

# **Nutraceutical potential of lycopene in management of oxidative stress mediated disease conditions**

By

**Reshmitha T R**

**Enrollment No: 10BB17J39008**

A Thesis submitted to the  
Academy of Scientific and Innovative Research  
for the award of the degree of

**DOCTOR OF PHILOSOPHY**

in

**SCIENCE**

Under the supervision of

**Dr. P Nisha**

Principal Scientist



**CSIR-National Institute for Interdisciplinary  
Science and Technology (CSIR-NIIST),  
Thiruvananthapuram- 695019**



Academy of Scientific and Innovative Research  
AcSIR Headquarters, CSIR-HRDC campus  
Sector 19, Kamla Nehru Nagar,  
Ghaziabad, U.P. – 201 002, India

**August, 2022**

CSIR-NATIONAL INSTITUTE FOR INTERDISCIPLINARY SCIENCE AND  
TECHNOLOGY

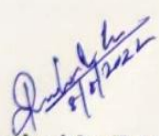


Council of Scientific & Industrial Research (CSIR)  
Industrial Estate (P.O), Thiruvananthapuram-695019, Kerala, India



Certificate

This is to certify that the work incorporated in this Ph.D. thesis entitled, "*Nutraceutical potential of lycopene in management of oxidative stress mediated disease conditions*", submitted by *Ms Reshmitha T R.* to the Academy of Scientific and Innovative Research (AcSIR) in fulfillment of the requirements for the award of the *Degree of Doctor of Philosophy in Sciences*, embodies original research work carried out by the student. We, further certify that this work has not been submitted to any other University or Institution in part or full for the award of any degree or diploma. Research materials obtained from other sources and used in this research work have been duly acknowledged in the thesis. Images, illustrations, figures, tables etc., used in the thesis from other sources, have also been duly cited and acknowledged.

  
Reshmitha T R

08-08-2022

  
8/8/22

Dr P Nisha  
(Thesis Supervisor)  
08-08-2022

## STATEMENT OF ACADEMIC INTEGRITY

I Reshmitha T R, a Ph.D. Student of Academy of Scientific and Innovative Research (AcSIR) with Registration No. 10BB17J39008 hereby undertake that, the thesis entitled “**Nutraceutical potential of lycopene in management of oxidative stress mediated disease conditions**” has been prepared by me and the document reports original work carried out by me and is free of any plagiarism in compliance with the UGC Regulations on “*Promotion of Academic Integrity and Prevention of Plagiarism in Higher Educational Institutions (2018)*” and the CSIR Guidelines for “*Ethics in Research and Governance (2020)*”.



**Reshmitha T R**

08-08-2022

Thiruvananthapuram

---

It is hereby certified that the work done by the student under my supervision, is plagiarism-free in accordance with the UGC Regulations on “*Promotion of Academic Integrity and Prevention of Plagiarism in Higher Educational Institutions (2018)*” and the CSIR Guidelines for “*Ethics in Research and Governance (2020)*”.



**Dr P Nisha**

08-08-2022

Thiruvananthapuram

## DECLARATION

I, Reshmitha T R bearing AcSIR Registration No. 10BB17J39008 hereby declare that my thesis entitled "**Nutraceutical potential of lycopene in management of oxidative stress mediated disease conditions**" is plagiarism-free in accordance with the UGC Regulations on "*Promotion of Academic Integrity and Prevention of Plagiarism in Higher Educational Institutions (2018)*" and the CSIR Guidelines for "*Ethics in Research and Governance (2020)*".

I would be solely held responsible if any plagiarised content in my thesis is detected, which is violative of the UGC regulation 2018.



Reshmitha T R

08-08-2022

Thiruvananthapuram



## ACKNOWLEDGEMENTS

*First and foremost, I thank **ALMIGHTY GOD** for being with me always and providing great mental support and strength throughout the completion of my research work.*

*I express my deep sense of gratitude to my research guide, **Dr. P. Nisha**, Principal scientist, Agro-processing and Technology division (APTD), CSIR-National institute for interdisciplinary science and Technology (CSIR-NIIST), who has been the true inspiration and guided me throughout my research work with inspiring suggestions, scholarly guidance, motivation, patience and also she gave full freedom to make use of all available facilities and fulfilled all the necessary requirements for my work, that have helped me to carrying out the present research work. I consider myself extremely fortunate for having her as my research supervisor.*

*I am grateful to, **Dr. Ashish Kishore Lele**, Director, CSIR-NIIST, **Dr. A. Ajayaghosh** and **Dr. Suresh Das**, former Directors of CSIR-NIIST, for providing the necessary facilities to carry out my work in this prestigious institute.*

*I gratefully acknowledge present and former HODs of Agro-processing and Technology division, **Shri.V. V.Venugopalan**, **Dr. K.G Raghu**, **Dr. Dileep Kumar B. S**, and **Shri. M.M. Sreekumar** for the constant support and providing all the resources to accomplish my work.*

*I also take the opportunity to express a deep sense of gratitude to **Dr. K.V.Radhakrishnan**, **Dr. Binod Parameswaran** and **Dr. Jayamurthy P** (Doctoral Advisory Committee members) of CSIR-NIIST for their cordial support and guidance throughout my study.*

*I wish to extend my thanks to **V. V.Venugopalan**, **Dr Priya. S**, **Dr Reshma M.V**, **Mr. D.R.Sobhan Kumar**, Agro-processing and Technology Division, CSIR-NIIST for their support.*

*I am deeply obliged for the timely efforts of AcSIR coordinators, **Dr. Karunankaran. V**, **Dr. Suresh C.H.** and **Dr. Luxmi Varma** for providing all help regarding the coordination and completion of the course work and other AcSIR requirements for granting PhD degree*

*My deepest thanks to **Dr. Arun K.B**, **Dr. Sithara Thomas**, **Mr Billu Abraham**, **Dr. Syama H.P**, **Dr Padma Ishwarya**, **Dr. Chintu Udayaraj**, **Ms Geethanjali**, **Ms Navami M**, **Ms Kavya**, **Ms Shini M.S**, **Ms Nidhina. K**, **Ms Heeba**, **Ms Sannya sathyan**, for their whole hearted help and support throughout my life in CSIR-NIIST.*

*I have immense pleasure in expressing my gratitude to my friends and colleagues, **Dr Prabha, Ms Aswathy P.S, Ms Fazeela, Ms Habeeba, Ms Reshma, Ms Evelyn M.A, Ms Sudhina Azeem, Dr Preetha Rani, Dr Anupama R, Ms Sruthi, Dr Sreelakshmi, Dr Swapna, Ms Vini Sekhar, Ms Geethu Gopinath, Ms Archana Haridas, Ms Nisha Jose, Ms Janu Chandran, Ms Shamla L, Mr Shijin, Mr Rakesh, Ms Sandhya Rajan, Ms Roopasree O.J, Mr Hari, Mr Noor Mohammad.***

*I would like to thank **Dr. Veena K.S, Dr. Dhanya B R, Dr. Sasi Parameswaran, Dr. Shyni, Dr. Gini, Dr. Salinn Raj Dr. Sindhu, Dr. Jamsheena V, Mr Krishnakumar, Mr Syam, Ms Taniya, Ms Lekshmi, Ms Gopika, Ms Jamsheena, Ms Theertha, Mr Vishnu, and all friends of APTD and NIIST** for their help and support.*

*I express my sincere thanks to all my **teachers.***

*I am obliged to **Council of Scientific and Industrial Research (CSIR)** for the award of direct-Senior Research Fellowship that inducted me to research carrier.*

*I am greatly thankful to my **family members** for their blessings and prayers, without which I have not reached here. I express my deep sense of gratitude, especially to my husband **Mr Anoop Raj**, who has been a constant source of love, concern, support and strength all these years that helped me stay the same through these difficult years. It gives me great pleasure to acknowledge all my family members and for whom this dissertation is dedicated*

*Thanks to all those who cannot find a separate name but helped me directly or indirectly to achieve the goal.*

**Reshmitha T R**

*Dedicated to my Family members...*

## TABLE OF CONTENTS

Sr No	Contents	Page No.
1	<b>Chapter 1: Introduction and Review of Literature</b>	<b>1-40</b>
1.1	Oxidative stress	4
1.2	Antioxidants	7
1.2.1	Endogeneous antioxidants	7
1.2.2	Exogeneous antioxidants	8
1.3	Carotenoids	9
1.3.1	Lycopene	10
1.3.1.2	Dietary LYC: Sources and bioavailability	13
1.3.1.3	Extraction of Lycopene	16
1.3.1.4	LYC as a free radical scavenger	17
1.3.1.5	LYC: mechanism of action in cancer	19
1.3.1.6	Potential role of LYC in CRC prevention and therapy	19
1.4	Carrier for bioactive delivery	21
1.4.1	Liposomes	22
1.5	Future Prospects and Conclusion	23
1.6	References	25
2	<b>Chapter 2: Enzyme mediated Lycopene extraction from tomato peel and evaluation of antioxidant potency against oxidative stress in L6 myoblast</b>	<b>41-71</b>
2.1	Introduction	42
2.2	Objective	43
2.3	Materials and methods	44

2.3.1	Chemicals and Reagents	44
2.3.2	Experimental Design	45
2.3.3	Sample Preparation	45
2.3.3.1	Enzymatically assisted LYC extraction	45
2.3.4	Determination of total phenolic content	46
2.3.5	DPPH Free radical scavenging activity	47
2.3.6	Cell culture treatment conditions	47
2.3.7	Cell viability	48
2.3.8	Intracellular ROS analysis	49
2.3.9	DNA protection studies	49
2.3.9.1	Hochest nuclear staining	49
2.3.9.2	DNA Fragmentation assay	49
2.3.9.3	Estimation of 8-oxo-2'-deoxyguanosine (8-oxo-dG)	50
2.3.10	Mitochondrial Protection Studies	50
2.3.10.1	Mitochondrial membrane potential analysis	50
2.3.10.2	Adenosine Triphosphate production by HPLC analysis	50
2.3.11	Statistical analysis	51
2.4	Results and Discussion	51
2.4.1	Estimation of LYC content in the ETE	52
2.4.2	The total phenolic content	52
2.4.3	Scavenging effect on DPPH radicals	53
2.4.4	Cell viability by MTT assay	53
2.4.5	ETE Inhibits H <sub>2</sub> O <sub>2</sub> -Induced Reactive Oxygen Species production in L6 cells	55



2.4.6	ETE protects L6 cells from nuclear damage	57
2.4.7	ETE protected H <sub>2</sub> O <sub>2</sub> induced DNA fragmentation	58
2.4.8	ETE protects DNA from oxidative damage	60
2.4.9	ETE prevented H <sub>2</sub> O <sub>2</sub> -induced reduction of Mitochondrial membrane potential in L6 cells	61
2.4.10	ATP level by HPLC analysis	61
2.5	Conclusion	63
2.6	Graphical Abstract	65
2.7	References	66
3	<b>Chapter 3: Role of Lycopene in Mitigation of Acrylamide and Glycidamide induced Hepatotoxicity (HepG2 cells)</b>	<b>72-114</b>
3.1	Introduction	73
3.2	Objectives	76
3.3	Materials and methods	76
3.3.1	Chemicals and Reagents	76
3.3.2	Experimental Design	77
3.3.3	Cell culture and treatment conditions	77
3.3.4	Cytotoxicity by MTT ssay	77
3.3.5	Lactate dehydrogenase lekeage	78
3.3.6	Intracellular ROS level	79
3.3.7	Antioxidant enzyme analysis	79
3.3.7.1	Superoxide Dismutase (SOD) and catalase (CAT) activity	79
3.3.7.2	Measurement of glutathione (GSH) concentration	79
3.3.8	Oxidative marker analysis	80

3.3.8.1	Measurement of lipid peroxidation	80
3.3.8.2	Estimation of 8-oxo-2'-deoxyguanosine (8-oxo-dG) level	80
3.3.9	Mitochondrial membrane potential ( $\Delta\Psi_m$ )	80
3.3.10	Mitotracker staining	81
3.3.11	Apoptosis by Flow Cytometry Analysis	81
3.3.12	Caspase 9 assay	81
3.3.13	Caspase 3 assay	82
3.3.14	Immunoblotting analysis	82
3.3.15	Statistical analysis	83
3.4	Results and Discussion	83
3.4.1	Cytotoxicity assessment of ACR, GLY and LYC	83
3.4.2	Cytoprotective potential of LYC against ACR and GLY-Induced toxicity	83
3.4.3	LYC protects HepG2 cells morphology from ACR and GLY induced alterations	85
3.4.4	Protective effect of LYC against ACR and GLY-induced LDH leakage	86
3.4.5	Protective potential of LYC against CAR and GLY induced ROS generation	87
3.4.6	Estimation of cellular antioxidant enzyme activity	89
3.4.6.1	LYC improved Superoxide dismutase and catalase activity	89
3.4.6.2	LYC improved ACR and GLY induced GSH depletion	90
3.4.7	Estimation of oxidative markers formation	92
3.4.7.1	Effect of LYC on lipid peroxidation induced by ACR and GLY	92

3.4.7.2	LYC protects DNA from ACR and GLY induced oxidative damage	93
3.4.8	Protective effect of LYC against ACR and GLY induced mitochondrial membrane potential	94
3.4.9	LYC protects mitochondrial membrane integrity against ACR and GLY induced cells	95
3.4.10	LYC protects ACR and GLY induced apoptosis in HepG2 cells	97
3.4.11	LYC downregulates caspase 9 activity	98
3.4.12	LYC downregulates caspase 3 activity	99
3.4.13	Protein expression by Western blotting	101
3.5	Conclusions	102
3.6	Graphical abstract	104
3.7	References	105
4	<b>Chapter 4: Lycopene regulates colon tumorigenesis via suppressing ROS mediated P13/Akt/mTOR signaling in HCT 116 cells</b>	<b>115-152</b>
4.1	Introduction	116
4.2	Objectives	119
4.3	Materials and methods	119
4.3.1	Chemicals and Reagents	119
4.3.2	Experimental Design	120
4.3.3	Cell culture and treatment conditions	121
4.3.4	Cytotoxicity by MTT assay	121
4.3.5	Morphological analysis	121

4.3.6	Cell death detection by AO/EtBr staining	122
4.3.7	Intracellular ROS level	122
4.3.8	Antioxidant enzyme analysis	122
4.3.8.1	Catalase activity	122
4.3.8.2	Measurement of glutathione (GSH) concentration	123
4.3.9	Nuclear staining with Hoechst 33342	123
4.3.10	Mitochondrial membrane potential ( $\Delta\Psi_m$ )	123
4.3.11	Mitotracker/DAPI staining	124
4.3.12	Apoptosis by Flow Cytometry Analysis	124
4.3.13	Caspase-3 Assay	125
4.3.14	Immunoblot analysis	125
4.3.15	Cell cycle analysis	126
4.3.16	Statistical analysis	126
4.4	Results and Discussion	126
4.4.1	LYC reduces cell viability in HCT 116 cells	126
4.4.2	Cell morphology by phase contrast microscope	128
4.4.3	Live/Dead assay by AO/EtBr dual staining	129
4.4.4	Measurement of intracellular ROS level in HCT 116	130
4.4.5	LYC reduced Antioxidant enzyme activity HCT 116	131
4.4.6	LYC promotes nuclear fragmentation in HCT 116 cells	133
4.4.7	LYC Induced MMP Loss in HCT 116 cells	134
4.4.8	Mitotracker/DAPI Staining	135
4.4.9	LYC promotes apoptosis in HCT 116 cells	137
4.4.10	LYC initiates caspase 3 activity	138

4.4.11	LYC supress PI3K/AKT/mTOR signalling pathway	139
4.4.12	LYC initiate G2Phase arrest	142
4.6	Graphical Abstract	145
4.7	References	146
5	<b>Chapter 5: Development and characterization of chitosan coated lycopene nanoliposomes with inulin for colon delivery</b>	<b>153-189</b>
5.1	Introduction	154
5.2	Objectives	157
5.3	Materials and methods	157
5.3.1	Chemicals nad Reagents	157
5.3.2	Experimental Design	158
5.3.3	Liposomal (LP) preparation	158
5.3.4	CS coating of Liposomes	160
5.3.5	Physicochemical characterization of CS coated LPs	161
5.3.5.1	Particle size, PDI and Zeta potential	161
5.3.5.2	Entrapment efficacy (EE)	161
5.3.5.3	ATR-Fourier-transform infrared (FTIR) spectroscopy	162
5.3.6	Color analysis	162
5.3.7	<i>In vitro</i> digestion	162
5.3.8	Mucin adsorption study	163
5.3.9	Cell culture and treatment	164
5.3.9.1	Determination of cell viability	164
5.3.9.2	Morphological anlaysis	164



5.3.9.3	BRdu cell proliferation assay	165
5.3.9.4	Colony formation assay	165
5.3.9.5	Apoptosis estimation by Annexin V	165
5.3.10	Statistical analysis.	166
5.4	Results and Discussion	166
5.4.1	Formation of Uncoated and CS coated LP	166
5.4.2	Particle size distribution, PDI and zeta potential	167
5.4.3	Encapsulation efficiency (EE)	169
5.4.4	Fourier Transform Infrared Spectroscopy (FTIR)	170
5.4.5	<i>In Vitro</i> LYC Release	171
5.4.6	Mucoadhesive property	173
5.4.7	Cell viability	174
5.4.8	Cell Morphology	176
5.4.9	Brdu cell proliferation	177
5.4.10	Colony formation assay	178
5.4.11	Cell death by apoptosis	179
5.5	Conclusion	180
5.6	Graphical Abstract	183
5.7	Reference	184
<b>6</b>	<b>Chapter 6 : Summary and Conclusion</b>	<b>190-198</b>
<b>7</b>	<b>Appendix</b>	<b>199</b>
<b>8</b>	<b>One page Abstract</b>	<b>200</b>
<b>9</b>	<b>List of Publications</b>	<b>201</b>

## LIST OF TABLES

<b>Table No.</b>	<b>Title</b>	<b>Page No.</b>
Table 1.1	LYC Content in different food sources	14
Table 5.1	The Composition of developed uncoated and CS coated nanoliposomes	159
Table 5.3	The physicochemical characterization of uncoated and CS coated different liposomal system by using DLS analysis	168

## LIST OF FIGURES

---

<b>Figure No</b>	<b>Title</b>	<b>Page No.</b>
Fig 1.1	Balance between dietary antioxidant and unhealthy lifestyle induced oxidative damage.	3
Fig 1.2	Oxidative stress resulting from an imbalance between ROS generation and antioxidant system and its consequences on cellular macromolecules	5
Fig 1.3	Schematic representation of the link between ROS, oxidative stress and their effects on the human body	6
Fig 1.4	Role of different types of carotenoids in disease suppression	10
Fig 1.5	Chemical structure of LYC	12
Fig 1.6	Transport and absorption of dietary LYC	15
Fig 1.7	Lycopene, protects the cellular biomolecules from oxidation by quenching reactive oxygen species (ROS)	18
Fig 1.8	Mechanisms of cancer chemoprevention by LYC	19
Fig 2.1	Outline of Chapter 2	43
Fig 2.2	Experimental methods used for the study	45
Fig 2.3	Schematic representation of enzyme assisted LYC extraction from tomato peel	46
Fig 2.4	The Effect of ETE, H <sub>2</sub> O <sub>2</sub> and pretreatment of cells with	54

	ETE before exposure with H <sub>2</sub> O <sub>2</sub> , on viability of L6 cells by MTT assay	
Fig 2.4a	Cytotoxicity of ETE to L6 cells	54
Fig 2.4b	Cytotoxicity of L6 cells following different concentrations of H <sub>2</sub> O <sub>2</sub> exposure	54
Fig 2.4c	The effect of ETE on L6 cell viability against 100μM H <sub>2</sub> O <sub>2</sub>	54
Fig 2.5	Measurement of ROS production in L6 cells.	56
Fig 2.5a	Fluorescent intensity measurement indicate in % ROS production	54
Fig 2.5b	Fluorescent imaging	54
Fig 2.5c	Represent flow cytometric analysis of ROS production in L6 cells by plotting cell count against FITC	54
Fig 2.6a	Chromatin condensation observed using Hoechst 33342 staining	59
Fig 2.6b	DNA damage was analyzed by DNA Fragmentation assay	59
Fig 2.7	The level of 8-oxo-dG in cells	60
Fig 2.8	Quantification of Mitochondrial membrane potential by Rhodamine 123 staining and ATP level by HPLC method	62
Fig 2.8a	Mitochondrial membrane potential by Rhodamine 123 staining	62
Fig 2.8b	Represents the restoration of mitochondrial membrane potential in percentage on ETE treatment.	62

Fig 2.8c	ETE treatment increases mitochondrial capacity to produce ATP	62
Fig 2.10	Enzyme assisted LYC rich tomato peel extract (ETE) exhibit a promising antioxidant potential by protecting stress induced L6 myoblast cells by inhibiting ROS production and cellular damage.	65
Fig 3.1	Outline of Chapter 3	76
Fig 3.2	Experimental methods used for the study.	77
Fig 3.3	Determination of cytotoxic effect on HepG2 cells by MTT Assay	84
Fig 3.3a	Cell viability of various concentrations of LYC	84
Fig 3.3b	Cell viability of ACR and GLY treated cells.	84
Fig 3.3c	The LYC on viability of L6 cell against 500 $\mu$ M ACR and GLY induced toxicity	84
Fig 3.4	Morphological analysis by Phase contrast microscopy	85
Fig 3.5	LDH release in HepG2 cells	86
Fig 3.6	Estimation of ROS formation by HDCFDA Staining	88
Fig 3.6a	Estimation of ROS formation by Fluorescence spectrophotometer	88
Fig 3.6b	Represent flow cytometric analysis of ROS production	88
Fig 3.7	Effects of LYC on SOD, CAT and GSH in HepG2 cells	91
Fig 3.7a	Protective effect of LYC on SOD activity in presence of	91



	ACR and GLY (500 $\mu$ M)	
Fig 3.7b	Protective effect of LYC on CAT activity in presence of ACR and GLY (500 $\mu$ M)	91
Fig 3.7c	Protective potential of LYC on reduction in the level of glutathione when exposed to ACR and GLY (500 $\mu$ M)	91
Fig 3.8	Quantification of oxidative stress markers.	93
Fig 3.8a	Lipid peroxidation determined by MDA level	93
Fig 3.8b	Figure represent the 8-oxo-dG level in cells	93
Fig 3.9	Estimation of Mitochondrial membrane potential by Rhodamine123 staining	95
Fig 3.10	Staining of HepG2 cells with mitotracker Red.	96
Fig 3.11	Flow cytometric analysis of cells undergoing apoptosis by Annexin V-FITC/propidium iodide staining	97
Fig 3.12	Bar diagram represent the caspase 9 activity	99
Fig 3.13	Bar diagram represent the caspase 3 activity	100
Fig 3.14	Effects of LYC against ACR AND GLY induced toxicity on the expression of apoptotic related proteins.	101
Fig 3.15	Schematic representation of LYC ameliorate ACR AND GLY induced ROS mediated apoptosis in HepG2 cells	104
Fig 4.1	Illustration of cancer cell hallmarks	117
Fig 4.2	Outline of Chapter 4	119
Fig 4.3	Experimental methods used for the study	120

Fig 4.4	The Effect of LYC on HCT 116 cell viability by MTT assay	127
Fig 4.5	Morphological analysis of HCT 116 cells by phase-contrast microscopy	128
Fig 4.6	Live and dead cell analysis by AO/EtBr double staining	130
Fig 4.7	Estimation of ROS level by DCFH-DA staining	131
Fig 4.8	The levels of catalase activity was reduced after treatment with LYC	132
Fig 4.8a	Bar diagram represent CAT activity	132
Fig 4.8b	Bar diagram represent GSH level	132
Fig 4.9	Chromatin condensation observed using Hoechst 33342 staining	133
Fig 4.10	Mitochondrial membrane potential loss was quantified by Rhodamine 123 staining. HCT 116 cells	135
Fig 4.11	Staining of HCT 116 cells with mitotracker Red and DAPI dual staining	136
Fig 4.12	Effect of LYC on colorectal cancer cell apoptosis	138
Fig 4.12a	Representative flow cytometry graphs of HCT 116 cells	138
Fig 4.12b	Bar diagram represent apoptosis rate was expressed in %.	138
Fig 4.13	Bar diagram represent the caspase 3 activity in percentage	139
Fig 4.14	Effect of LYC on the protein expression level in PI3K/AKT/mTOR pathway in HCT 116 cells	141

Fig 4.14a	Represent the protein expression level	141
Fig 4.14b	Quantification of protein expression by immunoblotting	141
Fig 4.15	Cell cycle arrest of HCT 116 cells treated with LYC was analysed by detecting Propidium iodide stained cells using a flow cytometer	143
Fig 4.16	Schematic representation of possible mechanism by LYC regulate signalling events to induce cell death by apoptosis in HCT 116 colon cancer cells	145
Fig 5.1	Outline of Chapter 4	157
Fig 5.2	Experimental methods used for the study	158
Fig 5.3	Schematic representation of CS coated LYC and INU incorporated liposome preparation by using thin film hydration method	160
Fig 5.4	Schematic representation of CS coated liposome preparation	166
Fig 5.5	Developed uncoated (LYC-LP and LYC-I-LP) and CS coated nanoliposomes (CS-LYC-LP and CS-LYC-I-LP)	167
Fig 5.6	Encapsulation efficiency (%) of developed LYC incorporated uncoated and CS coated samples	169
Fig 5.7	FTIR Spectra of LYC and developed CS Coated nanolipoosmes	171

Fig 5.8	Percentage LYC releases from uncoated and CS coated nanoliposomes after <i>in vitro</i> digestion	172
Fig 5.9	Bar diagram represent mucoadhesiveness of developed CS coated nanoliposomes	174
Fig 5.10	Cell viability was assessed by MTT Assay	175
Fig 5.11	Morphological analysis by light microscopy morphological changes of HCT 116 cells treated with developed nanoliposomes	176
Fig 5.12	Cell proliferation was assessed by Brdu staining	178
Fig 5.13	Colony formation assay by crystal violet staining	179
Fig 5.14	Nanoliposomes-induced apoptosis in HCT 116 cells was determined by flow cytometric method using Annexin FITC-PI staining	180
Fig 5.14a	Represent the cell sorted graph based on Annexin V-FITC staining.	180
Fig5.14b	Represent the percentage evaluation of necrotic cells, live cell early and late apoptotic cells	180
Fig 5.15	Schematic representation of developed nanoliposomes induces apoptosis in HCT 116 cells	183
Fig 8.1	Graphical representation of chapters which brief demonstration of the work flow.	198

## ABBREVIATIONS

---

BrdU	Bromodeoxyuridine
8-oxo-dG	8-Oxo-2'-deoxyguanosine
ACR	Acrylamide
AKT	Protein Kinase B
ANOVA	Analysis of variance
AO	Acridine orange
ATP	Adenosine triphosphate
ATR	attenuated total reflectance
ATSDR	Agency for Toxic Substances and Disease Registry
Bax	BCL2-Associated X Protein
BCA	Bicinchoninic acid
Bcl-2	B-cell lymphoma 2
Bcl-x1	B-cell lymphoma-extra large
CaCl <sub>2</sub>	Calcium chloride
CAT	Catalase
C-LP	Control liposomes
CO <sub>2</sub>	Carbon dioxide
CRC	Colorectal Cancer
CS	Chitosan
CS-C-LP	Chitosan coated control liposomes
CS-I-LP	Chitosan coated inulin incorporated liposomes

CS-LYC-I-LP	Chitosan coated lycopene and inulin incorporated liposomes
CS-LYC-LP	Chitosan coated lycopene incorporated liposomes
Cu	Copper
CYP2E1	Cytochrome P450 2E1
Cyt C	Cytochrome C
DAB	3,3'-Diaminobenzidine
DAPI	4',6-diamidino-2-phenylindole
DCF	Dichloro fluorescein
DCFH-DA	Dichloro-dihydro-fluorescein diacetate
DMEM	Dulbecco's Modified Eagle's Medium
DMSO	Dimethyl sulfoxide
DNA	Deoxyribonucleic acid
DPPH	2,2-diphenyl-1-picryl-hydrazyl-hydrate
DTNB	Dithionitro benzoic acid
EC	Epicatechin
EC	Enzyme Commission
EDTA	Ethylenediamine tetra acetic acid
EE	Entrapment efficacy
EGCG	Epigallocatechin gallate
ELISA	Enzyme-linked immunosorbent assay
EtBr	ethidium bromide
ETC	Electron Transport Chain
FACS	Fluorescence-Activated Cell Sorting

FBS	Fetal Bovine Serum
FITC	Fluorescein isothiocyanate
FTIR	Fourier-transform infrared
GAE	Gallic acid equivalent
GI	Gastrointestine
GLY	Glycidamide
GM	Gut microbiota
GSH	$\gamma$ -glutamy-l-cysteinyl-l-glycine
GSH	Glutathione
GSSG	Glutathione disulfide
H <sub>2</sub> O <sub>2</sub>	Hydrogen Peroxide
HCl	Hydrochloric acid
HFD	High-fat diet
HPLC	High Performance Liquid Chromatography
HRP	Horseradish peroxidase
Ig	Immunoglobulin
IGF	Insulin-like growth factor
IGFBP-1	Insulin-like growth factor binding protein-1
I-LP	Inulin incorporated liposomes
INU	Inulin
K <sub>2</sub> HPO <sub>4</sub>	Dipotassium hydrogen phosphate
KH <sub>2</sub> PO <sub>4</sub>	Potassium dihydrogen phosphate
KOH	Potassium Hydroxide
LC	Liquid Chromatography

LDH.	Lactate dehydrogenase
LDL	Low-density lipoproteins
LEHD	(Leu-Glu-His-Asp)
LP	Liposome
LPO	Lipid Peroxidation
LUVs	large unilamellar vesicles
LYC	Lycopene
LYC-I-LP	Lycopene and inulin incorporated liposomes
LYC-LP	Lycopene incorporated liposomes
MDA	Malondialdehyde
MLVs	Multilamellar vesicles
MMP	Mitochondrial membrane potential
Mn	Manganese
mTOR	Mammalian target of rapamycin
MTT	3-(4,5-dimethylthiazol-2-yl)-2,5 diphenyltetrazolium bromide
NaCl	Sodium Chloride
NaHCO <sub>3</sub>	Sodium Bicarbonate
OD	Optical Density
OS	Oxidative stress
PAGE	Polyacrylamide gel electrophoresis
PBS	Phosphate buffered saline
PCNA	Proliferating cell nuclear antigen
PDGF	Platelet-derived growth factor



PDI	Polydispersity index
PI	Propidium Iodide
PI3K	Phosphoinositide 3-kinase
PVDF	Lipid Peroxidation
RNA	Ribonucleic acid
ROS	Reactive Oxygen Species
RT	Room Temperature
SD	Standard Deviation
SDS	Sodium dodecyl-sulfate
Se	Selenium
SGF	Stimulatory gastric Fluid
SIF	Stimulatory intestinal fluid
SOD	Superoxide dismutase
SSF	Simulated salivary fluid
SUVs	Small unilamellar vesicles (
TPC	Total phenolic content (
UV	Ultraviolet
VEGF	Vascular endothelial growth factor
Zn	Zinc

## SYMBOLS

---

$\beta$	Beta
$\alpha$	Alpha
$\mu$	Micro
$\mu\text{m}$	Micrometer
g	Gram
mg	Milligram
$\mu\text{g}$	Microgram
%	Percentage
$^{\circ}\text{C}$	Degree Celsius
mL	Milliliter
$\mu\text{l}$	Microliters
M	Molar
mM	Millimolar
w/v	Weight by volume
nm	Nanometre
V	Voltage
Da	Dalton
kDa	Kilo Dalton
Min	Minutes
Kb	Kilobase
mL	Milliliter
nm	Nanometer
h	Hour

## PREFACE

Dietary antioxidants play a major role in prevention and management of oxidative stress induced chronic diseases. Oxidative stress is generated in cells due to the oxidants and antioxidants imbalance in the body. When free radicals are generated beyond the limit of inherent antioxidant system to take care off, the free radicals can damage fatty tissue, DNA, and proteins in the body leading to vast number of diseases over a period of time. Consumption of diets rich in antioxidants is known to protect from free radical exposure and oxidative stress and growing evidence has suggested that functional food components could minimise the oxidative damage. Lycopene (LYC) is a major carotenoid present in red fruits and tomatoes are the largest contributor to the dietary LYC consumption of in humans. As one of the most promising antioxidants, high intake of LYC rich fruit and vegetables is reported to reduce the risk of chronic pathologies, such as diabetes, cancer and cardiovascular disease.

LYC is reported to exhibit both antioxidant as well as pro-oxidant activity in cells depending on the conditions. Reactive oxygen species (ROS) build up in the cells are the basic cause of most of the chronic diseases development. The present study is designed, **to elucidate the effect of LYC as antioxidant and pro-oxidant role in cells for the management of stress mediated disease conditions.**

**Chapter 1** gives a general introduction and review of literature about oxidative stress, antioxidants, Lycopene, colorectal cancer and bioactive carrier system of targeted delivery

The antioxidants play a crucial role in scavenging the active free radicals before they attack vital biomolecules. Interestingly, low physiological levels of reactive oxygen species are required for normal functioning of skeletal muscle but high ROS levels promote contractile dysfunction resulting in muscle weakness and fatigue. Skeletal muscle cells with higher ROS can cause pathogenesis and lead to different muscular degeneration and other related

diseased conditions including muscular dystrophy, diabetes mellitus, aging etc. **Chapter 2** deals with the extraction of LYC from tomato peel by using enzymes cellulase and pectinase, and the antioxidant activity of this LYC rich extract (ETE) against H<sub>2</sub>O<sub>2</sub> (100 μM) induced oxidative stress in LI6 muscle cells. It was observed that pre-treatment of cells with ETE (15 μg/mL) before exposure to H<sub>2</sub>O<sub>2</sub>, significantly enhanced cell viability, reduced ROS production, DNA fragmentation, chromatin condensation & 8-oxo-dG, an increased mitochondrial membrane potential and ATP levels. Results showed that ETE could protect cells from H<sub>2</sub>O<sub>2</sub> induced oxidative damage significantly, as compared to control. These results depicted the antioxidant potential of tomato peel extract which can counteract the redox imbalance in cells induced by oxidative stress condition.

Acrylamide (ACR) is a heat induced toxicant found in high temperature processed foods such as deep fat fried, baked, extruded and coffee bean-based products, that are rich in Asparagine and reducing sugar. Long term exposure to acrylamide is reported to cause genotoxicity and mutagenicity. Acrylamide is metabolized to glycidamide (GLY) in the body which is reported to be much more toxic than ACR. **Chapter 3** demonstrates the cytoprotective potential of LYC against ACR and GLY -induced cytotoxicity in HepG2 cells. The protective effect of LYC is mediated by inhibiting intracellular ROS generation, enhance antioxidants enzymes SOD, CAT and restoring the GSH level. LYC pretreatment (10 μM) exhibited a reduction in lipid (MDA) and DNA (8-oxo-Dg) oxidation biomarker level in the cells representing LYC inhibit free radicals before attacking the biomolecules. The study also revealed that ACR and GLY induced cell death was due to apoptosis and LYC effectively suppress apoptosis induction in HepG2 cells. The apoptosis was activated in HepG2 cells via ROS mediated intrinsic pathway by increased release of Cytochrome C and there activation in caspase 9 and 3. This was confirmed with analysis of protein expression by western blotting. Together, present study suggest that the LYC from natural

products can protect HepG2 cells against ACR and GLY -induced oxidative damage through antioxidant activity and also prevent ACR and GLY induced apoptosis by modulating ROS linked mitochondrial function. Reasonable supplement of LYC which are natural antagonists of ACR and GLY, can avoid the side effects caused by improper diet like fried food which leads to unavoidable acrylamide exposure.

Chapter 4 deals with the investigation of anticancer potential of LYC in colon cancer cell (HCT 116) by focussing PI3K/AKT/mTOR pathway. The above studies explored the antioxidant activity of LYC against stress induced conditions. Here, LYC act as a pro-oxidant, help in increased ROS level in HCT 116 cells. The different concentration of LYC (5  $\mu$ M, 10  $\mu$ M and 15  $\mu$ M) showed a dose dependent cell death and the morphology indicated the features of apoptotic cell death. LYC also exert a decrease in innate antioxidant enzymes CAT and GSH leads to enhanced ROS level and mitochondrial dysfunction. The ROS mediated mitochondrial dysfunction was analysed by MMP level and it was also visualised with higher number of disrupted mitochondrial membrane by using a mitotracker staining. The current study revealed that LYC can inhibit proliferation and successively induce apoptosis through the suppression of the PI3K/AKT/mTOR pathway in HCT 116 cells. The phosphorylated forms of PI3K/AKT/mTOR activate cell proliferation and cell survival. From the blotting results, LYC suppressed the activation of PI3K pathway and is verified by analysing changes in the expression levels of PI3K, p-PI3K, AKT, p-AKT, mTOR, p-mTOR, Bax and Bcl-2. A decrease in the level of p-PI3K p-AKT p-mTOR Bcl-2 and increased Bax level, indicated apoptotic induction in HCT 116 cells. Collectively protein expression studies revealed that LYC inhibited HCT 116 cell proliferation and apoptosis activation via activating mitochondrial mediated pathway and suppressing PI3K/AKT/mTOR cascade. Therefore, LYC may be a promising agent for the prophylactic management of CRC.

In continuation to the beneficial effect of LYC in CRC management, fabrication of nanoliposomes for colon targeted delivery was dealt which forms the subject matter under chapter 5. Preliminary studies were also carried out on its effect in colon cancer cell (HCT 116). The fabricated liposomes with LYC and inulin (INU) were coated with chitosan to improve its functionality. The results showed that the developed liposomes possess size ranges in nanoscale, better PDI and increased zeta potential. The final liposomal formulations (CS-C-LP, CS-I-LP, CS-LYC-LP, and CS-LYC-I-LP) had a marked positive charge, which can attach to the negative charge on tumour cells and then inhibit cellular growth. The encapsulation efficacy showed better incorporation of lycopene in liposomal system with 81% for CS-LYC-I-LP. The *in vitro* release of lycopene under stimulated gastric conditions shows very low LYC release kinetics in three stimulated gastro-intestinal fluids with different pH. The results suggest a synergetic effect of LYC and INU in encapsulated liposomes (CS-LYC-I-LP sample) in demonstrating higher antiproliferation and apoptotic effect in HCT116 cells. The chitosan coating of the liposomes led to further controlled LYC release and, higher mucoadhesiveness. The chitosan coated Liposomes would be promising delivery system and LYC release for long-circulating treatment and colon targeted therapeutic strategies.

Thus the present study demonstrated the LYC exhibited promising antioxidant and pro-oxidant activity against ROS mediated cellular damages focussing on chronic disease depending on cellular conditions. As a natural antioxidant, LYC can be used as an excellent nutraceutical against various stress related health conditions. Pharmaceuticals cannot be completely replaced by nutraceuticals but it can be a strong high-value implement for prevention and treatment of some pathological conditions.

**Chapter 1**

**Introduction and Review of Literature**

Modern lifestyle is linked with a higher intake of processed food, lack of exercise, and exposure to environmental pollution that lead to the onset of lifestyle-associated diseases. Food habits with excess energy consumption from high fat and sugar have been reported to induce the production of reactive oxygen species (ROS), which lead to chronic pathological responses like diabetes, neurodegenerative diseases, cardiovascular diseases, cancer, and aging (Salehi et al., 2020a; Aminjan et al., 2019; Mishra et al., 2018). Under normal cellular processes, the innate antioxidant defence system and dietary antioxidant intake helps to control the ROS level in physiological range. The balance between antioxidants and ROS levels helps to maintain cellular homeostasis. However, the imbalance in the formation of free radicals and antioxidant defence system results in oxidative stress induction and progression of cellular damage (Fig 1.1). Dietary antioxidants are the key factor in a healthy lifestyle to reduce the risk of chronic diseases by minimizing the detrimental effects of ROS and thereby help in stress-mediated disease management (Tan et al 2018; Liang et al., 2020). Scientific evidence suggests that the higher level of ROS accumulation in the body is the major cause of most chronic disease progression (Sharifi Rad et al., 2018).

A variety of bioactives such as dietary polyphenols, carotenoids, and vitamins (C, D, E) possess promising antioxidant property and have been investigated for their capability to prevent several oxidative stress-induced human pathological conditions (Salehi et al., 2020b; Da Pozzo et al., 2018; Salehi et al., 2019). Out of all dietary antioxidants, carotenoids consist of natural fat-soluble components present in various vegetables and fruits. Humans cannot synthesize carotenoids in their body and must get it from their diet. Out of all carotenoids, LYC exhibit a superior antioxidant property with most potent singlet oxygen scavenging activity (Khan et al., 2019, Dos et al., 2018). Due to its outstanding antioxidant property, LYC offers a potential functional foods and nutraceutical with a therapeutic ability against stress-mediated disease conditions.



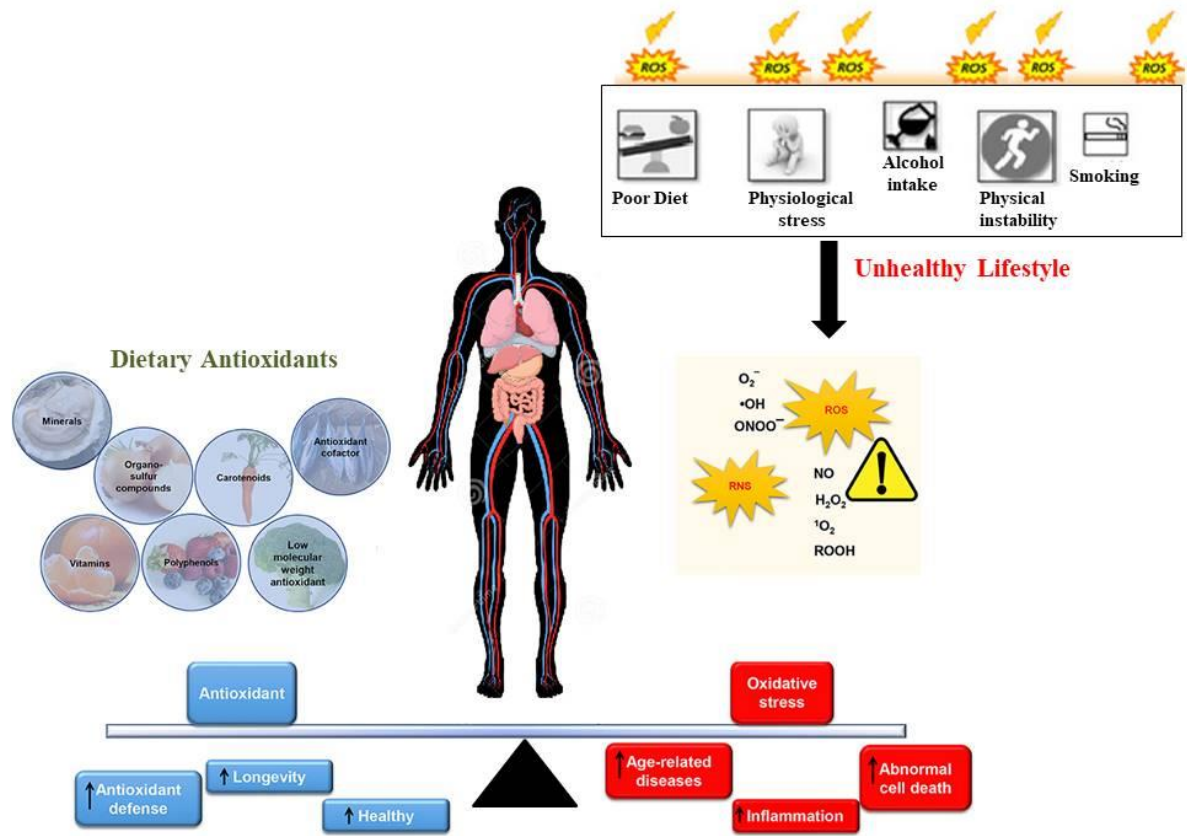


Fig 1.1: Balance between dietary antioxidant and unhealthy lifestyle induced oxidative damage.

## **1.1 Oxidative stress**

Many normal cellular processes in our bodies, such as respiration, digestion, detoxification of drugs, and fat metabolism produce harmful components called free radicals. For maintaining body homeostasis, ROS (Reactive Oxygen Species) plays a vital role as a regulatory mediator for signalling pathways (Tan et al., 2018). Under normal cellular conditions, innate antioxidant enzymes (catalase (CAT), superoxide dismutase (SOD), and glutathione (GSH)) converted these harmful intracellular ROS into less toxic compounds (Tsatsakis et al., 2019; Aminjan et al., 2019; Padureanu et al., 2019) by (Amir et al., 2016). Under pathological conditions, the overproduction of intracellular ROS overcomes the antioxidant defence mechanism leading to the formation of stress conditions known as oxidative stress (OS). If the free radical production exceeds beyond the efficiency of the innate defence systems or if the body's natural antioxidant defence system is not working properly, these free radicals can activate an adverse chain reaction in the body that results in plasma membrane damage, inhibition of the activity of enzymes, prevent cellular processes, inhibit cell division, induce deoxyribonucleic acid (DNA) damage and block ATP production (Sharifi-Rad et al., 2018; Tsatsakis et al., 2019; Kurutas, 2015). The imbalance in inherent antioxidant defence system in the body and free radicals leads to major cellular and tissue damage commonly by inducing DNA damage, lipid peroxidation, and protein denaturation (Fig.1.2). The impact of free radicals on health has been recognized for over 50 years, and potential of antioxidants on prevention and management of health have been documented (Liu, 2019). Under stress conditions or higher free radical build-up in the cells, ROS interrupts the antioxidant defence system to form irreversible changes in cellular biomolecules (DNA, Carbohydrates, protein, and fat) leads to disruption in normal cell signalling mechanism (Sharifi-Rad et al, 2018). The natural immune response in the body can also activate oxidative stress temporarily, which causes a minor inflammation that fades

once the body is out of infection. Numerous factors such as diet, lifestyle, and certain environmental factors like pollution, radiation, etc are reported to give rise to the oxidative stress development in the body.

Superoxide and hydroxyl radicals are primary oxygen free radicals. They are the derivatives of molecular oxygen formed under reduction conditions. Elevated ROS production in the cells leads to cellular mutations by interacting with DNA, potentially contributing the onset of tumour (Aminjan et al., 2019; Liang et al., 2020). Clinical research shows that antioxidant supplementation ameliorates endogenous antioxidant depletion and thereby minimizes stress-induced oxidative damage (Liu et al., 2019).

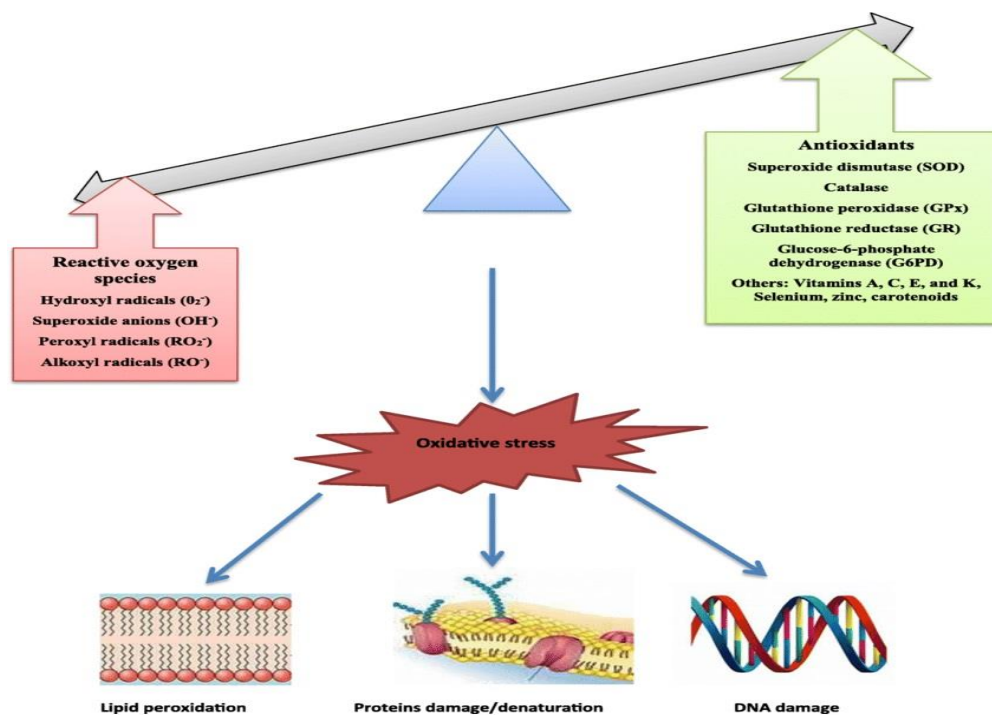


Fig 1.2: Oxidative stress resulting from an imbalance between ROS generation and antioxidant system and its consequences on cellular macromolecules (Roland et al., 2021; Lipid in health and disease).

Higher ROS level in cells regulate the protein configuration by modulating its structure and thereby induce functional changes results in the dysfunction of cellular system and disturbance in dynamic cellular processes (Sharifi-Rad et al, 2018). ROS-induced protein damage includes a site-specific amino acid alteration, crosslinked reaction product formation, peptide chain disintegration, electric charge variation, and enzymatic inactivation (Ayala et al., 2014). Free radicals can highly promote DNA damage via deoxyribose oxidation, DNA strand breakage, nucleotides deletion, bases modification, and DNA-protein cross-linkage (Liang et al., 2020; Cadet et al., 2017). In healthy organisms, the free radicals production are nullified by the innate antioxidant defense system of the body by keeping a delicate balance between free radicals (oxidants) and antioxidants in cells (Fig.1.3). Antioxidants in cells include enzymatic or non-enzymatic which prevent or neutralize the free radicals production (Sharifi-Rad et al, 2018).

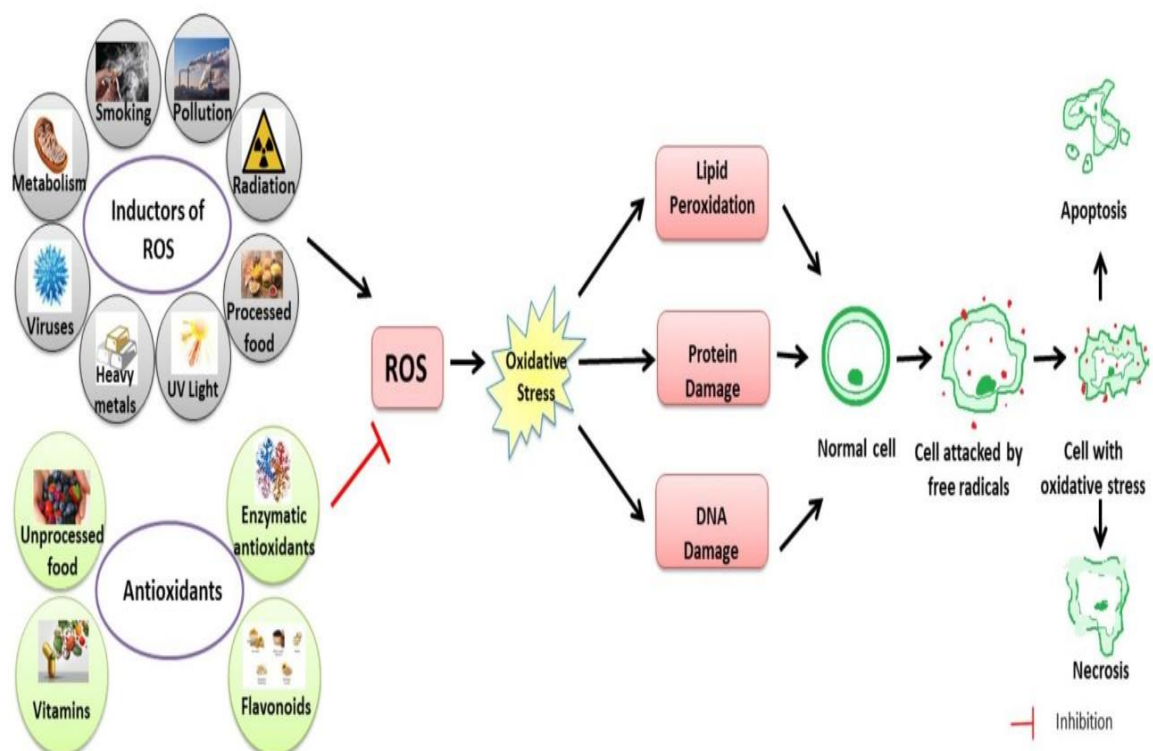


Fig 1.3: Schematic representation of the relation between ROS, oxidative stress and their effects on the human body (Sharifi-Rad et al., 2020; *Frontiers in Physiology*)

## **1.2 Antioxidants**

Antioxidants are the constituent that help in neutralizing free radicals by electron donation and thereby protects the body from oxidative stress. The oxidative stress in human body can be neutralized by innate antioxidants (endogenous) or externally provided through foods or supplements (exogenous) (Costa-Rodrigues et al., 2018). Both the antioxidants act as radical scavengers by inhibiting and restoring the damages caused by ROS; consequently enhances the defence system and lowers the risk of disease conditions (Sharifi Rad et al, 2020). The antioxidant mechanism can be both free radical quenching as well as chain-breaking. In the chain-breaking process, the chain breaking antioxidants e.g., vitamin C, E, carotenoids, etc, stabilizes free radicals thus resulting in a harmless product (Kurutas et al., 2015). One of the classic examples of chain reaction is lipid peroxidation in cells. The non-enzymatic antioxidant mechanism constitutes the second line of defence against ROS, characterized by the fast inactivation of oxidants and free radicals (Lazzarino et al., 2019). Exogenous antioxidants from the diet such as carotenoids, vitamin E, vitamin C, minerals (Zn, Se, Cu, Mn), and polyphenols (phenolic acids, flavonoids, lignans, stilbenes, etc) can improve the antioxidant activity.

### **1.2.1 Endogenous antioxidants**

One of the major enzymatic endogenous antioxidants that play the first line defence in cells is superoxide dismutase (SOD), which catalyzes the superoxide anion radical into hydrogen peroxide ( $H_2O_2$ ) by reduction. Some of the other antioxidants enzymes in first-line defence involved in the ROS neutralization are catalase (CAT), glutathione reductase (GRx), and glutathione peroxidase (GPx), (Curi et al., 2016; Hu and Ren, 2016). These enzymes neutralize  $H_2O_2$  into water and oxygen ( $O_2$ ) by GPx or CAT. The GPx enzyme helps in  $H_2O_2$  removal by oxidizing reduced glutathione (GSH) into oxidized glutathione (GSSG). The endogenous antioxidants (non-enzymatic) in the body are produced by normal cellular

metabolism, such as glutathione, lipoic acid, L-arginine, coenzyme Q10, melatonin, uric acid, bilirubin, transferrin, etc (Kucukgoncu et al., 2017; Tafazoli, 2017). GSH ( $\gamma$ -glutamyl-cysteinyl-glycine) is a tripeptide, commonly found in the cytoplasm, and also present in mitochondria, peroxisomes, and nuclei (Banafsheh and Sirous, 2018).  $\alpha$ -Lipoic acid is a organosulfur compound that regulates the oxidoreduction cycle similar to GSH. Subsequently,  $\alpha$ -Lipoic acid restores the active form of GSH, Vitamin C and Vitamin E by scavenging ROS (Kucukgoncu et al., 2017). Coenzyme Q10 is an isoprenoid antioxidant found in plasma membranes of the cell, it is crucial for Electron Transport Chain (ETC) and one of the rare fat soluble antioxidants, guaranteeing against lipid peroxidation and stress induced damage (Lee et al., 2017).

### **1.2.2 Exogenous Antioxidants**

Antioxidants present in fruits, vegetables, nuts, and cereal products contain higher amounts of exogenous antioxidants. These dietary antioxidants are reported to alleviate ROS-mediated cardiovascular disease (Costa-Rodrigues et al., 2018; Rowles et al., 2018), muscular dystrophy (Sitzia et al., 2019, Mensch and Zierz, 2020), diabetes (Imran et al., 2020), etc. Fruits and vegetable consumption deliver different vitamins, minerals, and phytochemicals as essential antioxidants, which cannot be synthesized inside the body. Phytochemical antioxidants comprises of vitamins E, C, and K; carotenoids like  $\beta$ -carotene, xanthophylls, lycopene, anthocyanins, and pheophytins; and secondary plant metabolites, like polyphenols (Lazzarino et al., 2019; Saheli et al., 2020). Phenolic compounds appear to be in variety of different structures, ranging from simple molecules (gallic acid, ferulic acid, vanillin, and caffeic acid) to complex polyphenols (flavonoids and tannins) (Fierascu et al., 2018). Vitamins C and E are the key vitamins exhibit highest antioxidant properties. Vitamin C is present in most vegetables and fruits and Vitamin E is a commonly present in cereals and legumes. Carotenoids are found in red colored vegetables and fruits. In

carotenoids,  $\alpha$ -carotene, lycopene,  $\beta$ -carotene, and lutein are the most important component with promising free radical scavenging (antioxidant) activity. These dietary antioxidants, particularly carotenoids and polyphenols, display a broad range of health benefits (Gulcin, 2020). Therefore to compensate for the increased oxidative stress, dietary antioxidant supplementation is suggested. Hence both endogenous and exogenous antioxidant defence system act synergistically to maintain redox homeostasis in the body. Nowadays, exogenous antioxidants present in foods and supplements are getting more attention in disease management and therapy.

### **1.3 Carotenoids**

Carotenoids are widely distributed pigments in nature, which imparts yellow to red and purple colors in fruits and vegetables. These carotenoids cannot be produced in the human body, so it depends entirely on dietary sources (Rosas-Saavedra et al., 2016). Based on conformation, carotenoids have been grouped into two category such as carotenes, ( $\beta$ -carotene, lycopene, and  $\alpha$ -carotene,) and xanthophylls ( $\beta$ -cryptoxanthin, lutein, astaxanthin, zeaxanthin, and fucoxanthin) (Maoka, 2020). Carotenoids comprise of basic eight isoprene units with a 40-carbon skeleton. Their common structures usually comprise of a polyene chain with nine conjugated double bonds and an end group (Kiokias et al., 2016). The chemical structure of carotenoid is responsible for its functional property. Carotenoids are responsible for the antioxidant activity by quenching singlet oxygen and protecting the cells against radical-induced damage (Black et al., 2020; Gulcin, 2020). Carotenoids exhibit a potent antioxidant effect by neutralizing oxidants that cause stress-mediated diseases including cancer (Fig 1.4) (Meena et al., 2019). The carotenoids benefits in human diets increased their scientific interest as a functional food and nutraceutical ingredient and had led to the development of different strategies to enhance their role in food products (Liu et al., 2015). Carotenoids intake from the diet is absorbed by the small intestine. These

carotenoids are combined with chylomicrons and then transported through the blood to the liver and various other organs (Von Lintig et al., 2019). Oxidative metabolites of lycopene, lutein, and zeaxanthin are also found in human plasma (Bohn, 2019).

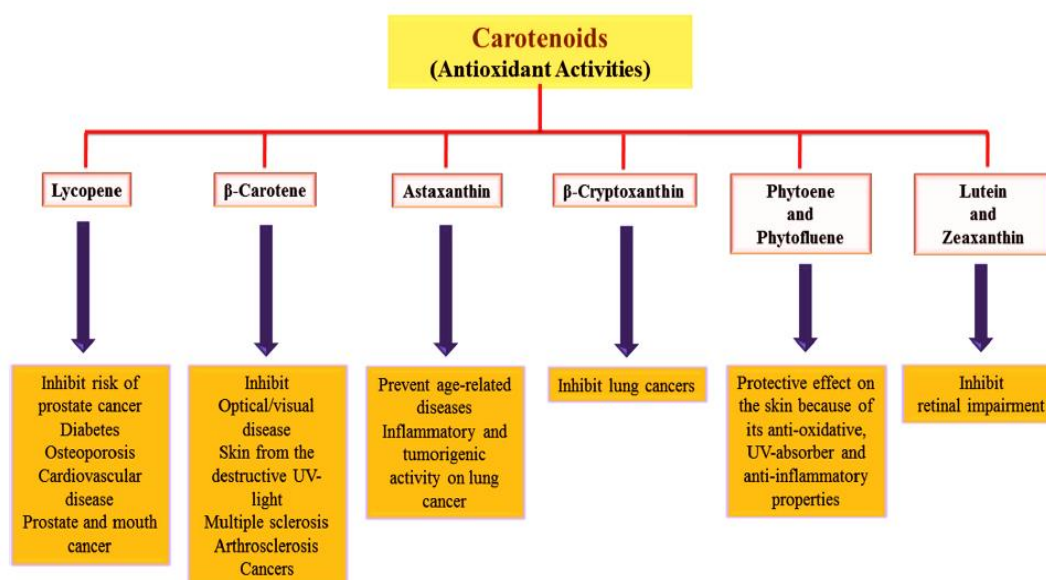


Fig 1.4: Role of carotenoids in disease suppression (Swapnil et al., 2021, *Current plant biology*).

Several studies showed that higher intake of dietary carotenoids are connected with reduced risks of serious disease conditions (Bhatt et al., 2020, Black et al., 2020). Lycopene is the rich carotenoid commonly found in the human diet (Kelkel et al., 2011). It is commonly present in red-colored vegetables and fruits and abundantly found in tomatoes. Among all carotenoids, lycopene is an emerging molecule, as a significant bioactive component with different biological properties.

### 1.3.1 Lycopene (LYC)

Among all carotenoids, LYC is a significant bioactive component with different biological properties. The activity of LYC in the body depends on several factors, like physical structure, dose, source, or specific site of action in the cells (Kong et al., 2010). It is also documented that, the LYC demonstrates a potential effect in the prevention and management



of most cancers (Vila et al., 2019) like prostate, bladder, cervical, leukemia, oral, pancreatic, colorectal, lung, and breast (Vila et al., 2019) by the reduction in tumor growth and inhibiting carcinogenesis (Sahin et al., 2019). LYC has a direct effect on redox imbalance and inflammation in which it activates antioxidant gene expression and regulates inflammatory mediators (Campos et al., 2017).

Epidemiological studies showed that LYC consumption and LYC level in blood plasma is correlated with a decreased risk for diabetes, cancer, neurodegenerative diseases, and cardiovascular disease (Rowles et al., 2020; Grabowska et al., 2019). Foods processing by thermal or mechanical methods contribute to the dissociation of LYC to become more bioavailable during intestinal absorption (Saini et al., 2020). A study showed that the LYC intake with fat content meals improves LYC absorption in the intestine. In contrast to other organs, higher LYC content was found in the cells of the gastrointestinal system after the consumption of LYC with a fat content meal (White et al., 2017).

The biological effects of LYC are associated with its native configurations in the form of *trans* or *cis* isomers and are mostly found in all-*trans* form which is converted to *cis* on cooking (Grabowska et al., 2019). LYC is a straight-chain unsaturated hydrocarbon comprising eleven conjugated and two non-conjugated double bonds (Fig 1.5), to form a chromophore (Pennathur et al., 2010). It is a red carotenoid, with a molecular mass of 536.89 g/mol, and its stability is exhibited at optimal pH of 3.5 to 4.5. It is an acyclic open-chain structure, an isomer of  $\beta$ -carotene, with the molecular formula of  $C_{40}H_{56}$ . This acyclic structure of LYC is a key factor for its chemical reactivity, physical properties, and biological functions (Meléndez et al., 2019). The conjugated double bonds in LYC undergo isomerization to different *cis* forms (*5-cis*, *9-cis*, *13-cis*, or *15-cis*) upon exposure to light, temperature, and chemical reactions (Grabowska et al., 2019). LYC is synthesized through phytoene and phytofluene precursors from mevalonate during the carotenoid biosynthesis

pathway (Meléndez et al., 2019; Yin et al., 2019). Because of this characteristic structure, it exhibits bright red color and powerful antioxidant property (Caseiro et al., 2020). Each double bond in LYC helps to decrease the energy required for the electrons transition, thus letting the molecule absorb light of longer wavelengths. It does not possess pro-vitamin A activity, due to its acyclic structure and the absence of a  $\beta$ -ionone ring (Pennathur et al., 2010). The most common LYC configuration found in foods are in *trans* form and it is present as *cis* in breastmilk, blood, and tissues (Saini et al., 2020). All *trans*-LYC isomers possess red color, whereas *cis*-configuration of LYC exhibit an orange hue color (Yin et al., 2019).

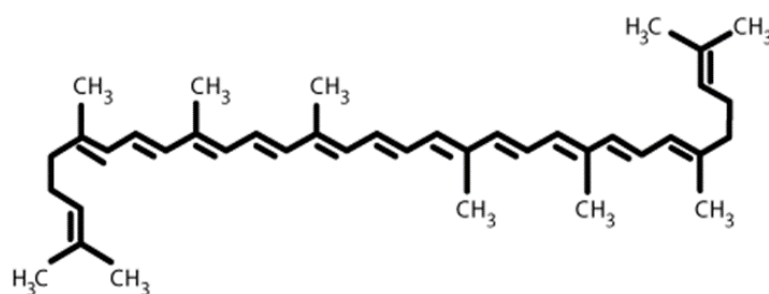


Fig 1.5: Chemical structure of LYC (Zuorro et al., 2020, *Molecules*).

The Partition coefficient of LYC is 17.64, making it nearly insoluble in ethanol, methanol, and water (Kong et al., 2010), and it is soluble in chloroform, tetrahydrofuran, benzene, hexane, petroleum ether, carbon disulfide, oil and acetone.. Because of its high hydrophobicity, LYC absorption from fruits and vegetables inside the body is very low. Because of its polyene structure, and a huge range of double bonds, it possesses many unique characteristics in mammalian systems. LYC shows a great quenching rate of singlet oxygen, which is directly associated to its free radical scavenging activity. The quenching efficacy of LYC is connected to the opening of the  $\beta$ -ionone ring to an open chain form. The antioxidant property of LYC is mainly due to the result of electron transfer from LYC to the

radical, the addition of the radical to the polyene chain, or the removal of a hydrogen atom from LYC (Pennathur et al., 2010). LYC is well studied to neutralize ROS effectively as twice as  $\beta$ -carotene and ten times as  $\alpha$ -tocopherol (Przybylska, 2020). It shows predominantly strong effects on superoxide radical, hydroxyl radical, and nitrogen dioxide.

#### **1.3.1.2 Dietary LYC: Sources and bioavailability**

Carotenoids are not biosynthesized in the body and are therefore completely obtained through the human diet. LYC is a major carotenoid found in red fruits, mostly in tomatoes, which are the largest dietary source of LYC in humans (Sokoloski et al., 2015). It is commonly found in red fruits and vegetables, generally tomato, carrot, papaya, cherry, watermelon, guava, and also in some vegetables that are not red, such as asparagus and parsley. LYC is present in tomato and tomato-related products, which contributes to more than 85% of dietary LYC (Przybylska, 2019). Tomatoes are an essential vegetable in the human diet and are usually consumed in fresh, cooked, or in processed forms like tomato paste, juice, ketchup, sauce, and soup. Epidemiologic evidence indicates that LYC-rich fruits and vegetable intake can reduce chronic disease conditions, such as cancer, diabetes, and cardiovascular disease (Dos Santos et al., 2018; Zhou et al., 2016; Bas et al., 2016; Sandikci et al., 2017). In recent years, LYC has been investigated for its possible health benefits, particularly in cancer prevention and treatment. The approximate LYC content of different food products is presented in Table 1.1 (Shi et al., 2000). LYC also appears in higher amounts in the seeds and peel of residues after the processing of watermelon (Okonkwo et al., 2018), tomato (Madia et al., 2021), Gac fruit (Saadedin et al., 2017), papaya (Desai et al., 2018), pomegranate (Sharmin et al., 2016) and carrot (Umair et al., 2021).

Table 1.1: LYC Content in different food sources (*Imran et al., 2020, Antioxidants*)

<b>Food Sources</b>	<b>LYC content (mg/100g)</b>
Tomatoes	0.7- 4.2
Boiled Tomatoes	3.7
Sun dried Tomatoes	45.9
Tomato paste	5.4 - 15
Tomato juice	8.2
Watermelon, fresh	4.5
Tomato, ketchup	9.9 - 13.4
Papaya, fresh	1.8
Pink guava	5.2–5.5
Rosehip	13
Pumpkin	0.3–0.4
Watermelon	2.3–7.2
Carrot	0.6–0.7

The bioavailability of LYC is high in processed products than in raw tomatoes. During food processing, certain factors like acid treatment, heat, and mechanical processing help tomato matrix disruption and LYC cis isomerization. LYC configuration influences the factors such as flavor, color, consistency and increase in biological activity by the formation of cis-isomers (Przybylska, 2020). Therefore, the bioavailability of LYC is low in fresh tomatoes compared to processed products like soup, sauce, juice, ketchup, etc. By passive diffusion, the LYC is entered into the intestinal cells through the brush border membrane. The gastrointestinal tract influences the bioavailability of dietary LYC. So, carotenoid release

from the food intake and its distribution in the digestive system was highly affected by several factors like food processing.

Dietary fat plays a major part in solubility and absorption of lipophilic carotenoids like LYC. It has the same absorption mechanism compared to dietary fat absorption (Srivastava et al., 2019). In Gastric phase, the food matrix is digested and LYC is released into the lipid medium. It is solubilized in the lipid medium and forms multilamellar lipid vesicles by the action of bile salts (Przybylska, 2020; Srivastava, 2019). In the small intestine, the LYC micelle is transferred into the mucosal cells through passive diffusion. Several factors influence micelle formation and mucosal transfer such as LYC structure, amount of fat intake, fatty acid composition, fiber content, etc (Asaduzzaman, 2022).

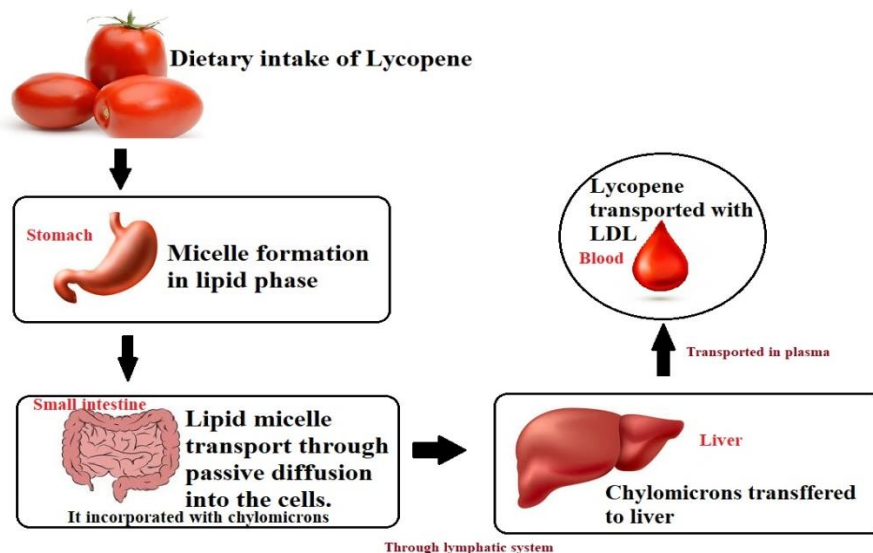


Fig 1.6: Transport and absorption of dietary LYC.

LYC leaves the intestinal mucosal cell and fused with chylomicrons, which are then transported through the lymphatic system to the liver (Durairajanayagam et al., 2014). In the liver, lipoprotein lipase acts on chylomicrons and releases LYC into the bloodstream and then transported with low-density lipoproteins (LDL) into other organs such as kidney, adrenal, adipose, reproductive organs, lung, and spleen (Arballo et al., 2021). The transport

and absorption process of dietary LYC is illustrated in Fig 1.6. LYC content is higher in adrenal gland, liver and reproductive tissues. In human serum, total carotenoids are found to be in the range 1–2  $\mu\text{M}$ , in which LYC constitute the major carotenoid present in serum. (Arballo et al., 2021; Su et al., 2002). The LYC accumulation may be found because of the higher lipoprotein receptors in the cells which enhance the lipoproteins uptake and higher oxidation rates in tissues. The studies suggest that dietary fiber consumption can reduce LYC adsorption by hindering its cellular uptake and thereby reducing the LYC level in blood plasma. And also the LYC absorption can be improved when it is consumed with other higher fat content food (White et al., 2017).

### **1.3.1.3 Extraction of lycopene**

The productive extraction and accurate evaluation of antioxidants from medicinal plants and food are essential for their application in pharmaceuticals and functional foods. Various extraction techniques, such as conventional and non-conventional extraction methods, can be selected to extract antioxidants from fruits or vegetables (Xu et al., 2017). The conventional extraction methods generally by using Soxhlet extraction and hot water bath are very time-consuming and need comparatively huge amounts of organic solvents with low extraction yields (Zhang et al., 2018; Saini et al., 2018). To obtain antioxidants in an economically acceptable approach, different techniques by using ultrasound, enzyme hydrolysis, microwave, high hydrostatic pressure, supercritical fluids, and pulsed electric field, have been studied as non-conventional methods (Zhang et al., 2018; Abdullah et al., 2019; Nour et al., 2018; Asaduzzaman, 2022). Enzyme-mediated extraction is a capable extraction method with mild extraction conditions. In this method, enzymes could hydrolyze the structural integrity of the cell wall, which aid to increase the release of bioactive (Popescu et al., 2022). The main enzymes used in enzyme-assisted extraction include cellulase, hemicellulose, pectinase, and  $\beta$ -glucosidase. Enzymatic methods have been

revealed to enhance the yield of antioxidants including carotenoids, flavonoids, phenolics, and anthocyanins, (Abdullah et al., 2019; Nguyen et al., 2022).

Currently, the utilization of by-products after different food processing is used as a source of healthy food components. Different studies were reported for the extraction of LYC from various fruits and vegetable sources. However, LYC can degrade rapidly and become isomerized when it is under strong and extreme processing methods (Asaduzzaman, 2022). Various methods that are used for LYC extraction include solvent extraction, hydrostatic pressure processing, enzymatic hydrolysis, ultrasonic extraction, supercritical fluid extraction (SFE), etc (Zhang et al., 2018; Asaduzzaman, 2022; Popescu et al., 2022; Romano et al., 2020). Recently an enzymatic extraction technique was used for the LYC extraction from tomato peels using rice bran oil (RBO) (Nguyen et al., 2022)

#### **1.3.1.4 LYC as a free radical scavenger**

The antioxidant efficacy of carotenoids is important to human health. Of all carotenoids, LYC is the most effective singlet oxygen scavenger *in vitro*. By ROS neutralization, LYC protects the cells from the oxidation of biomolecules such as DNA, proteins, and lipids (Fig 1.7). Epidemiological studies strongly support that adequate carotenoid supplementation may significantly reduce the risk of ROS-associated chronic conditions (Joshi et al., 2020). Because of its distinctive structure comprising of electron-rich system, the LYC displays an extreme reactivity towards free radicals (Caseiro et al., 2020). Molecular level studies have shown that the LYC is one of the most powerful antioxidants inhibiting the development of carcinogenesis and atherogenesis by protecting key biomolecules like proteins, DNA, and lipids (Bohn et al., 2019, Lim and Wang, 2020; Casiero et al., 2020.) In an animal study, the orally administrated LYC (10 or 100 mg/kg) alleviated hepatotoxicity by significantly reducing ROS production and regulating the antioxidant enzymes (CAT and GSH) in SK-Hep-1 cells (Bandeira et al., 2017). The antioxidative role of LYC exhibit a protective effect

against nephrotoxicity by increasing SOD activity , GPx, GSH, and antiapoptotic protein (Bcl-2) expression (Bayomy et al., 2017)

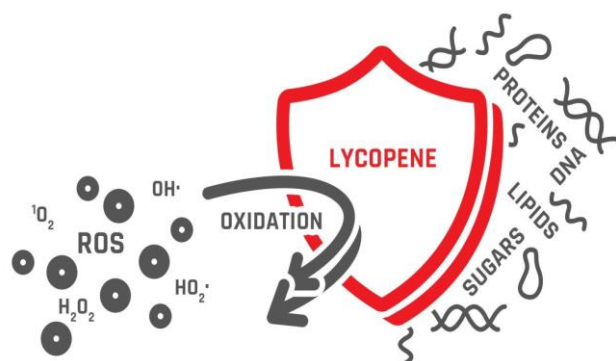


Fig 1.7: Lycopene, protects the cellular biomolecules from oxidation by quenching reactive oxygen species (ROS) (Grabowska *et al.*, 2019, *Food and function*)

LYC exhibited an alteration on the protein expression of Bcl-2 family in diabetic rats (Soleymaninejad et al., 2017). LYC significantly controlled glucose elevation, insulin intolerance, and lower glycogen level in the livers of HFD mice (Zeng et al., 2017). LYC is considered as a powerful nutraceutical, against cardiovascular diseases (CVD) and atherosclerosis (Costa-Rodrigues et al., 2018). LYC can scavenge some of the powerful oxidants associated with atherosclerosis by reducing cholesterol oxidation, which is considered as the initial step in atherosclerosis (Sen, 2019). In a study, tomato powder has been reported to have a protective effect against alcohol influenced hepatic toxicity by activating cytochrome p450 enzyme complex (Nedamani et al., 2019) Several studies exposed the antioxidant role of LYC against hepatotoxicity induced by mercuric chloride, carbon tetrachloride, methotrexate and acetaminophen in liver cells (Yucel et al., 2017; Nedamani et al., 2019; Imran et al., 2020).



### 1.3.1.5 LYC: mechanisms of action in cancer

High carotenoid content foods have been connected with decreased risk of different types of tumours by various mechanisms (Dos Santos et al., 2017; Ghadage et al., 2019). LYC has been verified to activate programmed cell death (apoptosis) in different cancer cell lines (Arathi et al., 2016). Different modes of action have been projected to describe the antitumorigenic activity of LYC in cancer cells (Casiero et al., 2020). It is one of the promising antioxidants, which has been lately stated to exhibit a dynamic role in antiproliferative activity at different stages of cancer (Ghadage et al., 2019). These include modulation of redox signalling, Antiproliferation, apoptosis induction, inhibition of cellular differentiation, cell cycle regulation, immune system modulation, cellular stress reduction by modifying ROS, detoxifying phase II enzymes, deactivation of growth factors such as IGF, VEGF, PDGF, triggered PI3K/AKT and MAPK signalling pathways (Fig 1.8) (Ghadage et al., 2019; Chen et al., 2018).

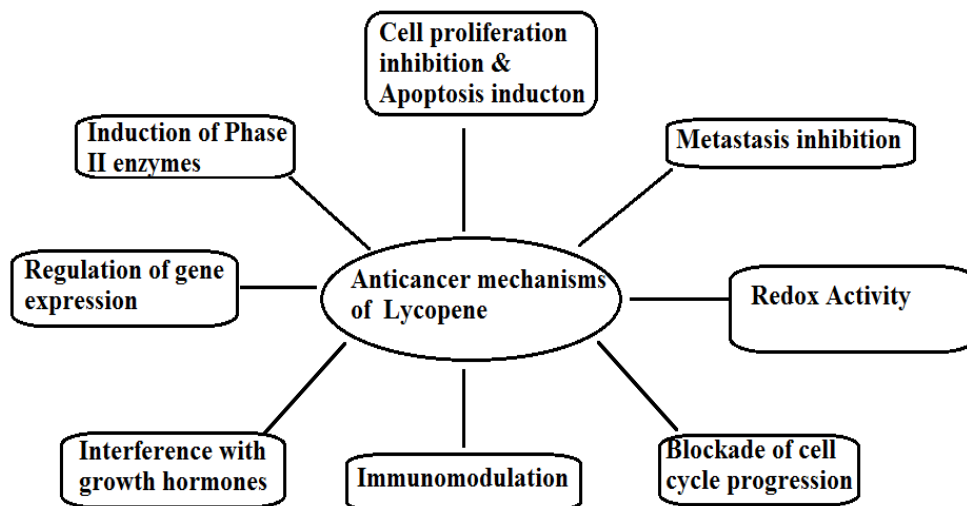


Fig 1.8: Mechanisms of cancer chemoprevention by LYC

### 1.3.1.6 Potential role of LYC in Colorectal cancer (CRC) prevention and therapy

Several studies have stated a positive relationship between LYC and tomato or tomato product intake in gastric and colorectal cancers (CRC) (Wang et al., 2021; Li et al., 2021;

Wang et al., 2018). Studies are reported on the connection between the LYC or LYC-rich food relationship in blood plasma levels and CRC risk (Langner et al., 2019; Li et al., 2021). Teodoro et al. have documented a substantial reduction in viable cell count when treated with LYC for 48 h in human colon adenocarcinoma (HT-29) cells and human colon carcinoma (T-84) cells (Teodoro et al., 2012). After 96 h LYC treatment triggered the cell cycle arrest in most of the common cancer cells as compared to control cells. Also, the LYC treatment in four cell lines such as HT-29, T-84, DU145, and MCF-7 exhibited a significant rise in apoptosis was detected. It also been demonstrated to prevent the cellular progression in HT-29 cells with an  $IC_{50}$  of 10  $\mu$ M. The LYC treatment also obstructed the Akt activation and  $\beta$ -catenin protein levels in non-phosphorylated form when studied in human colon cancer cells (Li et al., 2021). It was exposed in a different study that the tomato digestate inhibits HT-29 cell growth in a dose dependent mode and also triggers the cell cycle arrest and helps in apoptosis induction by down-regulating Bcl-2, Bcl-x1 and Cyclin D1, protein expression (Arbello et al., 2021).

A mouse model study, described that LYC blocked the nuclear expression of Proliferating cell nuclear antigen (PCNA) and  $\beta$ -catenin in cancer cells. LYC intake also enhances the E-cadherin expression and the cell cycle inhibitor p21 protein at nuclear levels (Wang et al., 2021). The inhibitory properties of LYC were also linked with the phosphorylated ERK1/2 proteins. In a randomized study, placebo-controlled men and women with high risk for CRC, administered with Lyc-o-Mato®, 30 mg/day LYC (tomato-based LYC supplementation) for eight weeks has been revealed the a surge in insulin-like growth factor binding protein-1 (IGFBP-1). The study also stated that the serum concentration of IGFBP-2 in both groups improved by 8.2 and 7.8%, respectively. The same placebo-controlled test conducted in patients plasma waiting for colectomy surgery, was reported a significant decrease of 25% IGF-I concentration on Lyc-o-Mato® administration (Walfisch et al.,

2017). The administration of LYC of different concentrations in gastric carcinoma in rats, upregulates the immune system, and thereby reduced the risk of gastric cancer.

Colon targeted delivery is a dynamic research area in for colon related diseases including colorectal cancer (CRC), as it delivers an improving therapeutic efficacy and reduces systemic toxicity. The oral administration is the most common route of drug delivery. Nanoformulations help to increase the therapeutics efficacy by site specific targeting and uptake into inflamed colon cells. Liposomes (LPs) can be a good delivery system for GI tract targeting, in which they can be modified by the addition of polymer coatings on the liposomal surface. These polymer coatings allow oral liposomal formulations to resist the deterioration of LPs in the gastric atmosphere of the gastrointestinal tract (GIT), which would normally dissolve the lipid bilayer.

#### **1.4 Carrier for bioactive delivery**

Most of the phytochemicals such as phenolic acids, flavonoids, carotenoids, and alkaloids possess extreme bioactivity such as antioxidant, antidiabetic, anti-inflammatory, anticancer, antimicrobial, etc. Though, some of them show poor solubility, low stability, and bioavailability limit in pharmaceutical applications (Rezaei et al., 2019). With this aspect, wide arrays of delivery systems have been formulated against gastrointestinal conditions to increase the component stability, enhance their solubility as well as targeted delivery.

Nanotechnology offers multiple benefits in therapeutics by site-specific delivery. It has made a great influence on food, biotechnology, cosmetics, and pharmaceutical. It plays a vital role in the lipophilic drugs to the targeted site delivery. Nano delivery systems can be categorized as emulsion-based delivery systems, solid lipid nanoparticulate systems, and vesicular delivery systems (Pandey et al., 2015; Singh et al., 2016). Nanotechnology represents an innovative area in research and development to overcome the limitations of conventional drug delivery systems. The limitations of the conventional delivery system can

be overcome by target-specific nanocarriers such as solid lipid nanoparticles (SLNs), liposomes, niosomes, colloidosomes, sphingosomes, and polymeric nanoparticles (Subramanian, 2021). Nanometer-sized (10–1,000 nm) particles are called nanoparticles, entrapped in the therapeutic molecules within the matrix, or conjugated onto the surface via functional modifications (Maurya et al., 2019; Awasthi et al., 2018). These nanocarriers protect the drug molecules against enzymatic degradation, and enhance its therapeutic benefits (Awasthi et al., 2020).

#### **1.4.1 Liposomes**

Liposomes are lipid vesicles with size ranges from nanometers to micrometers. They are highly effective in the targeted delivery of both hydrophilic and lipophilic molecules. The main constituents of a liposomal fabrication include phospholipids, sterols, and polymers. Liposomal vesicles are usually categorized depending on the diameter and number of layers in the vesicles, like multiple bilayers as multilamellar vesicles (MLVs), and with a single bilayer termed unilamellar vesicles. These unilamellar can again classify as small unilamellar vesicles (SUVs) and large unilamellar vesicles (LUVs) (Verma et al., 2019). An aqueous core was enclosed by the lipid bilayer of lamellar vesicles. Liposomes are likely to fuse and aggregate together leads to premature release of encapsulated components. Lipids on the surface of liposomes are vulnerable to oxidation. The main advantages of liposomal formulations are low toxicity, biocompatibility, and biodegradability (Khorasani et al., 2019). The liposomal surface can be easily manipulated by the addition of polymer coatings on the surface allow oral liposomal formulations to resist different pH in the GI tract (Xiuping et al., 2019)

In most cases, polyphenols were demonstrated in liposomal encapsulation due to their instability and low bioavailability (Gopi et al., 2018). A flavonol, quercetin, commonly found in grapes, onions, cherries, broccoli, citrus fruits, and berries, is one of the most

studied polyphenols for liposomal incorporation because of its varied bioactivity (Hadick et al., 2014). Quercetin-loaded liposomes show a protective effect against stress in cells (Li et al., 2018). A study reported in tumor-bearing mice treated with quercetin-loaded liposomes show a reduction in tumor growth compared to its free form (Ezzat et al., 2019). Curcumin also exhibits significant bioactive properties while its usage is limited because of low solubility, stability, and bioavailability. Compared to free curcumin, liposomal curcumin systems have demonstrated an enhanced anti-inflammatory and antioxidant activity (Fornasier et al., 2021; Caddeo et al., 2021).

### **1.5 Future prospects and conclusion**

The role of LYC as a powerful antioxidant against different disease conditions is well established and there is an increasing interest in developing LYC-containing supplements, nutraceuticals, and functional foods. Tomato is one of the major sources of industrial production of LYC. In industries, after tomato processing generates huge quantities of by-products, comprising of tomato peel, seeds, and pulp which could be exploited as a source of LYC with a circular economy point of view. Improvement in the efficiency of traditional extraction method is identified as a gap. With an eco-sustainable technique using cell wall degrading enzymes can help to recover LYC from tomato peel with high extraction yield.

One of the major causes for the onset of lifestyle associated diseases (including cancer) is exposure to process-induced toxicants in food products such as Heterocyclic aromatic amines, Acrylamide, Furan, nitrosamines, etc. Though LYC is affirmed as a potent antioxidant, its role in the mitigation of food toxicants-induced oxidative stress is not addressed. Acrylamide (ACR) is a process induced toxicant found in high temperature processed foods such as fried potatoes, cornflakes, potato chips or bread, etc. Toxic effects of acrylamide are reported to lead to carcinogenicity, neurotoxicity, and genotoxicity, which are facilitated by the formation of OS in cells and tissues. Glycidamide (GLY) is the primary

epoxide metabolite of ACR, and GLY is reported to be a more potent mutagen than ACR. Since LYC is a dietary antioxidant, its role in mitigating OS induced by acrylamide is worth exploring. With these backgrounds, the objectives of the proposed work are to

- Optimize the enzyme-assisted extraction of LYC from tomato peel using cell wall degrading enzymes and investigate the antioxidant potential of LYC-rich tomato peel extract against stress-induced L6 myoblast cells
- Evaluate the role of LYC in mitigation of acrylamide (ACR) and glycidamide (GLY) induced toxicity in HepG2 and elucidate the role of LYC in ACR/GLY induced cell death via ROS-regulated mitochondrial dysfunction.
- To study the antitumorigenic effect of LYC in colon cancer cell line ( HCT 116 cells) via suppressing P13/AKT/mTOR signalling
- To Develop LYC incorporated nanoliposomes for colon targeted delivery and to investigate its antitumorigenic effect in colon cancer cells (HCT 116)

## 1.6 References

- Abdullah, M. A., Dajah, S., Murad, A., El-Salem, A. M., Khafajah, A. M. (2019) Extraction, Purification, and Characterization of Lycopene from Jordanian Vine Tomato Cultivar, and Study of its Potential Natural Antioxidant Effect on Samen Baladi. *Current Research in Nutrition and Food Science*, 7(2).
- Aminjan, H. H., Abtahi, S. R., Hazrati, E., Chamanara, M., Jalili, M., and Paknejad, B. (2019). Targeting of oxidative stress and inflammation through ROS/NF kappa B pathway in phosphine-induced hepatotoxicity mitigation. *Life Sciences*, 232:116607.
- Amir Aslani, B., & Ghobadi, S. (2016). Studies on oxidants and antioxidants with a brief glance at their relevance to the immune system. *Life sciences*, 146, 163–173.
- Anwar, H., Hussain, G., Mustafa, I. (2018). 'Antioxidants from Natural Sources', in E. Shalaby, G. M. Azzam (eds.), *Antioxidants in Foods and Its Applications*, IntechOpen, London. 10.5772/intechopen.75961.
- Arathi, B. P., Sowmya, P. R., Kuriakose, G. C., Vijay, K., Baskaran, V., Jayabaskaran, C., & Lakshminarayana, R. (2016). Enhanced cytotoxic and apoptosis inducing activity of lycopene oxidation products in different cancer cell lines. *Food and chemical toxicology : an international journal published for the British Industrial Biological Research Association*, 97, 265–276.
- Arballo, J., Amengual, J., Erdman, J. W. (2021). Lycopene: A Critical Review of Digestion, Absorption, Metabolism, and Excretion. *Antioxidants*, 10(3):342.
- Asaduzzaman, M. (2022). Lycopene - A Review: Chemistry, Source, Health Role, Extraction, Applications. *Annual Research & Review in Biology*, 37, 87-101.
- Ayala, A., Muñoz, M. F., & Argüelles, S. (2014). Lipid peroxidation: production, metabolism, and signaling mechanisms of malondialdehyde and 4-hydroxy-2-nonenal. *Oxidative medicine and cellular longevity*, 2014, 360438.

- Banafsheh, A. A., and Sirous, G. (2016). Studies on oxidants and antioxidants with a brief glance at their relevance to the immune system. *Life Sciences*, 146, 163–173.
- Bandeira, A., da Silva, T. P., de Araujo, G. R., Araujo, C. M., da Silva, R. C., Lima, W. G., Bezerra, F. S., & Costa, D. C. (2017). Lycopene inhibits reactive oxygen species production in SK-Hep-1 cells and attenuates acetaminophen-induced liver injury in C57BL/6 mice. *Chemico-biological interactions*, 263, 7–17.
- Bas, H., & Pandir, D. (2016). Protective Effects of Lycopene on Furan-treated Diabetic and Non-diabetic Rat Lung. *Biomedical and environmental sciences, BES*, 29(2), 143–14.
- Bayomy, N. A., Elbakary, R. H., Ibrahim, M., & Abdelaziz, E. Z. (2017). Effect of Lycopene and Rosmarinic Acid on Gentamicin Induced Renal Cortical Oxidative Stress, Apoptosis, and Autophagy in Adult Male Albino Rat. *Anatomical record (Hoboken, N.J. : 2007)*, 300(6), 1137–1149.
- Bhatt, T., & Patel, K. (2020). Carotenoids: Potent to Prevent Diseases Review. *Natural*
- Black, H. S., Boehm, F., Edge, R., & Truscott, T. G. (2020). The Benefits and Risks of Certain Dietary Carotenoids that Exhibit both Anti- and Pro-Oxidative Mechanisms- A Comprehensive Review. *Antioxidants (Basel, Switzerland)*, 9(3), 264.
- Bohn T. (2019). Carotenoids and Markers of Oxidative Stress in Human Observational Studies and Intervention Trials: Implications for Chronic Diseases. *Antioxidants (Basel, Switzerland)*, 8(6), 179.
- Caddeo, C., Gabriele, M., Nácher, A., Fernández-Busquets, X., Valenti, D., Maria Fadda, A., Pucci, L., & Manconi, M. (2021). Resveratrol and artemisinin eudragit-coated liposomes: A strategy to tackle intestinal tumors. *International journal of pharmaceutics*, 592, 120083.



- Cadet, J., Davies, K. J. A., Medeiros, M. H. G., Di Mascio, P., and Wagner, J. R. (2017). Formation and repair of oxidatively generated damage in cellular DNA. *Free radical biology and medicine* 107, 13–34.
- Cadet, J., Davies, K., Medeiros, M. H., Di Mascio, P., & Wagner, J. R. (2017). Formation and repair of oxidatively generated damage in cellular DNA. *Free radical biology & medicine*, 107, 13–34.
- Campos, K. K. D., Araújo, G. R., Martins, T. L., Bandeira, A. C., Costa, B. G. et al. (2017). The antioxidant and anti-inflammatory properties of lycopene in mice lungs exposed to cigarette smoke. *Journal of Nutritional Biochemistry*, 48, 9–20.
- Caseiro, M., Ascenso A., Costa, A., Creagh-Flynn, J., Johnson, M., Simões S. (2020). Lycopene in human health. *LWT-Food Science and Technology*, 127, 109323.
- Chen, P., Xu, S., Qu, J. (2018). Lycopene protects keratinocytes against UVB radiation-induced carcinogenesis via negative regulation of FOXO3a through the mTORC2/AKT signaling pathway. *Journal of cellular Biochemistry*, 119, 366–377.
- Costa-Rodrigues, J., Pinho, O., & Monteiro, P. R. R. (2018). Can lycopene be considered an effective protection against cardiovascular disease?. *Food chemistry*, 245, 1148–1153.
- Costa-Rodrigues, J., Pinho, O., Monteiro, P. (2018). Can lycopene be considered an effective protection against cardiovascular disease?. *Food Chemistry* ,245, 1148–1153.
- Curi, R., Newsholme, P., Marzuca-Nassr, G. N., Takahashi, H. K., Hirabara, S. M., Cruzat, V., et al. (2016). Regulatory principles in metabolism then and now. *Biochemical Journal*, 473, 1845–1857.

- Curi, R., Newsholme, P., Marzuca-Nassr, G. N., Takahashi, H. K., Hirabara, S. M., Cruzat, V., et al. (2016). Regulatory principles in metabolism-then and now. *Journal of Biochemistry*. 473, 1845–1857.
- Da Pozzo, E., De Leo, M., Faraone, I., Milella, L., Cavallini, C., Piragine, E., Testai, L., Calderone, V., Pistelli, L., Braca, A., & Martini, C. (2018). Antioxidant and Antisenescence Effects of Bergamot Juice. *Oxidative medicine and cellular longevity*, 2018, 9395804.
- Da Pozzo, E., De Leo, M., Faraone, I., Milella, L., Cavallini, C., Piragine, E. (2018). Antioxidant and antisenescence effects of bergamot juice. *Oxidative Medicine and Cellular Longevity*. 2018:9395804.
- Desai, Pooja, H., Payal, M., Sangeeta, K., Bhushan, K., Vishal, K., Geetanjali, P., Rajeev, H., Shivaprakash, K. (2018). Studies on Isolation and Quantification of Lycopene from Tomato and Papaya and its Antioxidant and Antifungal Properties. *International Journal of Agriculture Innovations and Research*, 5, 257-260.
- Dos Santos, R.C., Ombredane, A. S., Souza, J. M. T., Vasconcelos, A.G., Plácido, A., Amorim, A.G.N. et al.(2018). Lycopene-rich extract from red guava (*psidium guajava L.*) Displays cytotoxic effect against human breast adenocarcinoma cell line MCF-7 via an apoptotic-like pathway. *Food Research International*, 105, 184-196.
- Durairajanayagam, D., Agarwal, A., Ong, C., & Prashast, P. (2014). Lycopene and male infertility. *Asian journal of andrology*, 16(3), 420–425.
- Ezzat, H.M., Elnaggar, Y.S.R., Abdallah, O.Y. (2019). Improved oral bioavailability of the anticancer drug catechin using chitosomes: Design, in-vitro appraisal and in-vivo studies. *International Journal for Pharmaceutics*, 565, 488–498.

- Fierascu, R.C., Ortan, A., Fierascu, I.C., Fierascu, I. (2018). In vitro and in vivo evaluation of antioxidant properties of wild-growing plants. A short review. *Current Opinion in Food Science*, 24, 1–8.
- Fornasier, M., Pireddu, R., Del Giudice, A., Sinico, C., Nylander, T., Schillén, K., Galantini, L., Murgia, S. (2021). Tuning lipid structure by bile salts: Hexosomes for topical administration of catechin. *Colloids and Surfaces B: Biointerfaces*, 199, 111564.
- Ghadage, S., Mane, K., Agrawal, R., Pawar, V. (2019). Tomato lycopene: Potential health benefits. *Pharma Innovation Journal*, 8, 1245–1248.
- Gopi, S., Amalraj, A., Jacob, J., Kalarikkal, N., Thomas, S., Guo, Q. (2018). Preparation, characterization and in vitro study of liposomal curcumin powder by cost effective nanofiber weaving technology. *New Journal of Chemistry*, 42, 5117–5127.
- Grabowska, M., Wawrzyniak, D., Rolle, K., Chomczyński, P., Oziewicz, S., Jurga, S., Barciszewski, J. (2019). Let food be your medicine: Nutraceutical properties of lycopene. *Food and Function*, 10, 3090–3102.
- Gulcin. (2020). Antioxidants and antioxidant methods: an updated overview. *Archives of Toxicology*, 94 (3), 651–715.
- Hu, N., and Ren, J. (2016). Reactive oxygen species regulate myocardial mitochondria through post-translational modification. *Reactive Oxygen Species*, 2, 264–271.
- Hu, N., and Ren, J. (2016). Reactive oxygen species regulate myocardial mitochondria through post-translational modification. *Reactive Oxygen Species* 2, 264–271.
- Imran, M., Ghorat, F., Ul-Haq, I., Ur-Rehman, H., Aslam, F., Heydari, M., Ali, M., Shariati, Okuskhanova, E., Yessimbekov, Z., Thiruvengadam, M., Hashem, M., & Rebezov, M. (2020). Lycopene as a Natural Antioxidant Used to Prevent Human Health Disorders. *Antioxidants*, 9(8):706.

- Joshi, B., Kar, S.K., Yadav, P.K., Yadav, S., Shrestha, L., Bera, T.K. (2020). Therapeutic and medicinal uses of lycopene: A systematic review. *International journal of Researchh in Medical Sciences*, 8, 1195.
- Kelkel, M., Schumacher, M., Dicato, M., & Diederich, M. (2011). Antioxidant and anti proliferative properties of lycopene. *Free Radical Research*, 45, 925–940.
- Khan, H., Reale, M., Ullah, H., Sureda, A., Tejada Gavela, S., Wang, Y et al. (2019). Anti-cancer effects of polyphenols via targeting p53 signaling pathway: updates and future directions. *Biotechnology Advances*, 38- 107385.
- Khorasani, S., Danaei, M., Mozafari, M. (2018). Nanoliposome technology for the food and nutraceutical industries. *Trends in Food Science and Technology*, 79, 106–115.
- Kiokias, S., Proestos, C., Varzakas, T. (2016). A review of the structure, biosynthesis, absorption of carotenoids-analysis and properties of their common natural extracts. *Current Research in Nutrition and Food Science*, 4, 25–37.
- Kong, K. W., Khoo, H. E., Prasad, K. N., Ismail, A., Tan, C.P., Rajab, N. F (2010).Revealing the power of the natural red pigment lycopene. *Molecules*,15(2), 959–987.
- Kucukgoncu, S., Zhou, E., Lucas, K. B., and Tek, C. (2017). Alpha-lipoic acid (ALA) as a supplementation for weight loss: results from a meta-analysis of randomized controlled trials. *Obesity Reviews*. 18, 594–601.
- Kucukgoncu, S., Zhou, E., Lucas, K. B., and Tek, C. (2017) Alpha-lipoic acid (ALA) as a supplementation for weight loss: results from a meta-analysis of randomized controlled trials. *Obesity Reviews*, 18: 594– 601.
- Kurutas, E.B. (2015). The importance of antioxidants which play the role in cellular response against oxidative/nitrosative stress: current state. *Nutrition journal*, 15(1), 71.

- Langner, E., Lemieszek, M.K. (2019). Lycopene, sulforaphane, quercetin, and curcumin applied together show improved antiproliferative potential in colon cancer cells *in vitro*. *Journal of Food Biochemistry*, 43, 12802
- Lazzarino, G., Listorti, I., Bilotta, G., Capozzolo, T., Amorini, A. M., Longo, S., et al. (2019). Water- and fat-soluble antioxidants in human seminal plasma and serum of fertile males. *Antioxidants*, 8:96.
- Lee, S. Q., Tan, T. S., Kawamukai, M., and Chen, E. S. (2017). Cellular factories for coenzyme Q10 production. *Microbial cell factories*, 16:39.
- Li, Z. L., Peng, S., Chen, X., Zhu, Y.-Q., Zou, L.-Q., Liu, W., Liu, C. M. (2018). Pluronic modified liposomes for curcumin encapsulation: Sustained release, stability and bio accessibility. *Food Research International*, 108, 246–253.
- Li, N., Wu, X., Zhuang, W., Xia, L., Chen, Y., Wu, C., Rao, Z., Du, L., Zhao, R., Yi, M., Wan, Q., Zhou Y. (2021). Tomato and lycopene and multiple health outcomes: umbrella review. *Food Chemistry*, 343,128396.
- Liang, J., Wu, M., Chen, C., Mai, M., Huang, J., & Zhu, P. (2020). Roles of Reactive Oxygen Species in Cardiac Differentiation, Reprogramming, and Regenerative Therapies. *Oxidative medicine and cellular longevity*, 2020, 2102841.
- Liang, X., Wang, S., Wang, L., Ceylan, A. F., Ren, J., and Zhang, Y. (2020). Mitophagy inhibitor liensinine suppresses doxorubicin-induced cardiotoxicity through inhibition of drp1-mediated maladaptive mitochondrial fission. *Pharmacological Research*, 157:104846.
- Liang, X., Wang, S., Wang, L., Ceylan, A. F., Ren, J., and Zhang, Y. (2020). Mitophagy inhibitor liensinine suppresses doxorubicin-induced cardiotoxicity through inhibition of drp1-mediated maladaptive mitochondrial fission. *Pharmacology Research*. 157:104846.

- Lim, J. Y., Wang, X. D. (2020). Mechanistic understanding of  $\beta$ -cryptoxanthin and lycopene in cancer prevention in animal models, *Biochimica et biophysica acta. Molecular and cell biology of lipids*, 1865(11), 158652.
- Liu, L. Shao, Z. Zhang, M. Wang, Q. (2015). Regulation of carotenoid metabolism in tomato. *Molecular plant*, 8(1), 28–39.
- Liu, Y., Shi, C., He, Z., Zhu, F., Wang, M., He, R., Zhao, C., Shi, X., Zhou, M., Pan, S., Gao, Y., Li, X., Qin, R. (2019). Inhibition of PI3K/AKT signaling via ROS regulation is involved in Rhein-induced apoptosis and enhancement of oxaliplatin sensitivity in pancreatic cancer cells. *International journal of biological sciences*, 17(2), 589–602.
- Liu, Z.-Q. (2019). Bridging free radical chemistry with drug discovery: a promising way for finding novel drugs efficiently. *The European Journal of Medicinal Chemistry*. 189:112020.
- Lourenco, S. C., Moldão-Martins, M., Alves, V. D. (2019) Antioxidants of Natural Plant Origins: From Sources to Food Industry Applications. *Molecules*, 15;24(22):4132.
- Madia, V. N., Vita, D., Ialongo, D., Tudino, V., Leo, A., Scipione, L., Messori, A. (2021). Recent Advances in Recovery of Lycopene from Tomato Waste Antioxidant with Endless Benefits. *Molecules*, 26:4495.
- Maoka, T. (2020). Carotenoids as natural functional pigments. *Journal of natural medicines*, 74 (1), 1–16.
- Meena, M., Samal, S. (2019) *Alternaria* host-specific (HSTs) toxins: an overview of chemical characterization, target sites, regulation and their toxic effects. *Toxicology Reports*, 6 , 745–758,
- Meléndez, A. J., Stinco, C. M., & Mapelli-Brahm, P. (2019). Skin Carotenoids in Public Health and Nutricosmetics: The Emerging Roles and Applications of the UV

Radiation-Absorbing Colourless Carotenoids Phytoene and  
Phytofluene. *Nutrients*, 11(5).

Mensch, A., Zierz, S. (2020). Cellular Stress in the Pathogenesis of Muscular Disorders-  
From Cause to Consequence. *International journal of molecular sciences*, 21(16),  
5830.

Mishra, A. P., Salehi, B., Sharifi-Rad, M., Pezzani, R., Kobarfard, F., Sharifi-Rad, J., et al.  
(2018). Programmed Cell death, from a cancer perspective: an overview. *Molecular  
Diagnosis and Therapy*, 22, 281–295.

Nedamani, A.R., Nedamani, E.R., Salimi, A. (2019). The role of lycopene in human health  
as a natural colorant. *Nutrition and Food Sciences*, 49, 284–298.

Nguyen, T. M., Trang, N., Ha M.D. (2022) 7<sup>th</sup> *analytica Vietnam Conference* lycopene  
extraction from tomato (*Lycopersicon esculentum*) peels using rice bran oil

Nour, V., Panaite, T. D., Ropota, M., Turcu R., Trandafir, I., Corbu, A. R. (2018).  
Nutritional and bioactive compounds in dried tomato processing waste. *CyTA-  
Journal of Food*, 16(1):222-9.

Okonkwo, Sylvia O., Nnamdi. (2018). Determination of lycopene from water melon  
(*Citrullus lanatus*). *International Journal of Scientific and Engineering*, 9, 5.

Padureanu, R., Albu, C. V., Mititelu, R. R., Bacanoiu, M. V., Docea, A. O., Calina, D.,  
Padureanu, V., Olaru, G., Sandu, R. E., Malin, R. D., & Buga, A. M. (2019).  
Oxidative Stress and Inflammation Interdependence in Multiple Sclerosis. *Journal of  
clinical medicine*, 8(11), 1815.

Pennathur, S., Maitra, D., Byun, J., Sliskovic, I., Abdulhamid, I., Saed, G.M., Diamond,  
M.P., Abu-Soud, H.M. (2010). Potent antioxidative activity of lycopene: A potential  
role in scavenging hypochlorous acid. *Free Radical Biology and Medicine*, 49, 205–  
213.

- Popescu, M., Iancu, P., Plesu, V., Todasca, M. C., Isopencu, G.O., Bildea, C.S. (2022). Valuable Natural Antioxidant Products Recovered from Tomatoes by Green Extraction. *Molecules*, 27, 4191.
- products and bioprospecting*, 10(3), 109–117.
- Przybylska, S. (2020) Lycopene – a bioactive carotenoid offering multiple health benefits: a review. *International Journal of Food Science and Technology*, 55: 11-32.
- Rezaei, A., Fathi, M., Jafari, S.M. (2019). Nanoencapsulation of hydrophobic and low-soluble food bioactive compounds within different nanocarriers. *Food Hydrocolloids*, 88, 146–162.
- Roland, A., Ajayi, A. (2021).The impact of reactive oxygen species in the development of cardiometabolic disorders: a review. *Lipids Health Diseases* 20, 23
- Romano, R., Aiello, A., Pizzolongo, F., Rispoli, A., De Luca, L., Masi, P. (2020). Characterisation of oleoresins extracted from tomato waste by liquid and supercritical carbon dioxide. *International Journal of Food Science*, 55, 3334–3342.
- Rosas-Saavedra, C., & Stange, C. (2016). Biosynthesis of Carotenoids in Plants: Enzymes and Color. *Sub-cellular biochemistry*, 79, 35–69.
- Rosas-Saavedra, C., Stange, C. (2016). Biosynthesis of carotenoids in plants: enzymes and color. *Carotenoids in Nature*, Springer, 35–69.
- Rowles, J. L., Erdman, J. W. (2020). Carotenoids and their role in cancer prevention. *Biochimica et biophysica acta. Molecular and cell biology of lipids*, 1865(11), 158613.
- Rowles, J.L., Ranard, K.M., Applegate, C.C., Jeon, S., An, R. Erdman, J.W. (2018). Processed and raw tomato consumption and risk of prostate cancer: a systematic review and dose-response meta-analysis. *Prostate Cancer and Prostatic Diseases*, 21, 319–336.



- Saadedin, I., Shurook, H.M., Awadi, A., Salwa, A. (2017). Solvents extraction efficiency for lycopene and  $\beta$ -carotene of GAC fruit (*Momordica cochinchinensis*, Spreng) cultivated in Iraq. *Bioscience Research*, 14, 788-800.
- Sahin, K., Orhan, C., Sahin, N., Kucuk, O. (2019). Anticancer properties of lycopene. *Bioactive Molecules in Food*, 935–969.
- Saini, R. K., Bekhit, A.E., Roohinejad, S., Rengasamy, K.R.R., Keum, Y.S. (2020). Chemical Stability of Lycopene in Processed Products: A Review of the Effects of Processing Methods and Modern Preservation Strategies. *Journal of Agriculture and Food Chemistry*, 68, 712–726.
- Saini, R. K., Moon, S. H., Keum, Y. S. (2018). An updated review on use of tomato pomace and crustacean processing waste to recover commercially vital carotenoids. *International Food Research journal*, 108, 516–529.
- Salehi, B., Calina, D., Docea, A. O., Koirala, N., Aryal, S., Lombardo, D., et al. (2020a). Curcumin's nanomedicine formulations for therapeutic application in neurological diseases. *Journal of Clinical Medicine*, 9:430.
- Salehi, B., Capanoglu, E., Adrar, N., Catalkaya, G., Shaheen, S., Jaffer, M., et al. (2019). Cucurbits plants: a key emphasis to its pharmacological potential. *Molecules*, 24:1854.
- Salehi, B., Rescigno, A., Dettori, T., Calina, D., Docea, A. O., Singh, L., et al. (2020b). Avocado–soybean unsaponifiables: a panoply of potentialities to be exploited. *Biomolecules*, 10:130.
- Sandikci, M., Karagenc, L., Yildiz, M. (2017). Changes in the Pancreas in Experimental Diabetes and the Effect of Lycopene on These Changes: Proliferating, Apoptotic, and Estrogen Receptor  $\alpha$  Positive Cells. *Anatomical Record*, 300, 2000–2007.

- Sen, S. (2019). The chemistry and biology of lycopene: Antioxidant for human health. *International journal of Advancement in Life Sciences*, 2, 8–14.
- Sharifi-Rad, M., Anil Kumar, N. V., Zucca, P., Varoni, E. M., Dini, L., Panzarini, E., Rajkovic, J., Tsouh Fokou, P. V., Azzini, E., Peluso, I., Prakash Mishra, A., Nigam, M., El Rayess, Y., Beyrouthy, M. E., Polito, L., Iriti, M., Martins, N., Martorell, M., Docea, A. O., Setzer, W. N., ... Sharifi-Rad, J. (2020). Lifestyle, Oxidative Stress, and Antioxidants: Back and Forth in the Pathophysiology of Chronic Diseases. *Frontiers in physiology*, 11, 694.
- Sharifi-Rad, M., Anil, K. N., Zucca V., Varoni, E. M., Dini, L., Panzarini, E., Rajkovic J., Tsouh, F., Patrick, V., Azzini, E., Peluso, I., Prakash, M. A., Nigam, M., El Rayess, Y., Beyrouthy, M. E., Polito, L., Iriti, M., Martins, N., Martorell, M. et al. (2020). Lifestyle, Oxidative Stress, and Antioxidants: Back and Forth in the Pathophysiology of Chronic Diseases. *Frontiers in physiology*, 11, 694.
- Sharmin, Tajnuba, A., Neaj, H., , Abul , H., Mojaffor, M., Shakti ,H., Almas,M., Siddik, M. D. (2016). Extraction of Bioactive Compound from Some Fruits and Vegetables (Pomegranate Peel, Carrot and Tomato). *American Journal of Food and Nutrition*, 4, 12.
- Shi, J., & Le Maguer, M. (2000). Lycopene in tomatoes: chemical and physical properties affected by food processing. *Critical reviews in biotechnology*, 20(4), 293–334.
- Sitzia, C., Meregalli, M., Belicchi, M., Farini, A., Arosio, M., Bestetti, D., Villa, C., Valenti, L., Brambilla, P., Torrente, Y. (2019). Preliminary Evidences of Safety and Efficacy of Flavonoids- and Omega 3-Based Compound for Muscular Dystrophies Treatment: A Randomized Double-Blind Placebo Controlled Pilot Clinical Trial. *Frontiers in Neurology*, 10:755.

- Sokoloski, L., Borges, M., & Bagatin, E. (2015). Lycopene not in pill, nor in natura has photoprotective systemic effect. *Archives of dermatological research*, 307(6), 545–549.
- Soleymaninejad, M., Joursaraei, S.G., Feizi, F., Jafari Anarkooli, I. (2017). The effects of lycopene and insulin on histological changes and the expression level of Bcl-2 family genes in the hippocampus of streptozotocin-induced diabetic rats. *Journal of diabetes research*, 2017, 4650939.
- Srivastava, S. (2019). Lycopene: Metabolism and Functional Aspects. In: Mérillon, JM., Ramawat, K. (eds) *Bioactive Molecules in Food. Reference Series in Phytochemistry*. Springer.
- Su, Q., Rowley, K. G., & Balazs, N. D. (2002). Carotenoids: separation methods applicable to biological samples. *Journal of chromatography. B, Analytical technologies in the biomedical and life sciences*, 781(1-2), 393–418.
- Subramanian, P. (2021). Lipid-Based Nanocarrier System for the Effective Delivery of Nutraceuticals. *Molecules*, 26, 5510.
- Swapnil, P., Meena, M., Singh, S. K., Dhuldhaj, U. P., Harish, Marwal, A. (2021). Vital roles of carotenoids in plants and humans to deteriorate stress with its structure, biosynthesis, metabolic engineering and functional aspects. *Current Plant Biology*, 26,100-203,
- Tafazoli, A. (2017). Coenzyme Q10 in breast cancer care. *Future Oncol.* 13, 1035–1041.
- Tan, B. L., Norhaizan, M. E., Liew, W. P. P., Rahman, H. S. (2018) Antioxidant and Oxidative stress: A Mutual Interplay in Age-Related Diseases. *Frontiers in pharmacology*, 9, 1162.

- Tang, F. Y., Pai, M. H., & Wang, X. D. (2011). Consumption of lycopene inhibits the growth and progression of colon cancer in a mouse xenograft model. *Journal of agricultural and food chemistry*, 59(16), 9011–9021.
- Teodoro, A.J., Perrone, D., Martucci, R.B., Borojevic, R. (2012). Lycopene isomerisation and storage in an in vitro model of murine hepatic stellate cells. *European Journal of Nutrition*, 48, 261–268.
- Tsatsakis, A., Docea, A. O., Constantin, C., Calina, D., Zlatian, O., Nikolouzakis, T. K., & Neagu, M. (2019). Genotoxic, cytotoxic, and cytopathological effects in rats exposed for 18 months to a mixture of 13 chemicals in doses below NOAEL levels. *Toxicology Letters*, 316, 154-170.
- Umair, M., Jabbar, S., Mustapha, M., Nasiru, Lu, Z., Zhang, J., Abid, M., Murtaza, A. M., Kieliszek, M., Zhao, L. (2021) Ultrasound-Assisted Extraction of Carotenoids from Carrot Pomace and Their Optimization through Response Surface Methodology. *Molecules*, 26(22): 6763.
- Verma, S., Utreja, P. (2019). Vesicular nanocarrier based treatment of skin fungal infections: Potential and emerging trends in nanoscale pharmacotherapy. *Asian Journal of Pharmaceutical Sciences*, 14, 117–129.
- Vila, E., Hornero-Méndez, D., Azziz, G., Lareo, C., Saravia, V. (2019) Carotenoids from heterotrophic bacteria isolated from Fildes Peninsula, King George Island, Antarctica. *Biotechnology Reports*, 21.
- Von Lintig J., Moon J., Lee J., Ramkumar S. (2019). Carotenoid metabolism at the intestinal barrier. *Biochimica et Biophysica Acta - Molecular and Cell Biology*, 158-580.
- Walfisch, S., Walfisch, Y., Kirilov, E., Linde, N., Mnitentag, H., Agbaria, R., Sharoni, Y., & Levy, J. (2007). Tomato lycopene extract supplementation decreases insulin-like

- growth factor-I levels in colon cancer patients. *European journal of cancer prevention : the official journal of the European Cancer Prevention Organisation (ECP)*, 16(4), 298–303.
- Wang J. Q., Wang, S. S., Chu, P., Ma, X., Tang, Z. Y. (2021). Investigating into anti-cancer potential of lycopene: Molecular targets. *Biomedicine & Pharmacotherapy*, 138, 111546.
- Wang, Y., Zhong, J., Bai, J., Tong, R., An, F., Jiao, P. et al. (2018). The Application of Natural Products in Cancer Therapy by Targeting Apoptosis Pathways. *Current Drug Metabolism*, 19:739–49
- White, W. S., Zhou, Y., Crane, A., Dixon, P., Quad, F., Flendrig, L.M. (2017). Modeling the dose effects of soybean oil in salad dressing on carotenoid and fat-soluble vitamin bioavailability in salad vegetables. *American Journal of Clinical Nutrition*, 106, 1041–1051.
- Xiuping, L., Cuicui, M., Xiaojia, Yan, X., Liu, F. (2019). Advances in research on bioactivity, metabolism, stability and delivery systems of lycopene. *Trends in Food Science & Technology*, 93, 185-196.
- Xu, D.P., Li, Y., Meng, X., Zhou, T., Zhou, Y., Zheng, J., Zhang, J. J., Li, H. B. (2017). Natural Antioxidants in Foods and Medicinal Plants: Extraction, Assessment and Resources. *International Journal of Molecular Sciences*, 5;18(1):96.
- Yin Y., Zheng Z., Jiang Z. (2019). Effects of lycopene on metabolism of glycolipid in type 2 diabetic rats. *Biomed. Pharmacotherapy*, 109:2070–2077.
- Yucel, Y., Oguz, E., Kocarlan, S., Tatli, F., Gozeneli, O., Seker, A., Sezen, H., Buyukaslan, H., Aktumen, A., Ozgonul, A. (2017). The effects of lycopene on methotrexate-induced liver injury in rats. *Bratislavske lekarske listy*, 118(4), 212–216.

- Zeng, Y. C., Peng, L. S., Zou, L., Huang, S.-F., Xie, Y., Mu, G.-P., Zeng, X. H., Zhou, X. L., Zeng, Y. C. (2017) Protective effect and mechanism of lycopene on endothelial progenitor cells (EPCs) from type 2 diabetes mellitus rats. *Biomedicine and Pharmacotherapy*, 92, 86–94.
- Zhang, Q. W., Lin, L. G., Ye, W. C. (2018). Techniques for extraction and isolation of natural products: A comprehensive review. *Chinese medicine*, 13(1):1-26
- Zhou, S., Zhang, R., Bi, T., Lu, Y., Jiang, L. (2016). Inhibitory effect of lycopene against the growth of human gastric cancer cells. *The African Journal of Traditional, Complementary and Alternative Medicines*, 13, 184–190.
- Zujko, M. E., Witkowska, A. M., Waskiewicz, A., Mironczuk-Chodakowska, I. (2015) Dietary antioxidant and flavonoid intakes are reduced in the elderly. *Oxidative Medicine and Cellular Longevity*, 2015:843173.
- Zujko, M.E., Witkowska, A.M., Waskiewicz, A., Sygnowska, E. (2012). Estimation of dietary intake and patterns of polyphenol consumption in Polish adult population. *Advances in Medical Sciences*, 57(2):375–84.
- Zuorro, A. (2020). Enhanced Lycopene Extraction from Tomato Peels by Optimized Mixed Polarity Solvent Mixtures. *Molecules*, 25. 2038.

**Chapter 2**

**Enzyme mediated lycopene extraction from tomato peel  
and evaluation of antioxidant potency against oxidative  
stress in L6 myoblast**

## 2.1 Introduction

Epidemiological studies suggest that lycopene (LYC) provides protection against free radical induced chronic diseased conditions including cancer and supplementation of diets rich in LYC is reported to reduce the risk of many chronic disease conditions (Joshi et al., 2020; Bandeira et al., 2017). LYC is a major carotenoid found in tomatoes and tomato products. The industrial waste after tomato processing leads to the formation of waste/tomato by-products such as seeds, skin, and pulp residues, consist of high level of LYC. Tomato processing industries generate a huge amount of residue in the form of peel, seeds, pomace, etc (Ravindran et al., 2016; Torres-Valenzuela et al., 2020). Studies have reported that tomato peel contains high levels of LYC, about five times more than that of pulp and seeds, which denotes more than 85% of the entire carotenoids. Despite of these advantages, carotenoids recovery from this material is not simple, as revealed by the low yields achievable with conventional solvent extraction procedures (Nayak et al., 2019) mainly due to the interference of matrix, which hinders solvent penetration and the possible degradation of the carotenoids during recovery. Enzymes that catalyze the cleavage of cell-wall polysaccharides have been effectively utilized to help the release of vegetable oils (Jablonsky et al., 2018), non-volatile aroma precursors (Sowbhagya et al., 2010), phenols (Heemann et al., 2019) and carotenoids (Popescu et al., 2022) from the plant materials. The food-grade enzymes with, pectinolytic, cellulolytic, and hemi cellulolytic activities were capable of considerably enhancing LYC recovery from tomato skins (Abdullah et al., 2019). Based on the previous reports that enzyme pretreatment improves the extraction of active ingredients (mainly carotenoids) from tomato peel, CSIR-NIIST has optimized a process for the enzyme assisted extraction of LYC rich oleoresin (types of enzyme, incubation time, temperature, etc) from tomato peel, as a part of network project entitled 'Bioprocessing of botanicals for active ingredient isolation-enzymatic route' (CSC 133), Cellulase (20 U/g),



and pectinase (30 U/g), at 50 °C for 60 min under dark was found to yield an oleoresin enriched with maximum LYC (ETE) compared to that of the extract without enzyme treatment (CTE). Further, to understand the beneficial role of ETE as an antioxidant in protecting DNA damage and mitochondrial membrane potential from ROS induced by H<sub>2</sub>O<sub>2</sub> in L6 muscle cells, preliminary studies were carried out which forms the subject matter under **chapter 2**.

## 2.2 Objective

To determine the LYC content in the tomato peel extract obtained by enzyme assisted extraction and to investigate the antioxidant potential of LYC-rich tomato peel extract against stress-induced L6 myoblast cells.

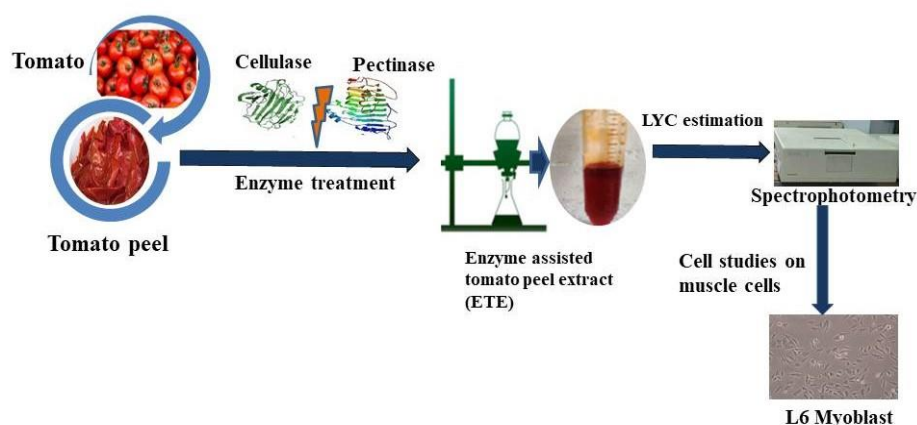


Fig 2.1: Outline of Chapter 2

## 2.3 Materials and methods

### 2.3.1. Chemicals and Reagents

Cellulase (EC 3.2.1.4) and pectinase (EC 3.2.1.15) enzymes were procured from Sigma-Aldrich (Bangalore, India), both derived from a selected strain of *Aspergillus niger*. The claimed activity of cellulase is 1.08 U/mg where, one unit will liberate 1.0  $\mu$ M of glucose from cellulose in 1 h at pH 5.0 at 37 °C. The claimed activity of pectinase is 1.02 U/mg where, one unit will liberate 1.0  $\mu$ M of galacturonic acid from poly- galacturonic acid per h at pH 4.0 at 25 °C.

Folin–Ciocalteu reagent, Sodium carbonate, 2,2-diphenyl-1-picrylhydrazyl (DPPH), Ethylene diamine tetraacetic acid (EDTA), Hydrogen peroxide (H<sub>2</sub>O<sub>2</sub>), Triton X, Sodium chloride (NaCl), Tris- HCl, perchloric acid, potassium hydroxide (KOH) were obtained from MERCK. Gallic acid, Dulbecco's Modified Eagle's Medium(DMEM), Dimethyl sulfoxide (DMSO), 2,7-Dichlorodihydrofluorescein diacetate (DCFH-DA), Fetal Bovine Serum (FBS), Ethidium bromide, 1Kb DNA ladder, Glycerol, Hoechst33342, Adenosine Triphosphate (ATP), 3-(4,5-dimethylthiazol-2-yl)-2,5 diphenyltetrazolium bromide (MTT), Bromophenol Blue, Rhodamine123 dye, Agarose for electrophoresis and Mammalian genomic DNA isolation kit were procured from Sigma- Aldrich Chemicals (St Louis, MO, USA). DNA/RNA Oxidative damage ELISA kit was purchased from Cayman chemicals (MI-USA). Trypsin-EDTA and Antibiotic-antimycotic mix were purchased from Gibco Invitrogen (Carlsbad, CA, USA). All the chemicals used were of high quality analytical grade chemicals.

### 2.3.2 Experimental Design

The experimental protocol for the study is given in Fig 2.2

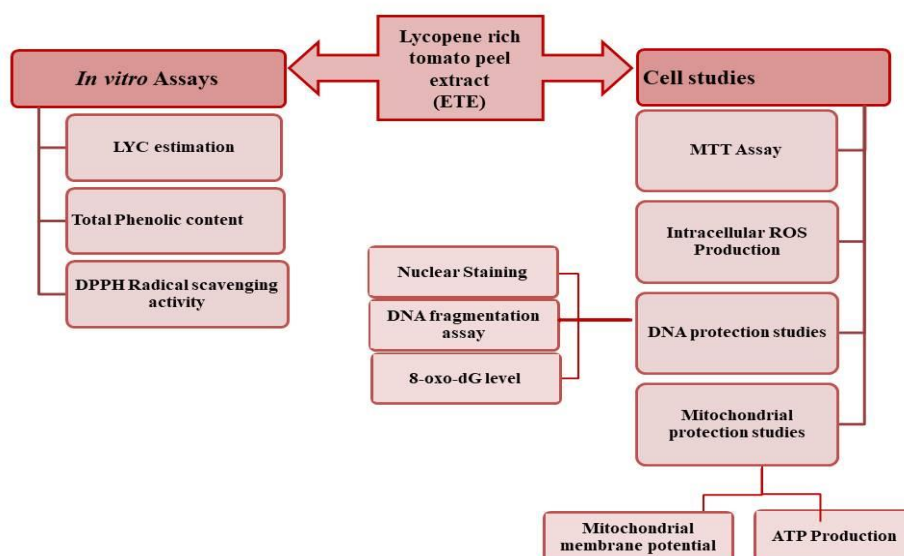


Fig 2.2 Experimental methods used for the study.

### 2.3.3 Sample preparation

#### 2.3.3.1. Enzymatically assisted LYC extraction

Tomatoes (*Solanum lycopersicum* L.) were purchased from local market of Trivandrum district in Kerala, India. After removal of damaged parts and washing, whole tomato fruits were immersed in warm water (80 °C) for 2 min. Then they were cooled under tap water, hand peeled and the peel was freeze dried (VirTis genesis 25EL, USA). It was then extracted using the following pre-optimized conditions

**Enzymes pretreatment** – Cellulase (20 U/g), pectinase (30 U/g), at 50 °C for 60 min under dark.

**Extraction of LYC** – After the pretreatment with enzymes, the LYC was extracted with petroleum ether, thrice, in a separating funnel for 20-25 min each time and allowed to stand for 10 min. Upper nonpolar phase which contains LYC were pooled together and filtered. It

is made up to known volume and analysed for LYC content spectrophotometrically (Fig 2.3).

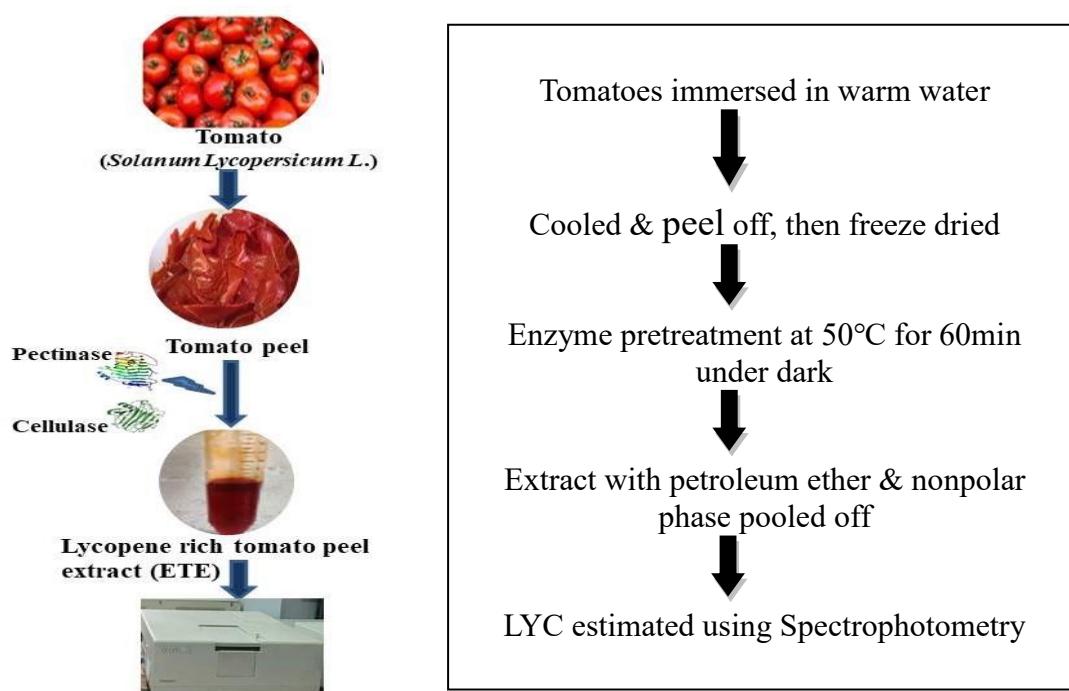


Fig 2.3: Schematic representation of enzyme assisted LYC extraction from tomato peel  
 A control without enzyme was also carried out simultaneously (CTE). The amount of LYC was calculated using the specific extinction coefficient ( $E = 3450$  in petroleum ether) (Ranganna, 1997).

$$\text{Lycopene (mg)} = \frac{(A \times \text{dil. factor} \times \text{mL} \times 10)}{E^{1\%1 \text{ cm}}}$$

where A - absorbance of the solution in 1 cm cuvette, dil - dilution factor, mL - total mL of the sample and  $E^{1\%1 \text{ cm}}$ , specific extinction coefficient for LYC in petroleum ether.

The solvent was then evaporated off to get the oleoresin (CTE and ETE respectively for control and enzyme assisted extracts) which is used for further biological studies.

### 2.3.4 Determination of total phenol content

Total phenol content (TPC) in tomato peel extracts CTE and ETE (Enzyme assisted tomato peel extract) were measured by the Folin–Ciocalteu method (Singleton & Rossi, 1965; Hudz

et al., 2019). Briefly, 20 µL of samples were mixed with Folin–Ciocalteu reagent followed by the addition of sodium carbonate (7.5%, w/v) and mixed, allowed to stand for 90 min at room temperature (RT) and absorbance was measured against the blank at 750 nm using multimode reader (Synergy Biotek). Total phenol content of the extract was expressed in terms of milligrams of gallic acid equivalents per gram sample (mg GAE/g).

### **2.3.5. DPPH Radical scavenging assay**

The antioxidant effect of tomato peel extract CTE and ETE was measured by the DPPH radical scavenging assay as reported earlier (Yen & Duh, 1994) with slight modifications. DPPH assay constitutes a rapid and low cost method, which has commonly been used for the estimation of the antioxidative potential of diverse natural products. The extracts of different concentrations in methanol were mixed with 0.2 mM methanolic solution of DPPH. The mixture was shaken vigorously and kept in dark at RT for 30 min, and the absorbance was then measured by spectrophotometer at 517 nm against the corresponding control.

$$\% \text{ Inhibition} = \frac{\text{Absorbance of Control} - \text{Absorbance of Sample}}{\text{Absorbance of Control}} \times 100$$

### **2.3.6. Cell culture and treatment conditions**

Skeletal muscle cell has been reported as *in vitro* model to study the effect of ROS production on the biomolecular system and the cellular machinery (Maurya et al., 2015, Dhanya et al., 2015). Therefore rat skeletal muscle cells, L6 myoblast, were used in the present study. L6 myoblast cells were acquired from NCCS, Pune and the cells were cultured in Dulbecco's modified Eagle's medium (DMEM) supplemented with (10%) fetal bovine serum and (0.5%) Antibiotic-antimycotic in a humidified atmosphere containing 5% CO<sub>2</sub> at 37 °C. Petroleum ether used for extraction procedure was removed by vacuum and

reconstituted in 50% DMSO. Prior to the cell based assays, it was further diluted in such a way that the absolute concentration of DMSO was less than 0.1%. The cells were grown at density of  $1 \times 10^4$  cells/well on 96-well black plate (Becton Dickinson Bioscience) and 12-well plates for staining and Fluoresce Activated Cell Sorter (FACS) analysis.

### **2.3.7. Cell viability assay**

Cellular toxicity of the extract and  $H_2O_2$  were standardized based on the concentration using MTT assay (Mosmann, 1983). L6 myoblast cells were treated with various concentrations of ETE (30- 150  $\mu\text{g}/\text{mL}$ ) and  $H_2O_2$  (10- 500  $\mu\text{M}$ ) for 24 h and 20 min respectively. After treatment, cells were incubated with MTT reagent (0.5 g/L) for 4 h. The principle behind the study depicts MTT, yellow dye converted to a purple colored formazan crystal by mitochondrial dehydrogenase enzyme, which is active only in live cells. The developed formazan crystals were dissolved in DMSO and the absorbance was read at 570 nm using multimode reader (Synergy 4 Biotek multiplate reader, USA).

For evaluating how ETE protect L6 cells against  $H_2O_2$  induced OS, the cells were first treated with different concentrations of tomato peel extract, ETE (20 -100  $\mu\text{g}/\text{mL}$ ) and incubated at 37 °C for 24 h followed by treatment with 100  $\mu\text{M}$   $H_2O_2$  for 20 min. Cells without treatment were used as negative control and 100  $\mu\text{M}$   $H_2O_2$  alone treated cell were used as positive control. After treatment, cell viability was determined as above. Each assay was carried out three times, and the results were expressed as the mean  $\pm$  SD. The percentage viability was calculated as

$$\% \text{ cell viability} = \frac{\textit{The absorbance of test}}{\textit{The absorbance of control}} \times 100$$

### **2.3.8 Intracellular reactive oxygen species (ROS) levels**

The influence of ETE on ROS levels was analysed by using DCFH-DA staining (Cathcart, 1983). Different subtoxic concentrations of ETE were pre incubated in L6 cells, followed by H<sub>2</sub>O<sub>2</sub>. Cells were washed and incubated with DCFH-DA for 20 min and imaged with Fluorescent microscope (Pathway 855, BD Bioscience, USA) equipped with filters in the range, excitation, 490 nm; and emission, 525 nm. The fluorescent intensity was analyzed by BD Image Data Explorer software. ROS production in cells was also quantified by measuring the intracellular DCF fluorescent intensity by flow cytometry (BD FACS Aria II, BD Bioscience, USA).

### **2.3.9 DNA Protection studies**

#### **2.3.9.1 Nuclear Staining with Hoechst 33342**

The nuclear morphology of the cells was observed using the cell-permeable DNA dye, Hoechst 33342 for checking the presence of chromatin condensation in nucleus (Hickman, 1992). After incubation with ETE and H<sub>2</sub>O<sub>2</sub>, L6 cells were stained with Hoechst 33342 (10 µg/mL) for 10 min at 37 °C followed by washing with PBS for 3 times and the nuclei were observed under a confocal fluorescence microscope (Pathway 855, BD Bioscience, USA) to examine the degree of nuclear condensation.

#### **2.3.9.2 DNA Fragmentation assay**

DNA fragmentation assay was carried out by gel electrophoresis (Chandna, 2004) for determining the genomic DNA protection ability of ETE against H<sub>2</sub>O<sub>2</sub> induced oxidative stress. After the treatment with ETE followed by H<sub>2</sub>O<sub>2</sub> as described earlier, the cells were pelleted. It was then lysed in 0.5 mL lysis buffer (10 mM Tris-HCl, pH 8.0, 20 mM EDTA, and 0.2% Triton X-100) and incubated at 37 °C for 60 min. After centrifugation, chromosomal DNA in the supernatant was extracted with ethanol and 4M NaCl at -20 °C for overnight. DNA was pelleted by centrifugation and re-suspended in Tris-EDTA buffer. It

was then subjected to electrophoresis in 1.8% agarose gel (60V), stained with ethidium bromide, and visualized under UV light.

### **2.3.9.3 Estimation of 8-oxo-2'-deoxyguanosine (8-oxo-dG)**

The effect of ETE on oxidative DNA damage induced by 100  $\mu\text{M}$   $\text{H}_2\text{O}_2$  was measured using 8-oxo-dG assay. The cells were pre incubated with different subtoxic concentrations of ETE followed by exposure to  $\text{H}_2\text{O}_2$ . Cells were trypsinized and DNA was isolated by using mammalian genomic DNA isolation kit. The level of 8-oxo-dG, marker of oxidative damage of DNA in the cell, was determined by DNA/RNA Oxidative damage ELISA kit (Gan et al., 2012). The estimation of 8-oxo-dG generated in the samples was carried out spectrophotometrically at 410 nm.

### **2.3.10. Mitochondrial protection studies**

#### **2.3.10.1. Mitochondrial membrane potential ( $\Delta\Psi_m$ )**

A major response to oxidative stress is loss of mitochondrial membrane potential (MMP) and dysfunction. MMP was investigated using Rhodamine123, a fluorescent dye that accumulates within the mitochondria in a membrane potential depending way (Zhang & Wang, 2008). Protection of mitochondrial membrane potential requires a proton motive force which is generated through respiration by ATP hydrolysis via ATP synthase. Following ETE treatment and stress induction, the cells were directly incubated with 2  $\mu\text{M}$  Rhodamine 123 for 25 min in the dark, followed by washed with PBS, then fluorescence was detected by FACS Aria II (BD Bioscience, USA). A reduction in green rhodamine 123 fluorescence indicates reduced mitochondrial membrane potential.

#### **2.3.10.2. Adenosine Triphosphate (ATP) production by HPLC analysis**

Levels of ATP, an indicator of the energy state in living cells, are dependent mainly on mitochondrial function. In L6 cells, mitochondrial protection activity of ETE against oxidative stress was determined by measuring ATP levels using HPLC method (Liu et



al.,2006). After treatment, the cells were trypsinized and centrifuged at  $800\times g$  for 3 min and the pellets were suspended in 4% perchloric acid on ice for 30 min. The pH of the lysates was adjusted between 6 and 8 with 2 M KOH. Precipitated salt was separated from the liquid phase by centrifugation at  $13,000\times g$  for 10 min at  $4^{\circ}\text{C}$ . ATP was quantified on a Prominence HPLC system (Shimadzu, Japan) containing LC-20 AD system controller, Phenomenex Gemini C18 column ( $250 \times 4.6$  mm, 5  $\mu\text{m}$ ), a column oven (CTO-20A), a Rheodyne injector (USA) with a loop of 20  $\mu\text{L}$  volume and a diode array detector (SPD-M20A). A buffer 20 mM  $\text{KH}_2\text{PO}_4$  and 3.5 mM  $\text{K}_2\text{HPO}_4 \cdot 3\text{H}_2\text{O}$  (pH 6.1) was used as the mobile phase. The flow rate was 1.0 mL/min, the injection volume was 20  $\mu\text{L}$  and column was at RT. The fractions were monitored at 259 nm. Sample peaks were identified by comparing with retention times of standard peaks. LC Lab Solutions software was used for data acquisition and analysis.

### **2.3.11. Statistical analysis.**

All the tests were repeated three times and results were expressed as means  $\pm$  standard deviations of the control and treated cells. The obtained results were subjected to one-way ANOVA and the significance  $P \leq 0.05$  was calculated by Duncan's multiple range test, using SPSS.

## **2.4 Results and Discussion**

Increased level of ROS leads to stress induced cellular damage of the biomolecules like proteins, DNA, and lipids, which causes many complications such as cancers, cardiovascular diseases (CVD), and neurological diseases. Epidemiological studies showed that people consuming more of antioxidant-rich fruits and vegetables are in better health thanks to increased mitigation of ROS. Studies have shown that antioxidants like flavonoids, polyphenolics, and vitamins from plant sources play vital role in evading cells and biomolecules from oxidative stress (Costa-Rodrigues et al., 2018; Mensch and Zierz, 2020;

Imran et al., 2020). Current study investigated free radical scavenging activity of tomato peel extract and its ability to protect cells from oxidative damage induced by H<sub>2</sub>O<sub>2</sub>, in L6 cells.

#### **2.4.1 Estimation of LYC content in the ETE**

The LYC content of CTE and ETE (tomato oleoresin) were  $86.99 \pm 0.404$  and  $677.298 \pm 0.418$  mg /kg dry weight of tomato peel respectively. From the data, it can be seen that the enzyme assisted extraction improved the extraction of LYC from tomato peel significantly. This may be due to the fact that on pretreatment of tomato peel with enzymes, cell wall components were degraded and which may assist in the release of intracellular contents. Pre-treatment of tomato peel with cellulase and pectinase under optimized conditions has been reported to increase the LYC yield in extraction (Choudhari & Ananthanarayan, 2007). Enzymatic pre-treatment has also reported to improve the recovery of total LYC from tomato paste (Popescu et al., 2022; Zuorro et al., 2011).

#### **2.4.2. The total phenolic content**

Total phenolic content (TPC) was as measured by the Folin-Ciocalteu method. TPC of the ETE was found to be  $235 \pm 0.9221$  and that of CTE was found to be  $208 \pm 0.9871$  mg GAE/g. A compound has been attributed to its antioxidant activity by various mechanisms such as prevention of binding of transition metal ion catalysts, decomposition of peroxides, reductive capacity and radical scavenging ability. Phenols are very important plant constituents due to their free radicals scavenging ability by virtue of its hydroxyl groups (Saheli et al., 2020). Several studies showed good correlation between the phenols and antioxidant activity (Gulcin, 2020). Tomato peel contains bioactives with useful effects for human health such as rutin, naringenin, lycopene and quercetin (Gonzalez et al., 2011). Major favourable actions accepted to LYC are that it quenches singlet oxygen, traps

peroxyl radicals, inhibits oxidative DNA damage, inhibits peroxidation and stimulates gap junction communication (Caseiro et al., 2020).

### **2.4.3 Scavenging effect on DPPH radicals**

DPPH radical scavenging model is a generally used method to assess free radical scavenging activity. The degree of discoloration indicates the scavenging potential of the antioxidant extract, which is due to the hydrogen donating ability (Jing et al., 2012). ETE showed a good scavenging activity of IC<sub>50</sub> value  $72.2 \pm 0.9931$   $\mu\text{g/mL}$  and for control it was  $88.58 \pm 0.8765$   $\mu\text{g/mL}$ , whereas the IC<sub>50</sub> of standard gallic acid was  $3.2 \pm 1.09$   $\mu\text{g/mL}$ . DPPH antioxidant activity of tomato peel extracts increased with the increase in concentration of extracts. These results point out that tomato peel has a noticeable effect on free radicals scavenging activity. ETE is found to be a rich source LYC as well as phenolic compounds which are good natural antioxidants (Pirayesh & Habib, 2015). Therefore the obtained activity of the extract may be attributed to the LYC as well as the phenolic content. The results indicated that the enzyme assisted tomato peel extract has a noticeable effect on scavenging free radicals.

Based on the above assays, it was found that ETE contain significantly higher content of LYC, phenolic compounds and free radical scavenging capacity, ETE was chosen for further studies.

### **2.4.4 Cell viability by MTT assay**

The cytotoxicity of ETE was examined in L6 myoblasts by MTT assay. In order to find out the working concentrations of ETE, cells were treated with different concentrations of ETE and cell viability was determined. It can be seen that (Fig 2.4a) the viability decreased significantly in a dose dependant manner ( $P \leq 0.05$ ). A concentration of  $100\mu\text{g/mL}$  of ETE caused cell viability to decrease by about 18.3 %. Therefore, for the further studies, the cells were exposed to the subtoxic concentration of  $100 \mu\text{g/mL}$  of ETE and below. The

preliminary study on the toxic effect of extract ETE demonstrated by MTT assay did not show harmful effects on L6 cells upto a concentration of 100  $\mu\text{g/mL}$ .

For inducing oxidative stress,  $\text{H}_2\text{O}_2$  has often been reported as a model in different cell types (Ransy et al., 2020; Sun et al., 2013).

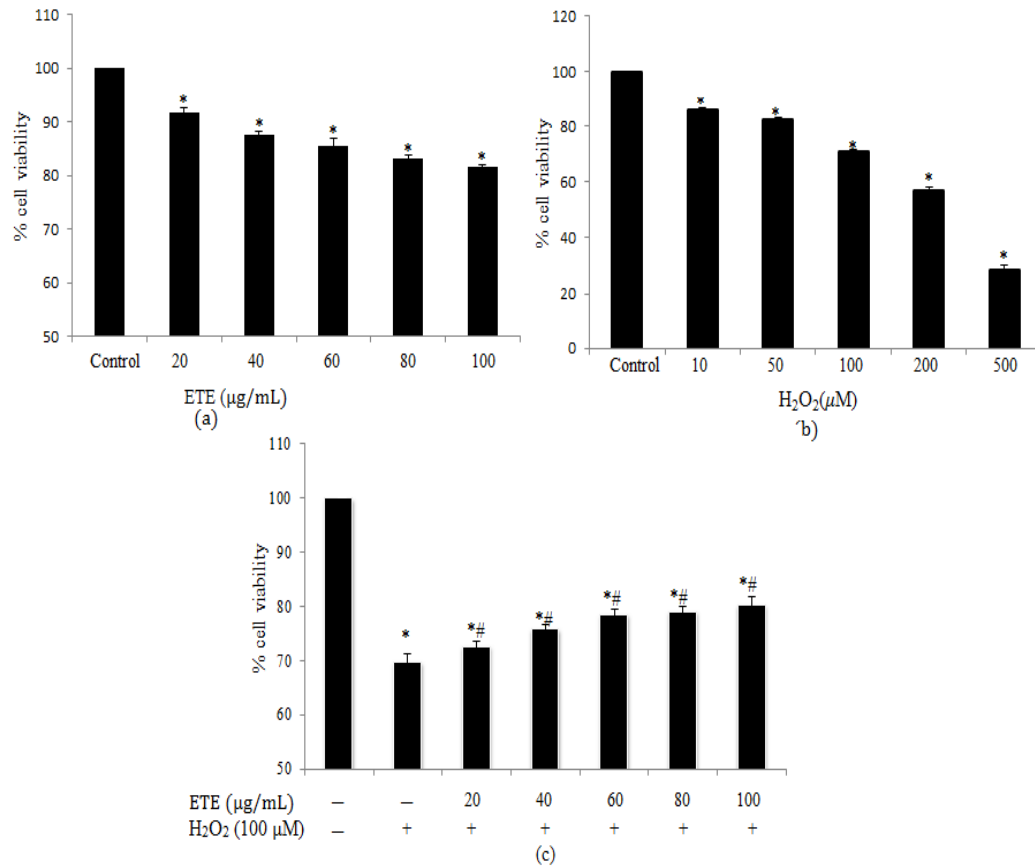


Fig 2.4: The Effect of ETE,  $\text{H}_2\text{O}_2$  and pretreatment of cells with ETE before exposure with  $\text{H}_2\text{O}_2$ , on viability of L6 cells by MTT assay. (a) Cytotoxicity in L6 cells at different concentration of ETE (b) Cytotoxicity of L6 cells following different concentrations of  $\text{H}_2\text{O}_2$  exposure (c) The effect of ETE on L6 cell viability against 100  $\mu\text{M}$   $\text{H}_2\text{O}_2$ . The results are expressed as percentage of control, and each value represents the mean  $\pm$  SD. The annotation \* indicates a  $P \leq 0.05$  versus control group. The annotation # indicates a  $P \leq 0.05$  versus  $\text{H}_2\text{O}_2$  group

In order to determine the sub toxic concentrations of H<sub>2</sub>O<sub>2</sub>, L6 cells were treated with H<sub>2</sub>O<sub>2</sub> (10 to 500 μM), for 20 min and assayed by MTT. As shown in the Fig 2.4b, it was found that different concentrations of H<sub>2</sub>O<sub>2</sub> significantly reduced cell viability after treatment ( $P \leq 0.05$ ) and 100 μM H<sub>2</sub>O<sub>2</sub> caused cell viability decrease by about 30%. Therefore the cells were exposed to a concentration of 100 μM H<sub>2</sub>O<sub>2</sub> for inducing oxidative stress for further assays. In order to find out the protective effect of ETE against H<sub>2</sub>O<sub>2</sub> induced toxicity, the cells (L6) were initially treated with subtoxic levels of ETE (20 to 100 μg/ml) for 24 h followed by H<sub>2</sub>O<sub>2</sub> at a concentration of 100 μM for 20 min. Subsequently we found that the extract protected cells from oxidative stress effectively in a dose-dependent manner ( $P \leq 0.05$ ) (Fig 2.4c). The data indicated that pre-treatment with ETE efficiently protected cells from H<sub>2</sub>O<sub>2</sub> induced toxicity. The study revealed that the ETE pre-treatment enhanced cell viability as compared to H<sub>2</sub>O<sub>2</sub> treated cells. These results suggest that treatment with H<sub>2</sub>O<sub>2</sub> results in cell death, which was prevented when the cells were pre-treated with ETE before H<sub>2</sub>O<sub>2</sub> treatment.

#### **2.4.5 ETE Inhibits H<sub>2</sub>O<sub>2</sub>-Induced Reactive Oxygen Species Production in L6 Cells.**

It is reported that OS induced by ROS plays an important role in cellular damage which leads to secondary injury to the cells (Sharifi-Rad et al., 2020; Tsatsakis et al., 2019). The production of ROS in the cells leads to depletion in the antioxidant mechanism in the body. Dietary supplementation of antioxidants can improve the antioxidant status of the body (Rowles et al., 2018; Liu et al., 2015). The free radical scavenging activity of the extracts and their potential against intracellular ROS was evaluated using H<sub>2</sub>DCFDA by fluorescent imaging and flow cytometric analysis. The fluorescence intensity of the images was visualized by BD Image Data Explorer software and has been illustrated in Fig 2.5a. The data indicated that untreated cells had little basal intracellular ROS. However, incubation of

cells with 100  $\mu\text{M}$   $\text{H}_2\text{O}_2$  caused a significant increase in ROS level as compared to the control.

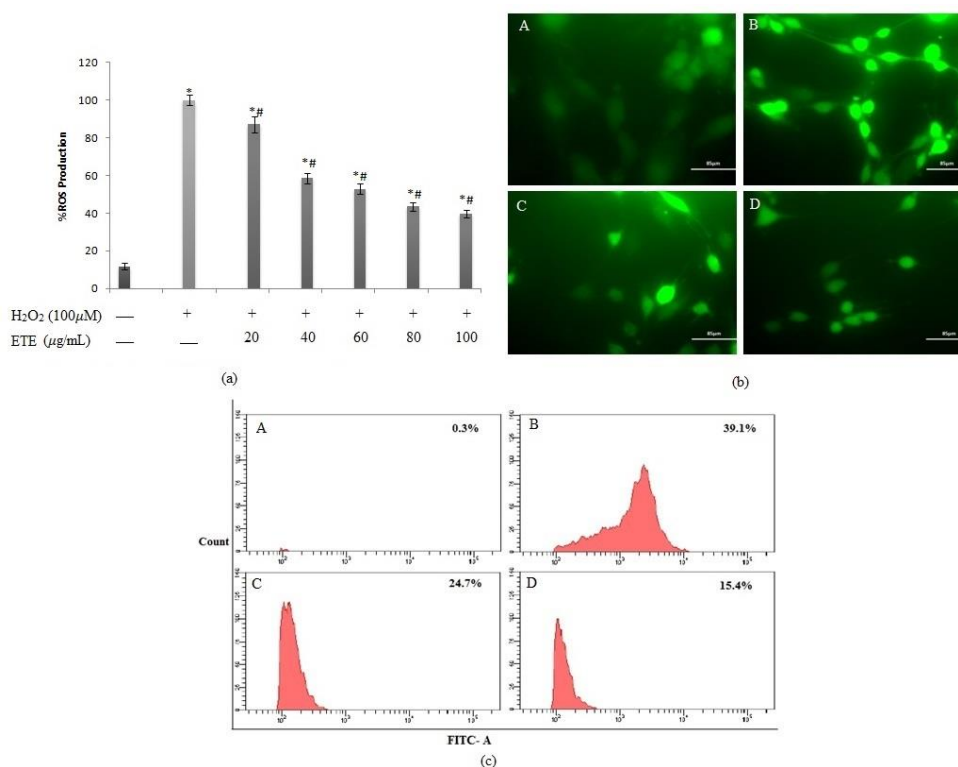


Fig 2.5: Measurement of ROS production in L6 cells. After treatment, the cells were stained with H<sub>2</sub>-DCFDA dye and then analyzed by fluorescence imaging. Fig (a) fluorescent intensity measurement indicate % ROS production; Fig (b) represent A-control, B-100  $\mu\text{M}$   $\text{H}_2\text{O}_2$ , C- 50  $\mu\text{g}/\text{mL}$  ETE +100  $\mu\text{M}$   $\text{H}_2\text{O}_2$ , D-100  $\mu\text{g}/\text{mL}$  ETE+100  $\mu\text{M}$   $\text{H}_2\text{O}_2$ . Fig(c) Represent flow cytometric analysis of ROS production in L6 cells by plotting cell count against FITC. Each value represents mean  $\pm$  SD from triplicate measurements of three different experiments. Significance levels between different groups were determined by using one way ANOVA, \* $P \leq 0.05$  versus Control; # $P \leq 0.05$  versus  $\text{H}_2\text{O}_2$ .

The ROS concentration was found to decrease significantly on preincubation with ETE (100  $\mu\text{g}/\text{mL}$ ) ( $P \leq 0.05$ ) as shown in Fig 2.5b. The intracellular ROS production was also

quantified by measuring the fluorescence of DCF by flow cytometry. The intensity of untreated and H<sub>2</sub>O<sub>2</sub> treated cells were 0.30± 0.081% and 39.1± 0.043% respectively. The fluorescence intensity of ETE treated group was 24.7 ± 0.121% and 15.4 ± 0.387% respectively for 50 µg/mL and 100 µg/mL of ETE, which was significantly lower than H<sub>2</sub>O<sub>2</sub> treated cells (Fig 2.5c).

The fluorescence intensity of the L6 control cells was significantly lower than that of cells with induced oxidative stress using 100 µM H<sub>2</sub>O<sub>2</sub>. Pre-treatment with ETE, could considerably reduce the ROS level when exposed to 100 µM H<sub>2</sub>O<sub>2</sub> exposure as indicated by reduction in fluorescence intensities than the positive cells. These results were further confirmed by quantifying the fluorescence intensity using flow cytometric analysis. The fluorescent intensity was reduced significantly on ETE treatment prior to H<sub>2</sub>O<sub>2</sub>. Overall, the cells treated with the extracts showed a decrease in the fluorescence intensity as compared with the 100µM H<sub>2</sub>O<sub>2</sub> group. It was also observed that cells treated with 100 µg/mL of ETE could reduce the ROS levels significantly as compared to 50 µg/mL, indicating that the extracts acted in a dose dependent manner. The concentration of ROS is directly proportionate to the fluorescence intensity. This activity of ETE may be correlated to the presence of various antioxidant molecules present in the extracts which can scavenge hydrogen peroxide.

#### **2.4.6 ETE protects L6 cells from nuclear damage**

ROS can damage nucleic acids by altering purine and pyrimidine bases and causing DNA fragmentation (Upadhyayula et al., 2019). DNA damage can lead to mutations, which are responsible for related diseases such as cancer, coronary heart disease, arteriosclerosis and inflammatory disorders. Dietary antioxidants have been reported to possess potential inhibitory effects against H<sub>2</sub>O<sub>2</sub>-mediated DNA damage and harmful free radicals. In this

respect we carried out further studies to find out the DNA protective potential of ETE against oxidative stress. Chromatin condensation and morphological changes in the cells (control, H<sub>2</sub>O<sub>2</sub> treated and ETE pre-treated) were examined with Hoechst staining under a confocal fluorescence microscope.

It can be seen that the control cells without treatment have intact nucleus whereas H<sub>2</sub>O<sub>2</sub> treatment resulted in increased number of cells with fragmented nucleus (Fig 2.6a). On pre-treatment with ETE at different concentrations, 50 µg/mL and 100 µg/mL, shows a reduction in nuclear fragmentation, in a dose dependent manner confirming that ETE protect cells from nuclear fragmentation. As can be seen from the Fig 2.6a, the control cells show intact nuclei whereas the cells induced with oxidative stress on treatment with H<sub>2</sub>O<sub>2</sub> exhibited significant chromatin condensation in the cells. DNA protection activity was exhibited by ETE against 100 µM H<sub>2</sub>O<sub>2</sub> induced DNA damage in L6 cells. The severity of H<sub>2</sub>O<sub>2</sub> treatment could be reduced on exposure of cells to ETE at a concentration of 100 µg/mL. However, ETE at 50 µg/mL concentration did not show much protective effect on the cells.

#### **2.4.7 ETE protected H<sub>2</sub>O<sub>2</sub> induced DNA fragmentation in L6 cells**

The protective effect of ETE on DNA was further confirmed using ladder assay where DNA from the cells were isolated and subjected to electrophoresis to check for DNA fragmentation. As shown in the Fig 2.6b, DNA from the untreated control cells were compact suggesting an intact DNA, whereas the treatment with H<sub>2</sub>O<sub>2</sub> causes a significant fragmentation as seen from laddering nature of DNA band. On treatment with ETE, the smearing nature of DNA gets diminished in a dose dependent manner suggesting that pre-incubating L6 cells with ETE effectively protected cells from DNA damage. This result shows that, antioxidants present in extract has the capacity to quench the free radicals generated in the reaction, thereby protecting the DNA from H<sub>2</sub>O<sub>2</sub> induced oxidative damage.



From the Fig 2.6b suggests that ETE at concentration of 100  $\mu\text{g}/\text{mL}$  could protect the DNA from the oxidative damage.

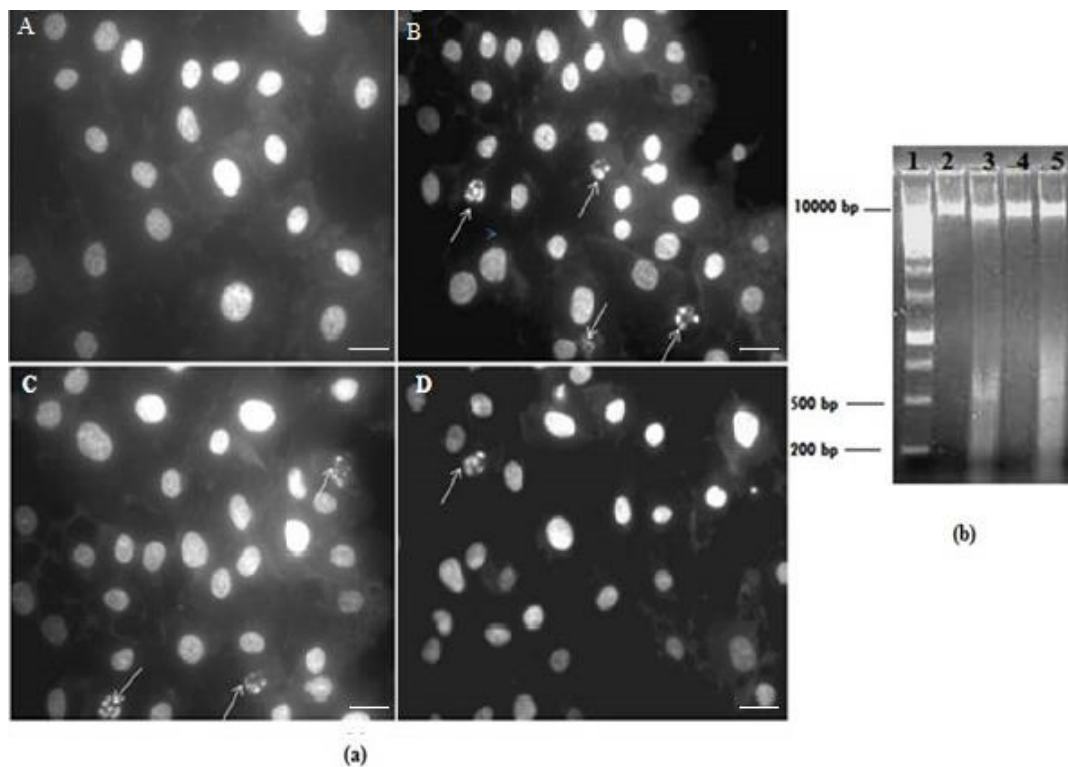


Fig 2.6: (a) Chromatin condensation observed using Hoechst 33342 staining: Figure represents A) control, B) 100  $\mu\text{M}$   $\text{H}_2\text{O}_2$ , C) 50  $\mu\text{g}/\text{mL}$  ETE +100  $\mu\text{M}$   $\text{H}_2\text{O}_2$ , D) 100  $\mu\text{g}/\text{mL}$  ETE +100  $\mu\text{M}$   $\text{H}_2\text{O}_2$  Arrows represent cells with chromatin condensation inside the nucleus.(b) DNA damage was analyzed by DNA Fragmentation assay Lane 1: 1kb DNA ladder, Lane 2 : control, Lane 3: 50  $\mu\text{g}/\text{mL}$  ETE +100  $\mu\text{M}$   $\text{H}_2\text{O}_2$ , Lane 4: 100  $\mu\text{g}/\text{mL}$  ETE +100  $\mu\text{M}$   $\text{H}_2\text{O}_2$  Lane :5 100  $\mu\text{M}$   $\text{H}_2\text{O}_2$ .

The data from Hoechst 33342 staining and ladder assay indicated that incubating cells in the presence of 100  $\mu\text{M}$   $\text{H}_2\text{O}_2$  causes a significant chromatin condensation/ DNA fragmentation, as compared to the control (without any treatment). At the same time, ETE promote genomic stability by preventing double-strand DNA breaks, which is associated with increased ROS production mediated by 100  $\mu\text{M}$   $\text{H}_2\text{O}_2$ . Ion radicals generated during oxidative stress lead to a chain reaction which form DNA adducts and lipid hydroperoxides

results in single and double strand breaks. The obtained results from Hoechst 33342 staining and ladder assay also support the antioxidant property of ETE which protects the nuclear DNA from oxidative stress induced by H<sub>2</sub>O<sub>2</sub>.

#### 2.4.8 ETE protects DNA from oxidative damage

The protective effect of ETE against oxidative damage of DNA was further confirmed by quantifying the oxidative damage indicator, 8-oxo-dG in the DNA. 8-Oxo-dG is the most abundant product of DNA oxidation (Nakabeppu et al., 2007; Bogdanov et al., 2001). Oxidative attack to DNA is of particular interest since DNA modifications can lead to mutations. DNA molecules have unique double helix structure, which undergo oxidation in presence of H<sub>2</sub>O<sub>2</sub>. Therefore the 8-Oxo-dG level in the cells was estimated to assess the DNA protecting effect of ETE against H<sub>2</sub>O<sub>2</sub> treatment.

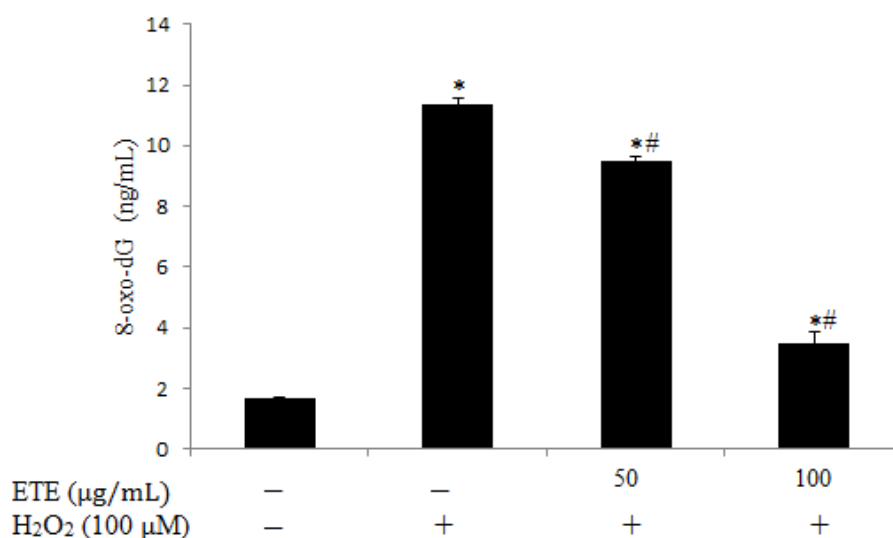


Fig 2.7: The level of 8-oxo-dG in cells. Each value represents the mean  $\pm$  SD of triplicate measurements. Significance levels between different groups were determined by using one way ANOVA, \*P  $\leq$  0.05 versus Control; #P  $\leq$  0.05 versus H<sub>2</sub>O<sub>2</sub>.

As shown in Fig 2.7, 8-oxo-dG level significantly increased on exposure to 100  $\mu$ M H<sub>2</sub>O<sub>2</sub> as compared to the control. However, on pretreatment with ETE prior to treatment with H<sub>2</sub>O<sub>2</sub>, the level of 8-oxo-dG decreased significantly. The oxidation of dsDNA was found to

decrease in a dose dependent manner on ETE pretreatment. Results from the present study indicate that ETE can prevent oxidation of DNA from ROS by scavenging free radicals in a dose dependent manner.

#### **2.4.9 ETE prevented H<sub>2</sub>O<sub>2</sub>-induced reduction of Mitochondrial membrane potential (MMP) in L6 Cells**

Mitochondrial membrane potential,  $\Delta\Psi_m$ , is an essential factor of mitochondrial function used as sign of cell health (Pal et al., 2016). A rapid reduction in the MMP was found when L6 cells were exposed to 100  $\mu\text{M}$  H<sub>2</sub>O<sub>2</sub>, as detected by a reduced fluorescence intensity of Rhodamine123. As compared to control cells, H<sub>2</sub>O<sub>2</sub> treatment decreased the fluorescence intensity in cells from  $79.6 \pm 0.772\%$  to  $37.4 \pm 0.875\%$  represents an increase in MMP loss. Pretreatment with 50  $\mu\text{g/mL}$  and 100  $\mu\text{g/mL}$  of ETE protected the cells against H<sub>2</sub>O<sub>2</sub> by retaining the mitochondrial membrane potential to  $47.1 \pm 0.567\%$  and  $72.6 \pm 0.765\%$  respectively. Fig 2.8a and 2.8b indicating that ETE could prevent H<sub>2</sub>O<sub>2</sub> induced loss of mitochondrial membrane potential significantly ( $p \leq 0.05$ ) in dose dependent way.  $\Delta\Psi_m$  is a sensitive indicator of mitochondrial function. Increasing evidence proposes that the  $\Delta\Psi_m$  assay can be used as a specific test for detecting early mitochondrial damage. Results indicated that 100  $\mu\text{M}$  H<sub>2</sub>O<sub>2</sub> group displayed a substantial decrease in mitochondrial membrane potential as compared to control. Interestingly, tomato peel extract ETE at 100  $\mu\text{g/mL}$  treatment preserved mitochondrial membrane potential, suggesting the inhibition of H<sub>2</sub>O<sub>2</sub> induced mitochondrial damage.

#### **2.4.10 ATP level by HPLC analysis**

ATP production in mitochondria is the main energy source for various metabolic pathways (Campanella et al., 2009). In normally functioning mitochondria,  $\Delta\Psi_m$  is high favoring ATP synthesis by ATP synthase (Jonckheere et al., 2011). When mitochondrial functioning is compromised and  $\Delta\Psi_m$  decreases below a threshold which leads to depletion of ATP

production. ATP production was estimated using HPLC method. From the Fig 2.8c, ATP productions by L6 cells at normal conditions were  $4.4 \pm 1.63 \mu\text{M}$ . On subjecting the cells to  $100 \mu\text{M H}_2\text{O}_2$  it was came down to  $1.5 \pm 0.229 \mu\text{M}$ , showing the inhibition of mitochondrial ATP synthesis. On pretreatment with ETE at  $50 \mu\text{g/mL}$  and  $100 \mu\text{g/mL}$ , ATP level was found to be  $2.32 \pm 0.031 \mu\text{M}$  and  $3.60 \pm 0.05 \mu\text{M}$ . Fig 2.8c suggests that  $100\mu\text{M H}_2\text{O}_2$  treated cells showed a decrease in ATP production, whereas ETE pretreated cells results in increase in ATP Production. Results indicate that mitochondrial capacity to produce ATP in oxidative stress conditions is low and it is reversed in the presence of ETE.

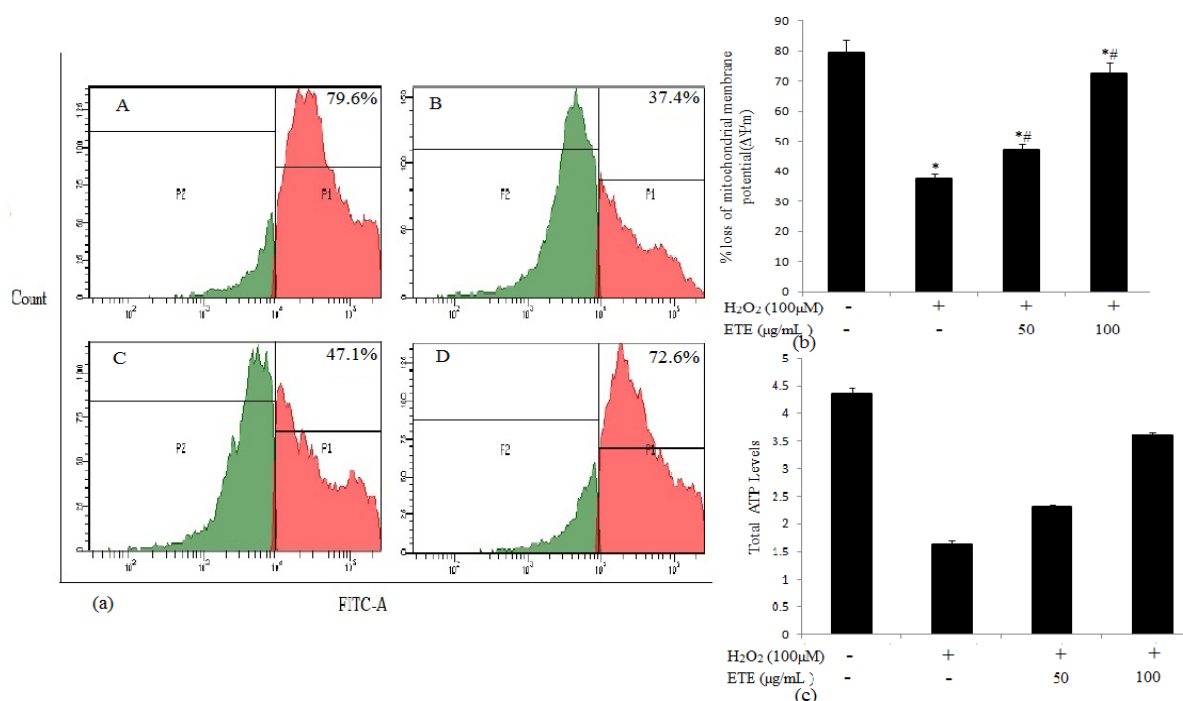


Fig 2.8: Quantification of Mitochondrial membrane potential by Rhodamine 123 staining and ATP level by HPLC method. Rhodamine 123 stained the cells after incubation and quantified by flow cytometer. In Image (a) indicate A- Control, B- $100 \mu\text{M H}_2\text{O}_2$ , C- $50 \mu\text{g/mL ETE} + 100 \mu\text{M H}_2\text{O}_2$ , D- $100 \mu\text{g/mL ETE} + 100 \mu\text{M H}_2\text{O}_2$ . The fluorescence of Rhodamine 123 reduction was attributed to loss in mitochondrial membrane potential. (b) Represents the restoration of mitochondrial membrane potential in percentage on ETE

treatment. (c) ETE treatment increases mitochondrial capacity to produce ATP. Results were expressed as mean  $\pm$  SD. Significance levels between different groups were determined by using one way ANOVA, \*P  $\leq$  0.05 versus Control; #P  $\leq$  0.05 versus H<sub>2</sub>O<sub>2</sub>.

It is reported that the electron-rich conjugated system of the polyene are responsible for the antioxidant activities of the carotenoids, by quenching singlet oxygen, and scavenging radicals to terminate chain reactions. Thus, the present study confirms that, tomato peel extract which is a rich source of carotenoids, especially LYC, acts as a potent antioxidant source which protects the L6 cells from hydrogen peroxide induced oxidative damage.

## **2.5 Conclusion**

In conclusion, enzyme assisted tomato peel extract (ETE) enriched with LYC helps in normalization of ROS, DNA protection and restoring mitochondrial membrane potential. ETE possess significantly higher content of LYC and radical scavenging activity as compared to the extract without enzyme. Tomato peel extracts demonstrated promising antioxidant potential and protected DNA and mitochondria against induced oxidative stress. This study demonstrated the effectiveness of extract, ETE, by counteracting redox imbalance under condition encountered in most of the disease by modulating the components involved in cellular antioxidant status. The results provide significant evidence for antioxidant rich tomato peel extracts to be considered as a dietary supplement with potential activity for the prevention of mitochondrial and DNA damage induced by oxidative stress-mediated pathophysiology. Supplementation of these would also address the free radicals induced complications arising from oxidative stress. At present, considerable amounts of tomato peel are produced in the world and disposed off as waste. As a result, the exploitation of this material as a source of natural antioxidants and LYC, not only provides economic-health benefits but also contribute to environmental protection.

**The key findings are summarized below:**

- Extraction of LYC from tomato peels significantly enhanced by enzyme assisted extraction.
- LYC enriched ETE helps in normalization of ROS, DNA protection, and restoration of mitochondrial membrane potential.
- ETE could counteract redox imbalance under stress induced conditions encountered in most of the diseases.

## 2.6 Graphical Abstract

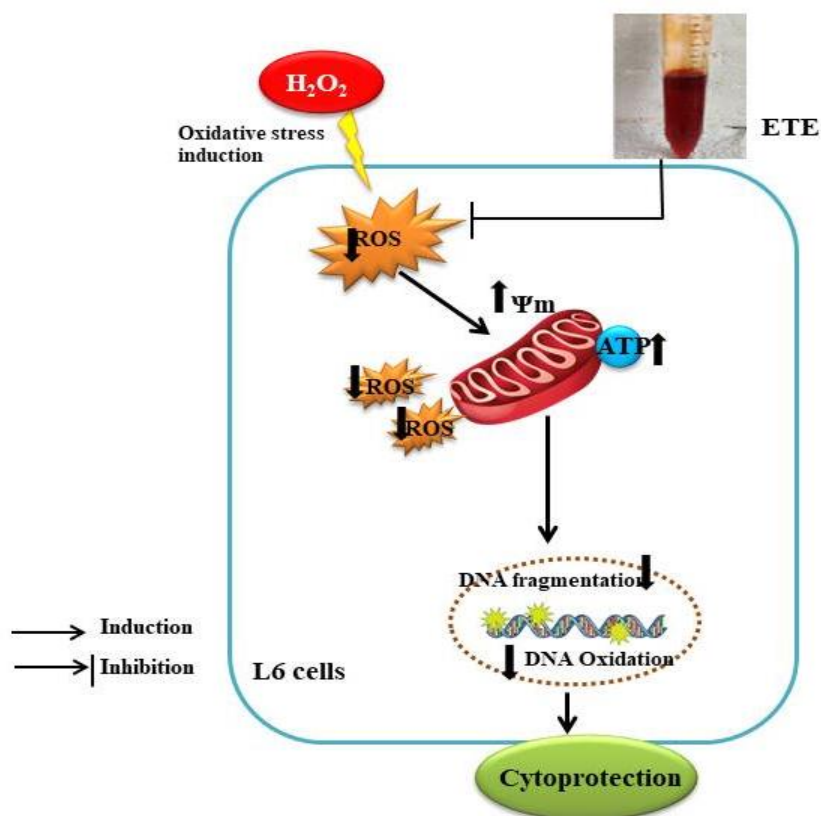


Fig 2.9: Enzyme assisted LYC rich tomato peel extract (ETE) exhibit a promising antioxidant potential by protecting stress induced L6 myoblast cells by inhibiting ROS production and cellular damage.

## 2.7 References

- Abdullah, M. A., Dajah, S., Murad, A., El-Salem, A. M., Khafajah, A. M. (2019). Extraction, Purification, and Characterization of Lycopene from Jordanian Vine Tomato Cultivar, and Study of its Potential Natural Antioxidant Effect on Samen Baladi. *Current Research in Nutrition and Food Science*, 7(2).
- Bandeira, A., da Silva, T. P., de Araujo, G. R., Araujo, C. M., da Silva, R. C., Lima, W. G., Bezerra, F. S., & Costa, D. C. (2017). Lycopene inhibits reactive oxygen species production in SK-Hep-1 cells and attenuates acetaminophen-induced liver injury in C57BL/6 mice. *Chemico-biological interactions*, 263, 7–17.
- Bogdanov, M. B., Andreassen, O. A., Dedeoglu, A., Ferrante, R. J., & Beal, M. F. (2001). Increased oxidative damage to DNA in a transgenic mouse model of Huntington's disease. *Journal of neurochemistry*, 79(6), 1246-1249.
- Campanella, M., Parker, N., Tan, C. H., Hall, A. M., & Duchen, M. R. (2009). IF(1), setting the pace of the F(1)F(o)-ATP synthase. *Trends in Biochemical Science*, 34, 343–350
- Caseiro, M., Ascenso A., Costa, A., Creagh-Flynn, J., Johnson, M., Simões S. (2020). Lycopene in human health. *LWT-Food Science and Technology*, 127, 109323.
- Cathcart, R., Schwieters, E., & Ames, B. N. (1983). Detection of picomole levels of hydroperoxides using a fluorescent dichlorofluorescein assay. *Analytical Biochemistry*, 134, 111–116.
- Chandna, S. (2004). Single-cell gel electrophoresis assay monitors precise kinetics of DNA fragmentation induced during programmed cell death. *Cytometry*, 61A, 127–133.
- Choudhari, S. M., & Ananthanarayan, L. (2007). Enzyme aided extraction of lycopene from tomato tissues. *Food chemistry*, 102(1), 77-81.



- Costa-Rodrigues, J., Pinho, O., Monteiro, P. (2018). Can lycopene be considered an effective protection against cardiovascular disease?. *Food Chemistry* ,245, 1148–1153.
- Dhanya, R., Arun, K.,B., Nisha, V., M. Syama, H., P, Nisha, P.,Santhosh Kumar, T., R., & Jayamurthy, P. (2015). Preconditioning L6 Muscle Cells with Naringin Ameliorates Oxidative Stress and Increases Glucose Uptake. *Plos one*, 10(7): e013242
- Gan, W., Nie, B., Shi, F., Xu, X. M., Qian, J. C., Takagi, Y., Hayakawa, H., Sekiguchi, M., & Cai, J. P. (2012). Age-dependent increases in the oxidative damage of DNA, RNA, and their metabolites in normal and senescence-accelerated mice analyzed by LC-MS/MS: urinary 8-oxoguanosine as a novel biomarker of aging. *Free Radical Biology and Medicine*, 52, 1700-1707.
- Gonzalez, I. N., Valverde, V. G., Alonso, J. G., & Periago, M. G. (2011). Chemical profile, functional and antioxidant properties of tomato peel fiber. *Food Research International*, 44, 1528–1535.
- Gulcin. (2020). Antioxidants and antioxidant methods: an updated overview. *Archives of Toxicology*, 94 (3), 651–715.
- Heemann, H., Winkler, A. C., and Rodrigo, K., Paloma, S., Michele, S., E. (2019). Enzyme-assisted extraction of polyphenols from green yerba mate. *Brazilian Journal of Food Technology*, 22.
- Hickman, J. A. (1992). Apoptosis induced by anticancer drugs. *Cancer and Metastasis Review*, 11, 121–139.
- Hudz, N., Yezerska, O., Shanaida, M., Horcinova, S. V., Wieczorek, P.P. (2019) Application of the Folin-Ciocalteu method to the evaluation of *Salvia sclarea* extracts. *Pharmacia*, 66(4): 209-215.

- Imran, M., Ghorat, F., Ul-Haq, I., Ur-Rehman, H., Aslam, F., Heydari, M., Ali, M., Shariati, Okuskhanova, E., Yessimbekov, Z., Thiruvengadam, M., Hashem, M., & Rebezov, M. (2020). Lycopene as a Natural Antioxidant Used to Prevent Human Health Disorders. *Antioxidants*, 9(8):706.
- Jablonsky, M. S., kulcova, A., Malvis, A., Ima, J. (2018). Extraction of value-added components from food industry based and agro-forest biowastes by deep eutectic solvents. *Journal of Biotechnology*, 282, 46–66.
- Jing, P., Zhao, S. J., Jian, W. J., Qian, B. J., Dong, Y., & Pang, J. (2012). Quantitative studies on structure-DPPH• scavenging activity relationships of food phenolic acids. *Molecules*, 17(11), 12910-12924.
- Jonckheere, A., Smeitink, J., Rodenburg, R. (2011). Mitochondrial ATP synthase: Architecture, function and pathology. *Journal of inherited metabolic disease*, 35. 211-25.
- Joshi, B., Kar, S.K., Yadav, P.K., Yadav, S., Shrestha, L., Bera, T.K. (2020). Therapeutic and medicinal uses of lycopene: A systematic review. *International journal of Researchh in Medical Sciences*, 8, 1195.
- Liu, H., Jiang, Y., Luo, Y., & Jiang, W. (2006). Simple and Rapid Determination of ATP, ADP and AMP Concentrations in Pericarp Tissue of Litchi Fruit by High Performance Liquid Chromatography. *Food Technology and Biotechnology*, 44, 531–534.
- Liu, L. Shao, Z. Zhang, M. Wang, Q. (2015). Regulation of carotenoid metabolism in tomato. *Molecular plant*, 8(1), 28–39.
- Maurya, C. K., Arha, D., Rai, A. K., Kumar, S. K., Pandey, J., Avisetti, D. R., Kalivendi, S. V., Klip, A., & Tamrakar, A. K.(2015). NOD2 activation induces oxidative stress

- contributing to mitochondrial dysfunction and insulin resistance in skeletal muscle cells. *Free Radical Biology and Medicine*, 89, 158–169.
- Mensch, A., Zierz, S. (2020). Cellular Stress in the Pathogenesis of Muscular Disorders- From Cause to Consequence. *International journal of molecular sciences*, 21(16), 5830.
- Mosmann, T. (1983). Rapid colorimetric assay for cellular growth and survival, Application to proliferation and cytotoxicity assays. *Journal of Immunological Methods*, 65, 55–63.
- Nakabeppu, Y., Tsuchimoto, D., Yamaguchi, H., Sakumi, K. (2007) Oxidative damage in nucleic acids and Parkinson's disease. *Journal of Neuroscience*, 85, 919–34.
- Nayak, A., Bhushan, B. (2019). An overview of the recent trends on the waste valorization techniques for food wastes. *Journal of Environmental Management*, 233, 352–370.
- Pal, M. K., Jaiswar, S.P., Srivastav, A.K. et al. (2016). Synergistic effect of piperine and paclitaxel on cell fate via cyt-c, Bax/Bcl-2-caspase-3 pathway in ovarian adenocarcinomas SKOV-3 cells. *Europeon Journal of Pharmacology*, 791, 751–762.
- Pirayesh, J., & Habib, M. (2015). Lycopene as a carotenoid provides radioprotectant and antioxidant effects by quenching radiation-induced free radical singlet oxygen: an overview. *Cell journal*, 16(4), 386–391.
- Popescu, M., Iancu, P., Plesu, V., Todasca, M. C., Isopencu, G.O., Bildea, C.S. (2022). Valuable Natural Antioxidant Products Recovered from Tomatoes by Green Extraction. *Molecules*, 27, 4191.
- Ranganna, S. (1997). Handbook of Analysis and Quality Control for Fruits and Vegetable Products, 2nd Ed., Tata McGraw Hill Pub Co Ltd, New Delhi, India. 1112p
- Ransy, C., Vaz, C., Lombès, A., & Bouillaud, F. (2020). Use of H<sub>2</sub>O<sub>2</sub> to Cause Oxidative Stress, the Catalase Issue. *International journal of molecular sciences*, 21(23), 9149.

- Ravindran, R., Jaiswal, A. K. (2016). Exploitation of food industry waste for high-value products. *Trends in Biotechnology*, 34 (1), 58–69.
- Rowles, J.L., Ranard, K.M., Applegate, C.C., Jeon, S., An, R. Erdman, J.W. (2018). Processed and raw tomato consumption and risk of prostate cancer: a systematic review and dose-response meta-analysis. *Prostate Cancer and Prostatic Diseases*, 21, 319–336.
- Salehi, B., Rescigno, A., Dettori, T., Calina, D., Docea, A. O., Singh, L., et al. (2020). Avocado–soybean unsaponifiables: a panoply of potentialities to be exploited. *Biomolecules*, 10:130.
- Sharifi-Rad, M., Anil, K. N., Zucca V., Varoni, E. M., Dini, L., Panzarini, E., Rajkovic J., Tsouh, F., Patrick, V., Azzini, E., Peluso, I., Prakash, M. A., Nigam, M., El Rayess, Y., Beyrouthy, M. E., Polito, L., Iriti, M., Martins, N., Martorell, M. et al. (2020). Lifestyle, Oxidative Stress, and Antioxidants: Back and Forth in the Pathophysiology of Chronic Diseases. *Frontiers in physiology*, 11, 694.
- Singleton, V. L., & Rossi, J. A. (1965). Colorimetry of total phenolics with phosphomolybdic-phosphotungstic acid reagents. *American journal of Enology and Viticulture*, 16(3), 144-158.
- Sowbhagya, H.B., and Chitra, V. (2010). Enzyme-Assisted Extraction of Flavorings and Colorants from Plant Materials. *Critical reviews in food science and nutrition*, 50. 146-61.
- Sun, G. B., Qin, M., Ye, J. X., Meng, X. B., Wang, M., Luo, Y & Sun, X. B. (2013). Inhibitory effects of myricitrin on oxidative stress-induced endothelial damage and early atherosclerosis in ApoE<sup>-/-</sup> mice. *Toxicology and applied pharmacology*, 271(1), 114-126.

- Torres-Valenzuela, L. S., Ballesteros-Gómez, A., Rubio, S. (2020). Green solvents for the extraction of high added-value compounds from agri-food waste. *Food Engineering Reviews*, 12 (1), 83–100.
- Tsatsakis, A., Docea, A. O., Constantin, C., Calina, D., Zlatian, O., Nikolouzakis, T. K & Neagu, M. (2019). Genotoxic, cytotoxic, and cytopathological effects in rats exposed for 18 months to a mixture of 13 chemicals in doses below NOAEL levels. *Toxicology Letters*, 316, 154-170.
- Upadhyayula, A., Srinivas, S., Bryce, W., Tan, Q., Balamurugan, A., Anand, D. (2019). ROS and the DNA damage response in cancer. *Redox Biology*, 25, 10108.
- Yen, G. C., & Duh, P. D. (1994. ). Scavenging effect of methanolic extract of peanut hulls on free radical and reactive oxygen species. *Journal of Agricultural. Food Chemistry*, 42, 629-63.
- Zhang, W. H., & Wang, H. (2008). Nortriptyline protects mitochondria and reduces cerebral ischemia/hypoxia injury. *Stroke*, 39, 455–462.
- Zuorro, A., Fidaleo, M., & Lavecchia, R. (2011). Enzyme-assisted extraction of lycopene from tomato processing waste. *Enzyme and microbial technology*, 49(6-7), 567-573.

### **Chapter 3**

## **Role of Lycopene in Mitigation of Acrylamide/ Glycidamide induced Hepatotoxicity (HepG2 cells)**

### 3.1 Introduction

Acrylamide (ACR) is a well-known food toxin, which can induce oxidative stress and related disease conditions including cancer. ACR is a recognized toxicant present in various carbohydrate rich foods exposed to higher temperature during food processing (Pedreschi, Mariotti, & Granby, 2014). Based on the studies conducted on lab animal models, Agency for Toxic Substances and Disease Registry (ATSDR), reported that the ACR is mostly carcinogenic to humans. ACR metabolised inside the body to form glycidamide, another genotoxic compound. Both ACR and GLY induce higher cellular toxicity by enhancing oxidative stress. Glycidamide (GLY), is the primary epoxide metabolite of ACR, which is catalysed by an enzyme complex Cytochrome P450 2E1 (CYP2E1). The ACR to GLY metabolic conversion via epoxidation is critical for the ACR toxicity, and GLY is reported to be a more potent mutagen than ACR as it causes genetic damage by binding to DNA (Manjanatha, Aidoo, Shelton, Bishop, Daniel, Lyn-Cook, 2006; Ghanayem, Witt, Kissling, Tice, & Recio, 2005). According to chemical activity, GLY is 70% more reactive than ACR, showing a high level of interaction with DNA and haemoglobin. According to Erdemli et al., 2021, ACR administration caused biochemical and histopathological disruption in pregnant rats and the consumption of vitamin E protected against neurotoxicity in rats (Erdemli et al., 2021).

Studies showed that ACR exposure gives rise to higher oxidative stress in cells and tissues (Zhao et al., 2015). Under oxidative stress conditions, the intracellular reactive oxygen species can oxidize biomolecules, which lead to protein oxidation, lipid peroxidation, DNA fragmentation, and most of the diseased conditions (Kunnel, Subramanya, Satapathy, Sahoo, & Zameer, 2019). Antioxidants are the scavengers in human body that confer protection against intracellular oxidative stress by providing electrons to ROS. Antioxidant enzymes like CAT, SOD, GPx, and GSH are integral parts of the innate antioxidant enzyme defense

system. It contributes the repair of damaged cellular components (Ren et al., 2017). Some non-enzymatic antioxidants such as ascorbic acid, flavonoids, tocopherol, and beta-carotene help in mitigating the oxidative stress in cells (Rahal et al., 2014). There are evidences suggesting that the animals exposed to acrylamide produced increased levels of ROS (Prasad, & Muralidhara, 2012). Studies on ACR discovered that the oxidative stress induction and mitochondrial dysfunction are the underlying mechanisms responsible for its cytotoxicity and genotoxicity (Liu et al., 2015). Accumulation of ROS or a compromised antioxidant defence leads to the disruption of redox balance in cells, causing cellular damage. Hence, the viable strategies to mitigate ACR induced toxicity are the need-of-the-hour.

Antioxidant activity is one of the possible mechanisms, to reduce the acrylamide toxicity by alleviating its free radical production. Recently, natural antioxidants are gaining more attention against ACR induced toxicity (Li et al., 2017, Sabah, Nikhat et al., 2016; Zhang, et al., 2013). Another study established that, due to the powerful antioxidant activity of crocin protects ACR induced liver damage in HepG2 cells (Soha, et al., 2020; Sema et al., 2017). Phytochemical treatments have been opted as a promising solution to overcome ACR induced toxicity and their protection induced by free radical regulation mechanisms (Mehri, Meshki, & Hosseinzadeh, 2015; Motamedshariaty, Farzad, Nassiri-Asl, & Hosseinzadeh, 2014).

From **Chapter 2**, it was understood that LYC rich ETE possess potential antioxidant and a strong free radical scavenging activity, which can be explored for mitigation of ACR and GLY induced cellular toxicity. It has a positive effect on redox imbalance, by which it activates antioxidant gene expression and regulates inflammatory mediators (Campos et al., 2017). Due to the presence of ACR in foods and its threat of massive intoxication, mechanisms to decrease the cytotoxicity and genotoxicity of ACR are of great importance.



Natural antioxidants as mitigating agents against ACR induced toxicity have attracted attention owing to their importance in food, nutraceutical and pharmaceutical sectors (Chu et al., 2017). Though, the cytoprotective role of LYC against GLY toxicity has not been reported so far, to the best of our knowledge. Identification of unfavourable health consequences due to ACR exposure is an important aspect of acrylamide risk management to avoid or mitigate its health risk. At the same time, it is also important to understand how the dietary antioxidant influence the ACR toxicity on stress induced chronic disease conditions and its molecular mechanisms of action. Liver is the major detoxification organ in human body. Hence, the use of HepG2 cells for the *in vitro* chemical toxicity assay is justified. Moreover, HepG2 cells are reproducible in human system and easy to maintain. Therefore, this current study, we explored the possible protective role of LYC against ACR and GLY induced cellular toxicity by modulating oxidative stress in HepG2 cells.

## 3.2 Objectives

To evaluate the role of LYC in mitigation of acrylamide (ACR) and glycidamide (GLY) induced cytotoxicity in HepG2 cells and elucidate the role of LYC in ACR and GLY induced cell death via ROS-regulated mitochondrial dysfunction (Fig 3.1).

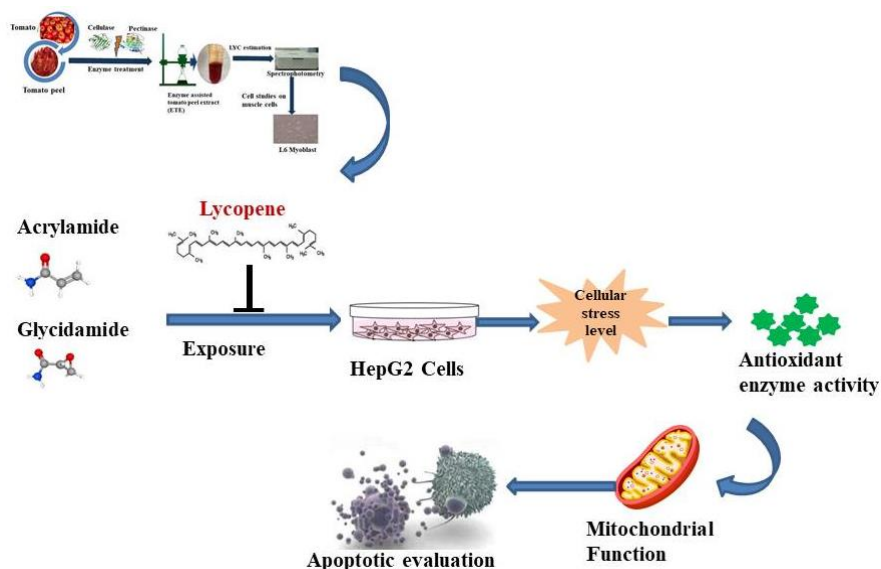


Fig 3.1: Outline of Chapter 3

## 3.3 Materials and methods

### 3.3.1 Chemicals and Reagents

Ethylene diamine tetra acetic acid (EDTA), sodium chloride (NaCl), hydrogen peroxide (H<sub>2</sub>O<sub>2</sub>), Triton X, Tris-HCl, perchloric acid, potassium hydroxide (KOH) from MERCK, India. acrylamide , glycidamide lycopene , 3-(4,5-dimethylthiazol-2-yl)-2,5 diphenyltetrazolium bromide (MTT), dimethyl sulfoxide , fetal bovine serum , Dulbecco's Modified Eagle's Medium , 2,7-Dichlorodihydrofluorescein diacetate, and Mammalian genomic DNA isolation kits , were procured from Sigma-Aldrich Chemicals (St Louis, MO, USA). Antibiotic-antimycotic solution and Trypsin-EDTA were purchased from Gibco

Invitrogen (Carlsbad, CA, USA). Kits for determining the activities of Superoxide Dismutase (SOD), Glutathione (GSH), Catalase, and Lipid Peroxidation (LPO) assay kit were purchased from Biovision Inc. (San Francisco, USA). DNA/RNA Oxidative damage Enzyme linked Immunosorbent Assay (ELISA) kit was procured from Cayman chemicals (MI-USA).

### 3.3.2 Experimental design

The experimental protocol for the study is given in Fig 3.2

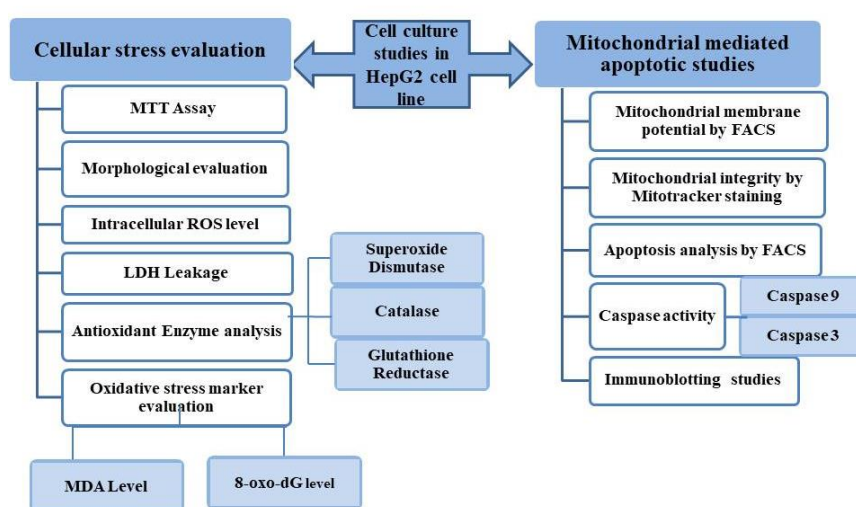


Fig 3.2: Experimental methods used for the study.

### 3.3.3 Cell culture and treatment conditions

HepG2 cells collected from National Centre for Cell Science, India were grown in DMEM containing 10% FBS and antibiotic-antimycotic solution (0.5%). Cells were kept in incubator with 37°C and 5% CO<sub>2</sub> humidified atmosphere. The cells were cultured on 96 or 12-well plates (1×10<sup>4</sup> cells/well) for staining and Flow cytometric analysis.

### 3.3.4 Cytotoxicity by MTT assay

The cytotoxicity of the Acrylamide (ACR), Glycidamide (GLY) and Lycopene (LYC) in HepG2 cells was estimated using MTT assay (Mosmann, 1983). Briefly, 96-well plates were

seeded with  $1 \times 10^4$  cells per well and were grown overnight. Then the cells were exposed to different concentrations of the ACR (0.1- 2 mM), GLY (0.1- 2 mM) and LYC (1- 50  $\mu$ M), for 24 h . After exposure, cells were treated with MTT (0.5 g/L) for 4 h. After exposure, cells were exposed to MTT reagent (0.5 g/L) for 4 h. Following the incubation, the reaction mixture was removed and added DMSO (200  $\mu$ L) to each well with gentle mixing (Orbit plate shaker, Labnet international, USA) and the absorbance was read at 570 nm (Synergy 4 Biotek multiplate reader, USA).

The cytoprotective role of LYC against ACR and GLY induced toxicity was assessed by pre-treating cells with LYC for 2 h prior to ACR and GLY treatment. Untreated cells were kept as negative control and cells exposed to 500  $\mu$ M ACR and GLY independently, were assigned as positive control. Each experiment was done in triplicate, and the results are represented as the mean  $\pm$  SD, using the following calculation

$$\% \text{ cell viability} = \frac{\text{The absorbance of test}}{\text{The absorbance of control}} \times 100$$

Morphological evaluation of cells after treatment conditions was observed using phase contrast microscope.

### **3.3.5 Lactate dehydrogenase leakage**

Upon cellular damage, cell membrane deterioration leads to the release of enzyme lactate dehydrogenase (LDH). It is recognised as cell damage marker under apoptosis, necrosis or other cellular damage conditions (Kaja, Payne, Naumchuk, & Koulen, 2017). LDH leakage in cells after incubation was estimated using an LDH assay kit (Sigma, India). A final coloured formazan derivative was read at 490 nm by spectrophotometer (Synergy 4 Biotek, USA).

### **3.3.6 Intracellular reactive oxygen species (ROS) levels.**

ROS productions in cells were estimated by DCFH-DA staining method (Cathcart, Schwiers, & Ames, 1983). The cells were exposed to various concentrations (sub toxic) of LYC followed by 500  $\mu$ M ACR and 500  $\mu$ M GLY. After the treatment, DCFH-DA stain were added to the cells and incubated for 20 min and then washed with PBS. The fluorescence intensity of produced DCF was read by using fluorescence spectrophotometer (Shimadzu RF5000U) with wavelength of excitation 480 nm and emission 520 nm (Synergy 4 Biotek multiplate reader, USA).

### **3.3.7 Antioxidant enzyme analysis**

#### **3.3.7.1. Superoxide Dismutase and catalase activity.**

The cells pre-treated with LYC, followed by incubation with ACR and GLY for 24 h, were rinsed with 1X PBS. Cells were lysed using specific enzyme buffer solution to estimate the antioxidant activity. A negative control (cells without treatment) and positive controls (ACR and GLY) were also kept. SOD and catalase activities were measured as per the directions provided by the manufacturers in the respective assay kits (K33-100 and K773-100).

#### **3.3.7.2 Measurement of glutathione (GSH) concentration.**

The lysate of the cells was prepared as mentioned under the above experiment and the clear supernatant was analysed for GSH level. The reduced GSH level of the treated lysates was found out based on the reaction of dithionitro benzoic acid with sulfhydryl groups that lead to the formation of yellow color. Glutathione assay kit was used for the estimation of glutathione level following the manufacturer instructions provided along with the kit (K261-100).

### **3.3.8 Oxidative marker analysis**

#### **3.3.8.1 Measurement of lipid peroxidation.**

Lipid peroxidation was quantified by lipid peroxidation (LPO) assay kit (K739-100). HepG2 cells were pre-treated with LYC (2 h) followed by incubation with ACR and GLY (24 h). Negative control and positive control were kept as described earlier. Malondialdehyde (MDA) level was tested using LPO Colorimetric/Fluorometric Assay Kit as per the directions given by the manufacturer. Absorbance measured at 532 nm (Synergy 4 Biotek multiplate reader, USA) was used to quantify the MDA content in the samples.

#### **3.3.8.2 Estimation of 8-oxo-2'-deoxyguanosine (8-oxo-dG) level**

The cytoprotective role of LYC against oxidative stress induced DNA damage by ACR and GLY was measured using 8-oxo-dG ELISA technique. Cells pre-incubated with LYC (10  $\mu$ M) followed by treatment with ACR and GLY (500  $\mu$ M) were trypsinized to extract the genomic DNA. 8-oxo-dG, the most abundant DNA oxidative marker, produced in the cells was quantified using Oxidative damage ELISA kit spectrophotometrically at 410nm.

#### **3.3.9 Mitochondrial membrane potential ( $\Delta\Psi_m$ ).**

Oxidative stress inactivates mitochondrial membrane potential and loss its function. Rhodamine123, a fluorescent indicator, accumulate in the mitochondria based on the membrane potential was used to assess  $\Delta\Psi_m$  (Zhang & Wang, 2008). The mitochondrial membrane potential is maintained by the proton motive force generated by ATP synthase present on the mitochondrial membrane. The cells were pre-incubated with LYC before it was exposed to ACR and GLY for stress induction. Then the cells were treated with 2  $\mu$ M Rhodamine 123 directly and rinsed with PBS many times and the fluorescence was read (FACS Aria II, BD Bioscience, USA). Suppression of  $\Delta\Psi_m$  is denoted by decreased level of green rhodamine 123 fluorescence.

### **3.3.10 Mitotracker staining**

The mitochondrial permeability (integrity) of HepG2 cells was observed by mitotracker-red fluorescent dye by using fluorescent imaging (Kholmukhamedov, Schwartz, & Lemasters, 2013). In brief, after exposure to the treatment conditions cells were dual stained with mitotracker (100 mM) for 15 min and then rinsed twice using 1× PBS, and the developed images were acquired by using a fluorescence microscope (Nikon Eclipse 80i with Nikon DS-Ri1).

### **3.3.11 Apoptosis by Flow Cytometry Analysis**

Annexin-V- /propidium iodide staining were used to quantify cellular apoptosis in HepG2 cells. Briefly, the cells were seeded at a density of  $1 \times 10^6$  cells in six well plates. After the treatment conditions described above, the cells were by harvested and centrifuged at 2300 rpm for 5 min. Then the cells were washed and resuspended in binding buffer and centrifuged at 400xg for 5min. Then the cell suspensions were stained with Annexin V-FITC and PI and kept at RT for 10 min. After incubation, the samples were again resuspended in binding buffer and analysed using FACS (BD FACS Aria II, BD Biosciences, United States). As per manufacturer instructions apoptotic cell ratio was quantified using flow cytometric methods with 10000 cells in each group. The data analysis was done using BD FACS Diva TM Software v6.1.2

### **3.3.12 Caspase 9 Assay**

Caspase 9 activity was analysed using caspase 9 Assay Kit (Abcam, USA) (Fluorometric) and the assay offers a simple and convenient method for evaluating caspase activity. The assay recognizes the LEHD (Leu-Glu-His-Asp) sequence and the detection of caspase activity was quantified using fluorimeter. After the cell treatments, the fluorescence emits a yellow-green fluorescence, which was quantified using fluorescence multimode reader (Synergy 4 Biotek multiplate reader, USA).

### **3.3.13 Caspase-3 Assay**

Caspase-3 activity was analysed by Assay Kit which recognize the sequence DEVD (Abcam, USA). Briefly after cell culture treatment, the sample lysate was added to the wells and incubated with reaction buffer and DEVD-*p*-NA substrate for 60 min at 37°C. Then the reaction absorbance was analysed by spectrophotometer at 400nm (Synergy 4 Biotek, USA).

### **3.3.14 Immunoblot analysis**

Briefly, after treatment conditions mentioned above, the cells were harvested and disintegrated by using lysis buffer (with protease inhibitor cocktail). The specific antibodies against -  $\beta$ -actin, Bax, Bcl-2, Cytochrome C, cleaved caspase 9, and cleaved caspase 3 were used in blotting. BCA protein assay kit was used to estimate the protein concentration in lysate. The extracted protein samples in reducing buffer was boiled at 75°C for 10 min. Then the lysate containing protein was subjected to SDS-PAGE (10% SDS polyacrylamide gel) and then transferred to a PVDF transfer membrane (Immobilon P™, Millipore154 R, USA) using Trans-Blot transfer system (Bio-Rad Laboratories, Germany). % skim milk in PBST blocking buffer were used to block the membranes by incubating at RT for 1 h and washed thrice with PBST and kept overnight at 4°C with primary antibodies ( $\beta$  actin, cleaved caspase 3, cleaved caspase 9, Bcl 2, Bax and Cytochrome) in the ratio 1:1000. After rinsing, IgG-HRP secondary antibody (1:2000) was incubated with the membrane. The blots bound antibodies were identified using DAB-Peroxidase substrate by chemiluminescence (Bio-rad, United States) and measured by densitometry using a ChemiDoc XRS digital imaging system and the Multi-Analyst software from Bio-Rad Laboratories (United States The density of particular protein bands were compared to that of housekeeping gene -  $\beta$  actin.



### **3.3.15 Statistical analysis.**

The Data are stated as means  $\pm$  standard deviations of minimum of triplicates. One-way ANOVA was used for analysing the results and the Duncan's multiple range tests was employed for assessing the significance  $P \leq 0.05$  using SPSS 16.0.

## **3.4 Results and Discussion**

### **3.3.1 Cytotoxicity assessment of ACR, GLY and LYC**

The toxicity level of ACR, GLY and LYC in HepG2 cells were evaluated using MTT assay. The results depicted that LYC did not alter cellular viability up to 10  $\mu\text{M}$  concentration (Fig 3.3A). Further, LYC at a concentration of 10  $\mu\text{M}$  and below was chosen for studying the hepatoprotective effect against ACR and GLY induced toxicity.

A dose-response assay was carried out with different concentrations of ACR and GLY (100  $\mu\text{M}$  to 2 mM) to identify the appropriate working concentrations of ACR and GLY to induce cytotoxicity. From the data shown in Fig 3.3B, ACR and GLY instigated cell death in a dose-dependent way. A concentration of 500  $\mu\text{M}$ , ACR and GLY caused about 30% decrease in cell viability (Fig 3.3B). Therefore, this concentration was chosen for inducing the cellular toxicity in further experiments. The concentration was consistent with the previous reports, as acrylamide at concentration above 250  $\mu\text{M}$  showed cytotoxicity in HepG2 cells (Sahinturk, Kacar, Vejselova, & Kutlu, 2018). Similar results were reported for Caco-2 cells (0.2–50 mM), NIH/3T3 fibroblasts, alveolar-basal epithelial cells (A549) and epithelial cells BEAS-2B (normal human lung) (Adriana, Szyda, Dorota, Agnieszka, Ilona, 2020; Kacar, Sahinturk, & Kutlu, 2019).

### **3.4.2 Cytoprotective potential of LYC against ACR and GLY-Induced toxicity**

To investigate the protective effects of LYC on HepG2 cells against ACR and GLY induced toxicity, the cells were pre-treated with two different concentrations (5  $\mu\text{M}$  and 10  $\mu\text{M}$ ) of LYC followed by the addition of ACR and GLY at their cytotoxic concentration (500  $\mu\text{M}$ ).

It was found that the pre-exposure of cells to LYC (Fig.3.3C) improved the cell viability in a concentration-dependent way compared to the cells that are treated only with ACR and GLY. Treatment of cells with 10  $\mu\text{M}$  concentration of LYC prior to ACR (500  $\mu\text{M}$ ) treatment increased the cell viability by 10%, compared to ACR treated cells. Likewise, the pre-exposure of LYC (10  $\mu\text{M}$ ) prior to GLY exposure (500  $\mu\text{M}$ ) also proved a similar trend where increased cell viability by 16.3% was observed (Fig. 3.3C). The results suggested that LYC could exert a hepatoprotective effects against toxicity induced by toxicants such as ACR and GLY in HepG2 cells. Earlier, a study by Chen et al. 2013, demonstrated that the flavonoid, myricitrin inhibit ACR cytotoxicity on Caco-2 cells (Chen et al, 2013).

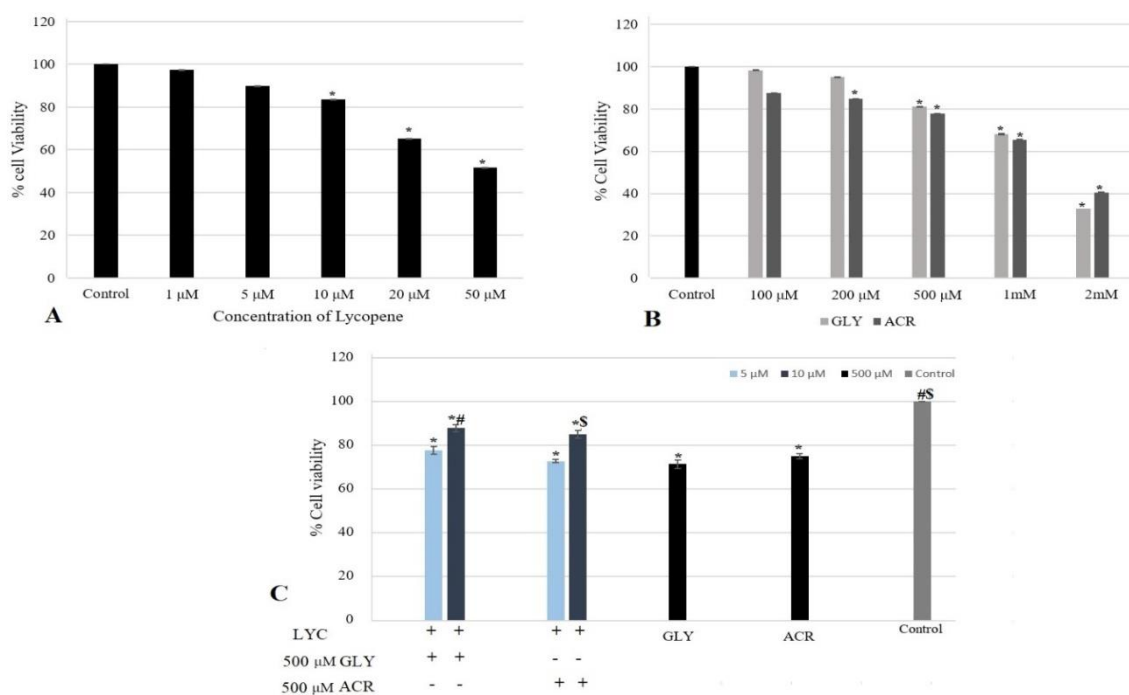


Fig 3.3: Determination of cytotoxic effect on HepG2 cells by MTT Assay. (A) Cell viability of various concentrations of LYC (B) Cell viability of ACR and GLY treated cells. (C) The LYC on viability of L6 cell against 500 $\mu\text{M}$  ACR and GLY induced toxicity. The data are expressed as the means  $\pm$  SD of triplicates. Annotation \* denotes a  $P \leq 0.05$  against control. # demotes  $P \leq 0.05$  against GLY and \$  $P \leq 0.05$  against ACR.

### 3.4.3 LYC protects HepG2 cells morphology from ACR and GLY induced alterations

Phase contrast microscopy was used to observe the morphological changes in HepG2 cells. As displayed in Fig 3.4, ACR and GLY at 500  $\mu\text{M}$  induced morphological changes in HepG2 cells. The image depicts a noticeable loss of the original cell shape, adhesion capacity, and cells became severely distorted, and rounded. A decline in cell number was also witnessed, indicating cell death progression. However, the restoration of cell morphology was prominent on LYC (10  $\mu\text{M}$ ) pretreatment of HepG2 cells and exhibited normal shaped cells with intact cell membrane, representing healthy cells.

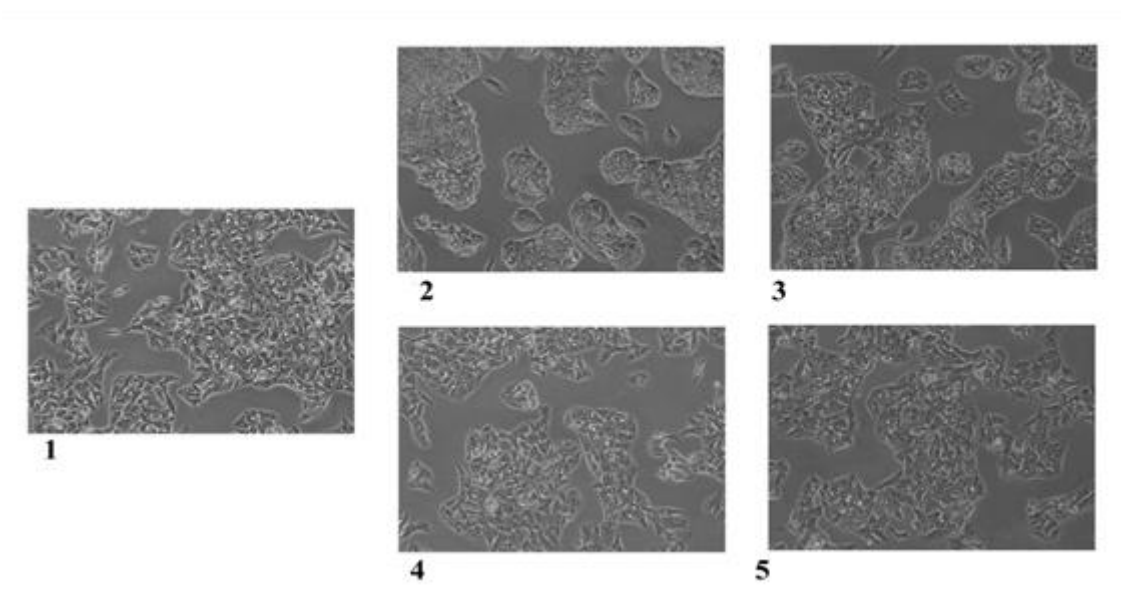


Fig 3.4: Morphological analysis by Phase contrast microscopy: Representative images shows morphological changes of HepG2 cells, indicate 1-Control, 2-500  $\mu\text{M}$  ACR, 3-500  $\mu\text{M}$  GLY, 4- 10  $\mu\text{M}$  LYC + 500  $\mu\text{M}$  ACR, 5- 10  $\mu\text{M}$  LYC + 500  $\mu\text{M}$  GLY were visualised using phase-contrast microscopy with magnification, 40X.

Li et al. showed similar findings on the morphological damage caused by ACR in HepG2 cells (Li et al., 2018). The phase contrast microscopic cell images indicate that LYC protects HepG2 cells from ACR and GLY induced cellular changes by minimizing its toxicity level.

### 3.4.4 Protective effect of LYC against ACR and GLY-induced LDH Leakage

When the cell membrane is compromised or damaged, lactate dehydrogenase releases into the extracellular space, which is used to analyse membrane integrity and cellular activity. Cell membrane permeability was evaluated in terms of LDH release from ACR and GLY exposed cells. LDH release from the cell into cytoplasm is considered as a marker for the disruption of plasma membrane during any type of cellular damage. Here LDH release assay was performed to explore the effects of pre-treatment 10  $\mu\text{M}$  LYC on cellular integrity before ACR and GLY (500  $\mu\text{M}$ ) exposure to HepG2 cells. ACR and GLY (500  $\mu\text{M}$ ) treatment exhibited a significant increase in LDH leakage; whereas the LYC (10  $\mu\text{M}$ ) pretreatment helped in the reduction of LDH release (Fig 3.5). The control cells exhibited no effect on LDH release. Pretreatment of cells with LYC treatment protected cells against ACR and GLY induced cellular damage, may be by protecting the cells from free radicals before it attack membrane proteins.

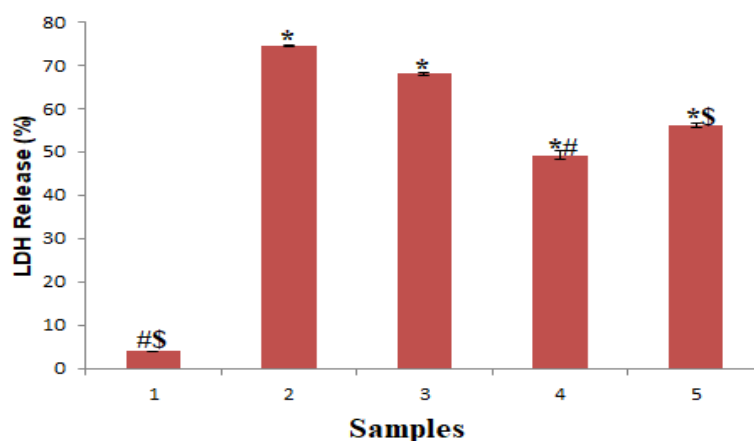


Fig 3.5: LDH release in HepG2 cells. In the figure numbers indicate, 1-Control, 2-500  $\mu\text{M}$  ACR, 3-500  $\mu\text{M}$  GLY, 4- 10  $\mu\text{M}$  LYC + 500  $\mu\text{M}$  ACR, 5- 10  $\mu\text{M}$  LYC + 500  $\mu\text{M}$  GLY significance levels between various cell groups were evaluated by one way ANOVA, and

Duncan's multiple range test. Annotation \* denotes a  $P \leq 0.05$  against Control group, \$ represent  $P \leq 0.05$  versus the ACR group and # represent  $P \leq 0.05$  against GLY group.

### **3.4.5 Protective potential of LYC against ACR and GLY-induced generation of ROS**

The toxicity of the external toxicants is manifested in cells when there is a biological oxidant to antioxidant imbalance induces oxidative stress. The overproduction of ROS causes the imbalance in the redox status of cells, and it is experimentally demonstrated that augmentation of antioxidants can modulate the cellular homeostasis by scavenging the ROS (Rodriguez, et al., 2011). Therefore, inhibition of ACR and GLY induced ROS formation by natural antioxidants from vegetables and fruits are a hopeful approach. To establish this concept, we analysed ROS using a fluorescence probe (DCFH-DA), to evaluate whether LYC could suppress ACR and GLY induced intracellular ROS generation in HepG2 cells. The cells were pre-exposed to 5 and 10  $\mu\text{M}$  of LYC and then treatment with 500  $\mu\text{M}$  ACR and GLY for 24 h incubation. The intensity of DCF fluorescence in HepG2 cells treated with ACR and GLY was significantly increased to 55.6 and 61.2%, respectively compared to the control group (15.0%) (Fig 3.6a). Interestingly, pre-treatment of 5 and 10  $\mu\text{M}$  LYC reduced ACR induced ROS production significantly to 34.0 and 23% whereas the same for GLY treated group was 41.6 and 34.0%, respectively. This result was further confirmed with quantitative analysis of ROS production by FACS method. In Fig 3.6b, the FACS data showed an increased ROS level in cells on ACR and GLY exposed cells by 37.9 and 36.7% respectively, compared to control cells which were reduced to 23% and 21.5% on pretreating the cells with 10  $\mu\text{M}$  LYC prior to ACR and GLY exposure. Results showed that LYC significantly scavenged the ROS generated by ACR and GLY in HepG2 cells in concentration dependent manner. Reduction in the generation of intracellular ROS in LYC pre-exposed HepG2 cells demonstrated the protective effect of LYC against ACR and GLY induced ROS generation in the cells.

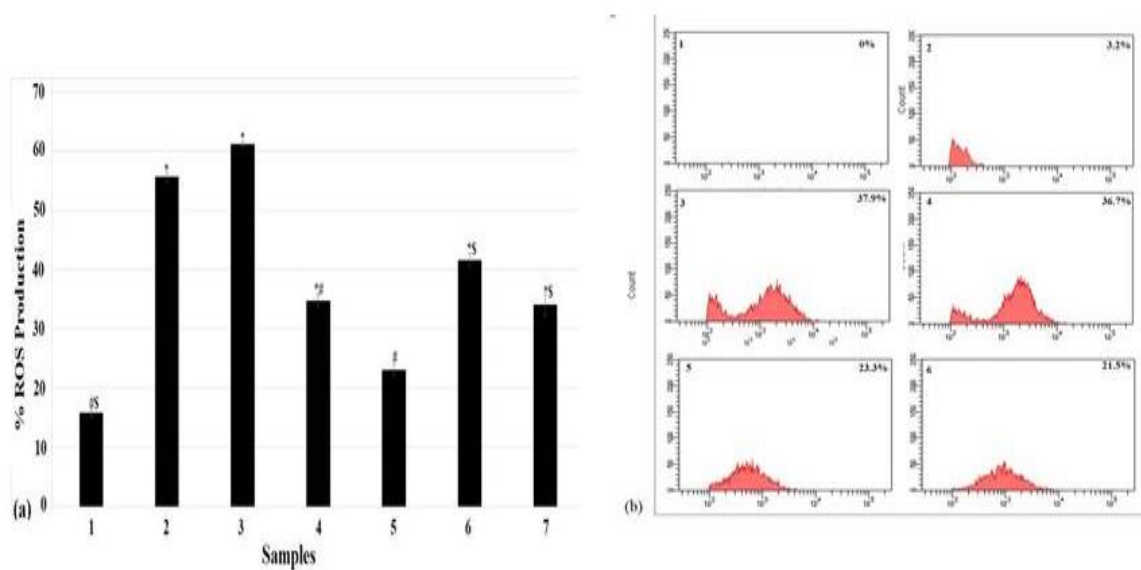


Fig 3.6: Estimation of ROS formation by HDCFDA Staining by Fluorescence spectrophotometer. (a) The numbers depict 1-Blank, 2-Control, 3-500  $\mu$ M ACR, 4-500  $\mu$ M GLY, 5- 10  $\mu$ M LYC + 500  $\mu$ M ACR, 6-10  $\mu$ M LYC + 500  $\mu$ M GLY. Results express the mean  $\pm$  SD of triplicates. The annotation \* denotes a  $P < 0.05$  against group Control, \$ represent  $P < 0.05$  versus the ACR group and # represent  $P < 0.05$  against GLY group.

Carotenoids in the foods possess excellent antioxidant activity, which have been studied for their ability to prevent chronic disease conditions. Beta-carotene, LYC and others carotenoids exhibit higher antioxidant properties in *in vitro* and *in vivo* models (Mueller, & Boehm, 2011; Bohm, Puspitasari, Ferruzzi, & Schwartz, 2002). It is reported that the ROS generation exerts a vital role in inducing hepatocellular damage. Previous studies confirmed that the ACR toxicity was connected with excessive intracellular ROS build-up in cells. Adriana et al., 2020, showed that after 24 h exposures of ACR (0.2 to 12.5 mM) exhibited a dose-dependent rise in ROS level in Caco2 cells. ACR and GLY induced ROS generation have been reported earlier and is known to be linked with oxidative stress (Prasad & Muralidhara, 2012; Mehri, Karami, Hassani, & Hosseinzadeh; 2014). Therefore, the

importance of LYC in cellular protection against ACR and GLY induced ROS generation is established in the present study.

### **3.4.6. Estimation of cellular antioxidant enzyme activity**

#### **3.4.6.1 LYC improved Superoxide Dismutase and catalase activity**

The two major antioxidant enzymes (SOD and CAT) play an important role in cellular redox homeostasis (Heikkila, Cabbat, & Cohen, 1976; Winterbourn & Stern, 1987) and protects cellular components from free radicals. Therefore, SOD and CAT activities are measured usually to evaluate the cellular oxidative stress level (Liu, Ma, & Sun, 2010; Duranti, et al., 2017). Hence, we evaluated the effect of LYC on SOD and CAT activity levels. As demonstrated in Fig 3.7A and 3.7B, exposure of HepG2 cells to ACR and GLY resulted in a significant decrease in both SOD ( $0.31 \pm 0.09$  &  $0.28 \pm 0.12$ U/mg, respectively) and CAT activity ( $3.4 \pm 0.03$  and  $3.10 \pm 0.05$ U/mg respectively), as compared to the untreated cells ( $0.5 \pm 0.06$  and  $5.4 \pm 0.09$  U/mg respectively for SOD & CAT). When cells were pre-incubated with LYC (10  $\mu$ M concentration), prior to ACR and GLY exposure, a striking and ( $p \leq 0.05$ ) significant rise in the activity of enzymes were noticed. The SOD activity was increased to 0.42 U/mg on pre-exposing the cells to LYC, (Fig. 3A) before ACR treatment. Similarly, SOD activity was increased to 0.41 U/mg when HepG2 cells were treated with LYC before GLY exposure.

Catalase (CAT) is very important in sustaining the cellular redox homeostasis (Autr aux, & Toledano, 2007). CAT activity is one of the commonly employed assays that can provide information about the cell antioxidant defence system. Fig. 3.7B illustrates the CAT activity in the untreated cells to be  $5.4 \pm 0.09$  U/mg, which on treatment with ACR and GLY decreased to  $3.4 \pm 0.03$  and  $3.1 \pm 0.05$ U/mg respectively. When cells were pre-incubated with LYC prior to ACR and GLY treatment, a significant ( $p \leq 0.05$ ) elevation in the enzyme activity (4.2 U/mg) was observed (Fig 3.7B). Similarly, for GLY exposure, the CAT activity

was observed in the order of 4.1U/mg on LYC pretreatment. From the assay, it was observed that the LYC exposure protected the cells from ACR and GLY induced oxidative damage by maintaining physiological antioxidant enzyme level. Recent studies report with a focus on the biological antioxidant and oxidant balancing. A study on the attenuation of crocin against ACR induced damage in male Wistar rats intestines revealed attenuation of ACR induced toxicity by inhibiting oxidative stress, specifically antioxidant enzyme defence system and stress markers (Gedik et al., 2018). A report by Gedik et al suggested that the crocin treatment removed ACR induced liver damage in male wistar rats due to its high antioxidant properties (Gedik et al., 2017)

#### **3.4.6.2 LYC improved ACR and GLY induced Glutathione (GSH) depletion**

Glutathione performs an important part in the free radicals (ROS) neutralization (Shan, Aw, & Jones, 1990). Previous studies reported that ACR exposure can lead to GSH depletion (Autréaux, & Toledano, 2007). Reports suggest that ACR can block the activity of glutathione S-transferase and thereby deplete the GSH level (Cuzzocrea, & Reiter, 2001; Hsu, Tsai, & Chen, 2009). Hence, we postulate that LYC could also attenuate ACR and GLY induced GSH depletion in cells. The results showed that GSH level in HepG2 cells treated with ACR and GLY was significantly depleted ( $8.3 \pm 0.12$  nmol/mg and  $7.9 \pm 0.18$  nmol/mg respectively), compared to the control ( $15.8 \pm 0.09$  nmol/mg) (Fig 3.7C). Exposing the cells to LYC before treating with ACR and GLY restored the GSH activity effectively by increasing it to 11.7 nmol/mg. A similar increase was also found in LYC pre-treatment before GLY exposure, which was 10.7nmol/mg.



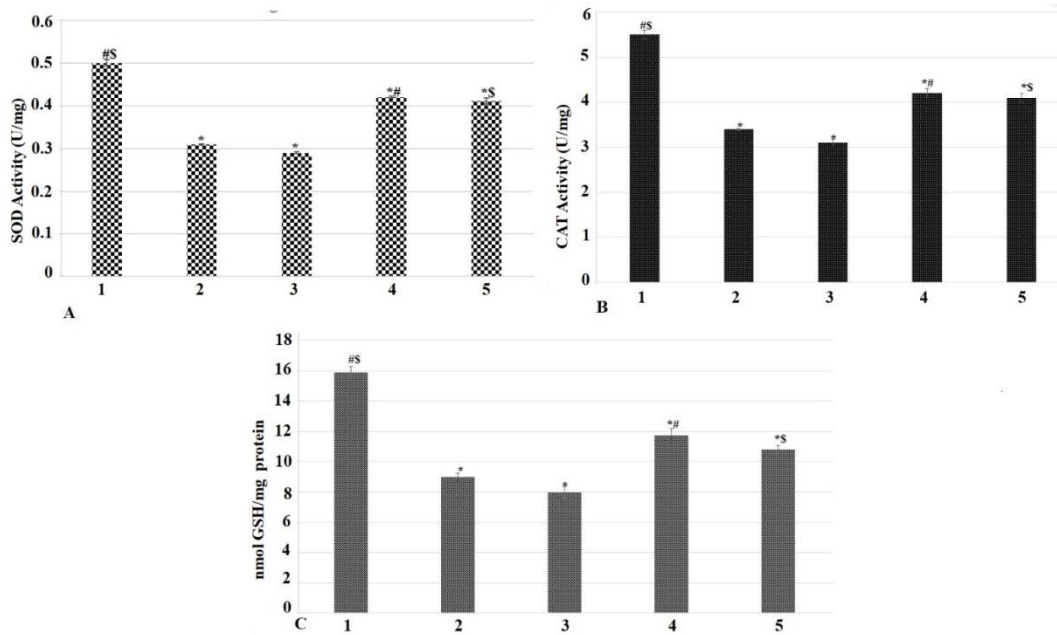


Fig 3.7: Effects of LYC on SOD, CAT and GSH in HepG2 cells (A) Protective effect of LYC on SOD activity in presence of ACR and GLY (500 μM) (B) Protective effect of LYC on CAT activity in presence of ACR and GLY (500 μM) (C) Protective potential of LYC on reduction in the level of glutathione when exposed to ACR and GLY (500 μM). The numbers depict 1-Control, 2- 500 μM ACR, 3- 500 μM GLY, 4- LYC+ 500μM ACR, 5- LYC+ 500μM GLY. Data are represented as the mean ± S.D. of three experiments carried out independently. The annotation \* represents  $P < 0.05$  against Control, # represents  $P < 0.05$  against ACR and \$ represents  $P < 0.05$  against GLY group.

It was observed in the study that exogenous exposure of ACR and GLY leads to rise in the generation of intracellular ROS and induce oxidative damage in hepatic cells, which can be counteracted by hepatocyte antioxidant defence mechanisms. Therefore, it may be inferred that on exposure of the HepG2 cells to LYC leads to the quenching of intracellular free radical production and elevate the level of glutathione. This enhances the antioxidant status of the cells, guarding against ACR and GLY -induced cellular impairment via controlling GSH antioxidant systems to subsist oxidative stress. These findings implied that LYC might

offer protection against ACR and GLY exerted stress induced oxidative damage in HepG2 cells by maintaining antioxidant defense systems to manage with oxidative stress.

Chronic dietary exposure of ACR induces oxidative stress by increasing ROS generation and thereby GSH oxidation was reported. After intestinal absorption, ACR combined with GSH and leads to a decline in intracellular GSH level. These low GSH, subsequently leads to an increase the ROS level in the cells. Experiment conducted by Seydi et al., 2015, which ACR treatment on male rats ensued a rapid GSH reduction, which is another stress marker of the cellular damage. The higher concentrations of polyphenols can prevent oxidative stress exerted by ACR in intestinal epithelium. A study in N-acetylcysteine administration shows, its antioxidant activity protect the cells against the ACR causes oxidative liver and intestinal damages (Altinoz, Turkoz, & Vardi, 2015).

### **3.4.7 Estimation of oxidative markers formation**

#### **3.4.7.1 Effect of LYC on lipid peroxidation induced by ACR and GLY**

Higher liver Malondialdehyde (MDA) levels indicate the enhanced lipid peroxidation that give rises to tissue impairment and leads to the failure of antioxidant defence mechanisms (Mohideen et al., 2021). Lipid peroxidation (MDA level) is broadly considered an oxidative stress marker (Mohideen et al., 2021). In this study, lipid peroxidation in the cells on exposure to 500  $\mu$ M ACR and GLY was analysed in terms of MDA level, in HepG2 cells. A significant increase in MDA level ( $3.9 \pm 0.72$  nmol/mg and  $4.7 \pm 0.91$  nmol/mg respectively for ACR and GLY respectively), compared to the control group (0.49 nmol/mg) was noted. Interestingly, pre-treatment with LYC significantly prevented the formation of MDA induced cellular damage caused by ACR and GLY in HepG2 cells (Fig 3.8A). Pre-treatment with LYC resultant in substantial decrease in the MDA levels to  $2.7 \pm 0.61$  nmol/mg, compared to ACR treated group ( $3.9 \pm 0.72$  nmol/mg) (Fig 3.8A). GLY treated cells with LYC preincubation also exhibited a reduction in MDA level to  $3.7 \pm 0.84$  nmol/mg,

compared to the GLY alone treated group ( $4.7 \pm 0.91$  nmol/mg). The results suggest that natural antioxidant LYC can protect against ACR and GLY induced lipid peroxidation in HepG2 cells.

### 3.4.7.2 LYC protects DNA from ACR and GLY induced oxidative damage

8-Oxo-dG is the major product of DNA oxidation due to increased oxidative stress (Nakabeppu et al., 2007). The cytoprotective role of LYC against ACR and GLY exerted oxidative DNA damage was quantified by analyzing the oxidative marker, 8-oxo-dG in DNA, which is a highly studied DNA oxidation product. In the presence of higher free radical accumulation, dsDNA molecules undergo oxidation to form an oxidized product (Bogdanov et al., 2001). Therefore, here 8-Oxo-dG level in the cells was assessed for investigating the DNA protective effect of LYC against ACR and GLY exposure.

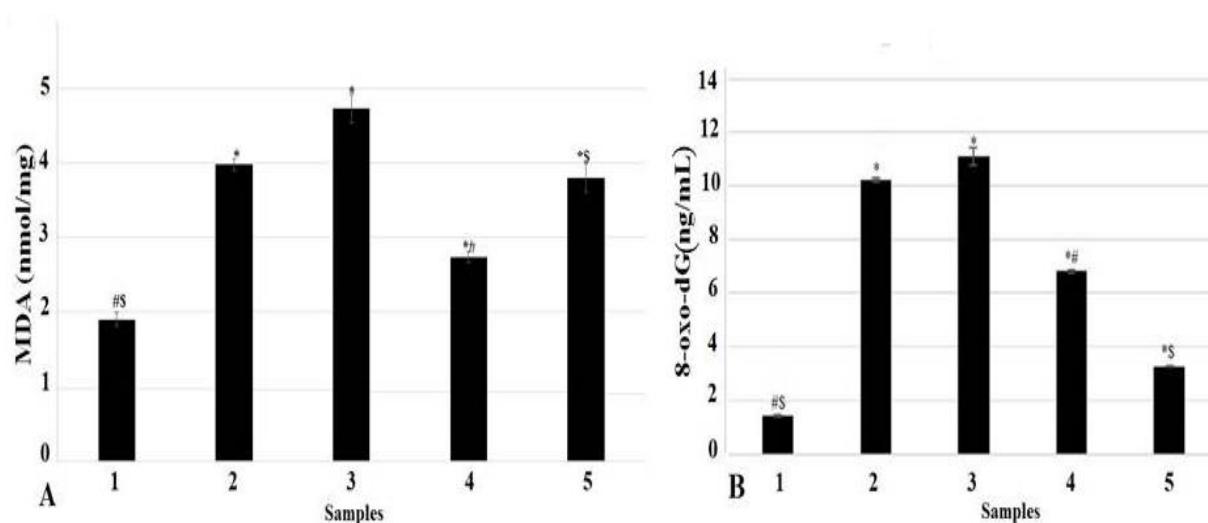


Fig 3.8: Estimation of oxidative stress markers. (A) Figure represent Lipid peroxidation determined by MDA level (B) Figure represent the 8-oxo-dG level in cells. The numbers depict 1-Control, 2- 500  $\mu$ M ACR, 3- 500  $\mu$ M GLY, 4- LYC+ 500 $\mu$ M ACR, 5- LYC+ 500 $\mu$ M GLY. Each value denotes the mean  $\pm$  SD of triplicates. And significance determined by using one-way ANOVA, \* $P \leq 0.05$  versus Control; # $P \leq 0.05$  versus ACR and \$  $P \leq 0.05$  versus GLY.

As shown in Fig 3.8B, 8-OH-dG level was significantly increased on exposure to 500  $\mu$ M ACR and GLY in cells,  $10.2 \pm 0.45$  and  $11.1 \pm 0.83$  ng/mL, to the control  $1.4 \pm 0.03$  ng/mL. However, on LYC pre-treatment prior to ACR and GLY exposure, the 8-OH-dG level was significantly decreased to  $6.8 \pm 0.03$  and  $3.2 \pm 0.04$  ng/mL. The dsDNA oxidation was found to increase in ACR and GLY exposure which was reduced upon LYC pre-treatment in a concentration dependent manner.

#### **3.4.8 Protective effect of LYC against ACR and GLY induced mitochondrial transmembrane potential ( $\Delta\psi_m$ ) loss**

It is reported that ROS accumulation results in the disruption of mitochondrial membrane potential (MMP) and ACR exposure to cells leads to mitochondrial dysfunction (Chen, et al., 2013). Based on these reports, the impact of LYC, being a potent antioxidant, against ACR and GLY induced mitochondrial transmembrane potential loss was investigated. To estimate the level of MMP, Rhodamine-123, a fluorescent cationic probe was used in this study. The higher the uptake of the Rhodamine-123, higher will be the loss of MMP. Fig 3.9 depicts ACR and GLY (500  $\mu$ M) treatment, which shows a remarkable decline of MMP level of 62 and 70.6 % respectively, as compared to the untreated cells (6.9%) (Fig 3.9). According to Zamani et al., 2017, ACR toxicity depends on mitochondrial dysfunction induced by oxidative damage, which activates cellular death. ACR exposure to hepatocytes also reported to result in mitochondrial injury by the decline of MMP (Seydi et al., 2015). Pre-treatment of cells with LYC was found to exert a protective effect in cells against the loss of mitochondrial transmembrane potential induced by ACR and GLY with 35.2 and 55.4%, respectively, when compared to cells exposed to ACR and GLY without pre-treatment. The results suggest that all the LYC-treated cells could significantly attenuate the ACR and GLY induced ROS associated mitochondrial dysfunction by retaining mitochondrial membrane integrity.

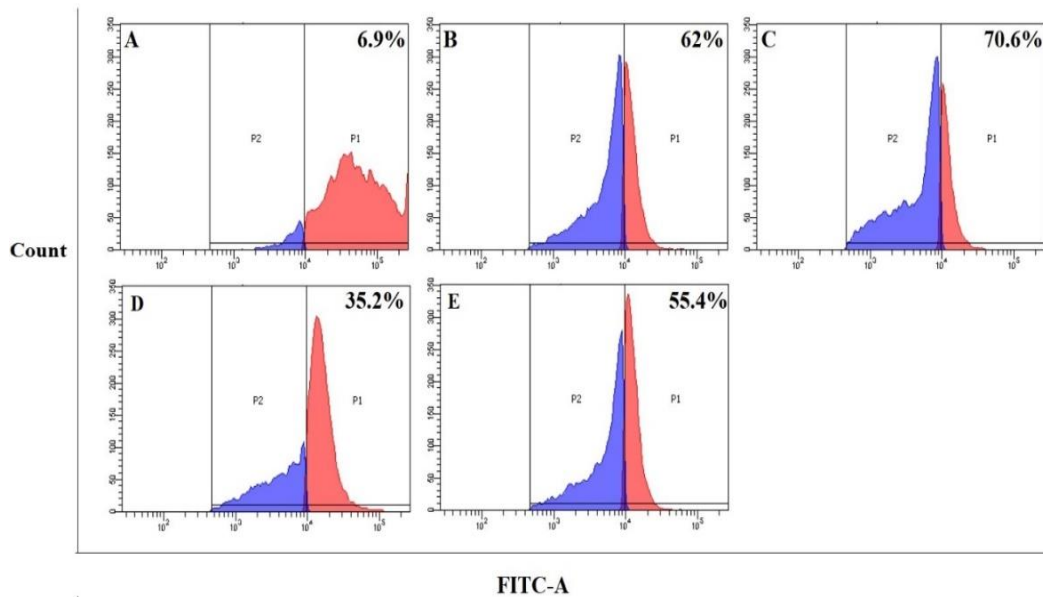
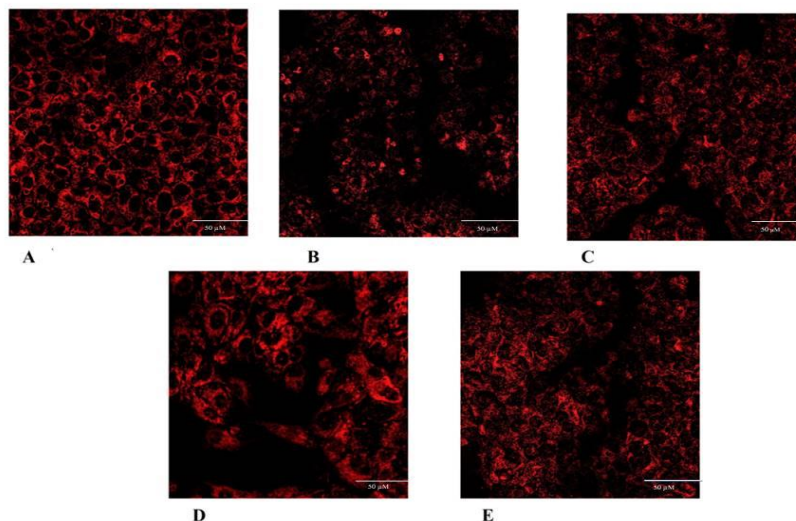


Fig 3.9: Estimation of Mitochondrial membrane potential by Rhodamine 123 staining which depicts restoration of MMP on LYC pre-treatment. After incubation, the cells were stained with Rhodamine 123 and read by flow cytometer. In data indicate A- Control, B-500  $\mu$ M ACR, C-500  $\mu$ M GLY, D- 10  $\mu$ M LYC+ 500  $\mu$ M ACR, E- 10  $\mu$ M LYC+ 500  $\mu$ M GLY.

### 3.4.9 LYC protect mitochondrial membrane integrity against ACR and GLY induced cells

Under normal cellular metabolism, a physiological level of ROS in cells function an important role in different signaling processes. An overproduction of cellular ROS lead to mitochondrial membrane disruption and permeability loss leads to mitochondrial dysfunction. To further analyse and confirm the cellular MMP from the above results, HepG2 cells were stained with mitotracker-red staining. From fig 3.10, it is visible that the mitochondrial membrane seems to be intact in the control cells, whereas ACR and GLY (500  $\mu$ M) exposed cells showed a reduction in mitochondrial membrane integrity. This disturbance in mitochondria leads to MMP loss, which is considered an initial sign of mitochondrial dysfunction. The MMP ( $\Delta\psi_m$ ) stability is highly dependent on mitochondrial

membrane integrity and MMP is considered as an essential indicator for mitochondrial function. Higher ROS in cells activates the opening of the mitochondrial transition pore which leads to an MMP loss (Wang et al., 2012). From the fig 3.10, shows a higher degree of compromised or ruptured mitochondria in ACR and GLY treated cells and a successive reduction can be seen in LYC pretreated cells. The enhanced ROS level in ACR and GLY exposed cells are directly linked with the increased mitochondrial-mediated cell death. Here, LYC pretreatment reasonably restored mitochondrial membrane integrity. Ginkgolic acids, a natural component found in nuts demonstrated a reduction in mitochondrial integrity leading to apoptosis and autophagy in HepG2 cells (Qi et al., 2018). Several studies exhibited restoration of mitochondrial membrane permeability by natural products in HepG2 cells (Al-Oqail, Farshori, & Al-sheddi, 2020; Li, et al., 2017).



**Fig 3.10:** Staining of HepG2 cells with mitotracker Red. (A) Control cells. (B) 500  $\mu$ M ACR exposed cells. (C) 500  $\mu$ M GLY exposed cells. (D) 10  $\mu$ M LYC + 500  $\mu$ M ACR exposed cells. (E) 10  $\mu$ M LYC + 500  $\mu$ M GLY exposed cells. The ACR and GLY alone treated display the highest number of disrupted (ruptured) mitochondria, which is linked with increased cell death.

### 3.4.10 LYC protects ARC and GLY induced apoptosis in HepG2 cells

The Annexin-V and propidium iodide were used for detecting cellular apoptosis by flow cytometric quantification. This method is used to detect necrotic as well as apoptotic cells, based on plasma membrane integrity. ROS shows a major role in stress induction in cells and leads to mitochondrial dysfunction. During ROS-induced cellular damage, mitochondria exhibit a significant part in apoptosis by triggering Cytochrome C release and caspase activation (Abd-Elsalam et al., 2021). The flow cytometry analysis (FACS) data confirmed that ARC and GLY (500  $\mu$ M) induced apoptosis in cells and was significantly higher in ACR and GLY exposed cells (48.1 and 45% respectively), compared to control (1.8%) (Fig 3.11). With LYC pretreatment, cells showed a reduction in apoptotic cells (27.1 and 25.6% for ACR and GLY respectively) when compared to ACR and GLY alone exposed cells. These results illustrated that LYC helps in the inhibition of ACR and GLY induced apoptosis in HepG2 cells.

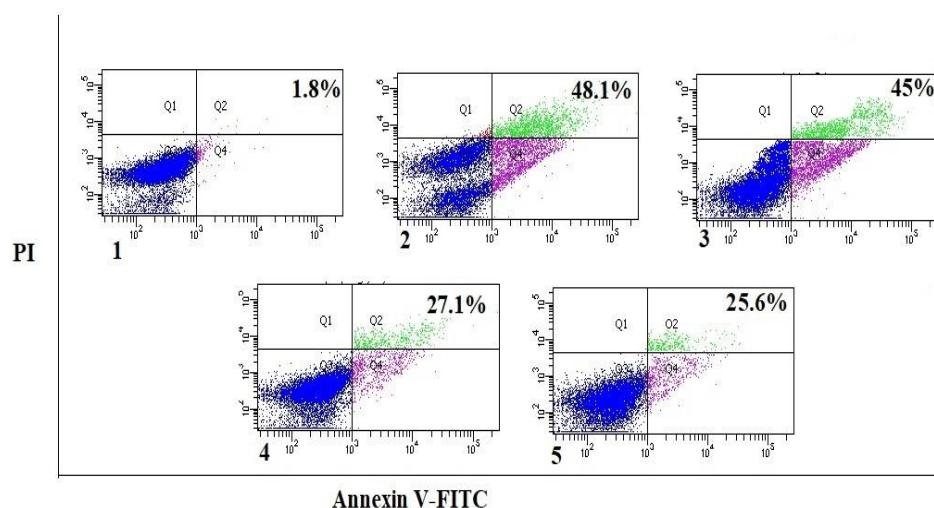


Fig 3.11 Flow cytometric analysis of cells undergoing apoptosis by Annexin V-FITC/propidium iodide staining; The numbers depict 1-Control, 2- 500  $\mu$ M ACR, 3- 500

$\mu\text{M}$  GLY, 4- 10  $\mu\text{M}$  LYC+ 500 $\mu\text{M}$  ACR, 5- 10  $\mu\text{M}$  LYC+ 500 $\mu\text{M}$  GLY. The percentage rate represents in the image shows early apoptotic cells.

A study revealed that rosmarinic acid reduced the oxidative stress exerted by ACR in BRL-3A cells, and thus inhibiting cellular apoptosis (Hong et al., 2021). Wang et al., 2022, reported that epigallocatechin gallate and epicatechin were effective in protecting ACR and GLY induced hepatotoxicity via rescuing cellular apoptosis in HepG2 cells. The current study confirmed that ACR/GLY induces hepatic dysfunction, characterized by increased ROS level, depleted mitochondrial integrity, and apoptotic induction

#### **3.4.11 LYC down regulates ACR and GLY induced Caspase 9 activity**

The caspase 9 works on activating executioner caspase (death caspase) and thereby initiating apoptotic events. The caspase 9 activity was significantly increased ( $P \leq 0.05$ ) in 500  $\mu\text{M}$  ACR and GLY exposed cells ( $18 \pm 0.91$  and  $16 \pm 0.50\%$ ) when compared to control cells ( $3.9 \pm 0.04 \%$ ) (Fig 3.12). However, on LYC pre-treatment prior to ACR and GLY exposure, the caspase 9 activity was significantly decreased to  $12.2 \pm 0.8$  and  $10.3 \pm 0.4\%$ . The initiation of the apoptotic cascade was accompanied by the activation of caspases 9 and 3, which are considered as main targets for anticancer agents. These caspase activation mainly involved in the mitochondrial-mediated intrinsic pathway. It was found that the pretreatment of cells with LYC prior to ACR and GLY treatment leads to the inactivation of caspases, which leads to the inhibition of apoptosis accompanied by intrinsic pathways. The inhibition of LYC against caspase-9 permits a controlled cytochrome c release in cells, was established by protein expression analysis using the blotting method.

A study in HepG2 cells reported that epigallocatechin gallate (EGCG) and epicatechin (EC) triggered caspase 9 activation and proceed to initiate apoptotic signaling (Wang et al., 2022). According to Hong et al, 2021 rosmarinic acid reduced the rate of apoptosis by down-regulating the expression of Caspase 9 in HepG2 cells. Here, the caspase 9 activity indicated



that the cell death was triggered via ROS-mediated mitochondrial apoptosis and it was then further confirmed with the analysis of the caspase 3 activity level.

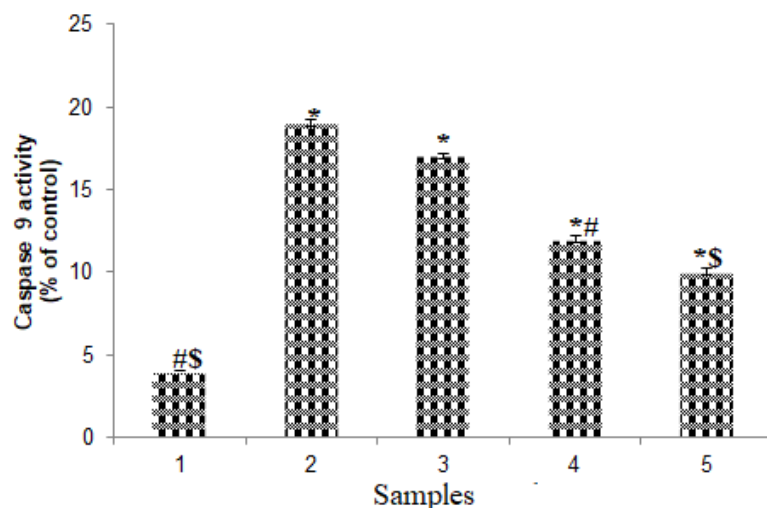


Fig 3.12: Bar diagram represent the caspase 9 activity in percentage with respect to control. The numbers depict 1-Control, 2- 500  $\mu$ M ACR, 3- 500  $\mu$ M GLY, 4- 10  $\mu$ M LYC+ 500 $\mu$ M ACR, 5- 10  $\mu$ M LYC+ 500 $\mu$ M GLY. Each value denotes the mean  $\pm$  SD of triplicates and significance between groups were analysed by one-way ANOVA, \* $P \leq 0.05$  versus Control; # $P \leq 0.05$  versus ACR and \$  $P < 0.05$  versus GLY

### 3.4.12 LYC down regulates ACR and GLY induced Caspase 3 activity

Caspase-3 employs vital roles in various cellular damages by initiating the apoptotic process (programmed cell death). It has been recognized as a major protein involved in the final stages of the apoptotic cascade known as executioner caspase (Soliman, et al., 2022). To analyze the role of LYC in mitigation of 500  $\mu$ M ACR and GLY induced cellular damage by apoptosis, caspase-3 activity was evaluated. The data revealed that the caspase 3 activity is relatively higher in ACR and GLY ( $24 \pm 0.44$  and  $23 \pm 0.31\%$  respectively) exposed cells compared to the control group (6%). LYC (10  $\mu$ M) pretreated cells prior to exposure to 500

$\mu\text{M}$  ACR and GLY were found to possess noticeably decreased caspase-3 activity ( $14.0 \pm 0.83$  and  $11 \pm 0.91\%$  respectively) (Fig 3.13). Initially, ACR and GLY activated caspase 9 and thereby caspase 3 to trigger an apoptotic pathway. LYC pretreatment showed a remarkable decrease in caspase-3 activity offers an ameliorating characteristic of LYC in protecting ACR and GLY induced cellular damage and also it provides a shred of evidence for its anti-apoptotic role in cells. A study by epigallocatechin gallate (EGCG) and epicatechin (EC) intervention down-regulated Caspase 3 activity on ACR and GLY exposed HepG2 cells (Wang et al., 2022). The major caspases included in the intrinsic apoptotic pathway such as caspase 3 and 9 exhibited a higher activity in  $500 \mu\text{M}$  ACR and  $500 \mu\text{M}$  GLY exposed cells and  $10 \mu\text{M}$  LYC pretreatment regulated its level by depleting caspase activity.

The proteins expressed in ACR and GLY induced hepatic apoptosis via mitochondrial intrinsic pathway were further confirmed by immunoblotting.

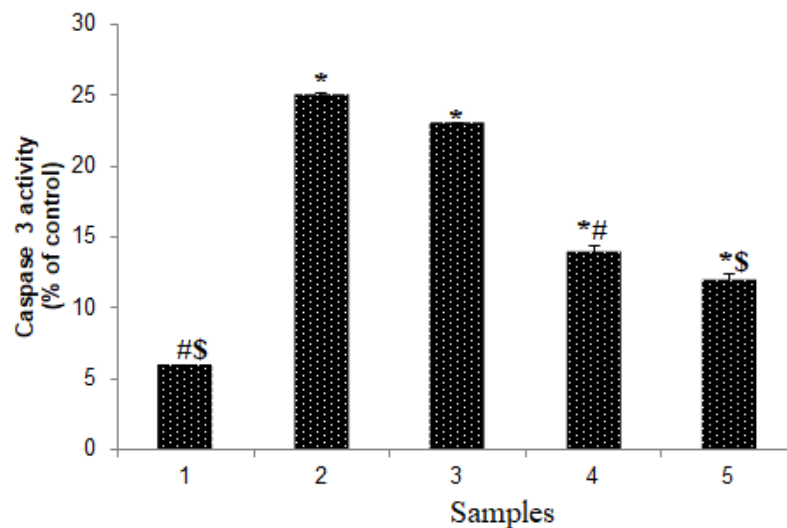


Fig 3.13: Bar diagram represent the caspase 3 activity in percentage with respect to control. The numbers depict 1-Control, 2-  $500 \mu\text{M}$  ACR, 3-  $500 \mu\text{M}$  GLY, 4-  $10 \mu\text{M}$  LYC+  $500 \mu\text{M}$  ACR, 5-  $10 \mu\text{M}$  LYC+  $500 \mu\text{M}$  GLY. Each value denotes the mean  $\pm$  SD of triplicates and

significance analysed by one-way ANOVA, \* $P \leq 0.05$  versus Control; # $P \leq 0.05$  versus ACR and \$  $P \leq 0.05$  versus GLY

### 3.4.13 Protein expression studies by western blotting

The biomolecular mechanism of LYC on ACR and GLY-induced apoptosis in HepG2 cells were investigated by an immunoblotting method. Using Immunoblotting, the protein expressions of Bax, Bcl-2, cleaved caspase 9, cleaved caspase 3, and Cytochrome C, were determined. Anti- and proapoptotic proteins such as Bcl-2/Bax play a significant role in regulating caspase-mediated apoptosis by the mitochondrial pathway (Mahmoud, Hussein, El-Twab, & Hozayen 2019). The Bax (pro-apoptotic protein) level increases during chronic liver diseases, inflammation to stimulate apoptosis (Temel et al., 2020).

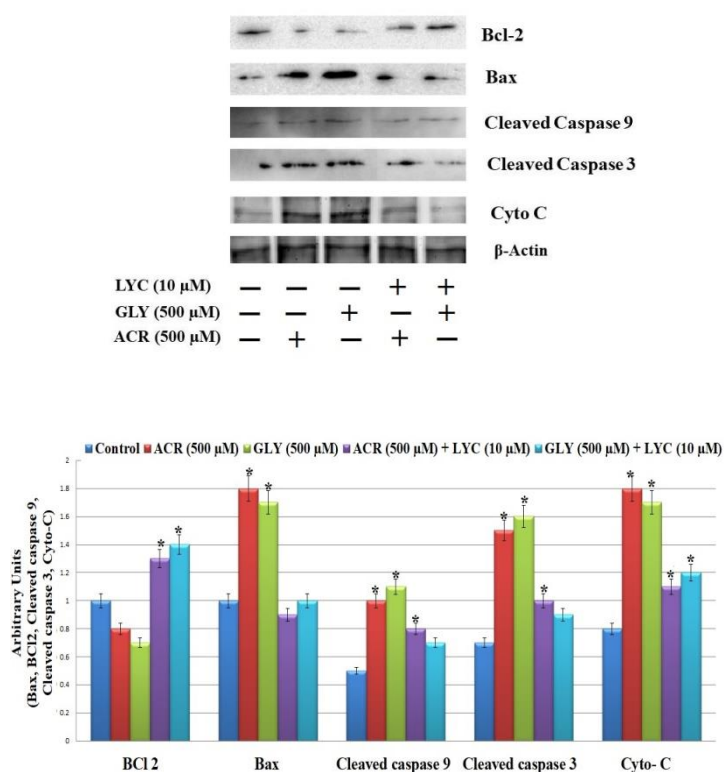


Fig 3.14: Effects of LYC against ACR and GLY induced toxicity on the proteins expression related to apoptosis. Western blot analysis for the expression of, Bcl2, Bax, cleaved caspase 3, cleaved caspase 9 and Cyto –C was carried out.

From the western blotting analysis, the Bax protein expression was significantly increased in ACR and GLY exposed cells which decreased upon LYC pretreated HepG2 cells (Fig 3.14). The Cytochrome c (Cyt-c) level was also increased in the ACR and GLY treated groups and extensive reduction was visible on LYC pretreated cells. The Cyt-c release from mitochondria activates caspase 9, finally resulting in programmed cell death. Activation of caspase directed to cleaved caspase 3 and cleaved caspase 9 levels were profoundly increased in ACR and GLY treated groups and decreased in LYC pretreated cell groups. The ACR and GLY exposure increased Cyt-C expression, cleaved caspase 3 and 9, confirming increased apoptosis via mitochondrial intrinsic pathway regulated by ROS. The blotting results revealed that 500  $\mu$ M ACR and GLY treated cells were upregulated the proapoptotic markers and the LYC pretreatment downregulated ROS-induced mitochondrial mediated apoptosis.

### **3.5 Conclusions**

The present study demonstrated the cytoprotective potential of LYC as a bioactive agent to attenuate ACR and GLY prompted cytotoxicity in HepG2 cells. ROS to antioxidant ratio imbalance leads to induce oxidative stress which is a key step for onset of different types of disease conditions. From the present study, the results indicate that the cytoprotective role of LYC is proposed to be facilitated by the inhibition of intracellular ROS production, restoration of mitochondrial membrane potential, enhanced antioxidant defense system of the body (SOD and CAT), restoration of the GSH level, and decreased oxidative product level (MDA and 8-oxo-dG). Collectively, the results of this study demonstrate that LYC can protect HepG2 cells against ACR and GLY induced oxidative damage through its antioxidant activity.

The ACR and GLY induced cell death was confirmed with apoptotic markers and LYC pretreatment exhibit a cytoprotection against cellular damage by alleviating ROS in cells. The apoptotic protein expression studies reveal that the ACR and GLY induced cell damage is activated by ROS dependent mitochondrial mediated intrinsic apoptotic pathway by triggering caspase 3 and 9. LYC pretreatment inhibit ACR and GLY induced cellular apoptosis by modulating ROS mediated apoptotic pathway. Therefore, reasonable supplements of the LYC or LYC enriched products can alleviate the harmful effects caused by dietary exposure to acrylamide.

**The key findings were summarized below:**

- LYC was found to attenuate ACR and GLY induced cytotoxicity in HepG2 cells by modulating cellular antioxidant status.
- The cell death induced by ACR and GLY is ascribed to mitochondrial-mediated cell apoptosis induced by ROS
- LYC alleviates ACR and GLY induced apoptosis via modulating ROS-mediated mitochondrial dysfunction in HepG2 cells

Supplement of LYC, a natural antagonist of ACR and GLY, could mitigate the side effects caused by the consumption of high-temperature processed foods.

### 3.6 Graphical Abstract

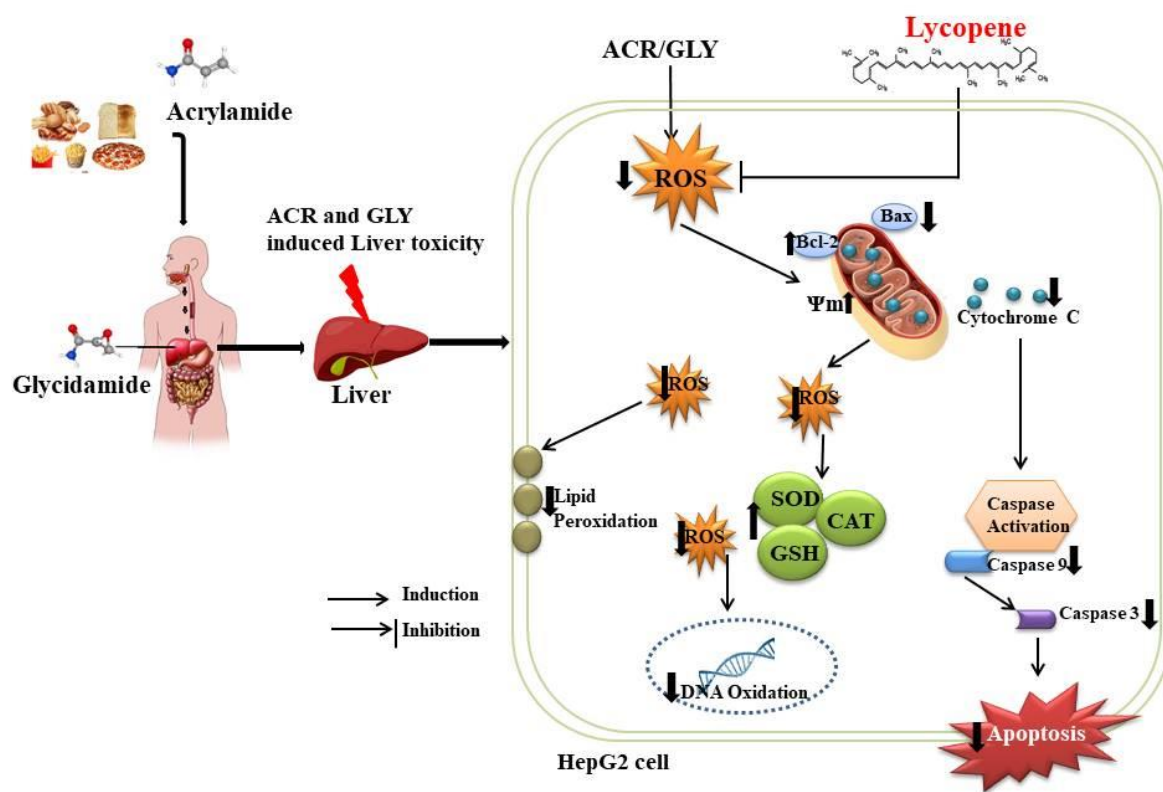


Fig 3.15: Schematic representation of LYC ameliorate ACR and GLY induced ROS mediated apoptosis in HepG2 cells

### 3.7 References

- Abd-Elsalam, R.M., El Badawy, S.A., Ogaly, H.A., Ibrahim, F.M., Farag, O.M., Ahmed, K.A. (2021). Eruca sativa seed extract modulates oxidative stress and apoptosis and up-regulates the expression of Bcl-2 and Bax genes in acrylamide-induced testicular dysfunction in rats. *Environmental Science and Pollution Research*, 28, 53249–66.
- Adriana, N., Szyda, M., Dorota, Z., Agnieszka, K., Ilona, M. (2020) Acrylamide Decreases Cell Viability, and Provides Oxidative Stress, DNA Damage, and Apoptosis in Human Colon Adenocarcinoma Cell Line Caco-2. *Molecules*, 25, 368;
- Agency for Toxic Substances and Disease Registry (ATSDR). (2012). Toxicological profile for Acrylamide. U.S. Department of Health and Human Services, Public Health Service.
- Al-Oqail, M. M., Farshori, N. N., Al-Sheddi, E.S. et al. (2020). Petroselinum sativum protects HepG2 cells from cytotoxicity and oxidative stress induced by hydrogen peroxide. *Molecular Biology Reports*, 47, 2771–2780
- Altinoz, E., Turkoz, Y., Vardi, N. (2015) The protective effect of N-acetylcysteine against acrylamide toxicity in liver and small and large intestine tissues. *Bratisl Lek Listy*, 116 (4)
- Autréaux, B. D., & Toledano, M. B. (2007). ROS as signalling molecules: mechanisms that generate specificity in ROS homeostasis. *Nature Reviews Molecular Cell Biology*. 8, 813–824.

- Bogdanov, M. B., Andreassen, O. A., Dedeoglu, A., & Ferrante, R. J. (2001) Increased oxidative damage to DNA in a transgenic mouse model of Huntington's disease. *Journal Neurochemistry*, 79, 1246–9
- Bohm, V., Puspitasari, N. L., Ferruzzi, M. G., & Schwartz, S. J. (2002). Trolox equivalent antioxidant capacity of different geometrical isomers of  $\alpha$ -carotene,  $\beta$ -carotene, lycopene, and zeaxanthin. *Journal of Agricultural and Food Chemistry*. 50, 221-226.
- Campos, K. K. D., Araújo, G. R., Martins, T. L., Bandeira, A. C. B., Costa, G., de, P., Talvani, A., & Bezerra, F. S. (2017) The antioxidant and anti-inflammatory properties of lycopene in mice lungs exposed to cigarette smoke. *Journal of Nutritional Biochemistry*, 48, 9–20.
- Cancer, IARC monographs on the evaluation of carcinogenic risks to humans: Some industrial chemicals. (International Agency for Research on Cancer).
- Cathcart, R., Schwiers, E., & Ames, B. N. (1983). Detection of picomole levels of hydroperoxides using a fluorescent dichlorofluorescein assay. *Analytical Biochemistry*. 134, 111–116.
- Chen, J. H., Yang, C.H., Wang, Y. S., Lee, J. G., Cheng, C.H., & Chou C. (2013)a. Acrylamide-induced mitochondria collapse and apoptosis in human astrocytoma cells, *Food and Chemical Toxicology*. 2013, 51, 446–452.
- Chen, W., Feng, L., Shen, Y., Su, H., Li, Y., Zhuang, J., Zhang, L., & Zheng, X. (2013)b. Myricitrin inhibits acrylamide-mediated cytotoxicity in human Caco-2 cells by preventing oxidative stress. *BioMed Research International*. 72,4183



- Chu, Q., Zhao, Y., Shi, X., Han, W., Zhang, Y., Zheng, X., & Zhu, J. (2017). *In vivo*-like 3-D model for sodium nitrite-and acrylamide-induced hepatotoxicity tests utilizing HepG2 cells entrapped in micro-hollow fibers. *Scientific Reports*. 7 (1), 14837.
- Cuzzocrea, S., & Reiter, R.J. (2001). Pharmacological action of melatonin in shock, inflammation and ischemia reperfusion injury. *European Journal of Pharmacology*. 426, 1–2.
- Duranti, G., Ceci, R., Sgro, P., Sabatini, S., & Di Luigi L. (2017). Influence of the PDE5inhibitor tadalafil on redox status and antioxidant defense system in C<sub>2</sub>C<sub>12</sub> skeletal muscle cells. *Cell Stress Chaperon*. 22, 389-396.
- Erdemli, Z., Erdemli, M. E., Turkoz, Y., Yigitcan, B., Aladag, M. A., Cigremis, Y., Cink, R. H., Altinoz, E., Bag, H. G. (2021) Vitamin E effects on developmental disorders in fetuses and cognitive dysfunction in adults following acrylamide treatment during pregnancy. *Biotechnic & Histochemistry*, 96(1):11-19
- Gedik, S., Erdemli, M. E., Gul, M., Yigitcan, B., Bag, H. G., Aksungur, Z., Altinoz, E. (2017) Hepatoprotective effects of crocin on biochemical and histopathological alterations following acrylamide-induced liver injury in Wistar rats. *Biomedicine and Pharmacotherapy*, 95:764-770.
- Gedik, S., Erdemli, M. E., Gul, M., Yigitcan, B., Bag, H. G., Aksungur, Z., Altinoz, E. (2018) Investigation of the protective effects of crocin on acrylamide induced small and large intestine damage in rats. *Biotechnic & Histochemistry*, 93(4):267-276.
- Ghanayem, B. I., Witt, K. L., Kissling, G. E., Tice, R. R., & Recio, L. (2005). Absence of acrylamide-induced genotoxicity in CYP2E1- null mice: evidence consistent with a glycidamide mediated effect. *Mutation Research*. 578:284-97

- Heikkila, R. E., Cabbat, F., & Cohen, G. (1976). *In vivo* inhibition of superoxide dismutase in mice by diethyldithiocarbamate, *Journal of Biological Chemistry*. 1976, 251, 182–2185 PMID: 5443
- Hong Y, Nan B, Wu X, Yan H, Yuan Y. (2019) Allicin alleviates acrylamide-induced oxidative stress in BRL-3A cells. *Life Sciences*, 231:116550.
- Hong, Z., Minghua, W., Bo, Nan., Chaoyue, Yang., Haiyang, Yan., Haiqing, Ye ., Chunyu, Xi., Yan, Zhang ., Yuan, Yuan. (2021).Rosmarinic acid attenuates acrylamide induced apoptosis of BRL-3A cells by inhibiting oxidative stress and endoplasmic reticulum stress. *Food and Chemical Toxicology*, 151,112156.
- Hsu, Y. W., Tsai, C. F., Chen, W. K. (2009). Protective effects of sea buckthorn (*Hippophaerhamnoides L.*) seed oil against carbon tetrachloride-induced hepatotoxicity in mice. *Food and Chemical Toxicology*. 47, 2281–2288.
- Kacar, S., Sahinturk, V., & Kutlu, H. M. (2019). Effect of acrylamide on BEAS-2B normal human lung cells: Cytotoxic, oxidative, apoptotic and morphometric analysis. *Acta Histochemica*. 121, 595–603
- Kacar, S., Vejselova, D., Kutlu, H.M., & Sahinturk, V. (2018). Acrylamide-derived cytotoxic, anti-proliferative, and apoptotic effects on A549 cells. *Human & Experimental Toxicology*. 37, 468–474.
- Kaja, S., Payne, A. J., Naumchuk, Y., & Koulen, P. (2017). Quantification of Lactate Dehydrogenase for Cell Viability Testing Using Cell Lines and Primary Cultured Astrocytes. *Current protocols in toxicology*, 72, 2.26.1–2.26.10.
- Kelkel, M., Schumacher, M., Dicato, M., & Diederich, M. (2011). Antioxidant and antiproliferative properties of lycopene. *Free Radical Research*, 45(8), 925–940.

- Kholmukhamedov, A., Schwartz, J. M., & Lemasters, J. J. (2013). Isolated mitochondria infusion mitigates ischemia-reperfusion injury of the liver in rats: mitotracker probes and mitochondrial membrane potential. *Shock (Augusta, Ga.)*, 39(6), 543.
- Kunnel, S.G., Subramanya, S., Satapathy, P., Sahoo, I., & Zameer, F. (2019). Acrylamide Induced Toxicity and the Propensity of Phytochemicals in Amelioration: Review. *Central Nervous System Agents in Medicinal Chemistry*, 19(2):100-13
- Li, L., Sun, H., Liu, W., Zhao, H., Shao, M. (2017) Silymarin protects against acrylamide-induced neurotoxicity via Nrf2 signalling in PC12 cells. *Food and chemical Toxicology*, 102:93-101
- Li, X., Liu, H., Lv, L. Y., Haiyang, Y. (2018). Antioxidant activity of blueberry anthocyanin extracts and their protective effects against acrylamide-induced toxicity in HepG2 cells. *International Journal of Food Science & Technology*.10- 678-797
- Liu, C. M., Ma, J. Q., Sun, Y. Z. (2010). Quercetin protects the rat kidney against oxidative stress-mediated DNA damage and apoptosis induced by lead. *Environmental Toxicology and Pharmacology*. 30, 264–271
- Liu,Z., Song, G.,Zou, C.,Liu, G.,Wu, W.,Yuan, T.,Liu, X. (2015) Acrylamide Induces mitochondrial dysfunction and apoptosis in BV-2 microglial cells. *Free radical biology and medicine*, 84:42-53
- Mahmoud, A.M., Hussein, O.E., Abd El-Twab, S.M., Hozayen, W.G. (2019) Ferulic acid protects against methotrexate nephrotoxicity via activation of Nrf2/ARE/HO-1

signaling and PPARgamma, and suppression of NF-kappaB/NLRP3 inflammasome axis. *Food and Function*, 10:4593–607.

Manjanatha, M. G., Aidoo, A., Shelton, S. D., Bishop, M. E., McDaniel, L. P., Lyn-Cook, L. E. (2006). Genotoxicity of acrylamide and its metabolite glycidamide administered in drinking water to male and female Big Blue mice. *Environmental and Molecular Mutagenesis*. 47:6-17. 5

Mehri, S. Karami, H. V., Hassani, F.V., & Hosseinzadeh, H. (2014). Chrysin reduced acrylamide-induced neurotoxicity in both *in vitro* and *in vivo* assessments, *Iranian Biomedical journal*. 2014, 18 (2),101–106.

Mehri, S., Meshki, M.A., Hosseinzadeh, H. (2015) Linalool as a neuroprotective agent against acrylamide-induced neurotoxicity in Wistar rats. *Drug and Chemical Toxicology*, 38 : 162–166.

Mohideen, K., Sudhakar, U., Balakrishnan, T., Almasri, M. A., Al-Ahmari, M. M., Al Dira, H. S., Suhluli, M., Dubey, A., Mujoo, S., Khurshid, Z., Raj, A. T., & Patil, S. (2021). Malondialdehyde, an Oxidative Stress Marker in Oral Squamous Cell Carcinoma-A Systematic Review and Meta-Analysis. *Current issues in molecular biology*, 43(2), 1019–1035.

Mosmann, T. (1983). Rapid colorimetric assay for cellular growth and survival, Application to proliferation and cytotoxicity assays. *Journal of Immunological Methods*. 65, 55–63

Motamedshariaty, V.S., Farzad, S.A., Nassiri-Asl, M., Hosseinzadeh H. (2014) Effects of rutin on acrylamide-induced neurotoxicity, *Journal of Pharmaceutical Sciences*, 22 (1)

- Mueller, L., & Boehm, V. (2011). Antioxidant Activity of  $\beta$ -Carotene Compounds in Different *in Vitro* Assays, *Molecules.*, 16, 1055-1069
- Nakabeppu, Y., Tsuchimoto, D., Yamaguchi, H., & Sakumi, K. (2007). Oxidative damage in nucleic acids and Parkinson's disease. *Journal of Neuroscience*, 2007, 85, 919–34
- Pedreschi, F., Mariotti, M. S., Granby, K. (2014). Current issues in dietary acrylamide: formation, mitigation and risk assessment. *Journal of the Science of Food and Agriculture.* 94, 9–20
- Prasad, S. N., Muralidhara. (2012). Evidence of acrylamide induced oxidative stress and neurotoxicity in *Drosophila melanogaster*—Its amelioration with spice active enrichment: relevance to neuropathy. *Neurotoxicology.* 33(5),1254–1264
- Qi, Q., Xue, Y., Lv, J., Sun, D., Du, J., Cai, S. ... Wang, M. (2018). Ginkgolic acids induce HepG2 cell death via a combination of apoptosis, autophagy and the mitochondrial pathway. *Oncology Letters*, 15, 6400-6408.
- Rahal, A., Kumar, A., Singh, V., Yadav, B., & Tiwari, R. Chakraborty, S. (2014). Oxidative stress, prooxidants, and antioxidants: the interplay. *BioMed Research International*, 761264
- Ren, X., Zou, L., Zhang, X., Branco, V., Wang, J., & Carvalho, C. (2017). Redox Signaling Mediated by Thioredoxin and Glutathione Systems in the Central Nervous System. *Antioxidant Redox Signal*, 27(13):989-101
- Rodriguez-Ramiro, I., Ángeles Martín, M., Ramos, S., Bravo, L., & Goya, L. (2011). Olive oil hydroxy tyrosol reduces toxicity evoked by acrylamide in human Caco-2 cells by preventing oxidative stress. *Toxicology.* 288 (1–3), 43–48.

- Rodriguez-Ramiro, I., Ramos, S., Bravo, L., Goya, L., & Angeles Martin, M. (2011). Procyanidin B2 and a cocoa polyphenolic extract inhibit acrylamide-induced apoptosis in human Caco-2 cells by preventing oxidative stress and activation of JNK pathway. *Journal of Nutritional Biochemistry*. 22 (12), 1186–1194.
- Sabah, A., Nikhat, J. S., Seema, Z., Majid, A.G., Manal, A. (2016). Hepatoprotective effect of Quercetin supplementation against Acrylamide-induced DNA damage in wistar rats. *BMC Complementary and Alternative Medicine*, 16(1): 327.
- Sahinturk, V., Kacar, S., Vejselova, D., Kutlu, H.M. (2018). Acrylamide exerts its cytotoxicity in NIH/3T3 fibroblast cells by apoptosis. *Toxicology and Industrial Health*. 34, 481–489.
- Sema, G., Mehmet, E. E., Gulc, M., Yigitcanc B., Harika, G. B., Zeynep, A., Eyup, A. (2017) Hepatoprotective effects of crocin on biochemical and histopathological alterations following acrylamide-induced liver injury in Wistar rats. *Biomedicine & Pharmacotherapy*, 95: 764-77
- Seydi, E., Rajabi, M. Salimi, A., Pourahmad, J. (2015) Involvement of mitochondrial-mediated caspase-3 activation and lysosomal labilization in acrylamide-induced liver toxicity. *Environmental Toxicology & Chemistry*, 97, 563–575.
- Shan, X. Q., Aw, T. Y., Jones, D. P. (1990). Glutathione-dependent protection against oxidative injury. *Pharmacology & Therapeutics* . 47, 61–71
- Soha, M. H., Zakaria, E. K., Abdel, R. F., Ola, N. S., Mervat, M. S., Diaa, M. (2020) Hepatoprotective effect of Raspberry ketone and white tea against acrylamide-induced toxicity in rats. *Drug and Chemical Toxicology*

- Soliman, M. M., Alotaibi, S. S., Sayed, S., Hassan, M. M., Althobaiti, F., Aldhahrani, A., Youssef, G., & El-Shehawi, A. M. (2022). The Protective Impact of *Salsola imbricata* Leaf Extract From Taif Against Acrylamide-Induced Hepatic Inflammation and Oxidative Damage: The Role of Antioxidants, Cytokines, and Apoptosis-Associated Genes. *Frontiers in veterinary science*, 8, 817183.
- Temel, Y., Kucukler, S., Yildirim, S., Caglayan, C., Kandemir, F.M. (2020). Protective effect of chrysin on cyclophosphamide-induced hepatotoxicity and nephrotoxicity via the inhibition of oxidative stress, inflammation, and apoptosis. *Naunyn-Schmiedeberg's Archives of Pharmacology*, 393:325–37.
- Wang, A., Chen, Xinyu., Wang, Laizhao., Jia, Wei., Wan, Xuzhi., Jiao, Jingjing., Yao, Weixuan., Zhang, Yu. (2022).Catechins protect against acrylamide- and glycidamide-induced cellular toxicity via rescuing cellular apoptosis and DNA damage. *Food and Chemical Toxicology*,167,113253.
- Winterbourn, C.C., & Stern, A. (1987). Human red cells scavenge extracellular hydrogen peroxide and inhibit formation of hypochlorous acid and hydroxyl radical. *Journal of Clinical Investigation*. 80, 1486
- Zamani, E., Shaki, F., Abedian Kenari, S., Shokrzadeh, M. (2017) Acrylamide induces immunotoxicity through reactive oxygen species production and caspase-dependent apoptosis in mice splenocytes via the mitochondria-dependent signaling pathways. *Biomedicine & Pharmacotherapy*, 94, 523–530.
- Zhang, L., Wang, E., Chen, F., Yan, H., Yuan, Y., 2013. Potential protective effects of oral administration of allicin on acrylamide-induced toxicity in male mice. *Food and Function*. 1229–1236.

Zhang, W. H., Wang, H., 2008. Nortriptyline protects mitochondria and reduces cerebral ischemia/hypoxia injury. *Stroke*. 39, 455–462.

Zhao, M., Wang, P., Zhu, Y., Liu, X., Hu, X., Chen, F. (2015) Blueberry anthocyanins extract inhibits acrylamide-induced diverse toxicity in mice by preventing oxidative stress and cytochrome P450 2E1 activation *Journal of Functional Foods*, 14:95-112.



**Chapter: 4**

**Lycopene regulates colon tumorigenesis via suppressing  
ROS mediated P13/Akt/mTOR signalling in HCT 116  
cells**

## 4.1 Introduction

Colorectal cancer (CRC), third most common cancer and one of the most prevalent leading causes of morbidity worldwide (Keum & Giovannucci, 2019). It is a major public health problem and its incidence has been increasing year by year (Siegal et al., 2016). Modifiable risk factors include bad dietary habits, smoking, a sedentary lifestyle; which significantly rise the chance of CRC progression (Vasen et al., 2014). Various studies indicated that low fruit and vegetable consumption in diets also displays a high risk for colon cancer (McGuire, 2015). The toxic side effects of chemotherapy drugs used in cancer treatment show increased toxicity in normal cells and also the failure of chemotherapy due to drug resistance are some of the drawbacks of clinical treatment (Tsuda et al., 2016; Tatsi et al., 2016). Recently, the researchers have concentrated on the alternative and complementary medicine approach, particularly as nutraceuticals or functional foods for the prevention, and management of various long-lasting diseased conditions, due to their ability to induce several important signalling pathways, and also enhance nutritional values without cellular toxicity (Saxena et al, 2016; Rouhi et a., 2017).

The elevation of apoptosis (programmed cell death) in tumor cells has been the key therapeutic target for several cancer treatments (Delbridge et al., 2012; Hassan et al., 2014). Cellular apoptosis can be initiated by two main signalling cascades such as the extrinsic (death receptor-mediated) way and the intrinsic (mitochondrial-mediated) way (Vyas et al., 2016). Both pathways finally lead to caspase activation which is responsible for the initiation of apoptosis via proteolytic cleavage (Ouyang et al., 2012). Six hallmarks that contribute to tumorigenesis and differentiate cancer cells from normal healthy ones are growth suppression, resistance to cell death, angiogenesis, replicative immortality, increased proliferative signalling, and metastasis (Fig 4.1). Some major target focused on

antitumorigenic activity is apoptotic induction and antiproliferation in cancer cells. The PI3K/Akt/mTOR cascade encompasses numerous normal functions like cellular growth, survival, proliferation, and angiogenesis (Morgensztern et al., 2005). The regulation of the PI3K/Akt/mTOR cascade in cancers has been recognized as a therapeutic target to treat cancer (Tang et al., 2009). PI3K/Akt/mTOR pathway normally acts to prevent proapoptotic factors and triggers anti-apoptotic factors via phosphorylation by activating a range of downstream factors, and then regulates cellular metabolism in colon cancer (Park et al., 2018). It has been confirmed that the PI3K/Akt/mTOR signalling mechanisms were highly stimulated in glandular in colorectal carcinoma and colorectal adenomas with intraepithelial neoplasia (Sui et al., 2017), indicating that blockers of PI3K/Akt/mTOR signalling may help as a possible anti-CRC agent. Inhibition of PI3K/Akt signalling can stimulate pro-apoptotic proteins such as Bax and Bad, leading to alteration in mitochondrial membrane potential ( $\Delta\psi_m$ ), which contributes to mitochondrial dysfunction and apoptosis (Yao et al., 2019; Franke, 2008). Hence, the importance of mitochondria-mediated apoptosis has been increasing attention in cellular death signalling.

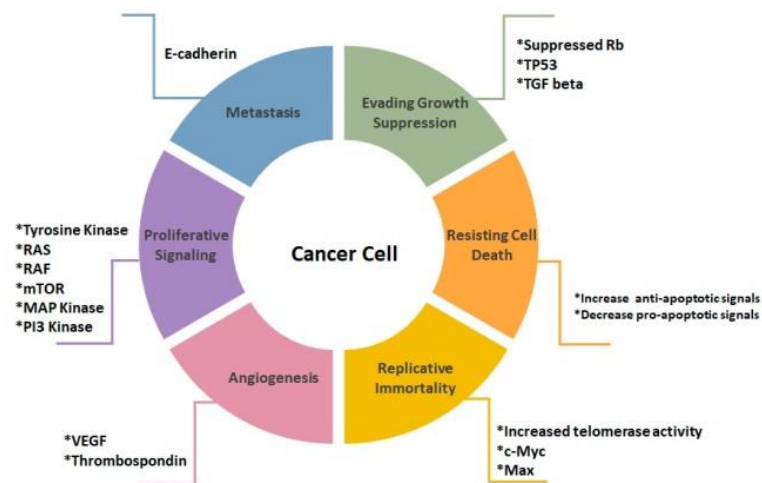


Fig 4.1: Illustration of cancer cell hallmarks (Abotaleb et al., 2018, *Cancers*)

Lycopene (LYC), a major pigment found in tomatoes, showed a potential anti-carcinogenic activity in different types of cancer [Schwartz et al., 2000]. LYC is commonly applicable for various chronic diseased conditions because of anti-diabetes, anti-inflammatory, anti-cancer, and antioxidant activities (Karas et al., 2000). Studies on tomato consumption in animals linked with a decreased malignancy in rodents. Epidemiologic studies also showed significant data that link tomato consumption and colon cancer development in humans. Lycopene (LYC) possesses powerful free radical scavenging property in the cells. In the previous chapters the antioxidant efficacy of LYC against stress-induced muscle cell, and food toxin mitigation against hepatotoxicity were investigated. LYC is mostly documented for its superior antioxidant property and cytoprotective abilities, though, under unbalanced and high intracellular stress conditions, LYC can also function as pro-oxidants. LYC is documented with potential antioxidant and cytoprotective properties, though, under unbalanced cellular stress mainly in cancer cells, in high oxygen tension, and low levels of antioxidants, LYC can function as pro-oxidants (Ribeiro et al., 2018; Arathi et al., 2016). Studies suggested that  $\beta$ -carotene (BCT) and LYC are strong antioxidants at low oxygen partial pressure ( $pO_2 < 150$ ) (Eghbaliferiz et al., 2016; Beutner et al. 2001). LYC can easily be autoxidized into a potent pro-oxidant at high  $pO_2$  (Eghbaliferiz et al., 2016; Beutner et al. 2001). LYC may act as pro-oxidants in relatively high intracellular ROS levels in cancer cells by triggering ROS-mediated apoptosis. The present study aimed to explore the efficacy of LYC on cell growth inhibition in the human colon cancer cell line (HCT-116) by focussing ROS dependent apoptosis. This chapter focused on the potential mechanisms of LYC, as a pro-oxidant by activating ROS generation in HCT 116 cells and the cells were investigated for their pro-apoptotic signalling induction and alterations on P13K/AKT/mTOR signalling.

## 4.2 Objective

- To investigate the antitumorigenic effect of LYC in HCT 116 (colon cancer cell line) (cells) via suppressing P13/AKT/mTOR signalling

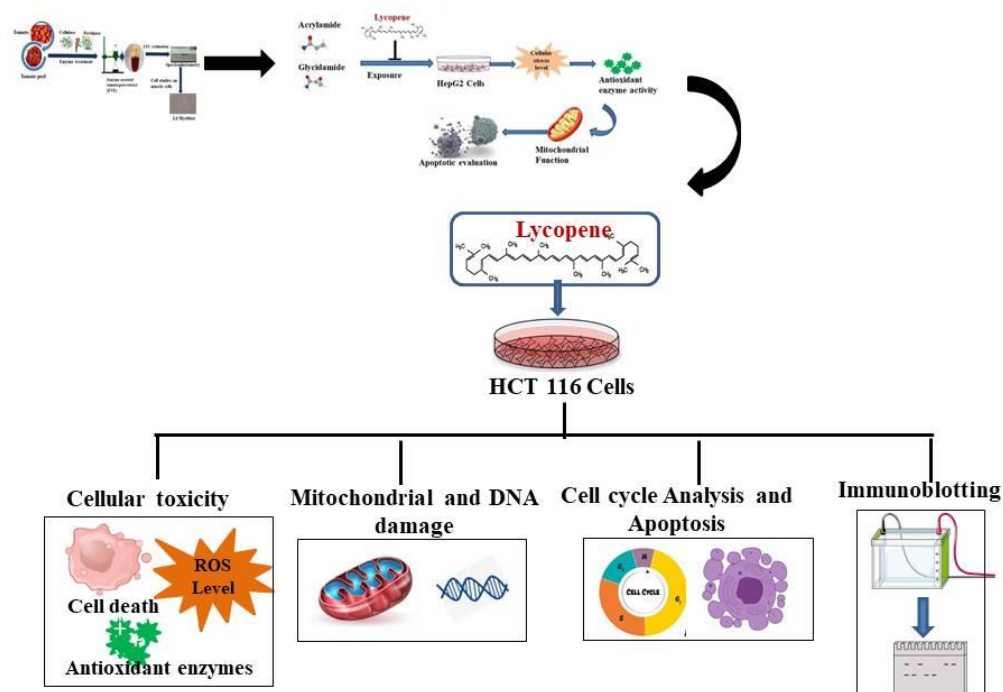


Fig 4.2: Schematic representation of methodology used for the objective

## 4.3 Materials and methods

### 4.3.1. Chemicals and Reagents

Lycopene, Dulbecco's modified eagle's media (DMEM), Dimethyl sulfoxide (DMSO), MTT (3-(4, 5-dimethylthiazol-2-yl)-2, 5-diphenyl tetrazolium bromide), 2,7-Dichlorodihydrofluorescein diacetate (DCFH-DA), Hoechst 33342, Rhodamine 123 (Rh123), Acridine orange, Propidium iodide, ethidium bromide and glutaraldehyde were obtained from Sigma-Aldrich Chemicals (St Louis, MO, USA) Fetal bovine serum (FBS), Trypsin-EDTA, Antibiotic-antimycotic was purchased from Gibco Invitrogen (Carlsbad, CA, USA). Ethylene diamine tetra acetic acid (EDTA), sodium chloride (NaCl), hydrogen peroxide ( $H_2O_2$ ), Triton X, Tris- HCl, perchloric acid, potassium hydroxide (KOH) from

MERK, India. Catalase Activity Colorimetric/Fluorometric Assay Kit, Glutathione (GSH) Colorimetric Assay Kit, Caspase 3 assay kit were purchased from Biovision Inc (San francisco, USA). Mitotracker-Red, DAPI were procured from Invitrogen. Annexin V – FITC was obtained from Cayman chemicals (MI-USA). BCA protein estimation kit, Primary antibodies ( $\beta$  actin, Bcl 2, Bax, P13K,p-P13K, Akt, p-Akt, m-TOR, p-mTOR) and secondary antibodies for immunoblotting were procured from Origin Diagnostics and Research, India. All other chemicals used were of the standard analytical grade.

### 4.3.2 Experimental Design

The experimental protocol for the study is given in Fig 4.3

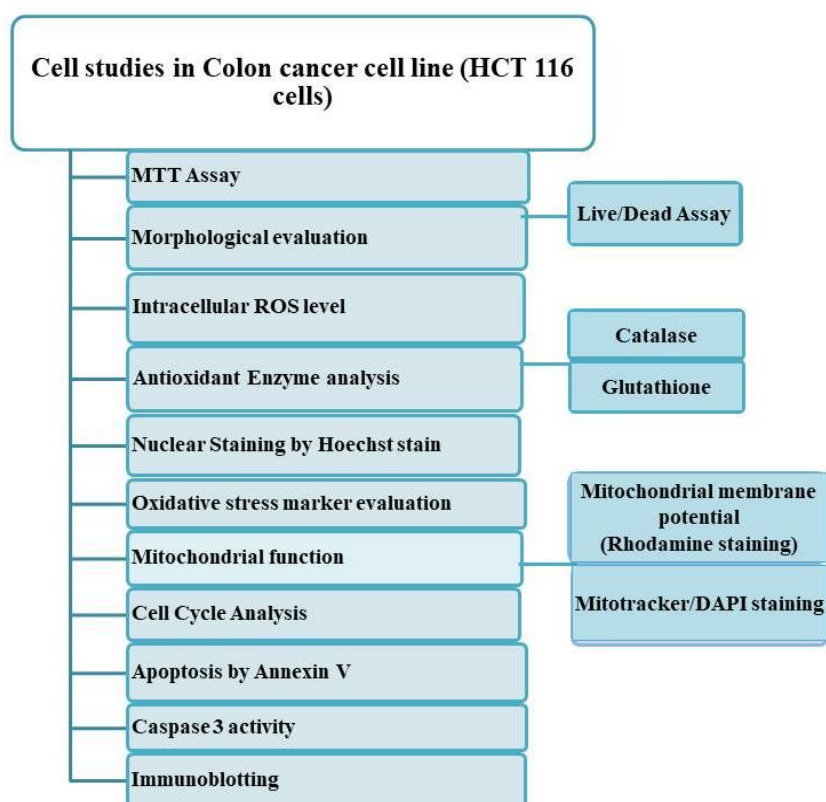


Fig 4.3: Experimental methods used for the study.

### **4.3.3 Cell culture and treatment conditions**

HCT 116 (human colon cell line) cells were purchased from NCCS, Pune, India. Cells were cultivated in DMEM with Fetal bovine serum (10%) and antibiotic-antimycotic (1%) solution at 37°C under 5% CO<sub>2</sub>. Cells were treated with different concentrations of LYC (5 µM, 10 µM, 15 µM) for 24 h and after treatment, the cells were trypsinized by using 0.25% Trypsin EDTA solution and resuspended in PBS for further studies.

### **4.3.4 Cytotoxicity by MTT assay**

The cytotoxicity of Lycopene (LYC) in HCT 116 cells was estimated using MTT assay (Mosmann, 1983). Briefly, after cellular treatment with LYC of different concentrations (5 µM, 10 µM, 15µM) for 24 h, cells were then exposed to MTT reagent (0.5 g/L) for 4 h. Media alone treated cells were taken as negative control, and H<sub>2</sub>O<sub>2</sub> (300 µM) treated cells as positive control. After incubation, reagent was removed and washed with 1X PBS and added DMSO (200 µL) to each well under gentle shaking (Orbit plate shaker, Labnet International, USA), and absorbance was read at 570 nm (Synergy 4 Biotek multiplate reader, USA). Each assay was done in three experiments, and the data are denoted as the mean ± SD, using the following calculation

### **4.3.5 Morphological analysis**

Cellular morphology of HCT 116 cells after sample treatment was observed by using phase-contrast microscopy. Different concentrations of LYC were incubated in cells under the above-mentioned conditions. The media were discarded after 24 h incubation with samples and washed thrice with PBS and visualized under phase contrast microscope

#### **4.3.6 Live/Dead Assay by AO/EtBr dual Staining**

Briefly, after treatment as per above mentioned treatment conditions, cells were stained with Acridine orange and Ethidium bromide for the detection of dead cells by analyzing the effect of LYC in cells (Pitchai et al., 2014). Based on apoptotic mediated cell death, changes in cell membranes indicate a clear distinction between normal cells, and apoptotic cells by AO/EtBr staining method. AO stained both live and dead cells, while EtBr stained only dead cells with compromised membrane integrity. The cell morphology after treatment was observed under a fluorescent microscope.

#### **4.3.7 Intracellular ROS levels.**

ROS levels in the cells were determined by DCFH-DA staining method (Cathcart, Schwiers, & Ames, 1983). After treatment, the cells were incubated with DCFH-DA for 20 min. For imaging, the cell medium with stain was removed and washed by using 1XPBS before fluorescent imaging. Quantitative analysis of ROS-generated in cells was measured by using FACS method. After 24 h cellular treatment and DCFH-DA staining, cells were harvested and evaluated by flow cytometric analysis (BD FACS Aria II, BD Biosciences, United States)

#### **4.3.8 Antioxidant enzyme analysis**

##### **4.3.8.1 Catalase (CAT) activity.**

Catalase activity in LYC treated cells was investigated by using Catalase colorimetric assay kit. As per the manufacturer's protocol, a Specific enzyme buffer solution was used for lysing the cells which were used for estimating the antioxidant activity. The negative control is cells without treatment and positive control with H<sub>2</sub>O<sub>2</sub> (300 μM) was also employed. The CAT activity in cells was quantified according to the Colorimetric Assay Kit (K773-100).



The absorbance was recorded by using spectrophotometry (Synergy 4 Biotek multiplate reader, USA.)

#### **4.3.8.2 Measurement of glutathione (GSH) level**

The cell lysate was prepared by lysis buffer as mentioned in the above experiment and the clear supernatant was analyzed for GSH level. The reduced GSH level of the treated lysates was found out based on the reaction of dithionitro benzoic acid (DTNB) with sulfhydryl groups that lead to the formation of yellow color. Glutathione assay kit was used for the estimation of glutathione levels following the manufacturer instructions provided along with the kit (K261-100). The absorbance was recorded by using spectrophotometry (Synergy 4 Biotek multiplate reader, USA).

#### **4.3.9 Nuclear Staining with Hoechst 33342**

The chromatin condensation ( nuclear morphology) of the treated cells was assessed by nuclear staining with a DNA dye, Hoechst 33342. DNA fragmentation (chromatin condensation) is considered as an apoptotic indicator. After the LYC treatment for 24 h, the cells were then washed off and add Hoechst 33342, a DNA-specific fluorescent dye( 10 µg/mL) and incubate in at 37°C for 10 m. The stained cells were then visualised under a fluorescence microscope to observe the degree of nuclear condensation.

#### **4.3.10 Mitochondrial membrane potential ( $\Delta\Psi_m$ ).**

LYC effect in the mitochondrial membrane was analyzed by using Rhodamine 123 staining. Increased cellular ROS production induces a loss in mitochondrial membrane potential, which leads to mitochondrial dysfunction. Rhodamine123, a fluorescent indicator used to monitor mitochondria based on the membrane potential was used for assessing the mitochondrial membrane potential (Zhang & Wang, 2008). One of the earliest changes that

occur in apoptosis is a change in mitochondrial transmembrane potential. Different concentration of LYC was added and incubated for 24 h. After treatment, the media was washed off and added 2  $\mu$ M Rhodamine 123 stain kept for 5min. After incubation, the fluorescence was quantitatively estimated by using Flow cytometric method (FACS Aria II, BD Bioscience, USA). Loss in mitochondrial membrane potential ( $\Delta\Psi_m$ ) is represented by decreased level of green rhodamine 123 fluorescence in cells.

#### **4.3.11 Mitotracker/DAPI staining**

The mitochondria permeability (integrity) of HCT 116 cells was observed by a mitotracker-red dye, using Fluorescent imaging (Pal et al., 2016). In brief, after LYC treatment for 24h, cells were dual stained with mitotracker (100 mM) for 15 min and washed twice with 1X PBS, and then incubated with DAPI (0.1  $\mu$ g/mL) at RT for 5 min. DAPI stains cellular DNA and the images were acquired by using a fluorescence microscope.

#### **4.3.12 Apoptosis by Flow Cytometry Analysis**

To quantify cellular apoptosis in HCT 116 cells, Annexin-V/PI staining was carried out. Briefly, after the treatment conditions described above, the cells were trypsinized and centrifuged for 5 min at 2300 rpm. Then the cells were washed with 1X PBS, suspended in binding buffer, and centrifuged at 400xg for 5min. Then the cell suspensions were stained with Annexin V-FITC and PI and incubated on ice for 10 min at RT in the dark. After incubation, the samples were resuspended in binding buffer and quantified using FACS (BD FACS Aria II, BD Biosciences, United States). As per manufacturer instructions, the apoptotic cell ratio was quantified using flow cytometric methods with 10000 cells in each group. The data analysis was done using BD FACS Diva™ Software 6.1.2

#### **4.3.13 Caspase-3 Assay**

Caspase-3 activity was analyzed by Assay Kit which recognizes the sequence DEVD (Abcam, USA). Briefly, after cell culture treatment, the sample lysate was added to the wells and incubated with reaction buffer and DEVD-p-NA substrate for 60 min at 37°C. Then the reaction absorbance was analyzed by spectrophotometer at 400nm (Synergy 4 Biotek, USA).

#### **4.3.14 Immunoblot analysis**

Briefly, after LYC treatment conditions, the cells were harvested and lysed with lysis buffer (protease inhibitor cocktail). The specific antibodies against -  $\beta$ -actin, BCL2, Bax, P13K, p-P13K, Akt, p-Akt, m-TOR, and p-mTOR were used as primary antibodies. BCA protein assay kit was used to quantify the protein concentration in lysate. The extracted protein in reducing buffer was boiled at 75°C for 10 min. Then the protein was subjected to SDS-PAGE, (10% SDS polyacrylamide gel), and then transferred to a PVDF transfer membrane (Immobilon P™, Millipore 154 R, the USA) by transfer system (Bio-Rad Laboratories, Germany). 5% skim milk in PBST blocking buffer containing 0.1% Tween was used to block the membrane by incubating for 1 h at RT. After that washed with PBST and kept overnight at 4°C with primary antibodies ( $\beta$ -actin, BCL2, BAX, P13K, p-P13K, Akt, p-Akt, m-TOR, p-mTOR) in the ratio 1:1000. After washing, the membrane was incubated with IgG-HRP secondary antibody (1:2000). The blots bound antibodies were detected using DAB-Peroxidase substrate solution by chemiluminescence (Bio-Rad, United States) and measured by densitometry using a ChemiDoc XRS digital imaging system and the Multi-Analyst software from Bio-Rad Laboratories (United States). The density of specific protein bands was compared to that of the housekeeping gene -  $\beta$  actin

#### **4.3.15 Cell cycle analysis**

Cell cycle arrest was analysed by propidium iodide (PI) staining. HCT 116 cells were treated with different concentrations of LYC for 24 h. After incubation, the cells were washed and then collected and fixed using 70% ethanol, mix gently and kept under the ice for 30 min. Then the samples were centrifuged for 5 min at 2000 rpm. Further, resuspended the cells in PBS and added 5  $\mu$ L RNase A. Again incubate the samples for 30 min at 37 °C, then add 10  $\mu$ l PI and kept for 30 min in dark at 4°C. Then again the cells were washed and then centrifuged for 5 min at 1500 rpm. The cell pellet was further resuspended in PBS and quantified in FACS (BD FACS Aria II, BD Biosciences, United States).

#### **4.3.16 Statistical analysis**

Data represented as mean  $\pm$  standard deviations of experiments in triplicates. One-way ANOVA was used for analyzing the results and Duncan's multiple range tests was employed for assessing the significance using SPSS 16.0. The significance was accepted at  $P \leq 0.05$ .

### **4.4 Results & Discussion**

#### **4.4.1 LYC reduces cell viability in HCT 116 Cells**

To investigate the antitumorigenic effect of LYC in HCT 116 cells (colon cancer cell line), LYC was initially verified for its cellular toxicity by using MTT assay. The cytotoxic effect of LYC at different concentrations (5  $\mu$ M, 10  $\mu$ M, 15  $\mu$ M) on HCT 116 cell was analysed. Untreated cells taken as negative control and H<sub>2</sub>O<sub>2</sub> (300  $\mu$ M) treated cells were taken as the positive control. Because of the wide cytotoxic effect in all cell types, H<sub>2</sub>O<sub>2</sub> was taken as the positive control, and it was reported as a good apoptotic inducer (Liu et al., 2013). The OD value of negative control cells was taken as 100% and then calculated the percentage reduction of OD in treated cells. MTT assay suggested that LYC exhibits a gradual increase

in cytotoxic effect in HCT 116 cells when exposed to lower to higher LYC concentrations of 5  $\mu$ M, 10  $\mu$ M, and 15  $\mu$ M in which the cell viability seems to be decreased as 91%, 68%, and 44%, respectively (Fig 4.4). It was observed that LYC inhibited HCT 116 cell viability in a concentration-dependent manner and its 50% inhibition rate of LYC on HCT 116 cells was at 12.5  $\mu$ M concentration after 24 h treatment.

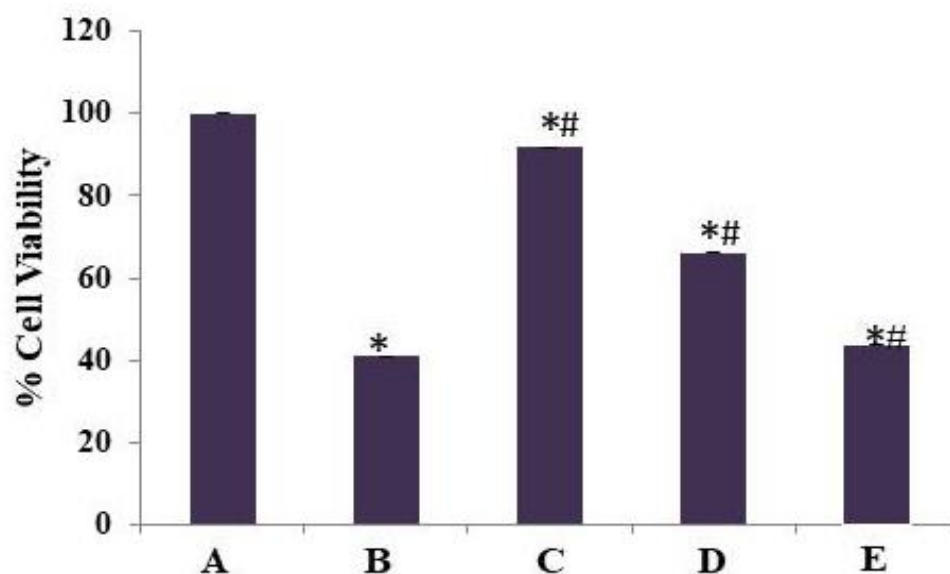


Fig 4.4: The Effect of LYC on HCT 116 cell viability by MTT assay. Bar diagram represent A- negative control, B- H<sub>2</sub>O<sub>2</sub> (300  $\mu$ M), C- 5  $\mu$ M LYC, D- 10  $\mu$ M LYC, E-15  $\mu$ M LYC. Data represents the mean  $\pm$  SD and significance between groups were analysed by one way ANOVA, followed by Duncan's multiple range test \* $p \leq 0.05$  versus control; # $p \leq 0.05$  versus control H<sub>2</sub>O<sub>2</sub>.

As shown in Fig 4.4, the 5  $\mu$ M LYC exposure in the culture moderately inhibited cell growth, while a more intense inhibition was visible in 15  $\mu$ M LYC exposed cells. Studies reported the cytotoxic effect of LYC in various cancer cell lines promoting antitumorigenic property (Magne et al., 2022; Khan et al., 2022; Langner et al., 2019). The anticancer effect of LYC was reported as dose and time dependent activity in cells with considerable

decrease in viable cells on different tumour cells (T84, HT-29, and MCF-7) (Wang et al., 2021). The data showed that the effect of LYC on the viability of cells is significant ( $p \leq 0.05$ ). The results indicated that LYC had a significant inhibitory effect on the HCT 116 proliferation, suggesting that LYC could efficiently inhibit cellular proliferation (Fig 4.4).

#### 4.4.2 Cell morphology by phase contrast microscope

After LYC exposure cell morphology of HCT 116 cell lines was observed by using a phase contrast microscope. As shown in Fig 4.5, LYC reduced the cell number and the cellular morphology seemed to be distorted and became round in shape. Morphology shows a minor change at the lower concentration of 5  $\mu\text{M}$  LYC treatment but at 15  $\mu\text{M}$  treated cells, morphology became a round shape and detached from the plate by losing its adherence and cell-cell connectivity.

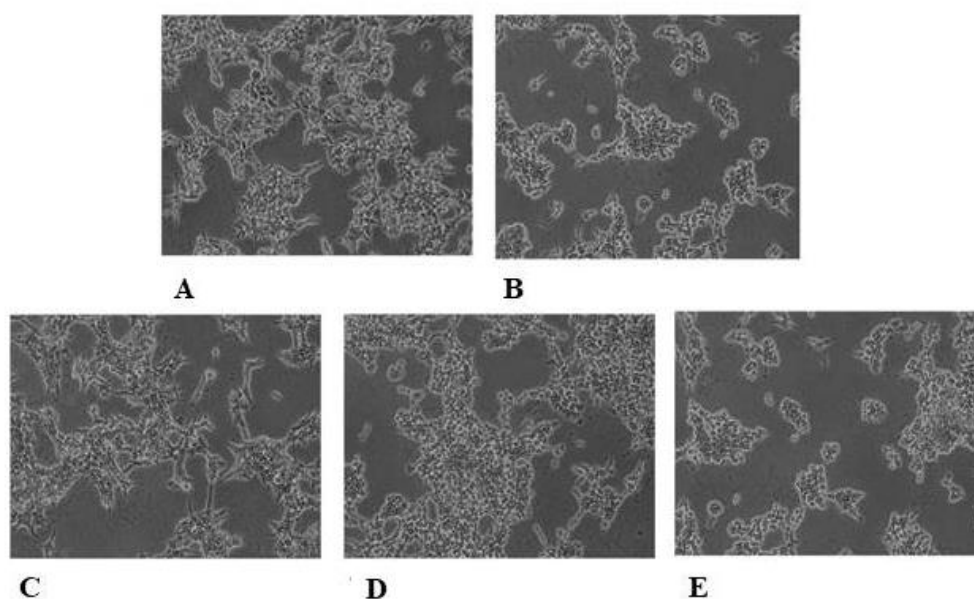


Fig 4.5: Morphological analysis of HCT 116 cells by phase-contrast microscopy: Images depict A- negative control, B-  $\text{H}_2\text{O}_2$  (300  $\mu\text{M}$ ), C- 5  $\mu\text{M}$  LYC, D- 10  $\mu\text{M}$  LYC, E-15  $\mu\text{M}$  LYC. Original magnification, 40X.

A declined cell number and higher degree of cell shrinkage indicates an increasing progression toward cell death. Meanwhile, in the untreated cell group, the cells displayed a cellular morphology of intact nucleus, cytoplasm, and cell membrane displayed active cells. Major characteristic features reported for an apoptotic cell include cell shrinkage, apoptotic body formation, alteration in cell shape, disconnection between neighbouring cells; etc (Zhang et al., 2022) According to the morphological observations in this study, the cytotoxicity of LYC is compatible with the morphological changes in dose-dependent way.

#### **4.4.3 Live/Dead assay by AO/EtBr dual staining**

The identification of live and dead cells using fluorescence microscopy was performed with AO/EtBr double staining method. In this method, AO stained both live and dead cells while EtBr stained only dead cells with depleted membrane integrity. Under fluorescent emission, AO-stained live cells exhibit green fluorescence, whereas EtBr-stained non-viable cells emit red fluorescence. Hence, the active cells are with green coloured nucleus and the green-yellow dots can be seen in early apoptotic nuclei and orange in late apoptotic cells indicating fragmented or condensed nuclei. After treatment, the morphological observation of HCT 116 cells was visualised using fluorescent microscope for control and 15 $\mu$ M LYC treated cells are represented in Fig 4.6. The cells with 15 $\mu$ M LYC exhibited variations in stained cellular nuclei when compared to the control cells. From the Fig 4.6, the control cells seemed to be stained by AO, and emit green fluorescence with an intact nucleus. The LYC (15  $\mu$ M) exposed cells displayed an early and late apoptotic nuclei stained in yellow and orange dots exhibited nuclear condensation, a remarkable apoptotic feature. The cell death mechanism (apoptosis or necrosis) of HCT 116 cells induced by LYC was further established by apoptotic evaluation using Annexin V/Propidium Iodide staining

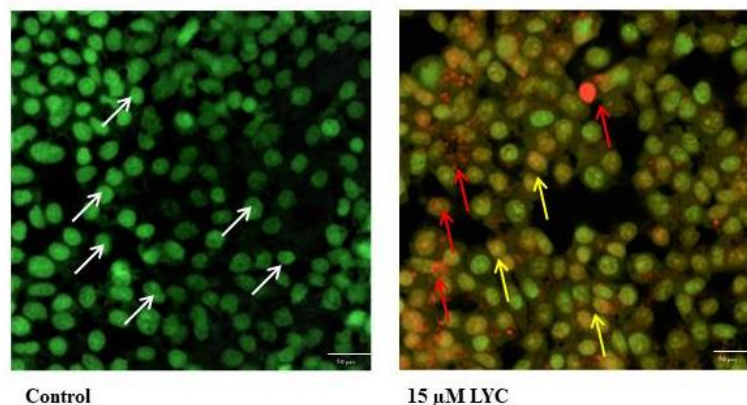


Fig 4.6: Live and dead cell analysis by AO/EtBr double staining visualised using fluorescent microscopy in HCT 116 cells treated with 15  $\mu$ M LYC. Control cells are visible in intact green colour indicated by white arrow; early apoptotic cells appear in greenish yellow indicated by yellow arrow; late apoptotic cells appear in orange or red colour indicated by red arrow. Original magnification 40x.

#### 4. 4.4 Measurement of intracellular ROS level in HCT 116 cells

The amount of oxidative stress after LYC treatment was analysed by intracellular ROS level on HCT 116 cells using flow cytometric method. Tumour cells are sensitive to ROS compared to normal cells and the rapid increase in the ROS level mediate proapoptotic effects in cancer cells (Engel and Evens, 2006; Gallego et al., 2008). ROS accumulation inside the cells was identified by using redox sensitive fluorescent labelled DCF-DA staining. HCT 116 cells were treated with different concentrations of LYC and as positive control,  $H_2O_2$  (300  $\mu$ M) measured for its fluorescent intensity. Cells treated with 5, 10, and 15  $\mu$ M LYC give rise to increase in intracellular ROS level by 13.1, 24.1 and 32.6%, respectively (Fig 4.7). LYC displayed a significant increase in the ROS level to 32% in LYC (15  $\mu$ M)-treated group after 24 h exposure compared to untreated cells with ROS 5.4%. Elevated intracellular ROS level damages cellular biomolecules via activation of a series of signalling cascades including mitochondrial mediated apoptosis and PI3K/Akt pathways (Dasari et al., 2014). Extensive scientific interest is shown recently on ROS and



mitochondria, their fundamental role in apoptosis in many chronic disease conditions. Cellular ROS is an intrinsic stimulus that rapidly activates the mitochondrial pathway in direct or indirect approach. As seen from the data, increased ROS level in cells expected to exhibit the anticancer effects of LYC linked to ROS mediated cell death. The results supported that LYC increases ROS level in cells in dose dependent way and which seems to be a critical factor for HCT 116 cell death

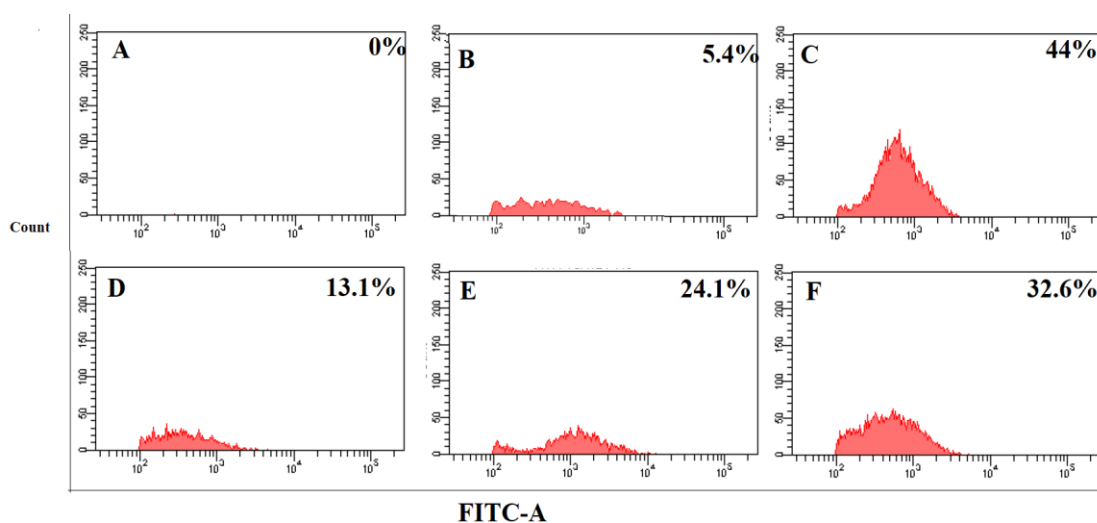


Fig 4.7: Estimation of ROS level by DCFH-DA staining. HCT 116 cells were exposed with different LYC concentrations (5, 10, and 15 μM) and H<sub>2</sub>O<sub>2</sub> (300 μM). After incubation, cells were stained with DCFH-DA and quantified using flow cytometer. A- Blank, B-negative control, C- H<sub>2</sub>O<sub>2</sub> (300 μM), D- 5 μM LYC, E- 10 μM LYC, F-15 μM LYC.

#### 4.4.5 LYC reduced Antioxidant enzyme activity in HCT 116

The role LYC in the alterations of antioxidant enzyme was investigated in HCT 116 cells, CAT and GSH content were estimated. It is well studied that a decreased cellular GSH levels is linked with ROS-mediated apoptosis by ROS-induced GSH oxidation in cells (Lu and Armstrong, 2007). The efficacy of ROS mediated apoptosis in cells exhibit an inactivation of intracellular catalase activity (Lu and Armstrong, 2007). After LYC

treatment, the results indicated a significant reduction in both CAT and GSH levels in HCT 116 cells, in a concentration dependent mode when compared to untreated cells ( $p \leq 0.05$ ). From the Fig 4.8, it may be noted that the cells treated with 15  $\mu\text{M}$  LYC showed a maximum decline in CAT and GSH activity level, compared to that of positive control used ( $p \leq 0.05$ ). Cancer cells with elevated antioxidant enzyme systems have been believed to initiates chemoresistance in cells (Derdak et al., 2008). Therefore, the oxidative stress modulation has been suggested as a remarkable approach for anticancer drugs. Intracellular ROS level and innate antioxidant enzyme system play a significant role in maintaining cellular redox system.

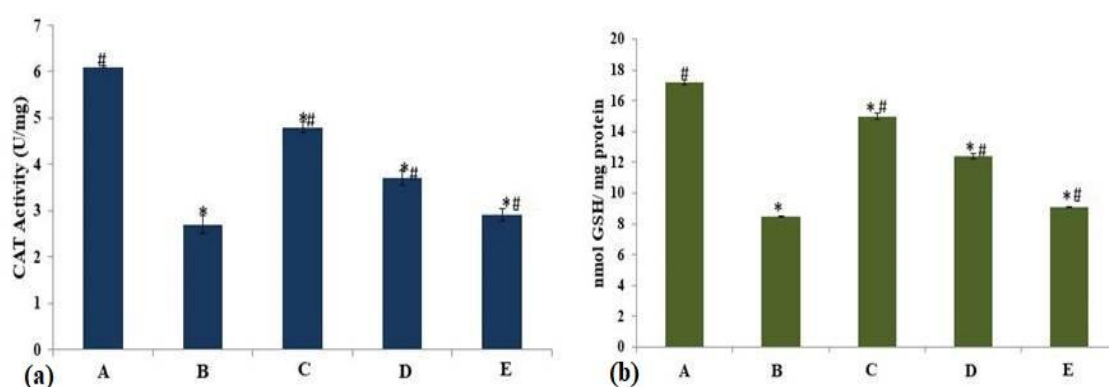


Fig 4.8: The levels of catalase activity and reduced glutathione were examined after treatment with LYC (5, 10, and 15  $\mu\text{M}$ ) and  $\text{H}_2\text{O}_2$  (300  $\mu\text{M}$ ). Figure (a) represent CAT activity, (b) represent GSH level. A- Negative control, B-  $\text{H}_2\text{O}_2$  (300  $\mu\text{M}$ ), C- 5  $\mu\text{M}$  LYC, D- 10  $\mu\text{M}$  LYC, E-15  $\mu\text{M}$  LYC. Data represents mean  $\pm$  SD from triplicate and significance were determined by one way ANOVA, followed by Duncan's multiple range test. \* $p \leq 0.05$  versus control, # $p \leq 0.05$  versus  $\text{H}_2\text{O}_2$ .

Under OS conditions, this ROS- antioxidant balance is disturbed and it can be seen in most of the cancer cells which make them more susceptible to further stress. Thus, any compounds that enhance intracellular ROS level in cancer cells leads to an increase in toxic

level result in cell death (Pramanik et al., 2011). The estimation of antioxidant enzyme showed that both CAT activity and GSH level decreased on treatment with 15  $\mu\text{M}$  LYC, similar to the of positive control ( $\text{H}_2\text{O}_2$  300  $\mu\text{M}$ ) (Fig 4.8). In the present study, an augmented ROS level along with reduced antioxidant enzyme status in LYC treated cells lead to the induction of ROS-mediated cell death in HCT 116 colon cancer cells.

#### 4.4.6 LYC promotes nuclear fragmentation in HCT 116 cells

Hoechst 33342 specifically binds on the minor groove of AT-rich region of DNA. The major hallmark of apoptosis include nuclear changes like DNA fragmentation and chromatin condensation, were determined by Hoechst 33342 staining. From the Fig 4.9 it can be noted that the control cells persisted an evenly stained intact nucleus and emitted a blue fluorescence demonstrating that the nuclei contain equally distributed chromatin. Meanwhile, LYC treated with different concentrations (5, 10, and 15  $\mu\text{M}$ ) exhibit highly condensed nucleus or fragmented chromatin indicated apoptosis induction in HCT 116 cells.

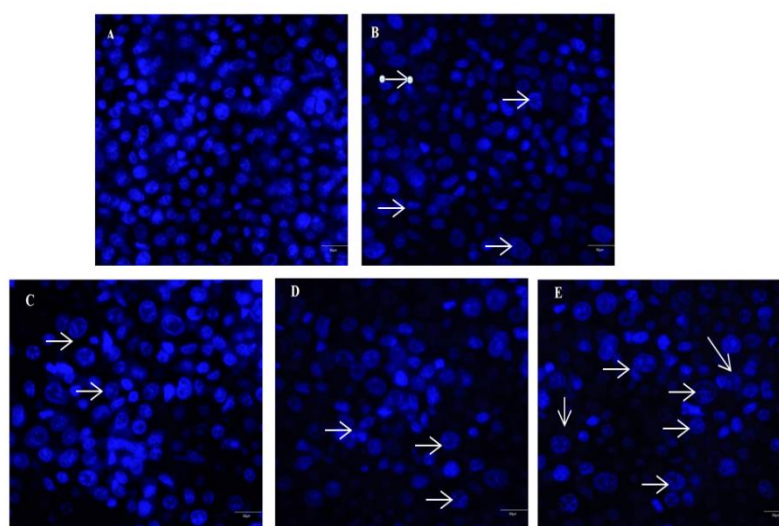


Fig 4.9: Chromatin condensation detected by Hoechst 33342 staining, arrows represent the cells with chromatin condensation inside the nucleus. A- Negative control, B-  $\text{H}_2\text{O}_2$  (300  $\mu\text{M}$ ), C- 5  $\mu\text{M}$  LYC, D- 10  $\mu\text{M}$  LYC, E-15  $\mu\text{M}$  LYC.

The LYC demonstrated a remarkable nuclear change of apoptosis with the increase in formation of apoptotic bodies and nuclear fragmentations. As visible in the Fig 4.9, the number of apoptotic cells or chromatin condensed cells was increased with the increase in LYC concentration. The apoptosis was further confirmation in the cells by Annexin V/PI staining.

#### **4.4.7 LYC Induced MMP Loss in HCT 116 cells**

Mitochondria play a significant role in bioenergetics and homeostasis in cells, during cell proliferation. In recent times, it is recognised as a innovative target for drug-induced apoptosis in cells. It plays an important role in apoptotic pathway by act as a centre of apoptotic signals for both (intrinsic and extrinsic)apoptotic cascade. Mitochondrial membrane potential is a vital indicator of mitochondrial function. Loss in mitochondrial membrane potential is mainly due to distracted mitochondrial membrane permeability, which is considered as an indicative of apoptosis. So, to evaluate the role of LYC treatment in mitochondrial induced apoptosis, the cells were treated with different concentration of LYC in HCT 116 cells. Mitochondrial membrane potential level was measured using rhodamine 123 stain. In active cell with intact mitochondrial membrane, Rh123 dye enters and retained in the mitochondria. The percentage loss of mitochondrial membrane potential is represented in the flow cytometric graph (Fig 4.10). From the Fig 4.10 the results showed that the loss of MMP in HCT 116 colon cancer cells was increased on treatment with LYC. The fluorescence increased in a dose dependent manner to 24.5, 37.9, and 55.4%, on treatment with 5, 10, and 15  $\mu$ M respectively. In the present study, a substantial reduction in mitochondrial membrane potential was detected in HCT 116 cells on LYC treatment. As showed in cytometric graph, LYC treatment at 15  $\mu$ M exhibited an increase in the loss of mitochondrial membrane potential similar to that of positive control  $H_2O_2$ . The decreased MMP in HCT 116 cells can lead to LYC-induced mitochondrial dysfunction and then

apoptosis induction. Mitochondrial apoptotic pathway is mostly triggered by a decrease in MMP and enhanced ROS production. To confirm this further mitotracker/DAPI staining dual staining was carried out.

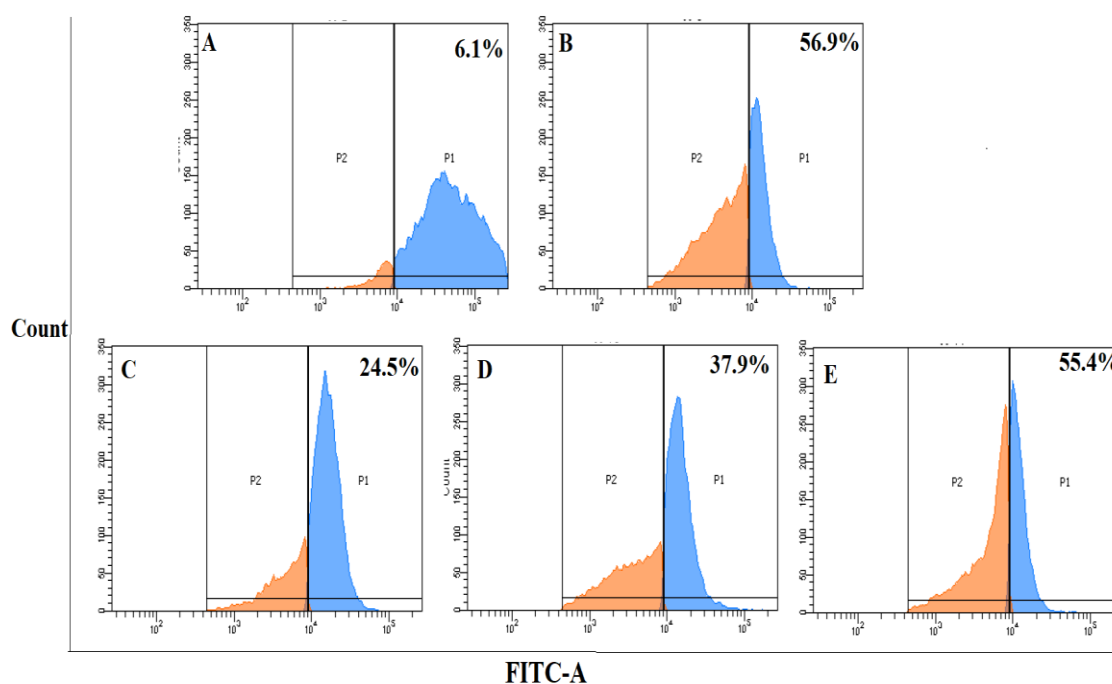


Fig 4.10: Mitochondrial membrane potential loss was quantified by Rhodamine 123 staining. HCT 116 cells were treated with LYC (5, 10, and 15  $\mu$ M) and  $H_2O_2$  (300  $\mu$ M). After LYC treatment, cells were stained with Rhodamine 123 and evaluated using flow cytometer.

#### 4.4.8 Mitotracker/DAPI Staining

The excess production of ROS leads to mitochondrial membrane disruption and loss in membrane permeability leading to mitochondrial dysfunction. To further confirm MMP loss, the HCT 1116 cells were stained with mitotracker/DAPI dual staining. Mitotracker is a red fluorescent dye, which binds to the mitochondrial membrane depends on mitochondrial integrity and DAPI is a DNA binding stain used to visualize DNA damages. The mitochondrial membranes of the control cells were intact, while in LYC exposure (5, 10, and 15  $\mu$ M) displayed loss of membrane integrity in a concentration dependent manner.

From the Fig 4.11, LYC at concentration of 15  $\mu\text{M}$  showed a higher degree of ruptured mitochondria in cells. The mitochondrial-mediated cell death in LYC treated cells are closely linked with increased levels of ROS. Several natural components found to be reported reduction in mitochondrial integrity leading to apoptosis (Qui et al., 2018). The MMP disturbance is an early indication of mitochondrial changes. The MMP ( $\Delta\psi\text{m}$ ) stability is highly dependent on mitochondrial membrane integrity and elevated ROS in cells trigger the opening of the mitochondrial transition pore which leads to an MMP loss (Wang et al., 2012).

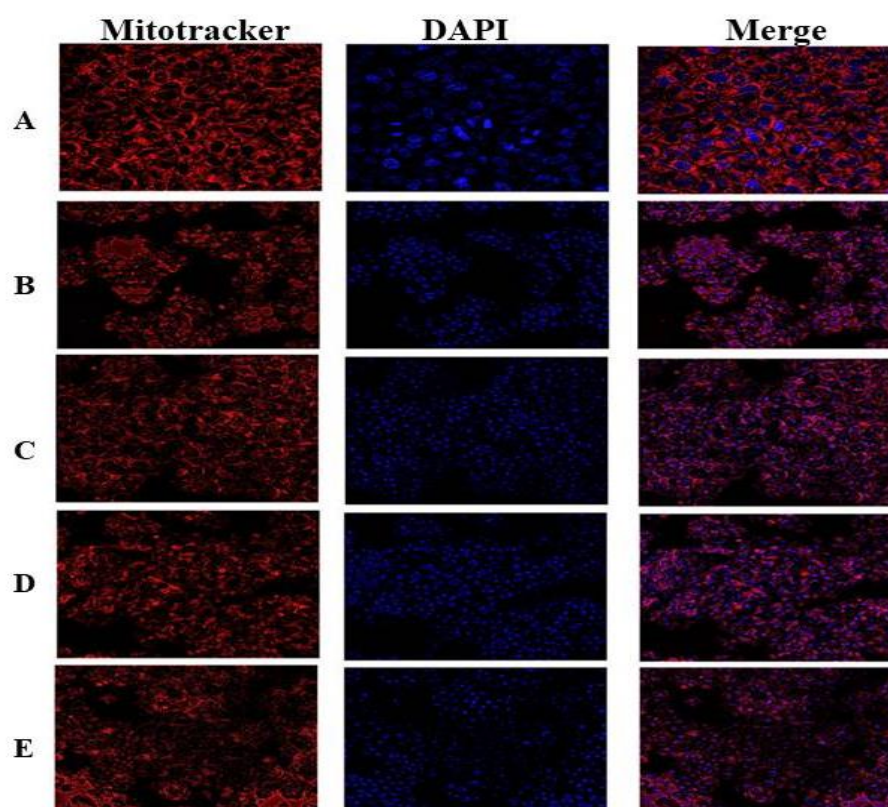


Fig 4.11: Staining of HCT 116 cells with mitotracker Red and DAPI dual staining. A- Negative control, B-  $\text{H}_2\text{O}_2$  (300  $\mu\text{M}$ ), C- 5  $\mu\text{M}$  LYC, D- 10  $\mu\text{M}$  LYC, E-15  $\mu\text{M}$  LYC. The  $\text{H}_2\text{O}_2$  and 15  $\mu\text{M}$  LYC treated shows the high number of damaged mitochondria that related to higher cell death.

#### **4.4.9 LYC promotes apoptosis in HCT 116 cells**

Previous studies explored the LYC effect in HCT 116 by a noted decrease in mitochondrial membrane potential, which point out a reduction in mitochondrial membrane integrity, is regarded as the prime centre for apoptosis activation. Annexin V–FITC/PI staining was conducted to explore the role of LYC on mitochondrial mediated cellular apoptosis in HCT 116 cells. Apoptosis is one of is a promising target in anticancer therapy, which is considered as one of the hallmarks of cancer drug, Briefly, the cells were treated with different concentrations of LYC (5, 10, and 15  $\mu\text{M}$ ) for 24 h and subjected to flow cytometric analysis. As shown in Fig 4.12, the percentage of total apoptotic cells (early and late apoptosis) was increased in a concentration dependent manner after LYC treatment. It was demonstrated that LYC promoted the apoptosis of HCT 116 cells (Fig 4.12). Flow cytometric data represent the percentages of both early and late apoptotic cells in 15  $\mu\text{M}$  LYC treated cells were 36 and 14.8%. As can be seen, the apoptotic cells in the late apoptotic stage increased from 4.4% in the control cells to 14.8% in LYC treated cells (15  $\mu\text{M}$  LYC). Studies reported that lycopene inhibits cell growth through multiple mechanisms such as growth factor regulation, cell cycle arrest, and/or apoptosis induction in the colon cancer cell (HT29) (Wang et al., 2021; Ono et al., 2015). Reports suggest that phytochemicals including carotenoids can induce the activation of intrinsic or extrinsic apoptosis in cancer cells (Pfeffer et al., 2018; Koklesova et al., 2020). The results obtained from MMP positively correlated with increase in apoptosis and MMP loss. Chemopreventive role of LYC induces apoptosis in chemically induced colon carcinogenesis in rat via alteration in nitric oxide synthase pathways (Magne et al., 2022). To determine the mechanisms of apoptosis induced by LYC, the activity level of caspases-3 was further analysed.

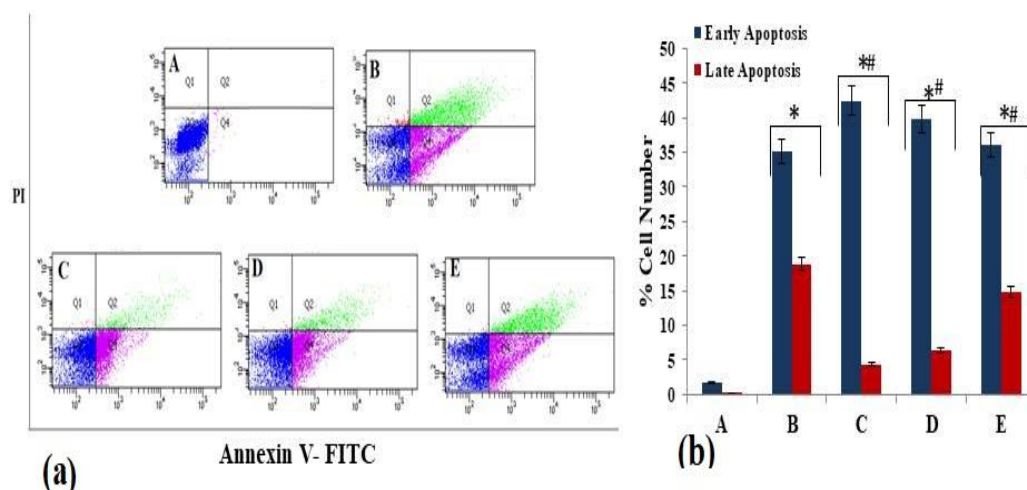


Fig 4.12: Effect of LYC on HCT 116 cell apoptosis. (A) Representative flow cytometry graphs of HCT 116 cells show the Q2 quadrant indicates late apoptosis and the Q4 quadrant indicate early apoptosis, Images represent A- negative control, B- H<sub>2</sub>O<sub>2</sub> ( 300 μM), C- 5 μM LYC, D- 10 μM LYC, E-15 μM LYC and (B) the apoptosis rate was expressed in %. Data are presented as the mean ± SD. \*P<0.05 versus control group and #P<0.05 H<sub>2</sub>O<sub>2</sub> treated group

#### 4.4.10 LYC initiates caspase 3 activity

Caspase-3 (Executioner caspase) is a key protein expressed in various cellular damages by initiating the apoptotic process (programmed cell death). It has been identified as key protein involved in the final stages of the apoptotic cascade known as executioner caspase (Porter et al., 2000). In the present study, the data revealed that the caspase 3 activity is slightly higher in 15 μM LYC exposed cells (26.2 ± 0.71%) than positive control H<sub>2</sub>O<sub>2</sub> (300 μM) (25 ± 0.96%). The LYC (5, 10, and 15 μM) treated cells noticeably increases the caspase-3 activity in a dose dependent manner with 10.8, 18.1 and 26.2% respectively (Fig 4.13). The remarkable increase in caspase-3 activity offers cell death by apoptosis and also it provides a shred of evidence for its mitochondrial mediated (intrinsic) apoptosis induction in



cells. The proteins expressed in apoptotic cells were further confirmed by immunoblotting focusing on PI3K/AKT/mTOR signalling.

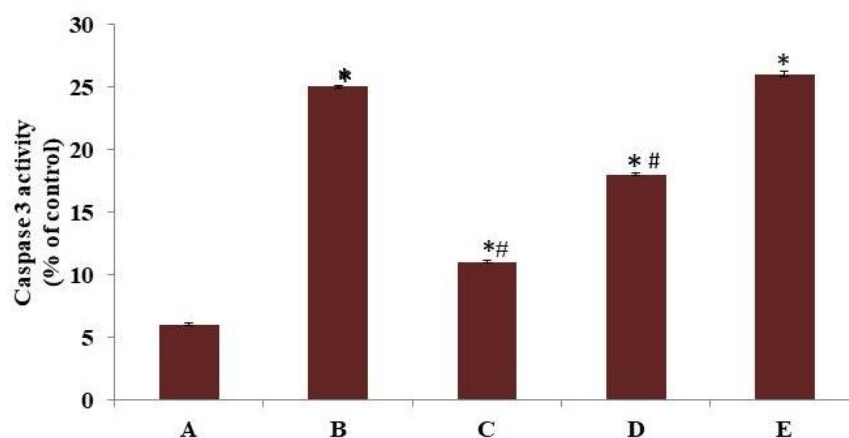


Fig 4.13: Bar diagram represent the caspase 3 activity in percentage with respect to control. The bar depict A- negative control, B- H<sub>2</sub>O<sub>2</sub> ( 300 μM), C- 5 μM LYC, D- 10 μM LYC, E- 15 μM LYC. Each value denotes the mean ± SD of triplicate. Significance levels determined by using one-way ANOVA, \*P ≤ 0.05 versus Control; #P ≤ 0.05 versus H<sub>2</sub>O<sub>2</sub>

#### 4.4.11 LYC inhibit PI3K/AKT/mTOR signalling pathway

The PI3K (Phosphoinositide 3-kinase), AKT (Protein Kinase B) and mTOR (mammalian target of rapamycin) signalling pathway shows a vital role in cell growth, proliferation, migration, and even in invasion (Murugan, 2019). These key proteins including their phosphorylation status were expressed by western blot assay, which are presented in the Fig 4.14. PI3K/AKT/mTOR promotes cell survival or cell proliferation via direct phosphorylation of the Bcl-2 family proteins (primary regulators) of the apoptosis pathway. Activated phosphorylated forms of these proteins (PI3K/AKT/mTOR) are linked with the dissociation of antiapoptotic protein (Bcl-2) protein, which effectively blocks apoptosis. After LYC treatment (5μM, 10μM, and 15μM), the protein expression levels of PI3K,

(phosphorylated) p-PI3K, AKT, (phosphorylated) p-AKT, mTOR and (phosphorylated) p-mTOR were identified using western blot assay. The downregulation of the PI3K/AKT/mTOR pathway is crucial in human oncogenesis, and as a chief effector of this signalling pathway, mTOR is broadly associated with cell transformation, proliferation, and survival. However, with increasing LYC concentrations the expression levels of p-PI3K, p-AKT and p-mTOR were significantly downregulated in HCT 116 cells (Fig 4.14a). This finding indicated that inhibition of the PI3K pathway by LYC is the underlying mechanism involved in HCT 116 apoptosis. After calculating the ratios of p-PI3K/PI3K, p-AKT/AKT and p-mTOR/mTOR, it was found that these three phosphorylated proteins were downregulated with increasing LYC concentrations in HCT 116 cells (Fig 4.14b). These results indicated that LYC has a dose-dependent inhibitory effect on the PI3K/AKT/mTOR signalling pathway in HCT 116 cells. Phosphorylated proteins help in cell proliferation and survival by activating Bcl-2 proteins and inhibiting Bax proteins. Therefore higher phosphorylated form of proteins (PI3K/AKT/mTOR) depicts an increased cell survival and apoptosis inhibition. From the blotting results showed the LYC inhibit the activation of PI3K/AKT/mTOR to its phosphorylated form in HCT 116 cells in a dose dependent manner. The PI3K/AKT/mTOR cascade is an important pathway for suppressing cellular functions (Pandurangan, 2021; Chen et al., 2018). The pro and anti-apoptotic proteins such as Bax and Bcl-2 are involved with the PI3K/AKT/mTOR signalling. Therefore, in this study the expression levels of Bax, and Bcl-2 were also investigated. The Data indicated that LYC successfully stimulated the expression of the pro apoptotic Bax, but inhibited the expression of anti-apoptotic Bcl-2 in a concentration-dependent mode (Fig 4.14). Higher Bax expression represents induction of apoptosis, while decreased Bcl-2 expression demonstrates a reduced capability to inhibit apoptosis. Bax is a pro-apoptotic member of the Bcl-2 family and it is closely related to PI3K pathway. From the blotting results, LYC suppressed the

activation of PI3K pathway and is verified by analysing changes in the expression levels of PI3K, p-PI3K, AKT, p-AKT, mTOR, p-mTOR, Bax and Bcl-2. Similar study by Cheng et al reported that Naringin promoted HT29 cell apoptosis by inhibiting PI3K/AKT/mTOR pathway (Chen et al., 2020). Also a study on CC139 fibroblast cells, found that PI3K inhibitors treated cells showed a downregulation of Bcl-2 and promote apoptosis (Wang et al., 2020). Another study by Liu et al reported that the pretreatment with the N-acetyl-L-cysteine (ROS scavenger) alleviate apoptosis and restored the level of phosphorylated AKT, indicating that ROS is an upstream regulator of the PI3K/AKT pathway (Liu et al., 2021). From the results, LYC induces apoptosis via intrinsic pathway and also suppressed the proteins involved in PI3K/AKT/mTOR pathway leading to the activation of apoptosis in HCT 116 cells.

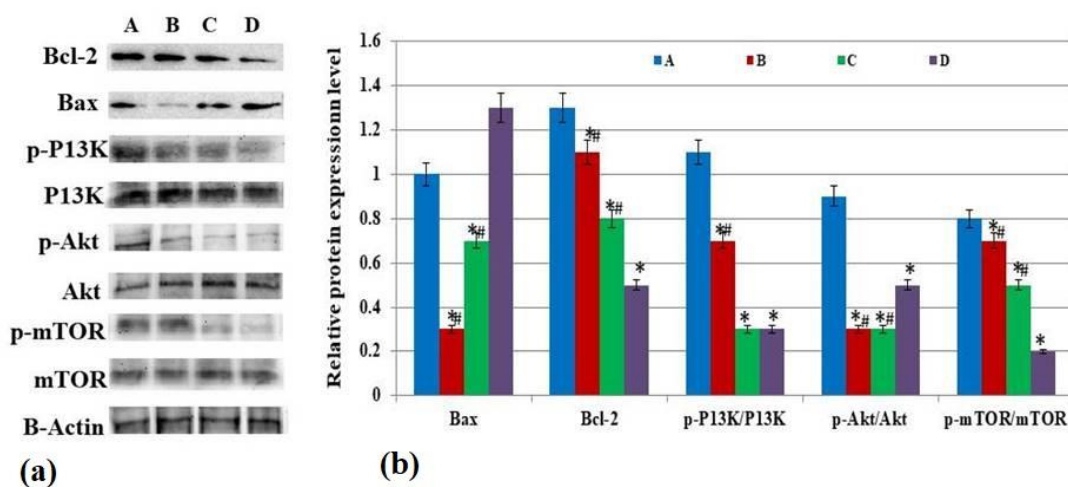


Fig 4.14: Effect of LYC on the protein expression level in PI3K/AKT/mTOR pathway in HCT 116 cells. Western blot analysis for the expression of, Bcl-2, Bax, PI3K, p-PI3K, Akt, p-Akt, mTOR, p-mTOR was carried out. The alphabet denotes A- negative control, B- H<sub>2</sub>O<sub>2</sub> (300 μM), C- 5 μM LYC, D- 10 μM LYC, E-15 μM LYC. (a) Represent the protein expression level (b) represents the quantification of expressed proteins Bcl-2, Bax, the ratio

of PI3K/p-PI3K, the ratio of Akt/p-Akt, the ratio of mTOR/p-mTOR. Data were expressed as mean $\pm$  SD, \*P  $\leq$  0.05 versus Control; #P  $\leq$  0.05 versus H<sub>2</sub>O<sub>2</sub>

#### **4.4.12 LYC initiates G2 phase arrest**

From the immunoblotting assay, confirmed that the LYC induce apoptosis in HCT 116 cells by inhibiting PI3K/AKT/mTOR pathway. Like apoptosis induction, cell cycle arrest is another important target for cancer treatment. Therefore, to analyse the cell cycle upon LYC treatment in HCT 116 cells, Propidium Iodide (PI) dye was used to stain the DNA distribution. The HCT 116 cells were treated with different concentrations of LYC (5 $\mu$ M, 10 $\mu$ M, and 15 $\mu$ M) and measured cells distribution in cell cycle phases (G1, S and G2/M) by flow cytometric method. The analysis of nuclear DNA distribution showed the G2 proportions of cells were increased after LYC treatment at different concentrations compared to the control groups (Fig 4.15), indicating that LYC could induce cell cycle arrest at the G2 phase in HCT 116 cells in a dose dependent manner. As shown in the Fig 4.15, LYC treatment significantly changed the distribution of cells in all phases of HCT 116 cellcycle. It showed that number of cells in G2/M phase is significantly increase and same way it is drecreased in G0/G1 Phase. Though, when compared to H<sub>2</sub>O<sub>2</sub> (300  $\mu$ M) treated cells, the activity of LYC is less. LYC was revealed to initiate G2/M phase arrest in cancer cells (A549, DU145, HepG2, and HT-29) (Wang et al., 2021). Several studies proposed LYC reduced cell cycle linked proteins and increased proapoptotic expressions in various cancer cell lines (Mekuria et al., 2020; Wang et al., 2021). From the results the LYC arrest the HCT 116 cell cycle at G2/M Phase in a concentration dependent way. As a basic assay, the role of LYC in HCT 116 cell cycle arrest was investigated and in future, role of LYC on cell cycle regulation needs to be explored.

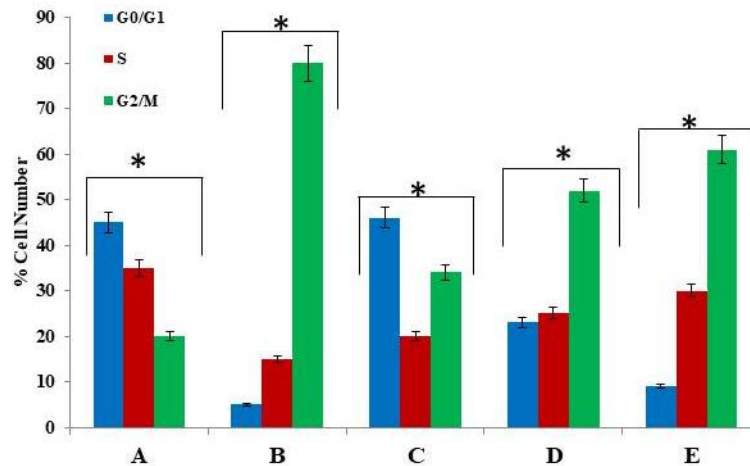


Fig 4.15: Cell cycle arrest of HCT 116 cells treated with LYC was analysed by detecting PI stained cells using a flow cytometer and the distribution of cells in each phase of cell cycle was determined. The Figure depicts A- negative control, B- H<sub>2</sub>O<sub>2</sub> (300 μM), C- 5 μM LYC, D- 10 μM LYC, E-15 μM LYC. Data are expressed as mean ± SD. p≤0.05 considered as significantly different. \*Each phase of various groups is significantly different from control group.

#### 4.5 Conclusion

In conclusion, LYC inhibited the CRC cells proliferation and apoptosis induction by suppressing the PI3K/AKT/mTOR signalling pathway, an important event in colorectal carcinogenesis. In addition, it plays a significant role in acquiring drug resistance as well as metastatic events of CRCs. LYC act as a pro-oxidant by inducing ROS level in cells and leads to mitochondrial dysfunction and triggering apoptosis in cells. Apoptosis activated by LYC was associated with a higher level of caspase-3 activity and increased BAX/Bcl-2 ratio in HCT 116 cells. Collectively protein expression studies revealed that LYC inhibited HCT 116 cell proliferation and apoptosis activation via suppressing PI3K/AKT/mTOR cascade. Therefore, LYC may be a promising therapeutic agent for the treatment and management of

CRC, by targeting PI3K/AKT/mTOR signalling pathway, is a possible way for future research.

**The key findings were summarized below:**

- LYC increases the ROS level in cells and decreases antioxidant enzyme activity as a pro-oxidant
- LYC promote mitochondrial dysfunction and DNA damage
- LYC triggered mitochondrial mediated apoptosis in HCT 116 cells by suppressing PI3K/AKT/mTOR signalling pathway

LYC may be a potential therapeutic agent for the treatment of CRC, which can inhibit the proliferation of CRC cells and induce apoptosis by inhibiting the PI3K/AKT/mTOR signalling pathway

## 4.6 Graphical Abstract

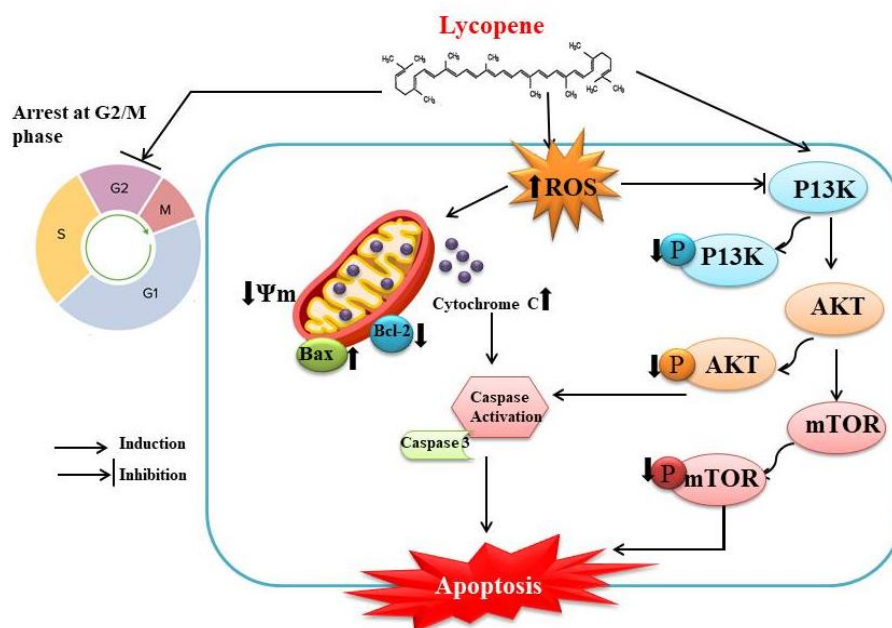


Fig 4.16 Schematic representation of possible mechanism by LYC regulate signalling events to induce cell death by apoptosis in HCT 116 colon cancer cells.

## 4.7 References

- Abotaleb, M., Samuel, S. M., Varghese, E., Varghese, S., Kubatka, P., Liskova, A., & Büsselberg, D. (2018). Flavonoids in Cancer and Apoptosis. *Cancers*, 11(1), 28.
- Arathi, B. P., Sowmya, P. R., Kuriakose, G. C., Vijay, K., Baskaran, V., Jayabaskaran, C., & Lakshminarayana, R. (2016). Enhanced cytotoxic and apoptosis inducing activity of lycopene oxidation products in different cancer cell lines. *Food and chemical toxicology : an international journal published for the British Industrial Biological Research Association*, 97, 265–276.
- Beutner, S., Bloedorn, B., Frixel, S., Hernández Blanco, I., Hoffmann, T., Martin, H.-D., Mayer, B., Noack, P., Ruck, C., Schmidt, M., Schülke, I., Sell, S., Ernst, H., Haremza, S., Seybold, G., Sies, H., Stahl, W. and Walsh, R. (2001). Quantitative assessment of antioxidant properties of natural colorants and phytochemicals: carotenoids, flavonoids, phenols and indigoids. The role of  $\beta$ -carotene in antioxidant functions. *Journal of the Science of Food and Agriculture*, 81: 559-568.
- Boussios, S., Seraj, E., Zarkavelis, G., Petrakis, D., Kollas, A., Kafantari, A., Assi, A., Tatsi, K., Pavlidis, N., & Pentheroudakis, G. (2016). Management of patients with recurrent/advanced cervical cancer beyond first line platinum regimens: Where do we stand? A literature review. *Critical reviews in oncology/hematology*, 108, 164–174.
- Chen, M., Peng, W., Hu, S., & Deng, J. (2018). miR-126/VCAM-1 regulation by naringin suppresses cell growth of human non-small cell lung cancer. *Oncology letters*, 16(4), 4754–4760.



- Cheng, H., Jiang, X., Zhang, Q., Ma, J., Cheng, R., Yong, H., Shi, H., Zhou, X., Ge, L., & Gao, G. (2020). Naringin inhibits colorectal cancer cell growth by repressing the PI3K/AKT/mTOR signaling pathway. *Experimental and therapeutic medicine*, *19*(6), 3798–3804.
- Dasari, S., & Tchounwou, P. B. (2014). Cisplatin in cancer therapy: molecular mechanisms of action. *European journal of pharmacology*, *740*, 364–378.
- Eghbaliferiz, S., & Iranshahi, M. (2016). Prooxidant Activity of Polyphenols, Flavonoids, Anthocyanins and Carotenoids: Updated Review of Mechanisms and Catalyzing Metals. *Phytotherapy research : PTR*, *30*(9), 1379–1391.
- Gansukh, E., Mya, K. K., Jung, M., Keum, Y. S., Kim, D. H., & Saini, R. K. (2019). Lutein derived from marigold (*Tagetes erecta*) petals triggers ROS generation and activates Bax and caspase-3 mediated apoptosis of human cervical carcinoma (HeLa) cells. *Food and chemical toxicology : an international journal published for the British Industrial Biological Research Association*, *127*, 11–18.
- Hassan, M., Watari, H., AbuAlmaaty, A., Ohba, Y., & Sakuragi, N. (2014). Apoptosis and molecular targeting therapy in cancer. *BioMed research international*, *2014*, 150845.
- Karas, M., Amir, H., Fishman, D., Danilenko, M., Segal, S., Nahum, A., Koifmann, A., Giat, Y., Levy, J., & Sharoni, Y. (2000). Lycopene interferes with cell cycle progression and insulin-like growth factor I signaling in mammary cancer cells. *Nutrition and cancer*, *36*(1), 101–111.

- Khan, A. W., Farooq, M., Haseeb, M., & Choi, S. (2022). Role of Plant-Derived Active Constituents in Cancer Treatment and Their Mechanisms of Action. *Cells*, 11(8), 1326.
- Koklesova, L., Liskova, A., Samec, M., Buhrmann, C., Samuel, S. M., Varghese, E., Ashrafizadeh, M., Najafi, M., Shakibaei, M., Büsselberg, D., Giordano, F. A., Golubnitschaja, O., & Kubatka, P. (2020). Carotenoids in Cancer Apoptosis-The Road from Bench to Bedside and Back. *Cancers*, 12(9), 2425.
- Langner, E., Lemieszek, M.K., Rzeski, W. (2019).Lycopene, sulforaphane, quercetin, and curcumin applied together show improved antiproliferative potential in colon cancer cells in vitro. *Journal of Food Biochemistry*. ; 43:e12802
- Liu, J., Wang, Y., Du, W., Liu, W., Liu, F., Zhang, L., Zhang, M., Hou, M., Liu, K., Zhang, S., & Yu, B. (2013). Wnt1 inhibits hydrogen peroxide-induced apoptosis in mouse cardiac stem cells. *PloS one*, 8(3), e58883.
- Liu, Y., Shi, C., He, Z., Zhu, F., Wang, M., He, R., Zhao, C., Shi, X., Zhou, M., Pan, S., Gao, Y., Li, X., & Qin, R. (2021). Inhibition of PI3K/AKT signaling via ROS regulation is involved in Rhein-induced apoptosis and enhancement of oxaliplatin sensitivity in pancreatic cancer cells. *International journal of biological sciences*, 17(2), 589–602.
- Magne, T.M., da Silva de Barros, A.O., de Almeida Fechine, P.B. *et al.* (2022)Lycopene as a Multifunctional Platform for the Treatment of Cancer and Inflammation. *Revista Brasileira de Farmacognosia*. 32, 321–330.

- McGuire, S. World Cancer Report 2014. Geneva, Switzerland: World Health Organization, International Agency for Research on Cancer, WHO Press, 2015. *Advances in Nutrition*. United States, 2016, 7: 418.
- Mekuria, A. N., Tura, A. K., Hagos, B., Sisay, M., Abdela, J., Mishore, K. M., & Motbaynor, B. (2020). Anti-Cancer Effects of Lycopene in Animal Models of Hepatocellular Carcinoma: A Systematic Review and Meta-Analysis. *Frontiers in pharmacology*, 11, 1306.
- Miller, K. D., Siegel, R. L., Lin, C. C., Mariotto, A. B., Kramer, J. L., Rowland, J. H., Stein, K. D., Alteri, R., & Jemal, A. (2016). Cancer treatment and survivorship statistics, 2016. *CA: a cancer journal for clinicians*, 66(4), 271–289.
- Morgensztern, D., & McLeod, H. L. (2005). PI3K/Akt/mTOR pathway as a target for cancer therapy. *Anti-cancer drugs*, 16(8), 797–803.
- Murugan A. K. (2019). mTOR: Role in cancer, metastasis and drug resistance. *Seminars in cancer biology*, 59, 92–111.
- Ono, M., Takeshima, M., & Nakano, S. (2015). Mechanism of the Anticancer Effect of Lycopene (Tetraterpenoids). *The Enzymes*, 37, 139–166.
- Ouyang, L., Shi, Z., Zhao, S., Wang, F. T., Zhou, T. T., Liu, B., & Bao, J. K. (2012). Programmed cell death pathways in cancer: a review of apoptosis, autophagy and programmed necrosis. *Cell proliferation*, 45(6), 487–498.
- Pal, M. K., Jaiswar, S. P., Srivastav, A. K., Goyal, S., Dwivedi, A., Verma, A., Singh, J., Pathak, A. K., Sankhwar, P. L., & Ray, R. S. (2016). Synergistic effect of piperine and paclitaxel on cell fate via cyt-c, Bax/Bcl-2-caspase-3 pathway

in ovarian adenocarcinomas SKOV-3 cells. *European journal of pharmacology*, 791, 751–762.

Pandurangan, A. K. (2013). Potential targets for prevention of colorectal cancer: a focus on PI3K/Akt/mTOR and Wnt pathways. *Asian Pacific journal of cancer prevention : APJCP*, 14(4), 2201–2205.

Park, S., Lim, W., Bazer, F. W., & Song, G. (2018). Apigenin induces ROS-dependent apoptosis and ER stress in human endometriosis cells. *Journal of cellular physiology*, 233(4), 3055–3065.

Pfeffer, C. M., & Singh, A. (2018). Apoptosis: A Target for Anticancer Therapy. *International journal of molecular sciences*, 19(2), 448.

Pitchai, D., Roy, A., & Ignatius, C. (2014). In vitro evaluation of anticancer potentials of lupeol isolated from *Elephantopus scaber* L. on MCF-7 cell line. *Journal of advanced pharmaceutical technology & research*, 5(4), 179–184.

Qui, W. J., Sheng, W. S., Peng, C., Xiaodong, M., & Yao, T. Z. (2021). Investigating into anti-cancer potential of lycopene: Molecular targets. *Biomedicine & pharmacotherapy*, 138, 111546.

Ribeiro, D., Freitas, M., Silva, A., Carvalho, F., & Fernandes, E. (2018). Antioxidant and pro-oxidant activities of carotenoids and their oxidation products. *Food and chemical toxicology : an international journal published for the British Industrial Biological Research Association*, 120, 681–699.

Rouhi Taheri, S. Z., Sarker, M., Rahmat, A., Alkahtani, S. A., & Othman, F. (2017). The effect of pomegranate fresh juice versus pomegranate seed powder on metabolic indices, lipid profile, inflammatory biomarkers, and the

- histopathology of pancreatic islets of Langerhans in streptozotocin-nicotinamide induced type 2 diabetic Sprague-Dawley rats. *BMC complementary and alternative medicine*, 17(1), 156.
- Saxena, R., Rida, P. C., Kucuk, O., & Aneja, R. (2016). Ginger augmented chemotherapy: A novel multitarget nontoxic approach for cancer management. *Molecular nutrition & food research*, 60(6), 1364–1373.
- Siegel, R. L., Miller, K. D., & Jemal, A. (2016). Cancer statistics, 2016. *CA: a cancer journal for clinicians*, 66(1), 7–30.
- Sui, Y., Yao, H., Li, S., Jin, L., Shi, P., Li, Z., Wang, G., Lin, S., Wu, Y., Li, Y., Huang, L., Liu, Q., & Lin, X. (2017). Delicaflavone induces autophagic cell death in lung cancer via Akt/mTOR/p70S6K signaling pathway. *Journal of molecular medicine (Berlin, Germany)*, 95(3), 311–322.
- Tang, F. Y., Cho, H. J., Pai, M. H., & Chen, Y. H. (2009). Concomitant supplementation of lycopene and eicosapentaenoic acid inhibits the proliferation of human colon cancer cells. *The Journal of nutritional biochemistry*, 20(6), 426–434.
- Tsuda, N., Watari, H., & Ushijima, K. (2016). Chemotherapy and molecular targeting therapy for recurrent cervical cancer. *Chinese journal of cancer research*, 28(2), 241–253.
- Vasen, H. F., Tomlinson, I., & Castells, A. (2015). Clinical management of hereditary colorectal cancer syndromes. *Nature reviews. Gastroenterology & hepatology*, 12(2), 88–97.

- Wang, Y., Gu, J., Hu, L., Kong, L., Wang, T., Di, M., Li, C., & Gui, S. (2020). miR-130a alleviates neuronal apoptosis and changes in expression of Bcl-2/Bax and caspase-3 in cerebral infarction rats through PTEN/PI3K/Akt signaling pathway. *Experimental and therapeutic medicine*, 19(3), 2119–2126.
- Yao, W., Lin, Z., Wang, G., Li, S., Chen, B., Sui, Y., Huang, J., Liu, Q., Shi, P., Lin, X., Liu, Q., & Yao, H. (2019). Delicaflavone induces apoptosis via mitochondrial pathway accompanying G2/M cycle arrest and inhibition of MAPK signaling cascades in cervical cancer HeLa cells. *Phytomedicine : international journal of phytotherapy and phytopharmacology*, 62, 152973.
- Zhang, X., Liu, Z., Chen, S., Li, H., Dong, L., & Fu, X. (2022). A new discovery: Total Bupleurum saponin extracts can inhibit the proliferation and induce apoptosis of colon cancer cells by regulating the PI3K/Akt/mTOR pathway. *Journal of ethnopharmacology*, 283, 114742.

## **Chapter 5**

### **Development and characterization of chitosan coated lycopene nanoliposomes with inulin for colon delivery**

## 5.1 Introduction

Bioactives in foods have been gaining interest in therapeutic applications for their potential role in preventive health and disease management, especially in the case of lifestyle associated diseases. Lycopene, one of the strong antioxidant pigments present in red fruits and vegetables (Nguyen, Schwartz, In Lauro, & Francis, 2000), has found applications in the prevention and management of various chronic diseased conditions because of its anti-diabetes, anti-inflammatory, anti-amyloid, and antioxidant activities (Souza et al., 2018). Although, it has several advantages, its therapeutic application is limited due to low bioavailability, poor water solubility, low stability against different pH conditions, fast metabolism and quick systemic removal (Perezmasia, Lagaron, & Lopezrubio, 2015).

The dietary intake of lycopene was suggested for promoting health through its powerful antioxidant property. In recent years, lycopene has increased attention for its promising anti-carcinogenic activity, especially in CRC treatment. CRC is the third most detected malignancy and the second top source of cancer death (Keum & Giovannucci, 2019). Clinical and epidemiological research has constantly highlighted the significant relationships between gut microbiota (GM), inflammation and colon carcinogenesis. Lycopene acts by various mechanisms in cancer cells including cell cycle arrest, growth factor signal regulation, apoptosis induction, inhibition metastasis, as well as by modifying phase II detoxification enzymes system, and the anti-inflammatory activity (Wang et al., 2018; Aktepe et al., 2021). Therapeutic applications of bioactives in cancer have increasingly been studied over the past two decades in particular with regards to CRC. Unhealthy food consumption is closely related to obesity, and increases the risk of CRC development. Noticeably, bioactives showed both chemopreventive and anti-tumor properties in CRC (Malki et al. 2020) contributing to the general concept that a healthy way of life, including a balanced diet, is protective of CRC.



Colon targeted delivery is a dynamic research area for the diseases affecting colon, as it shows an improved therapeutic efficacy and minimize systemic toxicity. Recently numerous studies have been showed on the development of various types of delivery systems for bioactive focus on increase in bioavailability, stability and maintaining the biological activity (Akhavan, Assadpour, Katouzian, & Jafari, 2018). Therefore, a designed carrier system could suggestively enable lycopene delivery, and which can lead to develop conceivable therapeutic applications in extensive area. Another important factor in colon cancer cell progression is the imbalance in gut health. Recent study found that inulin nanoparticle has therapeutic potential in colon cancer cells by promoting apoptosis (Yan et al., 2022).

Liposomes are highly structured delivery system of self-assembling vesicles with amphiphilic lipids (phospholipid such as lecithin or phosphatidylcholine, and cholesterol), which can incorporate both hydrophilic and lipophilic components, which possess promising area in food, functional food, nutraceutical applications as well as in medical research (He et al., 2019, Rasti, Erfanian, & Selamat, 2017). Phospholipid molecules that are arranged in such a way that they form a protective fat globule, where active ingredients were entrapped (Verma & Utreja, 2022). An important feature of liposomes is that they can incorporate both hydrophilic (core region) and hydrophobic (bilayer region) compounds and that they can be easily fused with the cell membrane because their composition is similar to that of the cell membrane (Olusanya et al., 2018).

Liposomes are totally biodegradable structures which makes them a perfect delivery system in functional food and pharmaceutical applications (Roy et al., 2016). Due to their potential role in transportation, controlled release, protection, entrapment efficacy for bioactive compounds, and targeted release applications, liposomes have been used to deliver different bioactive molecules especially antioxidants, peptides, flavors, and vitamins (Liu et al., 2020;

Sebaaly et al., 2015). Nanoliposomes have the ability to improve time-controlled drug release, and reduce the adverse effects of drugs on *in vitro* and *in vivo* (Li et al., 2022). One of the major drawbacks of liposomes as a carrier system is their fast removal from blood circulation and they are physically unstable, which depends on several factors which lead liposomal fusion, hydrolysis, degradation, and oxidation of phospholipids (He et al., 2019; Almaieda et al., 2020). Surface coating is hopeful way to improve liposome applicability by changes the surface characteristics of liposomes. Different studies have described on polymer coated (chitosan-CS) liposomes can increase their structural functionalities and applicability (Tan et al., 2016). Polymer coated liposome have shown an enhanced stability in *in vitro* simulated gastrointestinal fluids (Liu et al., 2020), as well as better drug uptake in *ex vivo* colon tissue in comparison to uncoated liposomes.

Studies in chapter 4 suggested the antitumor efficacy of LYC against CRC in HCT 116 cells and with this background the current study was designed to develop chitosan coated LYC/inulin incorporated nano liposomes with improved stability against gastrointestinal conditions for colon targeted delivery. The physicochemical stability of nano liposomes and its preliminary anticancer potential in colon cancer cell line were undertaken.

## 5.2 Objective

To develop LYC incorporated nanoliposomes for colon targeted delivery and to investigate its antitumorigenic effect in colon cancer cells (HCT 116).

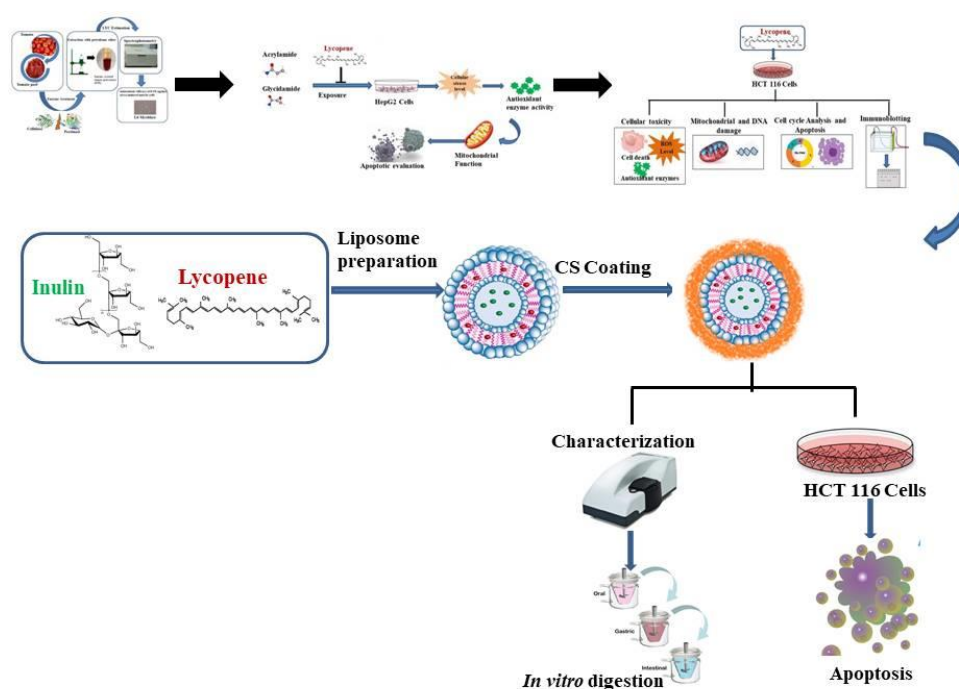


Fig 2.1: Outline of Chapter 5

## 5.3 Materials and Methods

### 5.3.1 Chemicals and Reagents

Chemicals such as chitosan, lycopene, inulin, lecithin, cholesterol, squalene,  $\alpha$ -amylase,  $\text{CaCl}_2$ , porcine pepsin, lipase, bile salts, pancreatin, potassium dihydrogen phosphate, sodium hydroxide, Dulbecco's Modified Eagle's Medium (DMEM), sodium bicarbonate, Dimethyl sulfoxide (DMSO), porcine mucin, Fetal Bovine Serum (FBS), 3-(4,5-dimethylthiazol-2-yl)-2,5 diphenyltetrazolium bromide (MTT) and Crystal violet were bought from Sigma (Sigma-Aldrich, St. Louis, MO, USA). Chloroform, HCl, and Acetic

acid were purchased from MERCK, India. Trypsin-EDTA, Antibiotic-antimycotic solution mixture was procured from Gibco Invitrogen (Carlsbad, CA, USA). Annexin V – apoptosis kit was obtained from Cayman chemicals (MI, USA). BrdU cell proliferation assay kit from BioVision (San Francisco, USA). All reagents used were of analytical grade.

### 5.3.2 Experimental Design

The experimental protocol for the study is given in the Fig 5.2.

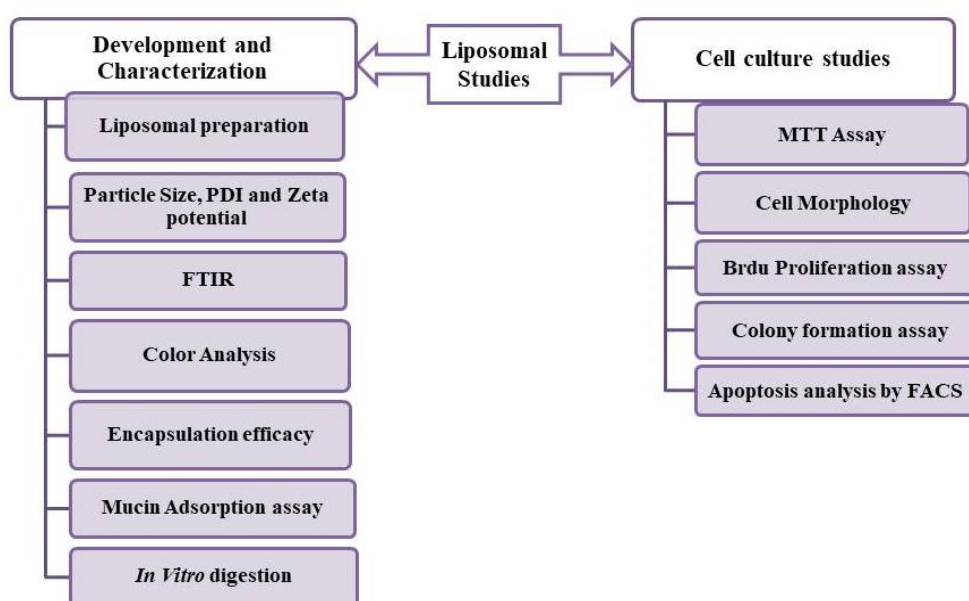


Fig 5.2: Experimental methods used for the study.

### 5.3.3 Liposomal (LP) preparation

LPs were developed by thin film hydration method combined with homogenization, to decrease the vesicle size and to create homogeneity (Hadian et.al., 2014). Briefly, soybean lecithin, cholesterol, and squalene were dissolved in chloroform (300: 50: 10 w/w/w), and LYC and INU of (30: 30 w/w) were added into the solvent mixture. A rotary evaporator at 37 °C, the prepared solvent mixture was evaporated to get a thin lipid film above the inner surface of a round-bottom flask. This process took 30 min to remove all the remaining chloroform. Then the developed thin lipid film was hydrated with PBS (0.05M) and exposed

to sonication (Equitron ultrasonic bath, Mumbai, India) for eluting the film easier at 25°C for 15 min. The formed uneven liposomal suspension was homogenized using homogenizer (T25 D S22 Digital Ultra Turrax, IKA Private Limited, Bengaluru, India) for 20 min (9000) for decreasing the vesicle sizes of LPs (Tsumoto et al., 2009). The developed uncoated liposomes were named as Control liposomes (C-LP), Inulin incorporated liposomes (I-LP), Lycopene incorporated liposomes (LYC-LP), and Lycopene and inulin incorporated liposomes (LYC-I-LP). The table 5.1 represents the composition used for the preparation of the liposomes in the study.

Table 5.1: The Composition of developed uncoated and CS coated nanoliposomes

<b>Liposomes</b>	<b>LEC (mg)</b>	<b>CL (mg)</b>	<b>SQE ( mg)</b>	<b>CS (%)</b>	<b>LYC (mg)</b>	<b>INU (mg)</b>
<b>Uncoated Liposomes</b>						
Control liposome (C- LP)	300	50	10	–	–	–
Inulin Liposome (I-LP)	300	50	10	–	–	10
LYC incorporated liposome(LYC –LP)	300	50	10	–	10	–
LYC and INU incorporated liposome (LYC-I-LP)	300	50	10	–	10	10
<b>CS coated Liposomes</b>						
CS coated control liposomes (CS-C-LP)	300	50	10	0.5	–	–
CS coated Inulin liposome (CS-I-LP)	300	50	10	0.5	–	10
CS coated LYC incorporated liposome (CS-LYC-LP)	300	50	10	0.5	10	–
CS coated LYC and INU incorporated liposome (CS-LYC-I-LP)	300	50	10	0.5	10	10

Lecithin- LEC; Cholesterol- CL; Squalene- SQE; Chitosan-CS; Lycopene-LYC; Inulin-INU

### 5.3.4 CS coating of Liposomes

Dropwise addition of Chitosan (CS) solution (0.5%, w/v) into the prepared liposome suspension under stirring for 60 min of 500 rpm to yield CS coated liposomes. The prepared liposomal dispersion was kept under RT with continuous stirring for 2 h. The developed chitosan-coated nanoliposomes were named as Chitosan coated control liposomes (CS-C-LP), chitosan coated inulin incorporated liposomes (CS-I-LP), chitosan coated lycopene incorporated liposomes (CS-LYC-LP), and chitosan coated lycopene and inulin incorporated liposomes CS-LYC-I-LP. All developed liposomal formulations were stored in the refrigerator at 4 °C until use. Both uncoated and coated liposome samples were used for characterization studies such as particle size, Polydispersity Index (PDI), zeta potential, entrapment efficacy and mucoadhesive ability. Based on the characterization and *in vitro* digestion assays, the liposomes that demonstrate potential activity was taken for cell culture studies to evaluate the anti-cancer activities in terms of antiproliferation and apoptotic induction in HCT 116 cells. The protocols followed for the development of uncoated and CS coated liposomes are represented in the fig.5.3.

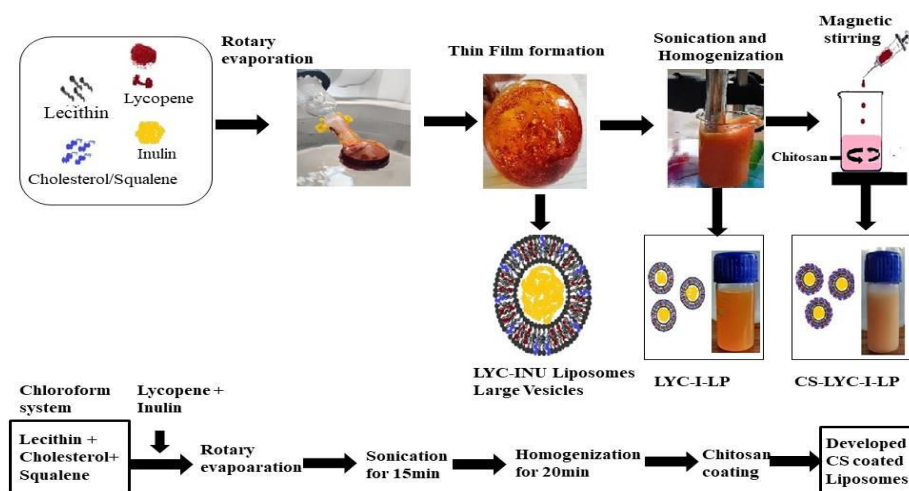


Fig 5.3: Graphical illustration of CS coated LYC and INU incorporated liposome preparation by using thin film hydration method

### 5.3.5 Physicochemical characterization of CS coated liposomes

#### 5.3.5.1 Particle size, PDI and Zeta potential

The particle size, PDI and zeta potential of uncoated (C-LP, I-LP, LYC-LP, and LYC-I-LP) and coated liposomes, (CS-C-LP, CS-I-LP, CS-LYC-LP, and CS-LYC-I-LP) were analysed using dynamic light scattering technique (DLS) by a Zetasizer (Malvern Instruments Ltd., UK). Developed liposomes were diluted in water and added to polystyrene latex cells, for mean particle size analysis and added to folded capillary cell for zeta potential, read at 25 °C with a detector angle of 90°. The liposomal suspensions were effectively diluted in deionized water to avoid the multiscattering phenomena. The average values from at least three measurements were reported, with the polydispersity index (PDI).

#### 5.3.5.2 Entrapment efficacy (EE)

The entrapment efficiency (EE) of LYC in developed liposomes was estimated by indirect method using centrifugation technique (Karim, Shishir, and Chen, 2020). The amount of LYC in the supernatant attained after centrifugation at 30,000 rpm for 15 min by refrigerated centrifuge (Beckman Coulter, Pasadena, CA, USA). LYC content in the LPs was evaluated by UV spectrophotometry (Shimadzu, Japan) at the wavelength of 470 nm. All samples were analysed in triplicate. The EE% was calculated based on following equations:

$$EE\% = \frac{LYC\ total - LYC\ free}{LYC\ total} \times 100$$

Where LYC added was taken as *LYC total* and the amount of LYC in the supernatant was *LYC free*.

### 5.3.5.3 ATR-Fourier-transform infrared (FTIR) spectroscopy

Fourier-transform infrared (FTIR) spectroscopy of LYC, CS-LP, CS-I-LP, CS-LYC-LP and CS-LYC-I-LP were recorded using an FTIR-ATR (Attenuated Total Reflection) spectrometer (Perkin Elmer, USA), equipped with an ATR accessory with a diamond crystal at an incidence angle of 45°. Transmittances were recorded at wave numbers between 4000 and 500 cm<sup>-1</sup>.

### 5.3.6 Color Analysis

The visual appearance of developed nanoliposomes were examined by L\*a\*b\* value. The color characteristics (L\*, a\*, and b\* values) of developed liposomes were measured by using color spectrophotometer (Hunder Lab, ColorFlex, Virginia). Hunter L,a,b color, represents L (lightness) axis, a (red-green) axis and b (blue-yellow) based on Opponent Colors theory.

### 5.3.7 *In vitro* digestion

The *in vitro* release kinetics of LYC from CS coated and uncoated liposomes were investigated using stimulated gastric fluids mimicking gastrointestinal phase (Li et al., 2020; Zhang et al., 2019). All the prepared solutions were pre-incubated at 37 °C using shaker to maintain this temperature during the digestion process.

**Oral phase:** Based on reported studies, the *in vitro* digestion starts in the oral cavity; we prepared simulated salivary fluid (SSF) using the salivary enzyme,  $\alpha$ -amylase and CaCl<sub>2</sub> salts to achieve 0.75 mM concentration as described in the method. In the initial phase, 3ml of LYC liposomal suspensions (LYC-LP, LYC-I-LP, CS-LYC-LP AND CS-LYC-I-LP) mixed with 3ml of SSF solution, and then the pH of the mixture was adjusted to 6.8 and incubated for 2 min in a shaker at 37°C.

**Gastric phase:** 5mL of salivary sample after incubation was mixed with 5 mL of Stimulatory gastric Fluid (SGF) electrolyte stock solution, (containing 3g/L porcine pepsin



in saline, 5 mM KCl, adjusted with 0.1M HCl to reach pH 3.0). The suggested time of digestion is 2 h at 37 °C in a shaking incubator

**Intestinal Phase:** The 5mL gastric samples after incubation mixed with 5mL Stimulatory intestinal fluid (SIF) electrolyte stock solution containing bile salts, intestinal solution (0.68g/L KH<sub>2</sub>PO<sub>4</sub>, 0.2M NaOH, 0.22g/L CaCl<sub>2</sub> and 1.3g/L NaHCO<sub>3</sub>), Lipase and pancreatin solution (1g/L, pancreatin from porcine pancreas). 1 M NaOH was used for pH adjustment in SIF to 7.0. The sample mixture was kept at shaking water bath for 2h at 37 °C. After incubation, the final digesta are used for the quantitative analysis of LYC release by using UV Spectrophotometric analysis (Shimadzu, Japan).

### 5.3.8 Mucin adsorption study

To investigate the mucoadhesive properties of developed liposomes, mucin adsorption (porcine stomach) by uncoated and CS coated liposomes was measured using Bradford method (Bradford, 1976). Briefly, equal quantity (1 mg/mL) of mucin solution and uncoated and chitosan-coated liposomes was agitated for 2 h at 37 °C. The mix was then centrifuged at 25,000 g (for 1 h) using refrigerated centrifuge. Free mucin content was estimated by using colorimetric method, and the variation between total and free mucin represents the quantity of mucin adsorbed on the liposomal surface. Briefly, all the samples were incubated with Bradford reagent for 10 min at 37 °C. After incubation, the absorbance was detected at 595 nm by using multimode reader (Synergy Biotek). Adsorption % was assessed for both uncoated liposomes and chitosan coated liposomes.

$$\text{Adsorption\%} = \frac{\text{Total amount of mucin used} - \text{free mucin}}{\text{Total amount of mucin used}} \times 100$$

### 5.3.9 Cell culture and Treatment

HCT 116 cells were purchased from NCCS, Pune, India and were cultured in DMEM with FBS (10%) (GibcoBRL) and 2% Antibiotic-antimycotic (GibcoBRL) at 37°C in a humidified atmosphere containing 5% CO<sub>2</sub>.

#### 5.3.9.1 Determination of cell viability

The cellular viability of the developed liposomes was estimated in colon adenocarcinoma cells, HCT 116 cells using MTT assay (Mosmann, 1983). Briefly, 96-well plates were seeded with cells and were grown overnight. To analyse the cytotoxicity of samples, cells were incubated with nanoliposomes CS-LP, CS-I-LP, CS-LYC-LP and CS-LYC-I-LP for 24 h followed by MTT reagent (0.5 g/L) for 4 h. After incubation, the reaction mixture was washed and DMSO (200 µL) was added to each well with gentle mixing (Orbit plate shaker, Labnet international, USA) and the absorbance was read at 570 nm (Synergy 4 Biotek multiplate reader, USA). Liposomes treated cells were compared to that of the cells exposed to 500µM H<sub>2</sub>O<sub>2</sub> taken as positive control. Each test was done in triplicate, and the results are represented as the mean ± SD, using the following calculation

$$\% \text{ cell viability} = \frac{\text{The absorbance of test}}{\text{The absorbance of control}} \times 100$$

#### 5.3.9.2 Morphological analysis

Cell morphology was visualized by phase-contrast microscopy. Cells were exposed with developed nanoliposomes CS-LP, CS-I-LP, CS-LYC-LP and CS-LYC-I-LP by above mentioned conditions. The media were discarded after 24 h incubation with samples and washed thrice with PBS and visualised under phase contrast microscope.

### **5.3.9.3 BrdU cell proliferation assay**

BrdU incorporation is a method used to analyse proliferating cells by incorporating into DNA of proliferating cells. After CS-LP, CS-I-LP, CS-LYC-LP and CS-LYC-I-LP treatment, cellular proliferation was measured using the BrdU Cell Proliferation ELISA kit (BioVision). As per manufacture instruction, absorbance was read within 5 min at 450 nm using an ELISA plate reader. Culture medium without BrdU was used as blank and the control were media without treatment.

### **5.3.9.4 Colony formation assay**

Evaluating the anchorage-dependent growth of colon cancer cells was done by using colony formation assays (Ayoub et al., 2021). Colony formation assay serve as a beneficial tool to analyse whether a compound can decrease the clonogenic survival of tumor cells. After CS-LP, CS-I-LP, CS-LYC-LP and CS-LYC-I-LP treatment, the cells were stained with 0.5% crystal violet solution and kept at RT for 30 min. The stained cells were visualised using phase contrast microscope (4x magnification).

### **5.3.9.5 Apoptosis by Annexin V**

Annexin V-fluorescein /PI staining was used to examine the effect of developed CS coated nanoliposomes on HCT 116 cells apoptosis. Briefly, the cells were exposed with developed nanoliposomes such as CS-LP, CS-I-LP, CS-LYC-LP and CS-LYC-I-LP incubated for 24 h. Untreated cells, as cells with media and positive control as H<sub>2</sub>O<sub>2</sub> (500 µM), LYC (10 µM) and INU (2 µg/ml) were also used to compare the samples . After incubation, cells were washed with PBS and suspended in binding buffer and then added Annexin V-FITC and incubated at RT for 15 min in the dark condition. Then the cells were stained with PI (5 µg/mL) and the ratio of apoptotic cells was measured by using FACS Aria II (BD Bioscience, USA).

### 5.3.10 Statistical analysis.

All the experiments were repeated thrice and data were expressed as means  $\pm$  SD. The obtained results were subjected to one-way ANOVA and the significance was calculated by Duncan's multiple range tests, using SPSS 16.0 and significance was accepted at  $P \leq 0.05$ .

## 5.4 Results & Discussion

### 5.4.1 Formation of Uncoated and CS coated LP

Four uncoated liposomes (LPs) and four CS coated LPs were fabricated as per the details given in Table 5.1 and figure 5.2. The representative figures of uncoated and CS coated LYC and INU incorporated liposomes (LYC-LP, LYC-I-LP, CS-LYC-LP, CS-LYC-I-LP) are given in fig 5.5. As discussed earlier, the gastrointestinal stability of the liposomes can be modified by the addition of polymer coatings on their surface. In the present study, nanoliposome formulations were provided with CS coating to resist gastro intestinal digestion for colon targeted delivery. Coatings allow oral liposomal formulations to resist enzymatic degradation in the GI tract, which would normally dissolve the lipid bilayer.

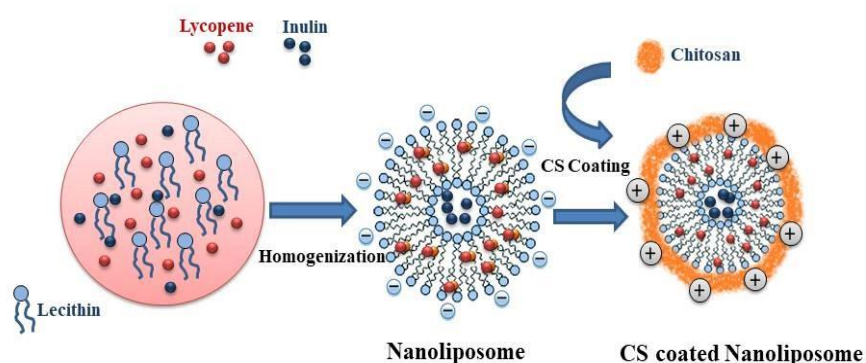


Fig 5.4: Schematic representation of CS coated liposome preparation

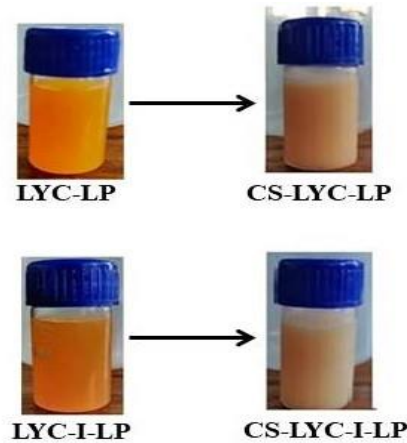


Fig 5.5: Developed uncoated (LYC-LP and LYC-I-LP) and CS coated nanoliposomes (CS-LYC-LP and CS-LYC-I-LP)

#### 5.4.2 Particle size distribution, PDI and zeta potential

The physical stability of the LPs was evaluated by analysing its PDI and zeta potential (Table 5.2). Dynamic light scattering was performed to obtain the hydrodynamic sizes of the liposomes in solution at 25 °C. The average size of prepared liposomes without CS coating showed a lower particle size compared to CS coated samples. Mean particle size of developed uncoated liposomes such as C-LP, I-LP, LYC-LP, and LYC-I-LP were 228, 238, 262 and 258 nm, with PDI values of 0.29, 0.29, 0.28, and 0.26 respectively, and CS coated liposomes CS-C-LP, CS-I-LP, CS-LYC-LP, and CS-LYC-I-LP were 350, 365, 351 and 365 nm, with PDI values of 0.48, 0.54, 0.49 and 0.54. From the table 5.2, there is a substantial change in the z-average particle diameter ( $p \leq 0.05$ ) which varied from 258 nm to 365 nm in CS-LYC-I-LP, and an increase in particle size of the CS-coated liposomes was compared to that of the corresponding uncoated liposomes. The enlargement in particle size in CS coated LPs can be attributed to the outer surface coating with CS layer (Zhao et al., 2015). All the samples yielded a size distribution curve suggesting relatively uniform size distribution. The polydispersity index (PDI) is generally used for assessing the stability of emulsion systems and a stable emulsion with uniform particle size distribution is denoted by a PDI value of 0.3

and below (Lee et al., 2018). PDI indicates homogeneous particle dispersion in all the liposomal dispersions, where the uncoated liposomes were more homogenous than the CS coated ones. In this study, values of PDI were within the range of 0.29 to 0.54 for both uncoated and CS coated systems, indicating an acceptable degree of polydispersity (Alshraim et al., 2019; Caddeo et al., 2016).

Table 5.2: The physicochemical characterization of uncoated and CS coated different liposomal system by using DLS analysis. Data represented as mean  $\pm$  SD, n = 3, p < 0.05.

Samples	DLS Analysis		
	Particle Size (nm)	Polydispersity index (PDI)	Zeta Potential (mV)
C-LP	228 $\pm$ 50	0.29	-28 $\pm$ 3.74
I-LP	238 $\pm$ 12	0.29	-29 $\pm$ 3.68
LYC-LP	262 $\pm$ 80	0.28	-29 $\pm$ 3.62
LYC-I-LP	258 $\pm$ 18	0.26	-29 $\pm$ 3.07
CS-C-LP	351 $\pm$ 89	0.48	23.6 $\pm$ 3.06
CS-I-LP	365 $\pm$ 38	0.54	23.9 $\pm$ 7.45
CS-LYC-LP	351 $\pm$ 99	0.49	25.1 $\pm$ 5.64
CS-LYC-I-LP	365 $\pm$ 46	0.54	24.6 $\pm$ 4.90

The surface charge and suspended particle stabilities are expressed by the Zeta potential. As can be noted, the uncoated liposomes showed negative charges in samples which depicted the surface charge of the outer lipid bilayer. The surface charge of the uncoated liposome suspensions changed from negative to positive charge in CS-coated samples. The chitosan possesses a positive charge, which can form a polyelectrostatic layer onto negatively charged liposomes, which was due to the interaction between the positive charge of CS and

the negative charge of the phospholipid head group (Zhou et al., 2018). Because of no significant differences in zeta potential among different chitosan-coated LPs, the surfaces of liposomes can be thought of as completely covered by chitosan and becomes positively charged. The formation of hydrogen bonding between phospholipids and CS results in the coating of liposomes with CS (Chen et al., 2016).

### 5.4.3 Encapsulation efficiency (EE)

Of the total eight coated and CS coated liposomal systems, four LPs such as LYC-LP, LYC-I-LP, CS-LYC-LP, and CS-LYC-I-LP were loaded with LYC. EE was evaluated to analyze the LYC incorporation in these four developed coated and CS coated liposomal systems. EE is key factor that defines the nanocarriers performance of in terms of stability and protection of pharmaceutical, nutritional and bioactive components for target delivery. EE is an expression of the quantity of the active ingredient incorporated into the liposomes and is a major factor in developing food, nutraceutical, and pharma products (Ong et al., 2020).

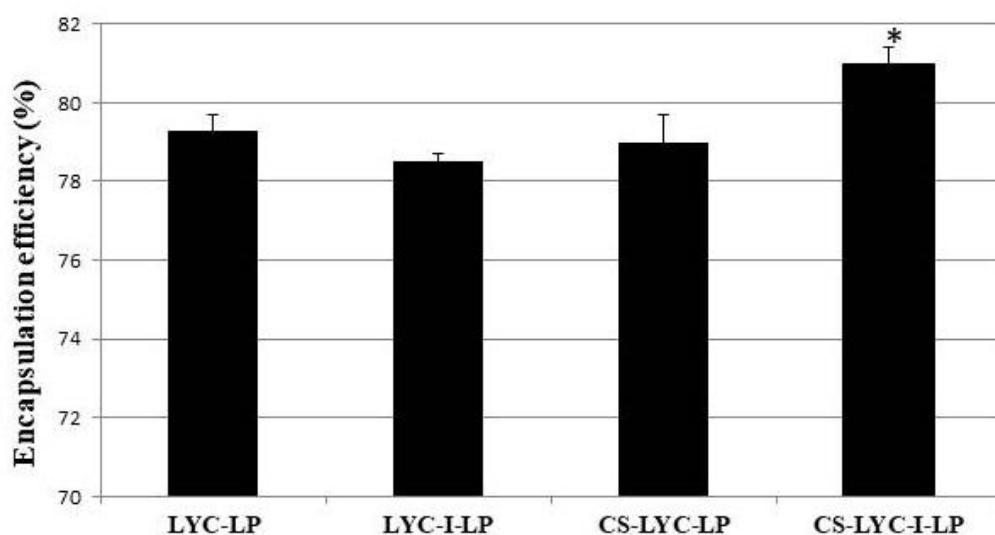


Fig 5.6: Encapsulation efficiency (%) of developed LYC incorporated uncoated and CS coated samples, represented as bars, Values are means  $\pm$  standard deviations (n=3). The annotation \* indicates a  $p \leq 0.05$  versus LYC-I-LP group.

As shown in Fig 5.6, the EE% for LYC-LP, LYC-I-LP, CS-LYC-LP, and CS-LYC-I-LP were  $79.3 \pm 1.4\%$ ,  $78.5 \pm 1.3\%$ ,  $79 \pm 1.1\%$ , and  $81 \pm 0.9\%$ , respectively. As can be seen, the CS coated liposomal system CS-LYC-I-LP exhibited a higher LYC encapsulation efficacy of 81% though there was no notable change in EE% between uncoated and CS coated LYC LPs. In CS coated liposomes, CS also acts as a barrier on the phospholipid bilayer surface which prevents the leakage of LYC from the liposome. Previous reports confirmed that chitosan coating in liposomes holds the drug inside the system due to CS adsorption on the surface of liposomes (Alomrani et al., 2019; Jiao et al., 2018).

#### **5.4.4 Fourier Transform Infrared Spectroscopy (FTIR)**

The IR spectra of LYC, CS-C-LP, CS-I-LP, CS-LYC-LP, and CS-LYC-I-LP were shown in Fig 5.7. Strong and broad absorption bands in the  $3700-3000\text{ cm}^{-1}$  and  $1600-1700\text{ cm}^{-1}$  range denote the presence of water. The presence of lipid groups from LYC is evidenced by the absorption at  $3000-2800\text{ cm}^{-1}$  and  $1730-1765\text{ cm}^{-1}$ . The bands range between  $1400$  and  $1477\text{ cm}^{-1}$  originate from C-H bending; the region  $1100-1400\text{ cm}^{-1}$  shows the C-C and C-C-H stretching. The region  $900 - 1200\text{ cm}^{-1}$  contains strips resulting from C-O stretching and C-O-C vibrations. The spectral signal at  $963\text{ cm}^{-1}$  can be attributed to trans C-H deformation vibrations and all types of deformations of the LYC molecule are found below  $1000\text{ cm}^{-1}$ . As it is evident from the figure, the characteristics peak of the LYC is visible in the FTIR spectrum of the control liposomes system which is another evidence of the perfect encapsulation of LYC. Results showed characteristic peaks of LYC in prepared liposomes are preserved between  $2800$  to  $2900\text{ cm}^{-1}$ . CS-LYC-LP and CS-LYC-I-LP show similar peaks with respect to control LYC, confirming that LYC is encapsulated in the system.



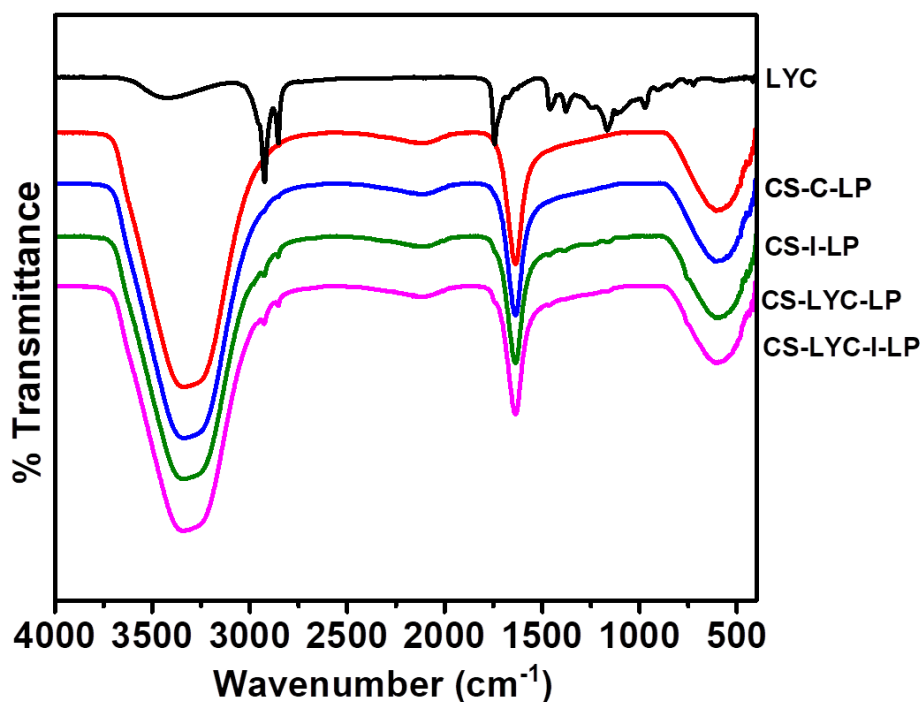


Fig 5.7: FTIR Spectra of LYC and developed CS Coated nanoliposomes (CS-C-LP, CS-I-LP, CS-LYC-LP and CS-LYC-I-LP)

#### 5.4.5 *In vitro* LYC release studies

To explore the release of developed liposome for LYC release in GI tract, *in vitro* digestion method was conducted. The *in vitro* release studies of the active ingredient are used to assess its incorporation, liposomal reliability, and the affinity of the bioactive to the carrier systems (Wang et al., 2017). In the present study, the *in vitro* LYC release from four uncoated and CS coated LYC incorporated liposomes, such as LYC-LP, LYC-I-LP, CS-LYC-LP, and CS-LYC-I-LP were examined by using *in vitro* digestion method using simulated salivary fluid (SSF), simulated gastric fluid (SGF), and simulated intestinal fluids (SIFs). SSF electrolyte stock solution creates oral phase with pH of about 6.8 and under this conditions, all the four liposomes LYC-LP, LYC-I-LP, CS-LYC-LP, and CS-LYC-I-LP exhibited very low percentage release of LYC of  $1.2 \pm 1.1$ ,  $1.1 \pm 0.07$ ,  $1.1 \pm 0.09$ ,  $0.2 \pm 1.01$  % respectively. From the data, under all the tested conditions, CS coated LPs (CS-LYC-

LP and CS-LYC-I-LP) show very low LYC release compared to uncoated liposomes. From the oral area the mixture is entered into gastric phase, and the system is exposed to SGF mimicking the gastric region of pH 2.6. Under SGF conditions, uncoated liposomes LYC-LP, LYC-I-LP shows a significant increase in LYC release of  $14 \pm 0.09$  and  $17 \pm 1.0$  % respectively, compared to CS coated samples CS-LYC-LP, and CS-LYC-I-LP of  $1.1\% \pm 0.76$ ,  $0.3 \pm 0.06\%$  respectively.

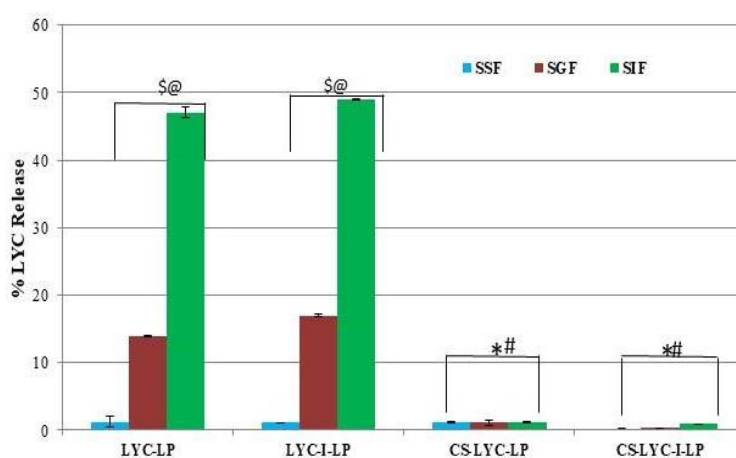


Fig 5.8: Percentage LYC releases from uncoated and CS coated nanoliposomes after in vitro digestion. Data expressed as mean  $\pm$  SD, The annotation \* denotes  $P < 0.05$  against LYC-LP group, # represent  $P < 0.05$  versus the LYC-I-LP group, \$ represent  $P < 0.05$  against CS-LYC-LP group and @ represent  $P < 0.05$  against CS-LYC-I-LP group,  $n = 3$ ,  $p < 0.05$ .

As can be seen, chitosan coated liposomes demonstrated least LYC release indicating CS offers protection to the active ingredient (Fig 5.8). From gastric phase the mixture is entered into intestinal phase where SIF mimics the intestinal area of pH 6.7. In SIF condition, as expected the uncoated LPs (LYC-LP and LYC-I-LP) showed a maximum LYC release of  $47 \pm 1.3$  and  $49 \pm 0.08\%$ , meanwhile CS-LYC-LP, and CS-LYC-I-LP exhibited very low LYC release of  $1.2\% \pm 0.22$  and  $0.9\% \pm 0.10$ , (Fig 5.8) of LYC. Under SIF conditions, uncoated LPs exhibited a fast LYC release within the intestinal phase and interestingly, CS

coated liposomal system shows a low amount of LYC release. This may be due to the CS coating in liposomes protects the liposomal system against pH degradation in GI tract conditions. The positively charged chitosan protected the liposomal surfaces from bile salts or lipase to reach the lipid bilayer. Chitosan coating helps to resist degradation in GI tract pH that would normally dissolve the lipid bilayer. Very low percent of LYC release was observed from CS-LYC-LP and CS-LYC-I-LP of lower than 2% in all stimulated gastrointestinal conditions, leading the intact liposomal system to the colonic region for targeted delivery.

#### **5.4.6 Mucoadhesive property**

Interaction between nanocarriers and mucins shows a vital role in the effective delivery of entrapped components to target area and their controlled release (Petrou, & Crouzier, 2018). Positively charged CS has an interaction with negatively charged mucin found in the intestinal epithelial cells. The mucoadhesive properties of uncoated LPs (C-LP, I-LP, LYC-LP, and LYC-I-LP) and CS coated LPs (CS-C-LP, CS-I-LP, CS-LYC-LP, CS-LYC-I-LP) were analysed by measuring their mucin adsorption capability. As illustrated in Fig 5.9, mucin adsorption by uncoated LPs exhibits less than 10% adsorption and which is significantly increased ( $p < 0.05$ ) to  $> 60\%$  in CS coated LPs. This result proposes that CS coated LPs might retain for a longer time in the GIT compared to uncoated liposomes. CS coating on the nano-carriers surface could be more effective in delaying the release of core materials by improving the interaction with the intestinal mucus. Mucins are hydro soluble coating present on many epithelial surfaces of cells, which are responsible for the gel properties of mucus (Sebaaly et al., 2021). The mucoadhesive property of CS coated liposomes are generally due to the electrostatic interaction between the chitosan (amine group-NH<sub>3</sub><sup>+</sup>) and mucin (carboxylate (COO<sup>-</sup>) or sulfonate (SO<sub>3</sub><sup>-</sup>) group) and also by other

non-covalent bonds (Imam et al., 2021; Sebaaly et al., 2021). Hence, the cationic charge of CS coated LPs (CS-C-LP, CS-I-LP, CS-LYC-LP, CS-LYC-I-LP) can facilitate the negatively charged cell membranes interaction and permeation across the cells. These LPs can easily interact with negatively charged mucin secreted from intestinal epithelial cells. Thus, the enhanced mucoadhesive capability of developed CS coated LPs possibly leads to a longer residence in gastric region and helps in the targeted release of LYC in the cell by interacting with the cell membrane.

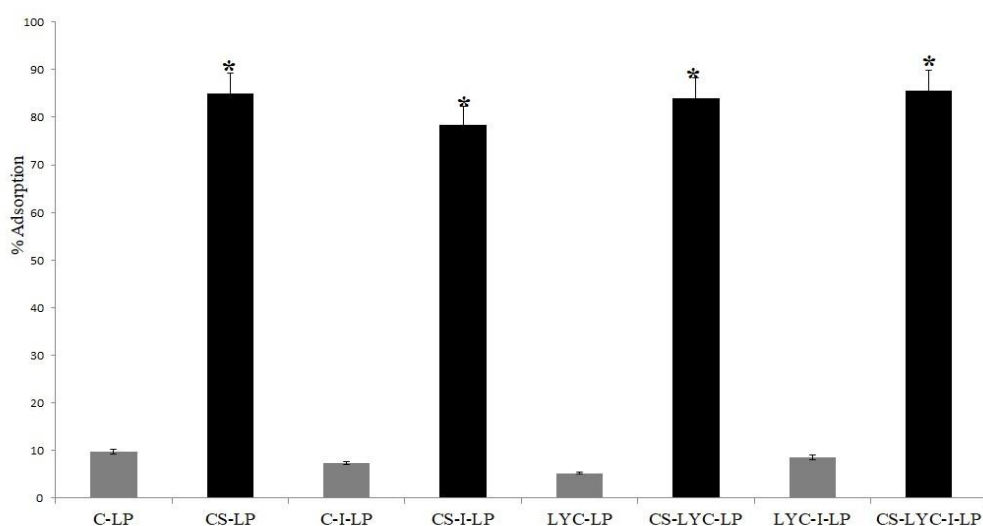


Fig 5.9: Bar diagram representing mucoadhesiveness of developed CS coated nanoliposomes (mean  $\pm$  SD, n = 4). \*p < 0.05, compared to uncoated LPs.

#### 5.4.7 Cell viability

After initial characterization of both uncoated and CS coated nanoliposomes in terms of particle size, zeta potential, encapsulation efficacy, in vitro digestion, and mucoadhesive property, the CS coated liposome samples (CS-C-LP, CS-I-LP, CS-LYC-LP, and CS-LYC-I-LP) were used for further cell culture studies. Nanoliposomes can be entered into cells by different routes such as non-specific endocytosis, receptor mediated endocytosis, phagocytosis etc. Here the surface charge of developed CS coated oral nanoliposomes are

identified as positive charge and is one of the possible ways to interact with the negative charge lipid layer of epithelial cells (presence of mucin), which promoted non-specific endocytosis. It has been recognised that liposome enter into the cells via endocytosis, that was directed by cell membrane and liposomal binding (Alshehri et al., 2018). The concentration of LYC in CS-LYC-LP, and CS-LYC-I-LP was estimated as  $13.2 \pm 0.92$  and  $14.9 \pm 1.1\mu\text{M}$ , used for further studies. Primarily, the antiproliferative effect of nanoliposomes was analyzed by MTT assay. At the same time, free LYC ( $15 \mu\text{M}$ ) and free INU ( $2 \mu\text{g/mL}$ ) were also evaluated for inhibition against HCT 116 cells. From the report,  $\text{IC}_{50}$  value of INU was reported as  $2.5 \mu\text{g/mL}$ . So in this study  $2\mu\text{g/mL}$  concentration was selected for the effect of free INU in cells (Yan et al., 2022).

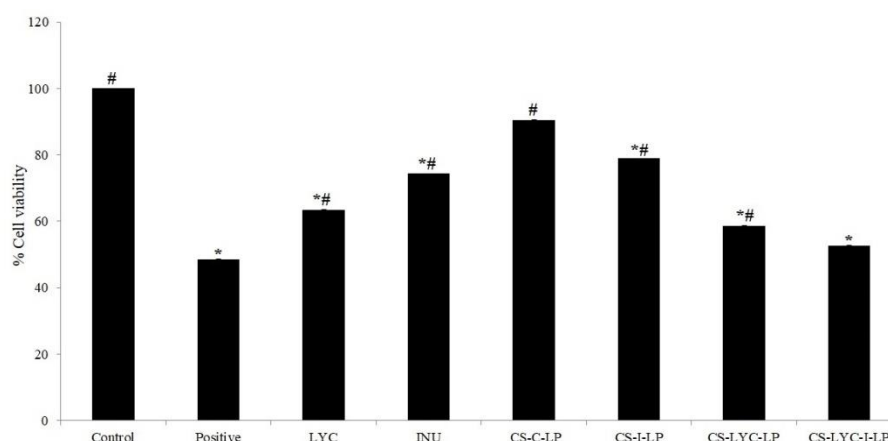


Fig 5.10: Cell viability was assessed by MTT Assay. Each data signifies the mean  $\pm$  SD of triplicate and the significance were analysed by one way ANOVA, \* $p \leq 0.05$  versus Control; # $p \leq 0.05$  versus  $\text{H}_2\text{O}_2$  (positive).

The results (Fig 5.10) indicated that CS-LYC-I-LP exhibited an effective increase in cell death, similar to a positive control ( $500 \mu\text{M H}_2\text{O}_2$ ). Both free LYC and free INU also showed a cell viability of 60 and 75% respectively whereas the CS-C-LP liposome showed low toxicity with 90 % cell viability. Treatment with CS-LYC-LP and CS-LYC-I-LP considerably decreased the cell viability compared to the control cells and showed

significantly ( $p < 0.05$ ) enhanced cytotoxicity level compared to other LPs. These higher cell death demonstrated by CS-LYC-I-LP indicating a synergetic effect of both incorporated LYC and INU in liposome system.

#### 5.4.8 Cell Morphology

The HCT 116 cells were exposed to LYC (15  $\mu\text{M}$ ), INU (2  $\mu\text{g/mL}$ ), and developed liposomes (CS-C-LP, CS-I-LP, CS-LYC-LP, and CS-LYC-I-LP) for 24 h and washed thrice with PBS. The cell morphology was observed at 200x magnification using a phase contrast microscope. Sample free media was taken as the negative control and  $\text{H}_2\text{O}_2$  was taken as the positive control. As shown in Fig 5.11, the numbers of cells were decreased and morphology of the cells became shrunken, cell membrane lysed suggesting that the samples exert cell death in HCT cells.

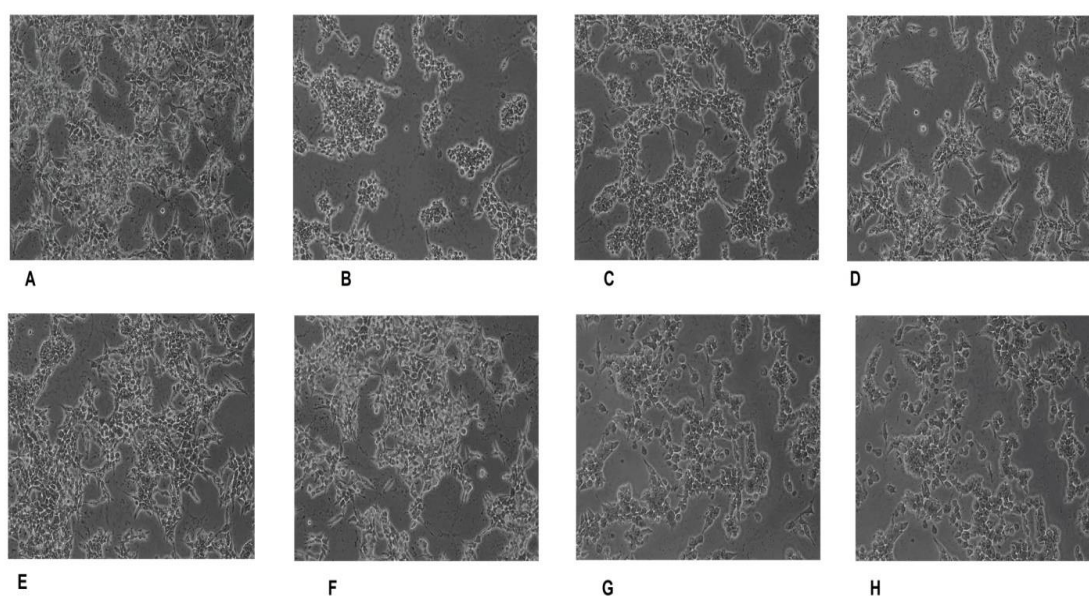


Fig 5.11: Morphological analysis of HCT 116 cells by Phase contrast microscopy: morphological changes of HCT 116 cells exposed to developed CS coated nanoliposomes,  $\text{H}_2\text{O}_2$  treated cells and untreated control cells were observed using phase-contrast microscopy. Original magnification, 40X. The figure depicts the images indicates, A=

Control cells, B= Positive control cells, C=LYC (15 $\mu$ M), D= INU (2 $\mu$ g/ml), E= CS-C-LP, F=CS-I-LP, G= CS-LYC-LP and H= CS-LYC-I-LP treated cells.

The CS-C-LP treated cells show a similar appearance to the control cells. This result indicated that the cells treated with CS-LYC-LP, and CS-LYC-I-LP show similar morphology to the positive control, where cells began to shrink and became irregularly shaped in culture. In CS-LYC-LP, and CS-LYC-I-LP treated cells, there was a loss in cell-to-cell contact; even different morphological distributions could be seen in HCT 116 cells. In HCT 116, filopodia and lamellipodial structures were seen in Fig 5.11A and these seemed to be shattered on CS- LYC-I-LP administered cells suggesting cell cytoskeleton modulation and cell death. Microscopic studies indicated that the cells exposed to developed CS coated nanoliposomes CS-LYC-LP and CS-LYC-I-LP show maximal growth inhibition by cellular shrinkage and induce cell death in HCT 116 cells.

#### **5.4.9 BrdU cell proliferation**

To elucidate the role of developed nanoliposomes (CS-C-LP, CS-I-LP, CS-LYC-LP, and CS-LYC-I-LP) in cellular proliferation was analyzed by BrdU cell proliferation kit. BrdU is a thymidine analogue used for the identification of proliferating cells by quantifying the BrdU incorporation in newly synthesized DNA. As shown in the Fig 5.12, the liposomal exposure, CS-LYC-LP, and CS-LYC-I-LP exerted a potential anti-proliferative effect on HCT 116 cell line by exhibiting a lower BrdU incorporation of  $56.2 \pm 0.083$  and  $54.4 \pm 0.78\%$ . Significant inhibition of cancer cell proliferation can be observed in CS coated samples, indicating a reduction in newly synthesized DNA in cells. From the MTT assay, the cell division rate diminished in nanoliposomes treated cells. Thus, we decided to confirm the anti-proliferative activity of the developed nanoliposomes. As expected, the percentage

of BrdU incorporation in cells diminished significantly in CS-LYC-LP, and CS-LYC-I-LP shows a reduced cellular DNA synthesis.

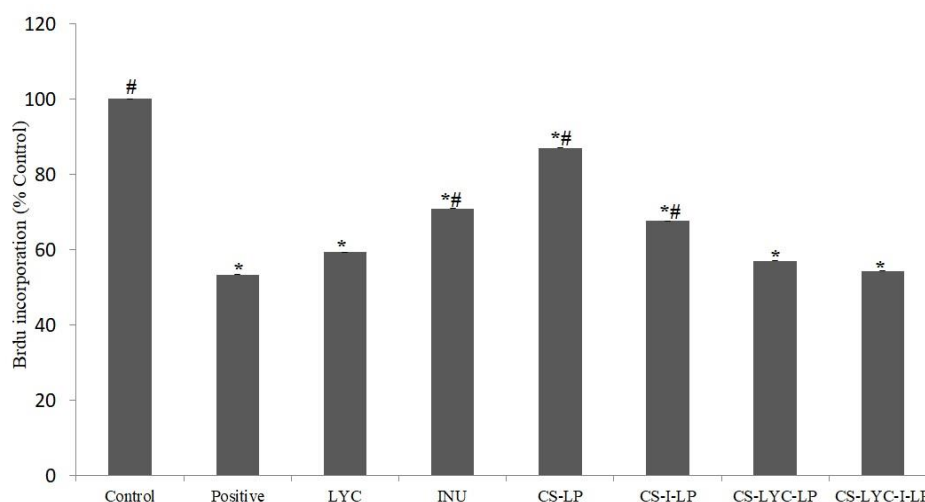


Fig 5.12: Cell proliferation was assessed by BrdU staining. Each data signifies the mean  $\pm$  SD of triplicate and the significance were analysed by one way ANOVA, \* $p \leq 0.05$  versus Control; # $p \leq 0.05$  versus  $H_2O_2$  (positive)

#### 5.4.10 Colony formation assay

To investigate the anti-proliferative effect of developed coated LPs (CS-C-LP, CS-I-LP, CS-LYC-LP, and CS-LYC-I-LP), colony formation assay was performed by using crystal violet staining method. From the data, the colony formation ability of HCT 116 cells was inhibited by the developed LPs especially, CS-LYC-LP, and CS-LYC-I-LP exposed cells, which is comparable to positive control ( $H_2O_2$ ). From the Fig 5.13, it can be noted that CS-LYC-LP and CS-LYC-I-LP exhibit promising inhibitory effect on HCT 116 cells in colony formation. The result showed that CS-C-LP, CS-I-LP shows higher colony formation in HCT 116 cells, while CS-LYC-I-LP shows a significant decrease in colony formation of cells, which indicates a combined effect of LYC and INU in CS-LYC-I-LP



actively suppress the cologenic property of cells. Colonies of cells were photographed using phase-contrast microscope (Fig 5.13)

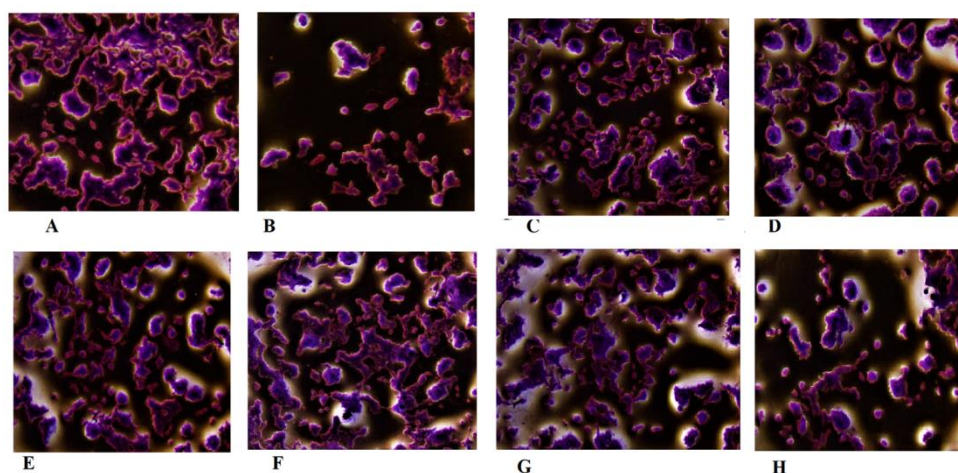


Fig 5.13: Colony formation assay by crystal violet staining: HCT 116 cells treated with developed CS coated nanoliposomes,  $H_2O_2$  treated as positive control and untreated taken as negative control and were observed using phase-contrast microscopy. Original magnification, 40X. The figure depicts the images indicates, A= Control cells, B=  $H_2O_2$ , C=LYC (15 $\mu$ M), D= INU (2 $\mu$ g/ml), E= CS-C-LP, F=CS-I-LP, G= CS-LYC-LP and H= CS-LYC-I-LP treated cells.

#### 5.4.11 Cell death by apoptosis

To investigate whether the reduction in cell viability by CS-C-LP, CS-I-LP, CS-LYC-LP, and CS-LYC-I-LP was connected with apoptotic cell death, Annexin V/PI staining method was studied.  $H_2O_2$  treated cells as positive control and untreated cells as negative control. In the Fig 5.14a, total apoptotic (early and late) population of cells treated with free LYC, free INU,  $H_2O_2$  were  $42 \pm 0.56$ ,  $38 \pm 0.99$  and  $55 \pm 0.68$ % respectively. However, after treatment with nanoliposomes, CS-LYC-I-LP shows a promising apoptotic induction similar to positive control as total apoptotic rate (early and late apoptosis) shows  $51 \pm 0.87$ %. For comparison, LYC and INU as such taken for the cell treatment. Both LYC and INU induce

cellular death by inducing apoptosis. The nanoliposomes, CS-LYC-I-LP possess a synergetic effect of LYC and INU on cells to promote higher programmed cell death. All the developed samples were demonstrating that nanoliposomes induced HCT 116 cell apoptosis, but not necrosis.

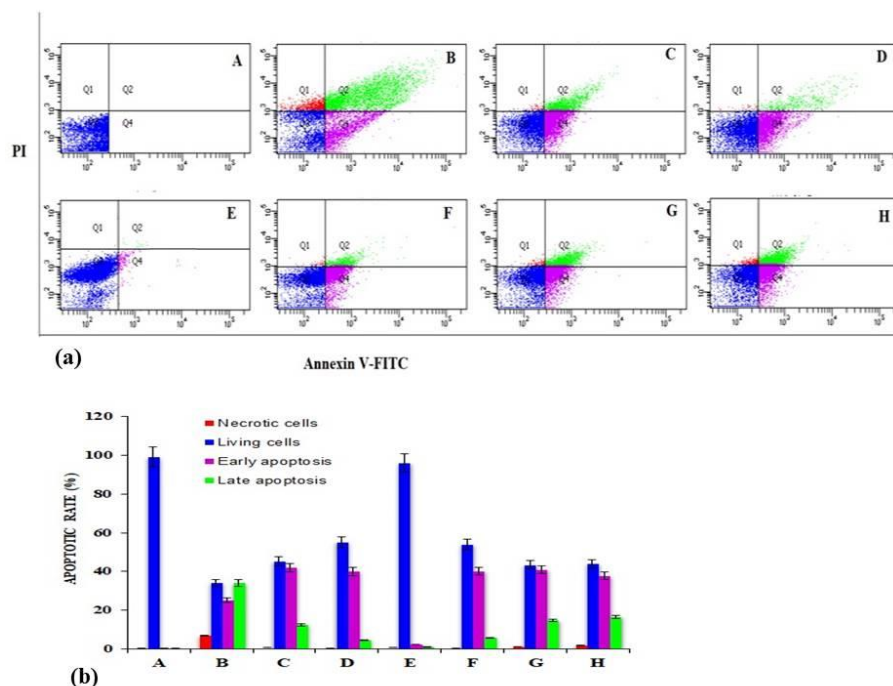


Fig 5.14: Nanoliposomes activates apoptosis in HCT 116 cells was analysed by flow cytometric method. A-Control cells, B- Positive control cells, C-LYC (15µM), D- INU (2µg/ml), E- CS-C-LP, F-CS-I-LP, G- CS-LYC-LP and H- CS-LYC-I-LP treated cells. In the figure (a), represent the cell sorted graph based on Annexin V-FITC staining. In bar diagram (b) represent the percentage evaluation of necrotic cells, live cells early and late apoptotic cells.

## 5.5 Conclusion

Fabrications of chitosan coated liposomes were successfully carried out for the delivery of LYC to the colon region. The results showed that the developed liposomes possess size

ranges in nano scale, better PDI and increased zeta potential. The encapsulation efficacy shows better incorporation of LYC in liposomal system. The *in vitro* release of LYC under stimulated gastric conditions shows very low LYC release kinetics for the chitosan coated liposomes in three stimulated gastro-intestinal fluids with different pH. The CS coating of those liposomes led to further controlled LYC release and, higher mucoadhesiveness. Subsequently, chitosan-coated liposomes appeared to exert antiproliferative effect on colon cancer cells. The results suggest a synergetic effect of LYC and INU in encapsulated liposomes (CS-LYC-I-LP sample) in demonstrating higher antiproliferation and apoptotic effect in HCT116 cells. The CS coated Liposomes would be a promising delivery system aid the controlled release of LYC for colon targeted therapeutic strategies. However, more studies are warranted to understand the mode of action by which the LYC is released in colon region. The prebiotic effect of INU in the liposomes needs to be studied further by *in vitro* prebiotic studies and *in vivo* studies. *In vivo* studies are warranted to conclusively elaborate the actual benefit of the developed system, which definitely is much more promising as indicted in the present study.

**The key findings were summarized below:**

- LYC was successfully incorporated in CS coated liposomal system
- Chitosan coating increased mucoadhesive property of liposomes
- The *in vitro* release of LYC, under stimulated gastric conditions, showed excellent retention of LYC
- The chitosan coated liposomes induced apoptosis in colon cancer cell (HCT 116)
- These oral liposomal formulations could be used for colon targeted therapeutic strategies
- Further studies (*in vitro* and *in vivo*) are necessary to understand exact mechanism by which the LYC is released in colon region and to understand the combined benefits of LYC and INU

## 5.6 Graphical Abstract

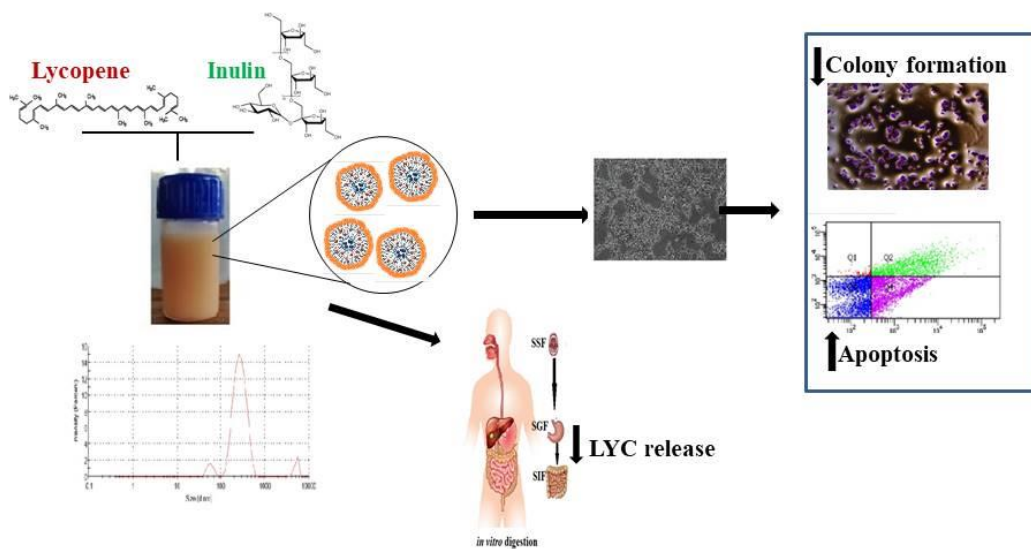


Fig 5.15 Schematic representation of developed nanoliposomes induces apoptosis in HCT 116 cells

## 5.7 Reference

- Akhavan, S., Assadpour, E., Katouzian, I., & Jafari, S. M. (2018). Lipid nano scale cargos for the protection and delivery of food bioactive ingredients and nutraceuticals. *Trends in Food Science & Technology*, 74, 132-146.
- Aktepe, O. H., Şahin, T. K., Güner, G., Arik, Z., & Yalçın, Ş. (2021). Lycopene sensitizes the cervical cancer cells to cisplatin via targeting nuclear factor- kappa B (NF-κB) pathway. *Turkish journal of medical sciences*, 51(1), 368–374.
- Almeida, B., Nag, O. K., Rogers, K. E., & Delehanty, J. B. (2020). Recent Progress in Bioconjugation Strategies for Liposome-Mediated Drug Delivery. *Molecules (Basel, Switzerland)*, 25(23), 5672.
- Alomrani, Abdullah & Badran, Mohammed & Harisa, Gamal & ALshehry, Mohamed & Alhariri, Moayad & Alshamsan, Aws & Alkholief, Musaed. (2019). The use of chitosan-coated flexible liposomes as a remarkable carrier to enhance the antitumor efficacy of 5-fluorouracil against colorectal cancer. *Saudi Pharmaceutical Journal*. 27.
- Alshehri, A., Grabowska, A., & Stolnik, S. (2018). Pathways of cellular internalisation of liposomes delivered siRNA and effects on siRNA engagement with target mRNA and silencing in cancer cells. *Scientific reports*, 8(1), 3748.
- Alshraim, M. O., Sangi, S., Harisa, G. I., Alomrani, A. H., Yusuf, O., & Badran, M. M. (2019). Chitosan-Coated Flexible Liposomes Magnify the Anticancer Activity and Bioavailability of Docetaxel: Impact on Composition. *Molecules (Basel, Switzerland)*, 24(2), 250.

- Ayoub, N.M., Alkhalifa, A.E., Ibrahim, D.R., Alhusban, A. (2021) Combined crizotinib and endocrine drugs inhibit proliferation, migration, and colony formation of breast cancer cells via downregulation of MET and estrogen receptor. *Medical Oncology*, 38(8).
- Bradford M. M. (1976). A rapid and sensitive method for the quantitation of microgram quantities of protein utilizing the principle of protein-dye binding. *Analytical biochemistry*, 72, 248–254.
- Caddeo, C., Díez-Sales, O., Pons, R., Carbone, C., Ennas, G., Puglisi, G., Fadda, A.M., Manconi, M.( 2016). Cross-linked chitosan/liposome hybrid system for the intestinal delivery of quercetin. *Journal of Colloid and Interface Science*, 461, 69–78.
- Chen, H., Pan, H., Li, P., Wang, H., Wang, X., Pan, W., & Yuan, Y. (2016). The potential use of novel chitosan-coated deformable liposomes in an ocular drug delivery system. *Colloids and surfaces. B, Biointerfaces*, 143, 455–462.
- Hadian Z, Sahari M.A., Moghimi HR, Barzegard M, et al.(2014) Formulation, characterization and optimization of liposomes containing eicosapentaenoic and docosahexaenoic acids, a methodology approach. *Iran Journal of Pharmaceutical Research*,13(2):393.
- He, H., Lu, Y., Qi, J., Zhu, Q., Chen, Z., & Wu, W. (2019). Adapting liposomes for oral drug delivery. *Acta pharmaceutica Sinica. B*, 9(1), 36–48.
- Imam, S. S., Alshehri, S., Altamimi, M. A., Hussain, A., Qamar, W., Gilani, S. J., Zafar, A., Alruwaili, N. K., Alanazi, S., & Almutairy, B. K. (2021). Formulation of Piperine-Chitosan-Coated Liposomes: Characterization and In Vitro Cytotoxic Evaluation. *Molecules (Basel, Switzerland)*, 26(11), 3281.

- Jiao, Z., Wang, X., Yin, Y., Xia, J., Mei, Y. (2018). Preparation and evaluation of a chitosan-coated antioxidant liposome containing vitamin C and folic acid. *Journal of microencapsulation*, 35(3), 272–280.
- Karim, N., Shishir, M. R. I., Xie, J., & Chen, W. (2020). Colonic delivery of pelargonidin-3-O-glucoside using pectin-chitosan-nanoliposome: Transport mechanism and bioactivity retention. *International journal of biological macromolecules*, 159, 341–355.
- Keum N, Giovannucci E. Global burden of colorectal cancer: emerging trends, risk factors and prevention strategies. *Nat Rev Gastroenterol Hepatol*. Springer Science and Business Media LLC. 2019,16(12):713–732.
- Lee H., Gaddy D., Ventura M., Bernards N., de Souza R., Kirpotin D., et al. (2018). Companion Diagnostic <sup>64</sup>Cu-Liposome Positron Emission Tomography Enables Characterization of Drug Delivery to Tumors and Predicts Response to Cancer Nanomedicines. *Theranostics* 8, 2300–2312.
- Li, H., Liu, S., Yue, L., Weinan, N., Ren, P., Yingying et al (2021). Effects of in vitro digestion and fermentation of Nostoc commune Vauch. polysaccharides on properties and gut microbiota. *Carbohydrate Polymers*. 281. 119055.
- Li, Y., Zhang, R., Xu, Z., & Wang, Z. (2022). Advances in Nanoliposomes for the Diagnosis and Treatment of Liver Cancer. *International journal of nanomedicine*, 17, 909–925.
- Liu, W., Hou, W., Jin, Y., Wang, Y., Xu, X., Han, Z. (2020) Research progress on liposomes: Application in food, digestion behavior and absorption mechanism, *Trends in Food Science & Technology*, 104, 177-189.



- Malki, A., ElRuz, R. A., Gupta, I., Allouch, A., Vranic, S., & Al Moustafa, A. E. (2020). Molecular Mechanisms of Colon Cancer Progression and Metastasis: Recent Insights and Advancements. *International journal of molecular sciences*, 22(1), 130.
- Mosmann, T. (1983). Rapid colorimetric assay for cellular growth and survival, Application to proliferation and cytotoxicity assays. *Journal of Immunological Methods*, 65, 55–63
- Nguyen, T.X., Huang, L., Liu, L., Abdalla, A.M.E., Gauthier, M., & Yang, G. (2014). Chitosan-coated nano-liposomes for the oral delivery of berberine hydrochloride, *Journal of Material Chemistry*, 7149–7159.
- Ong C. P., Lee W. L., Tang Y. Q., Yap W. H. (2020). Honokiol: A Review of its Anticancer Potential and Mechanisms. *Cancers* 12, 48. 10.3390/cancers12010048.
- Perezmasia, R., Lagaron, J. M., & Lopezrubio, A. (2015). Morphology and stability of edible lycopene-containing micro- and nanocapsules produced through electrospraying and spray drying. *Food and Bioprocess Technology*, 8(2), 459–470.
- Petrou, Georgia & Crouzier, Thomas. (2018). Mucins as multifunctional building blocks of biomaterials. *Biomaterials Science*. 6. 10.1039
- Rasti B, Erfanian A, Selamat J. (2017) Novel nanoliposomal encapsulated omega-3 fatty acids and their applications in food. *Food Chemistry*, 230:690-696.
- Roy, B., Guha, P., Bhattarai, R., Nahak, P., Karmakar, G., Chettri, P., & Panda, A.K. (2016). Influence of lipid composition, pH, and temperature on physicochemical properties of liposomes with curcumin as model drug, *J. Oleo Sci.* 65,399–411.
- Sarabandi, K., Peighambardoust, S. H., Mahoonak, A. S., & Samaei, S. P. (2017). Effect of carrier types and compositions on the production yield, microstructure and physical

- characteristics of spray dried sour cherry juice concentrate. *Journal of Food Measurement and Characterization*.
- Sebaaly, C., Jraij, A., Fessi, H., Charcosset, C., Greige-Gerges, H. (2015) Preparation and characterization of clove essential oil-loaded liposomes. *Food Chem.* 1,178:52-62.
- Sebaaly, C., Trifan, A.; Sieniawska, E., Greige-Gerges, H. (2021). Chitosan-Coating Effect on the Characteristics of Liposomes: A Focus on Bioactive Compounds and Essential Oils: A Review. *Processes*, 9, 445.
- Souza, A. L. R., Hidalgo-Chavez, D. W., Pontes, S. M., Gomes, F. S., Cabral, L. M. C., & Tonon, R. V. (2018). Microencapsulation by spray drying of a lycopene-rich tomato concentrate: Characterization and stability. *LWT-Food Science and Technology*, 91, 286–292.
- Tan, C., Feng, B., Zhang, X., Xia, W., & Xia, S. (2016). Biopolymer-coated liposomes by electrostatic adsorption of chitosan (chitosomes) as novel delivery systems for carotenoids, *Food Hydrocolloids*. 52, 774–784.
- Tsumoto, K., Matsuo, H., Tomita, M., et al., (2009). Efficient formation of giant liposomes through the gentle hydration of phosphatidylcholine films doped with sugar. *Colloids and Surfaces B : Biointerfaces*68 (1), 98–105.
- Verma, S.,& Utreja, P. (2021). Exploring Therapeutic Potential Of Invasomes, Transfersomes, Transethosomes, Oleic Acid Vesicles, And Cubosomes Adopting Topical/Transdermal Route. *Micro and Nanosystems*. 13. 10.2174.
- Wang, J., Li, L., Wang, Z., Cui, Y., Tan, X., Yuan, T., Liu, Q., Liu, Z., & Liu, X. (2018). Supplementation of lycopene attenuates lipopolysaccharide-induced

amyloidogenesis and cognitive impairments via mediating neuroinflammation and oxidative stress. *The Journal of nutritional biochemistry*, 56, 16–25.

Wang, M., Tingting, Z., Yanping, L., et al., (2017). Ursolic acid liposomes with chitosan modification: Promising antitumor drug delivery and efficacy. *Materials Science and Engineering: C*, 71, 1231–1240.

Yan, H., Jingzhe, J., Hongxia, D., Chao, L., Liqing, C., Wei, H., Zhonggao, G., Mingji, J. (2022). Targeted therapeutic effects of oral inulin-modified double-layered nanoparticles containing chemotherapeutics on orthotopic colon cancer. *Biomaterials*, 283, 0142-9612

Zhang, K., Wen, Q., Wang, Y., Li, T., Nie, B., & Zhang, Y. (2022). Study on the in vitro digestion process of green wheat protein: Structure characterization and product analysis. *Food science & nutrition*, 10(10), 3462–3474.

Zhao, T., Liu, Y., Gao, Z., Gao, D., Li, N., Bian, Y., Dai, K., & Liu, Z. (2015). Self-assembly and cytotoxicity study of PEG-modified ursolic acid liposomes. *Materials science & engineering. C, Materials for biological applications*, 53, 196–203.

Zhou H., Xia L., Zhong J., Xiong S., Yi X., Chen L., et al. (2019). Plant-derived Chlorophyll Derivative Loaded Liposomes for Tri-model Imaging Guided Photodynamic Therapy. *Nanoscale* 11, 19823–19831.

**Chapter 6**

**Summary and Conclusion**

LYC is one of the most important members of the carotenoid family with a tetraterpene structure. The unique structure of LYC is responsible for the bright red in many fruits and vegetables. It is associated with high antioxidant activity with wide variety of beneficial effects in the prevention and treatment of various diseases like diabetes mellitus, cardiovascular diseases, cancers, skin and bone ailments, neurological disorders, etc. LYC exhibits highest singlet oxygen quenching ability among all other carotenoids. LYC interacts with reactive oxygen species in mitigating their damaging effects on cellular biomolecules and play a significant role in preventing these diseases, thus presenting a potential candidate for nutraceutical and functional food applications.

During normal metabolic processes, cells produce free radicals in physiological level and cells also produce innate antioxidants that neutralize these free radicals. There are numerous factors that mainly include diet and lifestyle, which leads to oxidative stress formation by excess free radical production in the cells. These Oxidative stress is a resultant of the imbalance between oxidative and antioxidative mechanism in cells, which plays a vital role in the pathogenesis of numerous chronic disorders. ROS accumulation in the cells is the basic factor responsible for most of the chronic diseases development. Dietary antioxidants are known to play a significant role in curtailing the detrimental effects of ROS. The present study is **designed to elucidate the role of LYC as an antioxidant and prooxidant for the management of stress mediated disease conditions using *in vitro* studies.**

With this back ground the present investigation entitled “**Nutraceutical potential of lycopene in management of oxidative stress mediated disease conditions**” focussed on (1) investigating the antioxidant potential of LYC-rich tomato peel extract (ETE) against stress-induced L6 myoblast cells (2) Evaluate the role of LYC in mitigation of acrylamide (ACR) and glycidamide (GLY) induced toxicity in HepG2 and elucidate the role of LYC in ACR/GLY induced cell death via ROS-regulated mitochondrial dysfunction (3) To study the

antitumorigenic effect of LYC in colon cancer cell line ( HCT 116 cells) via suppressing P13/AKT/mTOR signalling (4)To Develop LYC incorporated nanoliposomes for colon targeted delivery and to conduct preliminary study on its antitumorigenic effect in colon cancer cells (HCT 116).

**Chapter 1** gives a general introduction and review of literature about Lycopene, stress related diseased conditions and colon targeted delivery system

*Enzyme assisted extraction of lycopene from tomato peel extract and evaluation of antioxidant potency against oxidative stress in L6 myoblast*

The role of LYC as a powerful antioxidant against different disease conditions is well established and there is an increasing interest in developing LYC-containing supplements, nutraceuticals, and functional foods. Tomato is one of the major sources of industrial production of LYC. The tomato processing industry generates significant amounts of by-products, consisting of tomato peel and seeds which could be exploited as a source of LYC with a circular economy point of view. Based on the previous reports that enzyme pretreatment improves the extraction of active ingredients (mainly carotenoids) from tomato peel, CSIR-NIIST has optimized a process for the enzyme assisted extraction of LYC rich oleoresin (ETE) from tomato peel. **Chapter 2** summarizes antioxidant potential of this LYC rich tomato peel extract (ETE) against stress induced skeletal muscle cell (L6 myoblast). ETE was found to help in normalization of ROS, DNA protection and restoring mitochondrial membrane potential of L6 cells which was pre-treated with H<sub>2</sub>O<sub>2</sub> for induction of stress. The potential of ETE to protect cells from oxidative damage was investigated in terms of cytotoxicity (MTT assay), reactive oxygen species (ROS) by 20, 70-dichlorofluoresceindiacetate (H<sub>2</sub>DCFDA), DNA damage (ladder assay, 8-oxo-dG), Hoechst 33342 nuclear staining, mitochondrial stability by ATP production and mitochondrial membrane potential by Rhodamine 123 staining. It was observed that treatment of cells with

ETE significantly increased cell viability, decreased ROS production, reduced DNA fragmentation, chromatin condensation & 8-oxo-dG, increased ATP levels and mitochondrial membrane potential. This study demonstrated the effectiveness of extract, ETE, in counteracting redox imbalance under condition encountered in most of the disease conditions by modulating the cellular antioxidant status. The results provide significant evidence for the potential of antioxidant rich tomato peel extracts against mitochondrial and DNA damage induced by oxidative stress-mediated pathophysiology .

***Role of Lycopene in Mitigation of Acrylamide/ Glycidamide induced Hepatotoxicity (HepG2 cells)***

Oxidative stress induced in the cells on exposure to food toxicants such as acrylamide (ACR) creates an imbalance between physiological reactive oxygen species (ROS) level and detoxification by antioxidant enzyme system leading to cytotoxicity and genotoxicity. Acrylamide is a heat induced food toxicant found high temperature processed foods such as deep fat fried, baked, extruded and coffee bean-based products. Long term exposure to ACR is reported to induce genotoxicity and mutagenicity. **Chapter 3** deals with the role of LYC in mitigating the oxidative stress developed in cells on exposure to Acrylamide (ACR) and its metabolite Glycidamide (GLY). The study demonstrated the cytoprotective potential of LYC (10  $\mu$ M) in attenuating ACR and GLY (500  $\mu$ M, each) induced cytotoxicity in HepG2 cells. HepG2 cells on pre-treatment with LYC could protect the cells from oxidative stress induced by exposure to ACR and GLY. The protective effect of LYC seems to be mediated by inhibiting intracellular ROS generation, enhance the activity of antioxidants enzymes superoxide dismutase (SOD), catalase (CAT) and glutathione (GSH) level, with reduction in malondialdehyde (MDA) and 8-oxo-dG level. Together, the results from the study suggested that the LYC from natural products can protect HepG2 cells against ACR and GLY -induced

oxidative damage by ameliorating the oxidative stress through enhancement of cellular antioxidant defence mechanism.

*Lycopene regulates colon tumorigenesis via suppressing ROS mediated P13/Akt/mTOR signalling in HCT 116 cells*

LYC is reported to exhibit both antioxidant and prooxidant property depending on the cellular conditions. The use of pro-oxidant agents is emerging as an exciting strategy for the selective target of tumor cells. This study investigated the multi-target mechanisms of LYC against colon cancer cells HCT 116 by evaluating the mitochondrial mediated apoptosis and abnormal regulation of the phosphoinositide 3-kinase/ Akt/ mTOR survival signalling pathway. **Chapter 4** summarizes the role of LYC as a prooxidant in inducing colon cancer cell death by apoptosis via inhibiting P13K/AKT/mTOR signalling cascade. The LYC (15 $\mu$ M) treated cells were evaluated for intracellular reactive oxygen species (ROS) level, antioxidant enzymes such as CAT and GSH activity, mitochondrial membrane potential, caspase 3 and 9 expression, and flow cytometric analysis of apoptosis by Annexin V-FITC/PI. The anti and pro apoptotic proteins and PI3K/AKT/mTOR cascade protein expression was investigated by Western blot analysis. Data showed that LYC significantly inhibited the cells viability in dose dependent manner at which 15 $\mu$ M exhibited  $56 \pm 0.91\%$  cell death, elevated intracellular ROS level of  $32.6 \pm 0.20\%$ , which leads to a decrease in CAT and GSH levels. ROS mediated mitochondrial membrane potential ( $\Delta\psi_m$ ) loss was higher at 15 $\mu$ M, of  $55.4 \pm 0.34\%$ . LYC resulted in externalization of phosphotidylserine in HCT116 cells suggesting that LYC induced mitochondrial- mediated apoptosis via augmentation of intracellular ROS with apoptotic rate of  $54 \pm 0.5\%$ . Western blot assays results further confirmed LYC induced ROS mediated, caspase-dependent apoptosis by increased Bax and decreased Bcl-2 expression and a suppression in PI3K/AKT/mTOR



signalling proteins. The downregulation of the PI3K/AKT/mTOR pathway is crucial in human oncogenesis, and as a chief effector of this signalling pathway, mTOR is broadly associated with cell transformation, proliferation, and survival. With increasing LYC concentrations the expression levels of p-PI3K, p-AKT and p-mTOR were significantly downregulated in HCT 116 cells in dose dependent way. Data suggest that LYC induced ROS-mediated cell cycle arrest and apoptosis through mitochondrial pathway accompanying with caspase-dependent cell death by inhibiting PI3K/AKT/mTOR cascade in human colorectal cancer HCT116 cells. Cell cycle analysis was also investigated and the results showed a G2/M phase arrest in HCT 116 cells. The Results suggested that, in addition to its antioxidant activity, lycopene also exhibit prooxidant activity by inducing ROS production in cells and thereby inhibit cell proliferation, cell cycle progression, and apoptosis induction, via regulating of PI3K/Akt/mTOR signal transduction pathways.

***Development and characterization of chitosan coated lycopene nanoliposomes with inulin for colon delivery***

.Nanoliposomes are reported to improve time-controlled drug releasing, and reduce the adverse effects of drugs in vitro and in vivo. One of the major drawbacks of liposomes as a carrier system is their fast removal from blood circulation and they are physically unstable, which depends on several factors which lead liposomal fusion, hydrolysis, degradation, and oxidation of phospholipids. Polymer coating is promising way to improve liposome applicability by change the surface characteristics of liposomes. Here we attempted to fabricate encapsulated liposomal formulations, Lycopene liposomes (LYC- LP) for colon delivery with improved stability for prevention and management of colorectal cancer. **Chapter 5** summarizes the development of chitosan coated LYC/INU (inulin) incorporated nanoliposomes, its gastro intestinal release and preliminary studies on its effect in colon

cancer cells (HCT 116). Chitosan-coated nanoliposomes were prepared using thin-film hydration method, as a practical oral delivery system for the encapsulation of LYC. The chitosan coated liposomal formulations (CS-C-LP, CS-I-LP, CS-LYC-LP, CS-LYC-I-LP) had a marked positive charges, which makes it possible to attach to the negative charged tumour cells leading to the inhibition of cellular growth as confirmed by mucin adsorption study. The average size of LYC and INU nanoliposomes (CS-LYC-I-LP) was 365 nm, with PDI value 0.54, and that was more easily entrapped into tumour cells. CS-LYC-I-LP showed much slower *in vitro* LYC release at all the stimulated phases (SSF, SGF, and SIF) in *in vitro* digestion method ( $0.2 \pm 1.01$ ,  $0.3 \pm 0.06$ , and  $0.9 \pm 0.02\%$ ), which ensured colon targeted delivery. The developed liposome CS-LYC-I-LP exhibit a higher apoptotic rate in colon cancer cells (HCT 116) of  $51 \pm 0.87 \%$ . The preliminary studies on developed liposomes indicates that the proper coating of liposomes with CS can not only improve gastrointestinal stability and colon target delivery of LYC, but also improved the antitumor efficacy in cancer cells, hence it is a most promising carrier system for lipophilic compounds like LYC for colon targeted delivery.

Nutraceuticals in numerous forms, including tablets, syrups, gums, and capsules, have fast become a staple in the healthcare market. It provides benefits in the prevention and treatment of various diseases. Results from the studies indicated that LYC is a promising antioxidant and prooxidant activity against ROS mediated cellular damages that leads to the development of chronic disease conditions. As a natural antioxidant, LYC can be used as an excellent nutraceutical against various stress related disease conditions. Nutraceuticals cannot replace pharmaceuticals but can be a strong high-value tool for prevention and aid in therapy of some pathological conditions.

## Conclusions

- Enzyme assisted tomato peel extract (ETE) enriched with LYC helps acts as a potent antioxidant source which protects the L6 cells from hydrogen peroxide induced oxidative damage.
- ETE (100 µg/mL) could counteract redox imbalance under stress induced conditions encountered in most of the diseases.
- LYC (10 µM) was found to attenuate ACR and GLY (500 µM.) induced cytotoxicity in HepG2 cells by modulating cellular antioxidant status.
- LYC (10 µM.) alleviates ACR and GLY induced apoptosis via modulating ROS-mediated mitochondrial dysfunction in HepG2 cells
- LYC (15 µM) increases the ROS level in cells and decreases antioxidant enzyme activity as a pro-oxidant in HCT 116
- LYC (15µM) triggered mitochondrial mediated apoptosis in HCT 116 cells by inhibiting PI3K/AKT/mTOR signalling pathway
- CS coated nanoliposomes with successfully incorporation of LYC in liposomal system was fabricated for colon delivery. The CS coated nanoliposomes exhibit excellent LYC retention ( $0.9 \pm 0.02\%$  LYC release,) under stimulated gastric conditions.
- Chitosan coating on liposomal surface increased mucoadhesive property of liposomes, which helps in cell mediated liposomal entry
- The chitosan coated liposomes induced cell death by apoptosis in colon cancer cell line (HCT 116), therefore these oral liposomal formulations could be used for colon targeted therapeutic strategies

## Future aspects

- The exploitation of Tomato peel as a source of natural antioxidants for developing functional foods/nutraceutical products based on waste to wealth concept needs to be explored further
- Supplementation of LYC, a natural antagonist of ACR and GLY, through diet could mitigate the side effects caused by the consumption of high-temperature processed foods. Further *in vivo* studies are warranted to substantiate these findings.
- The study proposes LYC as a potential candidate for the prevention and management of CRC, which can inhibit the proliferation of CRC cells and induce apoptosis by inhibiting the PI3K/AKT/mTOR signalling pathway. Further *in vivo* studies are warranted to substantiate these findings.
- The combined benefits of LYC and INU need to be further established using *in vitro* and *in vivo* models. The exact mechanism by which the LYC is released in the colon region needs to be established further. The impact of the prebiotic potential of INU on the activity of LYC needs to be investigated using *in vitro* and *in vivo* models.

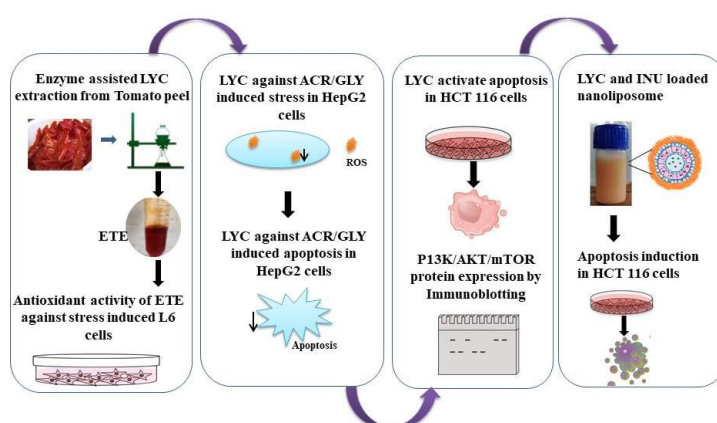


Fig 8.1 Graphical representation of chapters which brief demonstration of the work flow.

## APPENDIX

### List of Instruments

<b>Instruments</b>	<b>Manufacturer</b>
Homogenizer	T25 D S22 Digital ultra turrax, IKA private limited, Bengaluru, India
Micro-plate reader	Synergy 4 Biotek, USA
UV Spectrophotometr	Shimadzu, Japan
Gel electrophoresis system	Bio-Rad Laboratories, Germany
Zetasizer	Malvern Instruments Ltd., UK
FTIR spectrophotometer	Perkin Elmer, USA
HPLC	Shimadzu, Japan
FACS	BD FACS Aria II, BD Bioscience, USA
Fluorescent Microscopy	Olympus fluorescence microscope IX83, USA
Confocal Microscopy	Pathway 855, BD Bioscience, USA
Gel Doc	Bio-Rad Laboratories, Germany
Color Spectrophotometer	Hunder Lab, ColorFlex, Virginia
Refrigerated Centrifuge	Beckman Coulter, Pasadena, CA, USA

## ABSTRACT

<b>Name of the student: Reshmitha T R</b>	<b>Registration No.: 10BB17J39008</b>
<b>Faculty of study: Biological Science</b>	<b>Year of submission: 2022</b>
<b>ACSIR academic centre/CSIR Lab: CSIR-NIIST</b>	<b>Name of supervisor: Dr P. Nisha</b>
<b>Title of the thesis: ‘Nutraceutical potential of lycopene in management of oxidative stress mediated disease conditions’.</b>	

Disease management with the application of natural dietary products has been an opportunity for prophylactic and therapeutic use for different disease conditions. When free radicals are generated beyond the limit of inherent antioxidant system to tackle, free radicals can damage cellular biomolecules leading to onset of chronic disease conditions. Consumption of diets rich in antioxidants such as lycopene (LYC), which is a major carotenoid found in red fruits, is known to protect from free radical exposure and oxidative stress, and growing evidences suggest that dietary bioactive components could mitigate the oxidative damage. In the present study, we attempted to shed light on the protective effect LYC in cells on tackling oxidative stress induced by different conditions, using *in vitro* model. Chapter 1 gives a general introduction and review of literature about LYC, stress related diseased conditions and colon targeted delivery system. In the first experimental chapter (chapter 2), LYC enriched fraction (ETE) obtained by cell wall degrading enzymes from tomato peel was used to screen its antioxidant potential against stress induced L6 myoblast cells. ETE demonstrated promising antioxidant activity by normalization of ROS, reduced DNA fragmentation, chromatin condensation & 8-oxo-dG, increased ATP levels and mitochondrial membrane potential. In chapter 3, the role of LYC in mitigation of oxidative stress induced by exposure to food toxins (acrylamide and glycidamide) was investigated in HepG2 cells. In this study, LYC was found to attenuate ACR and GLY induced cytotoxicity by modulating cellular antioxidant status and also alleviates ACR and GLY induced apoptosis via modulating ROS-mediated mitochondrial dysfunction in HepG2 cells. LYC is also reported to possess pro-oxidant property in cells, according to the cellular conditions. Therefore, the chapter 4 focused on anticancer ability of LYC as a pro-oxidant in HCT 116. Study showed that LYC increased the ROS level with a reduction in antioxidant enzyme activity that triggered mitochondrial mediated apoptosis in HCT 116 cells by inhibiting PI3K/AKT/mTOR signalling pathway. Further to this, LYC was incorporated in a liposomal system coated with chitosan for the colon delivery which forms the content for chapter 5. The key point of this study is that, supplementation of LYC, a natural antagonist could mitigate the development and progression of stress mediated disease conditions.

## PUBLICATIONS

### Publications from thesis

- **Reshmitha, T. R.**, Sithara, T., Arun, K. B., and Nisha., P. (2017). DNA and Mitochondrial protective effect of lycopene rich tomato peel extract prepared by enzyme assisted extraction against H<sub>2</sub>O<sub>2</sub> induced oxidative damage in L6 Myoblasts, *Journal of Functional Foods* 28 ;147–156 (IF- 4.451)
- **Reshmitha, T. R.**, and Nisha., P. (2021). Lycopene mitigates acrylamide and glycidamide induced cellular toxicity via oxidative stress modulation in hepg2 cells, *Journal of functional foods*, 80, 104390

### Publications from other contributions as a co-author

- Sasikumar, P, Prabha, B, **Reshmitha, T. R.**, Sheeba Veluthoor, Pradeep, A. K., Rohit, K. R., Dhanya, B. P., Sivan, V. V., Jithin, M. M., Anil Kumar, N., Shibi, I. G., Nisha, P., and Radhakrishnan, K. V. (2016). Comparison of antidiabetic potential of (+) and (–)-hopeaphenol, a pair of enantiomers isolated from *Ampelocissus indica* (L.) and *Vateria indica* Linn., with respect to inhibition of digestive enzymes and induction of glucose uptake in L6 myotubes. *RSC Advances.*, 6, 77075
- Arun , K.B., Sithara Thomas , **Reshmitha , T.R.**, Akhil , G.C., and Nisha . P. (2017). Dietary fibre and phenolic-rich extracts from *Musa paradisiaca* inflorescence ameliorates type 2 diabetes and associated cardiovascular risks. *Journal of Functional Foods*, 31 ,198–207
- Greeshma, G., Dhanya, B. P., Saranya, J., **Reshmitha, T. R.**, Baiju, T.V., Meenu, M.T., Nair, M.S., Nisha, P., and Radhakrishnan, K. V. (2017) Metal-Free *trans*-Aziridination of Zerumbone: Synthesis and Biological Evaluation of Aziridine

Derivatives of Zerumbone. *European Journal of Organic Chemistry*  
10.1002/ejoc.201700410

- Dhanya, B. P. Greeshma G., **Reshmitha, T. R.**, Saranya, J., Sharathna, P., Shibi, I. G., Nisha, P., and Radhakrishnan, K. V. (2017) synthesis and *in vitro* evaluation of zerumbone pendant derivatives: potent candidates for anti-diabetic and anti-proliferative activities *new Journal of Chemistry.*, 41, 6960-6964
- Sithara, T., Arun, K. B., Syama, H. P., **Reshmitha, T. R.**, and Nisha, P. (2017). Morin Inhibits Proliferation of SW480 Colorectal Cancer Cells by Inducing Apoptosis Mediated by Reactive Oxygen Species Formation and Uncoupling of Warburg Effect. *Frontiers in pharmacology*, 8, 640.
- Arun ., K B., Madhavan, A., , **Reshmitha., T. R.**, Thomas, S., , and Nisha, P., (2018). Musa paradisiaca inflorescence induces human colon cancer cell death by modulating cascades of transcriptional events. *Food and function*, 9(1), 511–524.
- Gopalan, G., Prabha, B., Joe, A., **Reshmitha, T. R.**, Sherin, D. R., Abraham, B., Sabu, M., Manojkumar, T. K., Radhakrishnan, K. V., & Nisha, P. (2019). Screening of Musa balbisiana Colla. seeds for antidiabetic properties and isolation of apiforol, a potential lead, with antidiabetic activity. *Journal of the science of food and agriculture*, 99(5), 2521–2529.
- K B, Arun., , Aravind, M., Reshmitha, T. R., Sithara, T., and Nisha, P. (2019). Short chain fatty acids enriched fermentation metabolites of soluble dietary fibre from Musa paradisiaca drives HT29 colon cancer cells to apoptosis. *PloS one*, 14(5), e0216604.
- Billu, A., Reshmitha, T.R., Navami, M.M., Liza, G., , Venugopalan, V. V., and Nisha, P.. (2020) Phytochemical rich extract from the spent material generated from industrial dashamoola preparation (a medicinal ayurvedic decoction) with



antioxidant, antidiabetic and anti-inflammatory potential *industrial crops and products* 151. 112451. 10.1016/j.indcrop.2020.112451.

### **Book Chapter Publications**

- **Reshmitha T.R.**, Shini V.S., Nisha P. (2021) Nanotechnology Approaches for Colorectal Cancer Diagnosis and Therapy. In: Vishvakarma N.K., Nagaraju G.P., Shukla D. (eds) *Colon Cancer Diagnosis and Therapy*. Springer, Cham. [https://doi.org/10.1007/978-3-030-64668-4\\_8](https://doi.org/10.1007/978-3-030-64668-4_8)

## National/international conferences/seminars

- **Reshmitha T R.**, Sithara Thomas., Arun K B., Nisha, P. (2017) DNA and Mitochondrial protective effect of lycopene rich tomato peel extract prepared by enzyme assisted extraction against H<sub>2</sub>O<sub>2</sub> induced oxidative damage in L6 myoblast cells. Oral presentation in *International conference on “Food Value Chain: Innovations and Challenges”* from 17-19<sup>th</sup> March at Haryana conducted by NIFTEM.
- **Reshmitha T R.**, Aswathy P S., Oliya N, Nisha P.(2018) Development and optimization of antidiabetic functional beverages in the form of Bag based blends of green tea-spice/herb for making decoction. Poster presentation in 8<sup>th</sup> International food convention , Holistic approaches for start ups, Human Resources training for agricultural and food industry gemmation, “IFcON 18” from 12-15<sup>th</sup> December at CSIR-CFTRI, Mysore conducted by AFSTI.
- **Reshmitha T R.**, Aswathy P S, Oliya N, Nisha P. (2018). Antioxidant and hypoglycemic activity of functional beverage (health drink) developed from spices/herbs with bioactive rich fruits. Poster presentation in International Conference on Recent Advances in Food Processing Technology: Doubling Farmers Income through Food Processing, organized by IIFPT to be held on 17<sup>th</sup> to 19<sup>th</sup> August, 2018 at IIFPT, Thanjavur.



Contents lists available at ScienceDirect

Journal of Functional Foods

journal homepage: [www.elsevier.com/locate/jff](http://www.elsevier.com/locate/jff)

## DNA and mitochondrial protective effect of lycopene rich tomato (*Solanum lycopersicum* L.) peel extract prepared by enzyme assisted extraction against H<sub>2</sub>O<sub>2</sub> induced oxidative damage in L6 myoblasts



T.R. Reshmitha, Sithara Thomas, S. Geethanjali, K.B. Arun, P. Nisha\*

Agro Processing and Natural Products Division, CSIR-National Institute for Interdisciplinary Science and Technology (CSIR-NIIST), Industrial Estate P.O, Thiruvananthapuram 695019, Kerala, India

## ARTICLE INFO

## Article history:

Received 6 May 2016  
Received in revised form 29 September 2016  
Accepted 26 October 2016

## Keywords:

Tomato peel  
Enzyme assisted extraction  
Lycopene  
Free radicals  
Oxidative damage

## ABSTRACT

Lycopene rich extracts (ETE) were prepared by enzyme assisted extraction of tomato peel. Oxidative damage was induced in L6 myoblasts by exposing cells to H<sub>2</sub>O<sub>2</sub> in presence and absence (control) of ETE. The potential of ETE to protect cells from oxidative damage was investigated in terms of cytotoxicity (MTT assay), Reactive oxygen species (ROS) by 2', 7'-dichlorofluoresceindiacetate (H<sub>2</sub>DCFDA), DNA damage (ladder assay, 8-oxo-dG), Hoechst 33342 nuclear staining, mitochondrial stability by ATP production and mitochondrial membrane potential by Rhodamine 123 staining. It was observed that treatment of cells with ETE significantly increased cell viability, decreased ROS production, reduced DNA fragmentation, chromatin condensation & 8-oxo-dG, increased ATP levels and mitochondrial membrane potential. Results indicated that ETE could protect cells from H<sub>2</sub>O<sub>2</sub> induced oxidative damage significantly as compared to control. These results depicted the antioxidant potential of tomato peel extract which can counteract the redox imbalance in cells induced by oxidative stress condition.

© 2016 Elsevier Ltd. All rights reserved.

## 1. Introduction

Oxidative stress develops due to rise in free radical production and can exceed the antioxidant capacity of the normal biological system. The majority of free radicals that damage cellular system are oxygen-free radicals, generally known as 'reactive oxygen species' (ROS). Aerobic organisms have their own well-organized enzymatic and non-enzymatic self-defensive system against oxidative stress to maintain cellular homeostasis (Datta, Sinha, & Chathopathay, 2000). Excess ROS production, broadly damage the cellular biomolecules (Neeley & Essigmann, 2006) and finally contribute to the pathogenesis of several oxidative stress related diseases including cancer, heart failure, lung disease, diabetes, neurodegenerative disorders, aging and rheumatoid arthritis (Devasagayam et al., 2004). The antioxidants play a crucial role in scavenging the active free radicals before they attack vital biomolecules by donating hydrogen atom. H<sub>2</sub>O<sub>2</sub>, being a chief contributor to oxidative damage, is transformed from superoxide that leaks from the mitochondria. Interestingly, low physiological levels of reactive oxygen species are required for normal functioning of skeletal muscle (Droge, 2002), but high ROS levels promote con-

tractile dysfunction resulting in muscle weakness and fatigue (Powers & Jackson, 2008). Skeletal muscle cells with higher ROS can cause pathogenesis and lead to different muscular degeneration and other related diseased conditions including diabetes mellitus, aging etc (Dhanya et al., 2015)

Polyphenols are the most abundant antioxidants in the diet. Various biological effects of polyphenols in fruits and vegetables have been reported in the past two decades (Martinez-Valvercle, Perige, & Provan, 2002). Tomato (*Lycopersicon esculentum*) is one of the most important vegetables with a global production of 126 million tons in 2012 (FAOSTAT, 2012). It is a good source of various nutrients and secondary metabolites that are necessary for human health such as mineral matter, vitamins E, vitamin C, lycopene, β-carotene, flavonoids, phenolics and organic acids (Al-Wandawi, Abdul Rehman, & Al Shaikhly, 1985). Food by-products usually characterize an environmental problem for the industry. Various studies have been carried out on the possible consumption of several vegetable origin by-products for their inclusion in the human diet, which could reduce industrial costs providing a correct solution for the pollution problem connected with food processing (Singh & Goyal, 2008). Tomato processing industries generate a huge amount of residue in the form of peel, seeds, pomace etc (Shalini, Jyoti, Neetu, & Charanjit, 2015). Studies have reported that tomato peel contains high levels of lycopene, about five times more

\* Corresponding author.

E-mail addresses: [bp.nisha@yahoo.com](mailto:bp.nisha@yahoo.com), [pnisha@niist.res.in](mailto:pnisha@niist.res.in) (P. Nisha).

than that of pulp and seeds (Sharma & Le Maguer, 1996), which represents more than 85% of the total carotenoids. Recent epidemiological studies have shown that supplementation of diets rich in lycopene is related to reduce risk of many chronic diseases (Prakash, Gupta, & Sharma, 2012).

Despite of these advantages, carotenoids recovery from this material is not simple, as revealed by the low yields achievable with conventional solvent extraction procedures (Bushra, Anwar, & Ahraf, 2009). The reasons are to be found in the compactness of the material, which hinders solvent penetration and the possible degradation of the carotenoids during recovery. Enzymes catalyzing the cleavage of cell-wall polysaccharides have been effectively utilized to help the release of vegetable oils (Hammoungjai, Pyle, & Niranjan, 2002), non-volatile aroma precursors (Bautista Ortin, Martinez Cutillas, Ros Garcia, Lopez Roca, & Gomez Plaza, 2005), phenols (Pinelo, Zornoza, & Meyer, 2008) and carotenoids (Barzana et al., 2002) from plant materials. The food-grade enzymes with pectinolytic, cellulolytic and hemi cellulolytic activities were capable of considerably enhancing lycopene recovery from tomato skins (Choudhari & Ananthanarayan, 2007). With respect to above considerations, we have explored the feasibility of using cell-wall degrading enzymes as a way for improving carotenoid extraction from tomato peel.

Based on the previous reports that enzyme pretreatment improves the extraction of active ingredients (mainly carotenoids) from tomato peel, we carried out preliminary experiments to optimize the conditions (types of enzyme, incubation time, temperature etc) for enzyme assisted extraction of carotenoids from tomato peel (data not published). On evaluation using various biochemical assays it was found that the extract prepared by enzyme pretreatment exhibited better activity than that of the control without enzyme pretreatment (data not published). Therefore, in this work we aimed to evaluate the beneficial role of enzyme assisted tomato peel extracts in protecting DNA damage and mitochondrial membrane potential from ROS induced by H<sub>2</sub>O<sub>2</sub> in L6 muscle cells.

## 2. Materials and methods

### 2.1. Chemicals and reagents

Cellulase (EC 3.2.1.4) and pectinase (EC 3.2.1.15) enzymes were purchased from Sigma-Aldrich (St Louis, MO, USA), both derived from a selected strain of *Aspergillus niger*. The claimed activity of cellulase is 1.08 U/mg where, one unit will liberate 1.0 μmol of glucose from cellulose in one hour at pH 5.0 at 37 °C. The claimed activity of pectinase is 1.02 U/mg where, one unit will liberate 1.0 μmol of galacturonic acid from poly-galacturonic acid per hour at pH 4.0 at 25 °C. Folin-Ciocalteu reagent, sodium carbonate, 2,2-diphenyl-1-picrylhydrazyl (DPPH), Hydrogen peroxide (H<sub>2</sub>O<sub>2</sub>), Triton X, Ethylenediaminetetraacetic acid (EDTA), Sodium chloride (NaCl), Tris-HCl, perchloric acid, potassium hydroxide (KOH) were obtained from MERK. Gallic acid, Dulbecco's Modified Eagle's Medium (DMEM), Dimethyl sulfoxide (DMSO), 2,7-Dichlorodihydrofluorescein diacetate (DCFH-DA), Fetal Bovine Serum (FBS), Ethidium bromide, 1 Kb DNA ladder, Glycerol, Hoechst 33342, Adenosine Triphosphate (ATP), 3-(4,5-dimethylthiazol-2-yl)-2,5 diphenyltetrazolium bromide (MTT), Bromophenol Blue, Rhodamine123 dye, Agarose for electrophoresis and Mammalian genomic DNA isolation kit were purchased from Sigma-Aldrich Chemicals (St Louis, MO, USA). DNA/RNA Oxidative damage ELISA kit was purchased from Cayman chemicals (MI-USA). Trypsin-EDTA, Antibiotic-antimycotic were purchased from Gibco Invitrogen (Carlsbad, CA, USA). All the chemicals used were of high quality analytical grade chemicals.

### 2.2. Sample preparation

#### 2.2.1. Enzymatically assisted lycopene extraction

Tomatoes (*Solanum lycopersicum* L.) were purchased from local market of Trivandrum district of Kerala, India. After removal of damaged parts and washing, whole tomato fruits were immersed in warm water (80 °C) for 2 min. Then they were cooled under tap water, hand peeled and the peel was freeze dried (VirTis genesis 25EL, USA). It was then extracted using the following re-optimized conditions

Enzymes pretreatment – Cellulase at 20 U/g, pectinase at 30 U/g, 50 °C for 60 min under dark.

Extraction of lycopene – After the pretreatment with enzymes, the lycopene was extracted with petroleum ether, thrice in a separating funnel for 20–25 min each time and allowed to stand for 10 min. Upper nonpolar phase which contains lycopene were pooled together and filtered. It is made up to known volume and analyzed for lycopene content spectrophotometrically.

A control without enzyme was also carried out simultaneously (CTE). The amount of lycopene was calculated using the specific extinction coefficient (E = 3450 in petroleum ether) (Ranganna, 1997).

$$\text{Lycopene (mg)} = \frac{(A \times \text{dil. factor} \times \text{mL} \times 10)}{E^{1\%}_{1\text{cm}}}$$

where A – absorbance of the solution in 1 cm cuvette, dil – dilution factor, mL – total mL of the sample and E<sub>1%<sup>1</sup>cm</sub>, specific extinction coefficient for lycopene in petroleum ether.

The solvent was then evaporated off to get the oleoresin (CTE and ETE respectively for control and enzyme assisted extracts) which is used for further biological efficacy studies.

#### 2.3. Determination of total phenol content

Total phenol content in tomato peel extracts CTE and ETE (Enzyme assisted tomato peel extract) were measured by the Folin-Ciocalteu method (Singleton & Rossi, 1965). Briefly, 20 μL of samples were mixed with Folin-Ciocalteu reagent followed by the addition of sodium carbonate (7.5%, w/v) and mixed, allowed to stand for 90 min at room temperature and absorbance was measured against the blank at 750 nm using multimode reader (Synergy Biotek). Total phenol content of the extract was expressed in terms of milligrams of gallic acid equivalents per gram sample (mg GAE/g).

#### 2.4. DPPH radical scavenging assay

The antioxidant activity of tomato peel extract ETE was measured by the DPPH radical scavenging assay as reported earlier (Yen & Duh, 1994) with slight modifications. DPPH assay constitutes a rapid and low cost method, which has commonly been used for the evaluation of the anti-oxidative potential of diverse natural products. The extracts of different concentrations in methanol were mixed with 0.2 mM methanolic solution of DPPH. The mixture was shaken vigorously and left to stand for 30 min in dark at room temperature, and the absorbance was then measured at 517 nm against the corresponding control.

$$\% \text{ Inhibition} = \frac{\text{Absorbance of Control} - \text{Absorbance of Sample}}{\text{Absorbance of Control}} \times 100$$

#### 2.5. Cell culture and treatment conditions

Skeletal muscle cell has been reported as *in vitro* model to study the effect of ROS production on the biomolecular system and the



cellular machinery (Dhanya et al., 2015; Maurya et al., 2015). Therefore rat skeletal muscle cells, L6 myoblast, were used in the present study. These cells were obtained from NCCS, Pune and were cultured in Dulbecco's modified Eagle's medium (DMEM) supplemented with 10% Fetal bovine serum and 0.5% Antibiotic-antimycotic at 37 °C in a humidified atmosphere containing 5% CO<sub>2</sub>. Petroleum ether used for extraction procedure was removed by vacuum and reconstituted in 50% DMSO. Prior to the cell based assays, it was further diluted in such a way that the final concentration of DMSO was less than 0.1%. Cells were grown at density of  $1 \times 10^4$  cells/well on 96-well black plate (Becton Dickinson Bioscience) and 12-well plates for staining and Fluorescence Activated Cell Sorter (FACS) analysis.

#### 2.6. Cell viability assay

Cytotoxicity of the extract and H<sub>2</sub>O<sub>2</sub> were standardized based on the concentration using MTT assay (Mosmann, 1983). L6 myoblast cells were treated with different concentrations of the extract, ETE (30–150 µg/mL) and H<sub>2</sub>O<sub>2</sub> (10–500 µM) for 24 h and 20 min respectively. After treatment, cells were incubated with MTT reagent (0.5 g/L) for 4 h. Mitochondrial dehydrogenase enzyme, which is active only in live cells, reduces the yellow dye, MTT to purple formazan crystals. The formazan crystals were dissolved in DMSO and the absorbance was read at 570 nm using multimode reader (Synergy 4 Biotek multiplate reader, USA).

For evaluating how ETE protect L6 cells against H<sub>2</sub>O<sub>2</sub> induced oxidative stress, the cells were first treated with different concentrations of tomato peel extract, ETE (20–100 µg/mL) and incubated at 37 °C for 24 h followed by treatment with 100 µM H<sub>2</sub>O<sub>2</sub> (20 min). Cells without treatment were used as negative control and 100 µM H<sub>2</sub>O<sub>2</sub> alone treated cell were used as positive control. After treatment, cell viability was determined as above. Each assay was carried out three times, and the results were expressed as the mean ± SD. The percentage viability was calculated as

$$\% \text{ cell viability} = \frac{\text{The absorbance of test}}{\text{The absorbance of control}} \times 100$$

#### 2.7. Intracellular reactive oxygen species (ROS) levels

The effect of ETE on intracellular ROS levels was measured using DCFH-DA as described by Cathcart, Schwiers, and Ames (1983). The cells were preincubated with different subtoxic concentrations of ETE followed by H<sub>2</sub>O<sub>2</sub>. Cells were incubated with DCFH-DA for 20 min and imaged with Fluorescent microscope (Pathway 855, BD Bioscience, USA) equipped with filters in the range, excitation, 490 nm; and emission, 525 nm. The fluorescent intensity was measured by multimode reader. Quantification of ROS production by cells was also determined by measuring the intracellular DCF fluorescent intensity by flow cytometer (BD FACS Aria II, BD Bioscience, USA).

#### 2.8. DNA protection studies

##### 2.8.1. Nuclear staining with Hoechst 33342

The nuclear morphology of the cells were observed using the cell-permeable DNA dye, Hoechst 33342 for checking the presence of chromatin condensation in nucleus (Hickman, 1992). After incubation with ETE and H<sub>2</sub>O<sub>2</sub>, L6 cells were stained with Hoechst 33342 (10 µg/mL) for 10 min at 37 °C followed by washing with PBS for 3 times and the nuclei were observed under a confocal fluorescence microscope (Pathway 855, BD Bioscience, USA) to examine the degree of nuclear condensation.

##### 2.8.2. DNA fragmentation assay

DNA fragmentation assay was carried out by gel electrophoresis (Chandna, 2004) for determining the genomic DNA protection ability of ETE against H<sub>2</sub>O<sub>2</sub> induced oxidative stress. After the treatment with ETE followed by H<sub>2</sub>O<sub>2</sub> as described earlier, the cells were pelleted. It was then lysed in 0.5 mL lysis buffer (10 mM Tris-HCl, pH 8.0, 20 mM EDTA, and 0.2% Triton X-100) and incubated at 37 °C for 60 min. After centrifugation, chromosomal DNA in the supernatant was extracted with ethanol and 4 M NaCl at –20 °C for overnight. DNA was pelleted by centrifugation and re-suspended in Tris-EDTA buffer. It was then subjected to electrophoresis in 1.8% agarose gel (60V), stained with ethidium bromide, and visualized under UV light.

##### 2.8.3. Estimation of 8-oxo-2'-deoxyguanosine (8-oxo-dG)

The effect of ETE on oxidative DNA damage induced by 100 µM H<sub>2</sub>O<sub>2</sub> was measured using 8-oxo-dG assay. The cells were pre incubated with different subtoxic concentrations of ETE followed by exposure to H<sub>2</sub>O<sub>2</sub>. Cells were trypsinized and DNA was isolated by using mammalian genomic DNA isolation kit. The level of 8-oxo-dG, marker of oxidative damage of DNA in the cell, was determined by DNA/RNA Oxidative damage ELISA kit (Gan et al., 2012). The estimation of 8-oxo-dG generated in the samples was carried out spectrophotometrically at 410 nm.

#### 2.9. Mitochondrial protection studies

##### 2.9.1. Mitochondrial membrane potential

A major response to oxidative stress is loss of mitochondrial membrane potential and dysfunction. Mitochondrial membrane potential ( $\Delta\Psi_m$ ) was determined using Rhodamine 123, a cationic fluorescent indicator that selectively accumulates within mitochondria in a membrane potential dependent way (Zhang & Wang, 2008). Protection of mitochondrial membrane potential requires a proton motive force which is generated through respiration by ATP hydrolysis via ATP synthase. Following ETE treatment and stress induction, the cells were directly incubated with 2 µM Rhodamine 123 for 25 min in the dark, followed by rinsing with several changes of PBS, fluorescence was detected by FACS Aria II (BD Bioscience, USA). A reduction in green rhodamine 123 fluorescence indicates reduced  $\Delta\Psi_m$ .

##### 2.9.2. Adenosine triphosphate (ATP) production by HPLC analysis

Levels of ATP, an indicator of the energy state in living cells, are dependent mainly on mitochondrial function. In L6 cells, mitochondrial protection activity of extract against oxidative stress was determined by measuring ATP levels using HPLC method (Liu, Jiang, Luo, & Jiang, 2006). After treatment, the cells were trypsinized and centrifuged at 800g for 3 min and the pellets were suspended in 4% perchloric acid on ice for 30 min. The pH of the lysates was adjusted between 6 and 8 with 2 M KOH. Precipitated salt was separated from the liquid phase by centrifugation at 13,000g for 10 min at 4 °C. ATP was quantified on a Prominence HPLC system (Shimadzu, Japan) containing LC-20 AD system controller, Phenomenex Gemini C18 column (250 × 4.6 mm, 5 µm), a column oven (CTO-20A), a Rheodyne injector (USA) with a loop of 20 µL volume and a diode array detector (SPD-M20A). A buffer 20 mM KH<sub>2</sub>PO<sub>4</sub> and 3.5 mM K<sub>2</sub>HPO<sub>4</sub>·3H<sub>2</sub>O (pH 6.1) was used as the mobile phase. The flow rate was 1.0 mL/min, the injection volume was 20 µL and column was at room temperature. The fractions were monitored at 259 nm. Sample peaks were identified by comparing with retention times of standard peaks. LC Lab Solutions software was used for data acquisition and analysis.

### 2.9.3. Statistical analysis

All the experiments were repeated three times and results were expressed as means  $\pm$  standard deviations of the control and treated cells. The obtained results were subjected to one-way ANOVA and the significance was calculated by Duncan's multiple range test, using SPSS 16.0 and significance was accepted at  $p \leq 0.05$ .

## 3. Results

Studies have shown that antioxidants like flavonoids, polyphenolics, and vitamins from plant sources play vital role in evading cells and biomolecules from oxidative stress (Prasad, Srinivasan, Pugalendi, & Menon, 2006). The present study investigated free radical scavenging activity of tomato peel extract and its ability to protect cells from oxidative damage induced by  $H_2O_2$  in L6 cells. Antioxidants in extract assumed to be responsible for the scavenging activity of reactive oxygen species (ROS), resulting in the protection against DNA and mitochondrial damage induced by the oxidative stress.

### 3.1. Estimation of lycopene content in the ETE

The lycopene content of CTE and ETE (tomato oleoresin) were  $3.82 \pm 0.13\%$  and  $4.9 \pm 0.31\%$  respectively. As can be seen the enzyme assisted extraction improved the extraction of lycopene from tomato peel significantly. This may be due to the fact that on pretreatment of tomato peel with enzymes, cell wall components are degraded which may assist in the release of intracellular contents. Pretreatment of tomato peel with cellulase and pectinase under optimized conditions has been reported to increase the yield of lycopene extraction by 107 and 206, respectively (Choudhari & Ananthanarayan, 2007). Enzymatic pretreatment has also reported to improve the recovery of total lycopene from tomato paste (Zuorro & Lavecchia, 2011).

### 3.2. The total phenolic content

Total phenolic content (TPC) was as measured by the Folin-Ciocalteu method. TPC of the ETE was found to be  $235 \pm 0.9221$  and that of control was found to be  $208 \pm 0.9871$  mg GAE/g.

### 3.3. Scavenging effect on DPPH radicals

DPPH radical scavenging model is a commonly used method to evaluate free radical scavenging activity. The degree of discoloration indicates the scavenging potential of the antioxidant extract, which is due to the hydrogen donating ability (Jian, Peter, Qizhi, & Changyi, 2010). ETE showed a good scavenging activity of  $IC_{50}$  value  $72.2 \pm 0.9931$   $\mu$ g/mL and for control it was  $88.58 \pm 0.8765$   $\mu$ g/mL. The results indicated that the enzyme assisted tomato peel extract has a noticeable effect on scavenging free radicals. Based on the above assays, it was found that ETE contain significantly higher content of lycopene, phenolic compounds and free radical scavenging capacity, ETE was chosen for further studies.

### 3.4. Cell viability by MTT assay

The cytotoxicity of ETE was examined in L6 myoblasts by MTT assay. In order to find out the working concentrations of ETE, cells were treated with different concentrations of ETE and cell viability was determined. It can be seen that (Fig. 1a) the viability decreased significantly in a dose dependant manner ( $p \leq 0.05$ ). A concentration of 100  $\mu$ g/mL of ETE caused cell viability to decrease by about 18.3%. Therefore, for the further studies, the cells were exposed to

the subtoxic concentration of 100  $\mu$ g/mL of ETE and below. For inducing oxidative stress,  $H_2O_2$  has often been reported as a model in different cell types (Small et al., 2013; Sun, Qin, & Ye, 2013). In order to determine the sub toxic concentrations of  $H_2O_2$ , L6 cells were exposed to  $H_2O_2$  at concentrations ranging between 10 to 500  $\mu$ M, for 20 min and assayed by MTT. As shown in the Fig. 1b, it was found that different concentrations of  $H_2O_2$  significantly reduced cell viability after treatment ( $p \leq 0.05$ ) and 100  $\mu$ M  $H_2O_2$  caused cell viability decrease by about 30%. Therefore the cells were exposed to a concentration of 100  $\mu$ M  $H_2O_2$  for inducing oxidative stress for further assays. In order to find out the protective effect of ETE against  $H_2O_2$  induced toxicity, the cells (L6) were initially treated with subtoxic levels of ETE (20–100  $\mu$ g/ml) for 24hrs followed by  $H_2O_2$  at a concentration of 100  $\mu$ M (20 min). Subsequently we found that the extract protected cells from oxidative stress effectively in a dose-dependent manner ( $p \leq 0.05$ ) (Fig. 1c). The data indicated that pre-treatment with ETE efficiently protected cells from  $H_2O_2$  induced toxicity.

### 3.5. ETE inhibits $H_2O_2$ -Induced reactive oxygen species production in L6 cells

The protective effect of ETE on  $H_2O_2$ -induced intracellular ROS production was determined by measuring the intracellular ROS levels, by detecting dichlorofluorescein (DCF), derived from the oxidation of  $H_2DCFDA$ . The fluorescence intensity was measured by multimode reader (Synergy 4 Biotek multiplate reader, USA) and has been illustrated in Fig. 2a. The results indicated that untreated cells had little basal intracellular ROS. However, incubation of cells with 100  $\mu$ M  $H_2O_2$  caused a significant increase in ROS level as compared to the control. The ROS concentration was found to decrease significantly on preincubation with ETE (100  $\mu$ g/mL) ( $p \leq 0.05$ ). As shown in Fig. 2b the intracellular ROS production was visualized by Fluorescent microscope (Pathway 855, BD Bioscience, USA) and quantified by measuring the fluorescence of DCF by flow cytometry (BD FACS Aria II, BD Bioscience USA). The intensity of untreated and  $H_2O_2$  treated cells were  $0.30 \pm 0.081\%$  and  $39.1 \pm 0.043\%$  respectively. The fluorescence intensity of ETE treated group was  $24.7 \pm 0.121\%$  and  $15.4 \pm 0.387\%$  respectively for 50  $\mu$ g/mL and 100  $\mu$ g/mL of ETE, which was significantly lower than  $H_2O_2$  treated cells (Fig. 2c). This result suggests that  $H_2O_2$  could induce ROS accumulation in L6 cells and this ROS production was found to be effectively inhibited upon treatment with ETE extract.

### 3.6. ETE protects L6 cells from nuclear damage

To investigate chromatin condensation, cells were analyzed using Hoechst 33342 staining. It can be seen that the control cells without treatment have intact nucleus whereas  $H_2O_2$  treatment resulted in increased number of cells with fragmented nucleus (Fig. 3a). On pretreatment with ETE at different concentrations, 50  $\mu$ g/mL and 100  $\mu$ g/mL there is a reduction in number of cells with fragmented nucleus, in a dose dependent manner confirming that ETE protect cells from nuclear fragmentation.

### 3.7. ETE protected $H_2O_2$ induced DNA fragmentation in L6 cells

DNA protection activity was exhibited by ETE, against 100  $\mu$ M  $H_2O_2$  induced DNA damage in L6 cells. As shown in the Fig. 3b, DNA from the untreated control cells were compact suggesting an intact DNA, whereas the treatment with  $H_2O_2$  causes a significant fragmentation as seen from laddering nature of DNA band. On treatment with ETE, the smearing nature of DNA gets diminished in a dose dependent manner suggesting that preincubating L6 cells with ETE effectively protected cells from DNA damage. This



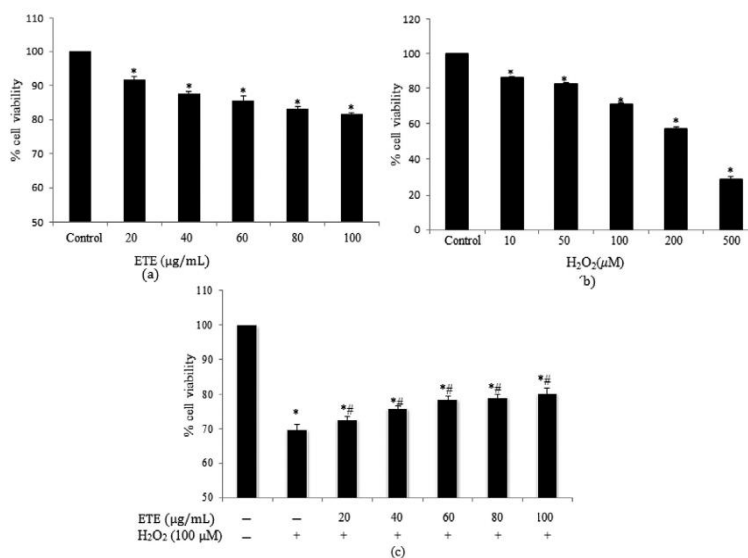


**Fig. 1.** The Effect of ETE, H<sub>2</sub>O<sub>2</sub> and pretreatment of cells with ETE before exposure with H<sub>2</sub>O<sub>2</sub>, on viability of L6 cells by MTT assay. (a) Cytotoxicity of ETE to L6 cells (b) Cytotoxicity of L6 cells following different concentrations of H<sub>2</sub>O<sub>2</sub> exposure (c) The effect of ETE on L6 cell viability against 100 μM H<sub>2</sub>O<sub>2</sub>. The results are expressed as percentage of control, and each value represents the mean ± SD. The annotation \* indicates a p value ≤ 0.05 versus control group. The annotation # indicates a p value ≤ 0.05 versus H<sub>2</sub>O<sub>2</sub> group.

result shows that, antioxidants present in extract has the capacity to quench the free radicals generated in the reaction, thereby protecting the DNA from H<sub>2</sub>O<sub>2</sub> induced oxidative damage.

### 3.8. ETE protects DNA from oxidative damage

8-Oxo-dG is the most abundant product of DNA oxidation (Nakabeppu, Tsuchimoto, Yamaguchi, & Sakumi, 2007). Therefore the level of 8-Oxo-dG in the cells was estimated to assess the DNA protecting effect of ETE against H<sub>2</sub>O<sub>2</sub> treatment. As shown in Fig. 4, 8-OH-dG level significantly increased on exposure to 100 μM H<sub>2</sub>O<sub>2</sub> as compared to the control. However, on pretreatment with ETE prior to treatment with H<sub>2</sub>O<sub>2</sub>, the level of 8-OH-dG decreased significantly. The oxidation of dsDNA was found to decrease in a dose dependent manner on ETE pretreatment.

### 3.9. ETE prevented H<sub>2</sub>O<sub>2</sub>-induced reduction of mitochondrial membrane potential (MMP) in L6 Cells

Mitochondrial membrane potential, ΔΨ<sub>m</sub>, is an important factor of mitochondrial function used as sign of cell health. A rapid reduction in the MMP was found when L6 cells were exposed to 100 μM H<sub>2</sub>O<sub>2</sub> as detected by a reduced fluorescence intensity of Rhodamine123. As compared to control cells, H<sub>2</sub>O<sub>2</sub> treatments decreased the fluorescence intensity in cells from 79.6 ± 0.772% to 37.4 ± 0.875%. Pretreatment with 50 μg/mL and 100 μg/mL of ETE protected cells against H<sub>2</sub>O<sub>2</sub> could retain the mitochondrial membrane potential to 47.1 ± 0.567% and 72.6 ± 0.765% respectively. Fig. 4a and b indicating that ETE could prevent H<sub>2</sub>O<sub>2</sub> induced reduction of mitochondrial membrane potential significantly (p ≤ 0.05).

### 3.10. ATP level by HPLC analysis

ATP production in mitochondria is the main energy source for various metabolic pathways (Campanella, Parker, Tan, Hall, & Duchon, 2009). In normally functioning mitochondria, ΔΨ<sub>m</sub> is high favoring ATP synthesis by ATP synthase (Schapira, 2006). When mitochondrial functioning is compromised and ΔΨ<sub>m</sub> decreases below a threshold which leads to depletion of ATP production. ATP production was estimated using HPLC method. From the Fig. 4c, ATP productions by L6 cells at normal conditions were 4.4 ± 1.63 μM. On subjecting the cells to 100 μM H<sub>2</sub>O<sub>2</sub> it was came down to 1.5 ± 0.229 μM, showing the inhibition of mitochondrial ATP synthesis. On pretreatment with ETE at 50 μg/mL and 100 μg/mL, ATP level was found to be 2.32 ± 0.031 μM and 3.60 ± 0.05 μM. Results suggest that mitochondrial capacity to produce ATP in oxidative stress conditions is low and it is reversed in the presence of ETE.

## 4. Discussion

Increased level of ROS leads to oxidative damage of the structural components like lipids, DNA and proteins of cells and potentiates many complications such as cancers, cardiovascular diseases, and neurological diseases etc. Epidemiological studies have shown that people consuming more of antioxidant-rich fruits and vegetables are in better health by increasing the degradation of ROS. In the present study, free radical scavenging activities of lycopene rich tomato peel extract (ETE) against oxidative stress induced in L6 cells were evaluated. Tomato, particularly peel, is a very good source of carotenoids, including lutein, zeaxanthin, β-cryptoxanthin, α-carotene, β-carotene and lycopene, and by virtue of its ability to interact with free radicals, can preserve the important cellular biomolecules such as proteins, lipids and DNA

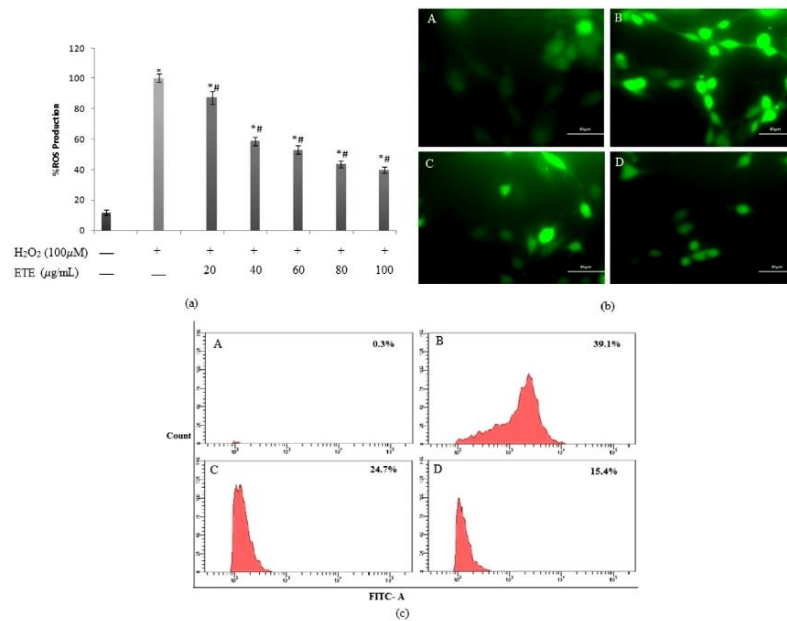


**Fig. 2.** Measurement of ROS production in L6 cells. After treatment, the cells were stained with H<sub>2</sub>-DCFDA dye and then analyzed by fluorescence imaging. (a) Fluorescent intensity quantified using multimode reader (% ROS production); (b) Fluorescent imaging using fluorescent microscope A- Control, B-100 µM H<sub>2</sub>O<sub>2</sub>, C- 50 µg/mL ETE +100 µM H<sub>2</sub>O<sub>2</sub>, D-100 µg/mL ETE +100 µM H<sub>2</sub>O<sub>2</sub>. (c) Represent flow cytometric analysis of ROS production in L6 cells by plotting cell count against FITC. Each value represents mean  $\pm$  SD from triplicate measurements of three different experiments. Significance levels between different groups were determined by using one way ANOVA,  $p < 0.05$  versus Control; \* $p < 0.05$  versus H<sub>2</sub>O<sub>2</sub>.

(Haslam, 1996; Riso & Porrini, 2001). It plays a significant role in the prevention of chronic diseases such as, gastrointestinal disorders, osteoporosis cardiovascular and prostate disorders (Astrog et al., 1997; Paiva & Russell, 1999). Lycopene, the major carotenoid present in tomato oleoresin, is reported to be responsible for the health protective activities of tomatoes. The lycopene content of the oleoresin, ETE, in the present study was found to be 4.9%. Riso et al. (2004) reported that the level of plasma concentration of lycopene increased from 0.347 µmol/L to 0.52 µmol/L on consumption of diet enriched with small amounts of different tomato products providing 8 mg lycopene for 3 weeks and there was an improved protection from DNA oxidative damage. A study by Paetau, Rao, Wiley, Brown, and Clevidence (1999) reported a 50% increase (from 2.05 to 4.95 mg/g protein) in lycopene concentration within buccal mucosal cells after the consumption of tomato oleoresin (about 75 mg/day lycopene for 4 weeks). In the present study we found that the ETE is a rich source of lycopene (4.95%) and this lycopene rich extract can impart a significant protection against oxidative stress induced damage.

Antioxidants are very useful for the management of these diseases due to their free radical scavenging activity. A compound has been attributed to its antioxidant activity by various mechanisms such as prevention of binding of transition metal ion catalysts, decomposition of peroxides, reductive capacity and radical scavenging ability. Phenols are very important plant constituents due to their free radicals scavenging ability by virtue of its hydroxyl groups (Haug, Ou, & Prior, 2005; Hemi, Taiglaferro, & Bobilya,

2002). Several studies showed good correlation between the phenols and antioxidant activity (Silva, Souza, Rogez, Rees, & Larondella, 2006). Tomato peel contains flavonoids with useful effects for human health such as rutin, naringenin, lycopene and quercetin (Gonzalez, Valverde, Alonso, & Periago, 2011). Major favorable actions accepted to lycopene are that it quenches singlet oxygen, traps peroxy radicals, inhibits oxidative DNA damage, inhibits peroxidation and stimulates gap junction communication (Jalil & Habib, 2015).

The stable radical DPPH has been used widely for the determination of primary antioxidant activity. The result revealed that the ETE exhibited the highest radical scavenging activity with IC<sub>50</sub> value 72.7  $\pm$  0.9771 µg/mL. DPPH antioxidant activity of tomato peel extracts increased with the increase in concentration of extracts. These results point out that tomato peel has a noticeable effect on free radicals scavenging. ETE is found to be a rich source lycopene as well as phenolic compounds which are good natural antioxidants (Jalil & Habib, 2015; Silva et al., 2006). Therefore the obtained activity of the extract may be attributed to the lycopene as well as the phenolic content.

A preliminary study on the toxic effect of extract ETE demonstrated by MTT assay did not show harmful effects on L6 cells up to a concentration of 100 µg/mL. The study revealed that the pretreatment with ETE increased the cell viability as compared to H<sub>2</sub>O<sub>2</sub> treated cells. These results suggest that treatment with H<sub>2</sub>O<sub>2</sub> results in cell death, which was prevented when the cells were pretreated with ETE before H<sub>2</sub>O<sub>2</sub> treatment.



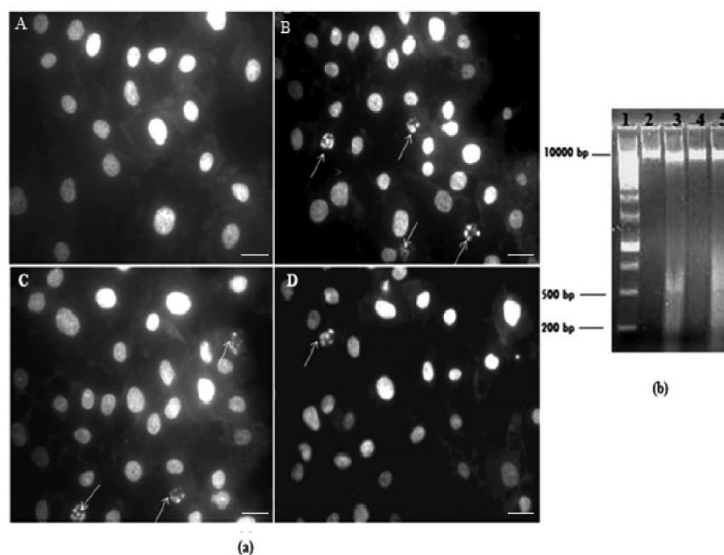


**Fig. 3.** (a) Chromatin condensation observed using Hoechst 33342 staining: Figure represents A) control B) 100  $\mu\text{M}$   $\text{H}_2\text{O}_2$  C) 50  $\mu\text{g}/\text{mL}$  ETE +100  $\mu\text{M}$   $\text{H}_2\text{O}_2$  D) 100  $\mu\text{g}/\text{mL}$  ETE +100  $\mu\text{M}$   $\text{H}_2\text{O}_2$ . Arrows represent cells with chromatin condensation inside the nucleus. (b) DNA damage was analyzed by DNA Fragmentation assay Lane 1: 1 kb ladder, Lane 2: control, Lane 3: 50  $\mu\text{g}/\text{mL}$  ETE +100  $\mu\text{M}$   $\text{H}_2\text{O}_2$ , Lane 4: 100  $\mu\text{g}/\text{mL}$  ETE +100  $\mu\text{M}$   $\text{H}_2\text{O}_2$  Lane 5: 100  $\mu\text{M}$   $\text{H}_2\text{O}_2$ .

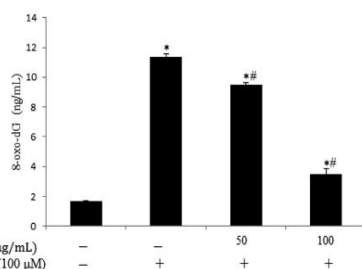


**Fig. 4.** The level of 8-oxo-dG in cells. Each value represents the mean  $\pm$  SD of triplicate measurements. Significance levels between different groups were determined by using one way ANOVA. \*  $p < 0.05$  versus Control; \*\*  $p < 0.05$  versus  $\text{H}_2\text{O}_2$ .

It is reported that oxidative stress induced by ROS plays a major role in cellular damage which leads to secondary injury to the cells (Kang et al., 2012). The production of ROS in the cells leads to depletion in the antioxidant mechanism in the body. Dietary supplementation of antioxidants can improve the antioxidant status of the body (Alvarado, Álvarez, Puerto, Gausserès, & Jiménez, 2006). The antioxidant activity of the extracts and their potential against intracellular ROS was evaluated using  $\text{H}_2\text{DCFDA}$  by fluorescent imaging and flow cytometric analysis. The fluorescence intensity of the L6 control cells was significantly lower than that of cells with induced oxidative stress using 100  $\mu\text{M}$   $\text{H}_2\text{O}_2$ . Pretreatment with ETE, could considerably reduce the ROS level when exposed to 100  $\mu\text{M}$   $\text{H}_2\text{O}_2$  exposure as indicated by reduction in fluorescence intensities than the positive cells. These results were further confirmed by quantifying the fluorescence intensity using flow cyto-

metric analysis. The fluorescent intensity was reduced significantly when cells were treated with ETE prior to  $\text{H}_2\text{O}_2$ . Overall, the cells treated with the extracts showed a decrease in the fluorescence intensity as compared with the 100  $\mu\text{M}$   $\text{H}_2\text{O}_2$  group. It was also observed that cells treated with 100  $\mu\text{g}/\text{mL}$  of ETE could reduce the ROS levels significantly as compared to 50  $\mu\text{g}/\text{mL}$ , indicating that the extracts acted in a dose dependent manner. The concentration of ROS is directly proportionate to the fluorescence intensity. This activity of ETE may be correlated to the presence of various antioxidant molecules present in the extracts which are can scavenge hydrogen peroxide.

ROS can damage nucleic acids by altering purine and pyrimidine bases and causing DNA fragmentation (Hemnani & Parihar, 1998). DNA damage can leads to mutations, which are responsible for related diseases such as cancer, coronary heart disease, arteriosclerosis and inflammatory disorders. Dietary antioxidants have been reported to possess potential inhibitory effects against  $\text{H}_2\text{O}_2$ -mediated DNA damage and harmful free radicals. In this respect we carried out further studies to find out the DNA protective potential of ETE against oxidative stress. Chromatin condensation and morphological changes in the cells (Control,  $\text{H}_2\text{O}_2$  treated and ETE pretreated) were examined with Hoechst staining under a fluorescence microscope. As can be seen from the Fig. 3a, the control cells shows intact nuclei whereas the cells induced with oxidative stress on treatment with  $\text{H}_2\text{O}_2$  exhibited significant chromatin condensation in the cells. The severity of  $\text{H}_2\text{O}_2$  treatment could be reduced on exposure of cells to ETE at a concentration of 100  $\mu\text{g}/\text{mL}$ . However, ETE at 50  $\mu\text{g}/\text{mL}$  concentration did not show much protective effect on the cells.

These results were further confirmed using ladder assay where DNA from the cells were isolated and subjected to electrophoresis to check for DNA fragmentation. DNA gel profile of untreated sample was compact with high molecular weight showing its integrity.

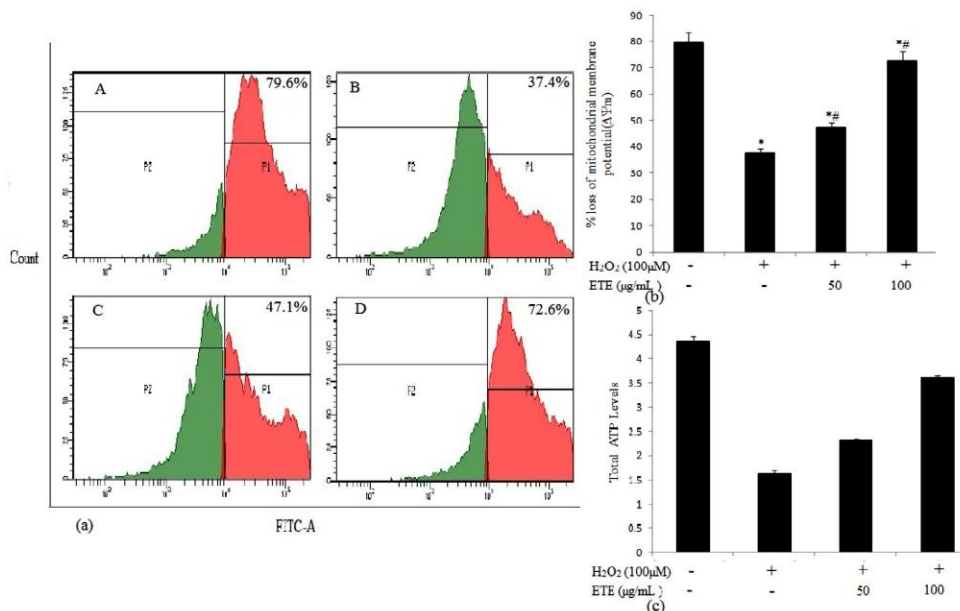


**Fig. 5.** Quantification of Mitochondrial membrane potential by Rhodamine 123 staining and ATP level by HPLC method. In (b) and (c) Restoration of mitochondrial membrane potential and ATP levels on ETE treatment. After incubation, cells were stained with Rhodamine 123 and analyzed by flow cytometer (a). In (b) indicate A – Control, B – 100 μM H<sub>2</sub>O<sub>2</sub>, C – 50 μg/mL ETE + 100 μM H<sub>2</sub>O<sub>2</sub>, D – 100 μg/mL ETE + 100 μM H<sub>2</sub>O<sub>2</sub>. The reduced fluorescence of Rhodamine 123 was determined as the reduced mitochondrial membrane potential. (c) ETE treatment increases mitochondrial capacity to produce ATP. Results were expressed as mean ± SD. Significance levels between different groups were determined by using one way ANOVA, \*p < 0.05 versus Control; #p < 0.05 versus H<sub>2</sub>O<sub>2</sub>.

DNA smearing was observed when cells were treated with H<sub>2</sub>O<sub>2</sub>. The intensity of smearing of DNA was minimized on treatment with ETE. From the Fig. 3b suggests that ETE at concentration of 100 μg/mL could protect the DNA from the oxidative damage. The data from Hoechst 33342 staining and ladder assay indicated that incubating cells in the presence of 100 μM H<sub>2</sub>O<sub>2</sub> causes a significant chromatin condensation/DNA fragmentation, as compared to the control (without any treatment). At the same time, ETE promote genomic stability by preventing double strand DNA breaks, which is associated with increased ROS production mediated by 100 μM H<sub>2</sub>O<sub>2</sub>. Ion radicals generated during oxidative stress lead to a chain reaction which form DNA adducts and lipid hydroperoxides results in single and double strand breaks. The obtained results from Hoechst 33342 staining and ladder assay also support the antioxidant property of ETE which protects nuclear DNA from oxidative stress induced by H<sub>2</sub>O<sub>2</sub>. The protective effect of ETE against oxidative damage of DNA was further confirmed by quantifying the oxidative damage indicator, 8-oxo-dG in the DNA. Oxidative attack to DNA is of particular interest since DNA modifications can lead to mutations. dsDNA molecules have unique double helix structure, which undergo oxidation in presence of H<sub>2</sub>O<sub>2</sub>. The most studied product of DNA oxidation is 8-oxo-dG (Bogdanov, Andreassen, Dedeoglu, Ferrante, & Beal, 2001; Nakabeppu et al., 2007). Results from the present study indicate that ETE can prevent oxidation of DNA from ROS by scavenging free radicals in a dose dependent manner.

As the primary cellular consumer of oxygen, together with redox enzymes and multiple electron carriers, mitochondria are considered as a main source of ROS production. However, mitochondria not only produce ROS, but also targets of oxidative stress.

In this way, ROS release contributes to oxidative damage and mitochondrial dysfunction in a wide range of diseases. The mitochondrial ATP synthase couples the electrochemical proton gradient to the synthesis or hydrolysis of ATP (Cross & Muller, 2004). Fig. 5c suggest that 100 μM H<sub>2</sub>O<sub>2</sub> treated cells showed a decrease in ATP production, whereas ETE pretreated cells results in increase in ATP Production. ΔΨm is a sensitive indicator of mitochondrial function. Increasing evidence suggests that the ΔΨm assay can be used as a more specific test for early mitochondrial injury. Results indicated that 100 μM H<sub>2</sub>O<sub>2</sub> group showed a significant decrease in mitochondrial membrane potential as compared to control. Interestingly, tomato peel extract ETE at 100 μg/mL treatment preserved mitochondrial membrane potential, suggesting the inhibition of mitochondrial membrane permeability. The reduced levels of the ATP production resulted in a decrease in membrane potential.

It is reported that the electron rich conjugated system of the polyene are responsible for the antioxidant activities of the carotenoids, by quenching singlet oxygen, and scavenging radicals to terminate chain reactions. Thus, the present study confirms that, tomato peel extract which is a rich source of carotenoids, especially lycopene, acts as a potent antioxidant source which protects the L6 cells from hydrogen peroxide induced oxidative damage.

## 5. Conclusion

In conclusion, antioxidants present in enzyme assisted tomato peel extract helps in normalization of ROS, DNA protection and restoring mitochondrial membrane potential. ETE possess significant bioactive compounds and radical scavenging activity as com-



pared to the extract without enzyme. Tomato peel extracts demonstrated promising antioxidant potential and protected DNA and mitochondria against induced oxidative stress. This study demonstrated the effectiveness of extract, ETE, by counteracting redox imbalance under condition encountered in most of the disease by modulating the components involved in cellular antioxidant status. The results provide significant evidence for antioxidant rich tomato peel extracts to be considered as a dietary supplement with potential activity for the prevention of mitochondrial and DNA damage induced by oxidative stress-mediated pathophysiology. The dietary supplementation of these would also address the free radical complications arising from oxidative stress. At present, considerable amounts of tomato peel are produced in the world and disposed off as waste. As a result, the exploitation of this material as a source of natural antioxidants, not only provides economic health benefits but also contribute to environmental protection.

#### Acknowledgment

The authors acknowledge CSIR-India (Network Project – CSC 0133) for research funding.

#### References

- Alvarado, C., Álvarez, P., Puerto, M., Gausserès, N., & Jiménez, L. (2006). Dietary supplementation with antioxidants improves functions and decreases oxidative stress of leukocytes from prematurely aging mice. *Nutrition*, *22*, 767–777.
- Al-Wandawi, H., Abdul Rehman, M. H., & Al Shaikhly, K. A. (1985). Tomato processing wastes as essential raw materials source. *Journal of Agriculture and Food Chemistry*, *33*, 804–807.
- Astrog, P., Gradelet, S., Berges, R., & Suschetet, M. (1997). Dietary lycopene decreases initiation of liver preneoplastic foci by diethylnitrosamine in rat. *Nutrition and Cancer*, *29*, 60–68.
- Barzana, E., Rubio, D., Santamaria, R. I., García-Correa, O., García, F., & RídauraSanz, V. E. (2002). Enzyme-mediated solvent extraction of carotenoids from marigold flowers (*Tagetes erecta*). *Journal of Agriculture and Food Chemistry*, *50*, 4491–4496.
- Bautista Ortin, A. B., Martínez Cutillas, A., Ros García, J. M., Lopez Roca, J. M., & Gomez Plaza, E. (2005). Improving colour extraction and stability in red wines, the use of maceration enzymes and enological tannins. *International journal of food science and technology*, *40*, 867–878.
- Bogdanov, M. B., Andreassen, O. A., Dedeoglu, A., Ferrante, R. J., & Beal, M. F. (2001). Increased oxidative damage to DNA in a transgenic mouse model of Huntington's disease. *Journal Neurochemistry*, *79*, 1246–1249.
- Bushra, S., Anwar, F., & Afraf, M. (2009). Effect of extraction solvent/technique on the antioxidant activity of selected medicinal plant extracts. *Molecules*, *14*, 2167–2180.
- Campanella, M., Parker, N., Tan, C. H., Hall, A. M., & Duchon, M. R. (2009). IF (1), setting the pace of the F(1)F(o)-ATP synthase. *Trends in Biochemical Science*, *34*, 343–350.
- Cathcart, R., Schwieters, E., & Ames, B. N. (1983). Detection of picomole levels of hydroperoxides using a fluorescent dichlorofluorescin assay. *Analytical Biochemistry*, *134*, 111–116.
- Chandna, S. (2004). Single-cell gel electrophoresis assay monitors precise kinetics of DNA fragmentation induced during programmed cell death. *Cytometry*, *61A*, 127–133.
- Choudhari, S. M., & Ananthanarayan, L. (2007). Enzyme aided extraction of lycopene from tomato tissue. *Food Chemistry*, *102*, 77–81.
- Cross, R. L., & Muller, V. (2004). The evolution of A-, F-, and V-type ATP synthases and ATPases, reversals in function and changes in the H<sup>+</sup>/ATP coupling ratio. *FEBS Letters*, *576*(1–4), 2004.
- Datta, K., Sinha, S., & Chathopathy, P. (2000). Reactive oxygen species in health and disease. *National Medical Journal of India*, *13*, 304–310.
- Devasagayam, T. P. A., Tilak, J. C., Boloor, K. K., Sane, K. S., Ghaskadbi, S. S., & Lele, R. D. (2004). Free radicals and antioxidants in human health, current status and future prospects. *Journal of Association of Physicians India*, *52*, 794–804.
- Dhanya, R., Arun, K. B., Nisha, V. M., Syama, H. P., Nisha, P., Santhosh Kumar, T. R., & Jayamurthy, P. (2015). Preconditioning L6 muscle cells with naringin ameliorates oxidative stress and increases glucose uptake. *PLoS One*, *10*(7), e013242.
- Droge, W. (2002). Free radicals in the physiological control of cell function. *Physiological Reviews*, *82*, 47–95.
- FAOSTAT (2012). *Agriculture production database*.
- Gan, W., Nie, B., Shi, F., Xu, X. M., Qian, J. C., Takagi, Y., et al. (2012). Age-dependent increases in the oxidative damage of DNA, RNA, and their metabolites in normal and senescence-accelerated mice analyzed by LC-MS/MS: urinary 8-oxoguanosine as a novel biomarker of aging. *Free Radical Biology and Medicine*, *52*, 1700–1707.
- Gonzalez, I. N., Valverde, V. G., Alonso, J. G., & Periago, M. G. (2011). Chemical profile, functional and antioxidant properties of tomato peel fiber. *Food Research International*, *44*, 1528–1535.
- Hanmoungjai, P., Pyle, D. L., & Niranjan, K. (2002). Enzyme-assisted water-extraction of oil and protein from rice bran. *Journal of Chemical Technology and Biotechnology*, *77*, 771–776.
- Haslam, E. (1996). Natural polyphenols (vegetable tannins) as drugs: Possible modes of action. *Journal of Natural Products*, *59*, 205–215.
- Huang, D., Ou, B., & Prior, R. L. (2005). The chemistry behind antioxidant capacity assays. *Journal of Agriculture and Food Chemistry*, *53*, 1841–1856.
- Hemi, K. E., Taigialferro, A. R., & Bobilya, D. J. (2002). Flavonoids antioxidant chemistry, metabolism and structure activity relationship. *Journal of Nutritional Biochemistry*, *13*, 572–584.
- Hemmani, T., & Parihar, M. S. (1998). Reactive oxygen species and oxidative DNA damage. *Indian Journal of Physiology and Pharmacology*, *42*, 440–452.
- Hickman, J. A. (1992). Apoptosis induced by anticancer drugs. *Cancer and Metastasis Review*, *11*, 121–139.
- Jalli, P. I., & Habib, M. (2015). Lycopene as a carotenoid provides radioprotectant and antioxidant effects by quenching radiation-induced free radical singlet oxygen: An overview. *Cell Journal*, *16*(4), 386–391.
- Jian, M. L., Peter, H. L., Qizhi, Y., & Changyi, C. (2010). Chemical and molecular mechanisms of antioxidants, experimental approaches and model systems. *Journal of Cellular and Molecular Medicine*, *14*, 840–860.
- Kang, K. A., Zhang, R., Piao, M. J., Chae, S., Kim, H. S., Park, J. H., et al. (2012). Baicalein inhibits oxidative stress-induced cellular damage via antioxidant effects. *Toxicology and Industrial Health*, *28*, 412–421.
- Liu, H., Jiang, Y., Luo, Y., & Jiang, W. (2006). Simple and rapid determination of ATP, ADP and AMP concentrations in pericarp tissue of litchi fruit by high performance liquid chromatography. *Food Technology and Biotechnology*, *44*, 531–534.
- Martinez-Valvercle, M. J., Periage, G., & Provan, A. (2002). Phenolic compounds, lycopene and antioxidant activities in commercial varieties of tomato (*Lycopersicon esculentum*). *Journal of the Science of Food and Agriculture*, *82*, 323–330.
- Maurya, C. K., Arha, D., Rai, A. K., Kumar, S. K., Pandey, J., Avisetti, D. R., et al. (2015). NOD2 activation induces oxidative stress contributing to mitochondrial dysfunction and insulin resistance in skeletal muscle cells. *Free Radical Biology and Medicine*, *89*, 158–169.
- Mosmann, T. (1983). Rapid colorimetric assay for cellular growth and survival, application to proliferation and cytotoxicity assays. *Journal of Immunological Methods*, *65*, 55–63.
- Nakabeppu, Y., Tsuchimoto, D., Yamaguchi, H., & Sakumi, K. (2007). Oxidative damage in nucleic acids and Parkinson's disease. *Journal of Neuroscience*, *85*, 919–934.
- Neeley, W. L., & Essigmann, J. M. (2006). Mechanisms of formation, genotoxicity, and mutation of guanine oxidation products. *Chemical Research in Toxicology*, *19*, 491–505.
- Paetau, I., Rao, D., Wiley, E. R., Brown, E. D., & Clevidence, B. A. (1999). Carotenoids in human buccal mucosa cells after 4 wk of supplementation with tomato juice or lycopene supplements. *American Journal of Clinical Nutrition*, *70*, 490–494.
- Paiva, S., & Russell, R. (1999). Beta carotene and other carotenoids as antioxidants. *The Journal of the American College of Nutrition*, *18*, 426–433.
- Pinelo, M., Zornosa, B., & Meyer, A. S. (2008). Selective release of phenols from apple skin, mass transfer kinetics during solvent and enzyme-assisted extraction. *Separation and Purification Technology*, *63*, 620–627.
- Powers, S. K., & Jackson, M. J. (2008). Exercise-induced oxidative stress: Cellular mechanisms and impact on muscle force production. *Physiological Reviews*, *88*, 1243–1276.
- Prakash, D., Gupta, C., & Sharma, G. (2012). Importance of phytochemicals in nutraceuticals. *Journal of Chinese Medical device*, 70–78.
- Prasad, N. R., Srinivasan, M., Pugalendi, K. V., & Menon, V. P. (2006). Protective effect of ferulic acid on  $\alpha$ -radiation induced micronuclei, dicentric aberration and lipid peroxidation in human lymphocytes. *Mutation Research*, *603*, 129–134.
- Ranganna, S. (1997). *Manual of analysis of fruit and vegetable products* (9th ed.). New Delhi: India, (Chapter 4).
- Riso, P., & Porrini, M. (2001). Tomatoes and health promotion. In R. R. Watson (Ed.), *Vegetables, fruits, and herbs in health promotion* (pp. 45–70). Boca Raton.
- Riso, P., Visioli, F., Erba, D., Testolin, G., & Porrini, M. (2004). Lycopene and vitamin C concentrations increase in plasma and lymphocytes after tomato intake. Effects on cellular antioxidant protection. *European Journal of Clinical Nutrition*, *58*, 1350–1358.
- Schapiro, A. H. (2006). Mitochondrial disease. *Lancet*, *368*, 70–82.
- Shalini, G., Jyoti, N., Neetu, J., & Charanjit, K. (2015). Food industry waste, mine of nutraceuticals. *International Journal of Environmental Science and Technology*, *4*, 205–229.
- Sharma, S. K., & Le Maguer, M. (1996). Lycopene in tomatoes and tomato pulp fractions. *Italian Journal of Food Science*, *8*(2), 107–113.
- Silva, E. M., Souza, J. N. S., Rogez, H., Rees, J. F., & Larondella, Y. (2006). Antioxidant activities and polyphenolic contents of fifteen selected plant species from the Amazonian region. *Food Chemistry*, *101*, 1012–1018.
- Singh, P., & Goyal, G. K. (2008). Dietary lycopene, its properties and anticarcinogenic effects. *Comprehensive Review on Food Science and Food Safety*, *7*(3), 255.
- Singleton, V. L., & Rossi, J. A. (1965). Colorimetry of total phenolics with phosphomolybdic-phosphotungstic acid reagents. *American Journal of Enology and Viticulture*, *16*, 144–158.

- Small, D. M., Bennett, N. C., Roy, S., Gabrielli, B. G., Johnson, D. W., & Gobe, G. C. (2013). Oxidative stress and cell senescence combine to cause maximal renal tubular epithelial cell dysfunction and loss in an in vitro model of kidney disease. *Nephron Experimental Nephrology*, *122*, 123–130.
- Sun, G. B., Qin, M., & Ye, J. X. (2013). Inhibitory effects of myricitrin on oxidative stress-induced endothelial damage and early atherosclerosis in ApoE<sup>-/-</sup> mice. *Toxicology and Applied Pharmacology*, *271*, 114–126.
- Yen, G. C., & Duh, P. D. (1994). Scavenging effect of methanolic extract of peanut hulls on free radical and reactive oxygen species. *Journal of Agricultural Food Chemistry*, *42*, 629–632.
- Zhang, W. H., & Wang, H. (2008). Nortriptyline protects mitochondria and reduces cerebral ischemia/hypoxia injury. *Stroke*, *39*, 455–462.
- Zuorro, A., & Lavecchia, R. (2011). Mild enzymatic method for the extraction of lycopene from tomato paste. *Biotechnology and Biotechnological Equipments*, *24*, 1854–1857.



## Lycopene mitigates acrylamide and glycidamide induced cellular toxicity via oxidative stress modulation in HepG2 cells

T.R. Reshmitha<sup>a,b</sup>, P. Nisha<sup>a,b,\*</sup>

<sup>a</sup> Agro Processing and Natural Products Division, CSIR-National Institute for Interdisciplinary Science and Technology (CSIR-NIIST), Industrial Estate P.O., Thiruvananthapuram 695019, Kerala, India

<sup>b</sup> Academy of Scientific and Innovative Research (AcSIR), Ghaziabad 201002, India

### ARTICLE INFO

#### Keywords:

Acrylamide  
Glycidamide  
Antioxidants  
Free radicals  
Oxidative damage  
Lycopene

### ABSTRACT

Acrylamide (ACR), a carcinogen and neurotoxin formed in carbohydrate-rich high temperature processed foods, undergo epoxidation in cells to form more toxic metabolite glycidamide (GLY). The present study investigated antioxidant potential of lycopene (LYC) against ACR and GLY induced toxicity in human liver cell line (HepG2). The treatment of HepG2 cells with LYC for 2 h prior to ACR and GLY exposure enhanced cell viability by 10% and 8% and decreased reactive oxygen species (ROS) production in a dose dependent manner. Also, significantly increased antioxidant enzyme activity such as superoxide dismutase (SOD), catalase (CAT) activity and glutathione (GSH) level, with reduction in malondialdehyde (MDA) and 8-oxo-dG level on LYC pre-treatment. Mitochondrial function on LYC pre-treated cells exhibit an increased mitochondrial membrane potential (MMP) level. Data supports the enhancement of antioxidant defence by LYC, against ACR and GLY-induced toxicity.

### 1. Introduction

Acrylamide (ACR) is a recognized toxicant present in various carbohydrate rich foods exposed to higher temperature during food processing (Pedreschi, Mariotti, & Granby, 2014). Based on the studies conducted on lab animal models, Agency for Toxic Substances and Disease Registry (ATSDR), reported that the ACR is mostly carcinogenic to humans. Also, in 1994, ACR was documented by the International Agency for Research on Cancer (IARC) as 'probably carcinogenic to humans' (ATSDR, 2012; IARC, 1994). It has been recognized that the amino acid asparagine and reducing sugars in the food are the main precursors for ACR production via Maillard reaction. Due to high consumption of baked goods globally, a long-term exposure to ACR formed in these products could induce genotoxicity, cytotoxicity and neurotoxicity and have a negative effect on human health (Prasad, & Muralidhara, 2012). Glycidamide (GLY), is the primary epoxide metabolite of ACR, which is catalysed by an enzyme complex Cytochrome P450 2E1 (CYP2E1). The ACR to GLY metabolic conversion via epoxidation is critical for the ACR toxicity, and GLY is reported to be a more potent mutagen than ACR as it causes genetic damage by binding to DNA (Manjanatha et al., 2006; Ghanayem, Witt, Kissling, Tice, & Recio,

2005). According to chemical activity, GLY is 70% more reactive than ACR, showing a high level of interaction with DNA and haemoglobin. According to Erdemli et al (2021), vitamin E consumption provided protection against neurotoxicity induced by ACR administration in both fetuses and adult rats.

Studies showed that ACR exposure gives rise to higher oxidative stress in cells and tissues (Zhao et al., 2015). Under oxidative stress conditions, the intracellular reactive oxygen species can oxidize biomolecules, which lead to protein oxidation, lipid peroxidation, DNA fragmentation, and most of the diseased conditions (Kunnel, Subramanya, Satapathy, Sahoo, & Zameer, 2019). Antioxidants are the scavengers in human body that confer protection against intracellular oxidative stress by providing electrons to ROS. Antioxidant enzymes like catalase (CAT), superoxide dismutase (SOD), glutathione peroxidase (GPx) and glutathione (GSH) are integral parts of the antioxidative defense system. It contributes to the repair of damaged cellular components (Ren et al., 2017). Some non-enzymatic antioxidants such as ascorbic acid, flavonoids, tocopherol, and beta-carotene help in mitigating the oxidative stress in cells (Rahal et al., 2014). There are evidences suggesting that the animals exposed to acrylamide produced increased levels of ROS (Prasad, & Muralidhara, 2012). Studies on ACR

\* Corresponding author at: Agro Processing and Natural Products Division, CSIR-National Institute for Interdisciplinary Science and Technology (CSIR-NIIST), Industrial Estate P.O., Thiruvananthapuram 695019, Kerala, India.

E-mail address: [pnisha@niist.res.in](mailto:pnisha@niist.res.in) (P. Nisha).

<https://doi.org/10.1016/j.jff.2021.104390>

Received 1 October 2020; Received in revised form 26 December 2020; Accepted 21 January 2021

Available online 19 February 2021

1756-4646/© 2021 The Authors. Published by Elsevier Ltd. This is an open access article under the CC BY license (<http://creativecommons.org/licenses/by/4.0/>).



discovered that the oxidative stress induction and mitochondrial dysfunction are the underlying mechanisms responsible for its cytotoxicity and genotoxicity (Liu et al., 2015). Accumulation of Reactive Oxygen Species (ROS) or a compromised antioxidant defense system could disrupt cellular redox balance, resulting in cellular injury. Hence, the viable strategies to mitigate ACR induced toxicity are the need-of-the-hour. Recently, growing attention has been paid to natural antioxidants from vegetables and fruits for the protection against ACR induced toxicity (Erdemli et al., 2021; Li et al., 2017; Soba et al., 2020; Sabah et al., 2016; Zhang, Wang, Chen, Yan, & Yuan, 2013). A reduction in acrylamide induced liver damage was reported on treatment with crocin (Gedik et al., 2017; Gedik et al., 2018). Treatment with phytochemicals have been shown promising results in overcoming ACR induced toxicity which is correlated with the protection induced by free radical regulation mechanisms [Mehri, Meshki, & Hosseinzadeh, 2015; Motamed-shariaty, Farzad, Nassiri-Asl & Hosseinzadeh, 2014].

Lycopene (LYC) is the most common and rich carotenoid in the human diet, worldwide (Kelkel, Schumacher, Dicato, & Diederich, 2011). It has a positive effect on redox imbalance, by which it activates antioxidant gene expression and regulates inflammatory mediators (Campos et al., 2017). LYC is a powerful antioxidant molecule that is particularly effective at ROS scavenging activity. Of all carotenoids known, LYC is the most effective singlet oxygen scavenger *in vitro* (Sies & Stahl, 1995). Clinical and epidemiological studies propose that carotenoid supplementation may reduce the risk of reactive oxygen species-associated chronic conditions. Due to its unique structure comprising electron-rich system, the LYC is a suitable target for all electrophilic components. Due to the presence of ACR in foods and its threat of massive intoxication, mechanisms to decrease the cytotoxicity and genotoxicity of ACR are of great importance. Natural antioxidants as mitigating agents against ACR induced toxicity have attracted attention owing to their importance in food, nutraceutical and pharmaceutical sectors (Chu et al., 2017). However, the protective effect of LYC against GLY toxicity has not been reported so far, to the best of our knowledge. Identification of unfavourable health consequences due to ACR exposure is an important aspect of acrylamide risk management to avoid or mitigate its health risk. At the same time, it is also important to understand how the dietary antioxidant influence the ACR toxicity on stress induced chronic disease conditions and its molecular mechanisms of action. Liver is the major detoxification organ in human body. Hence, the use of HepG2 cells for the *in vitro* chemical toxicity assay is justified. Moreover, HepG2 cells are reproducible in human system and easy to maintain. Therefore, in this study, we investigated the possible protective role of lycopene against ACR and GLY induced cellular toxicity by modulating oxidative stress in HepG2 cells.

## 2. Materials and methods

### 2.1. Chemicals and reagents

Acrylamide (ACR), Glycidamide (GLY), Lycopene (LYC) were purchased from Sigma-Aldrich (Bangalore, India). Ethylene diamine tetra acetic acid (EDTA), sodium chloride (NaCl), hydrogen peroxide (H<sub>2</sub>O<sub>2</sub>), TritonX, Tris- HCl, perchloric acid, potassium hydroxide (KOH) from MERK, India. Dimethyl sulfoxide (DMSO), Fetal Bovine Serum (FBS), Dulbecco's Modified Eagle's Medium (DMEM), 2,7-Dichlorodihydrofluorescein diacetate (DCFH-DA), 3-(4,5-dimethylthiazol-2-yl)-2,5-diphenyltetrazolium bromide (MTT) were purchased from Sigma-Aldrich Chemicals (St Louis, MO, USA). Trypsin-EDTA, Antibiotic-antimycotic was purchased from Gibco Invitrogen (Carlsbad, CA, USA). Superoxide Dismutase (SOD) Activity Assay Kit, Catalase Activity Colorimetric/Fluorometric Assay Kit, Glutathione (GSH) Colorimetric Assay Kit, Lipid Peroxidation (LPO), Colorimetric/Fluorometric Assay Kit were purchased from Biovision Inc (San Francisco, USA). Mammalian genomic DNA isolation kit were purchased from Sigma- Aldrich Chemicals (St Louis, MO, USA). DNA/RNA Oxidative damage Enzyme linked

Immunosorbent Assay (ELISA) kit was purchased from Cayman chemicals (MI-USA). All the chemicals used were of analytical grade high quality.

### 2.2. Cell culture and treatment conditions

HepG2 cells were procured from National Centre for Cell Science, Pune, India. Cells were grown in DMEM consisting of Fetal bovine serum (10%) and antibiotic-antimycotic solution (0.5%, 1 mL/100 mL of medium) at 37 °C in 5% CO<sub>2</sub> containing humidified atmosphere. The cells were cultured on 96-well plate and 12-well plates (1 × 10<sup>4</sup> cells/well) for staining and Flow cytometric analysis.

### 2.3. Cytotoxicity by MTT assay

The cytotoxicity of the Acrylamide (ACR), Glycidamide (GLY) and Lycopene (LYC) in HepG2 cells was estimated using MTT assay (Mossman, 1983). Briefly, 96-well plates were seeded with 1 × 10<sup>4</sup> cells per well and were grown overnight. To analyse the toxicity level of each samples, cells were treated with different concentrations of the LYC (1–50 μM), ACR (0.1–2 mM) and GLY (0.1–2 mM) for 24 h. After exposure, cells were exposed to MTT reagent (0.5 g/L) for 4 h. Following the incubation, the reaction mixture was removed and added DMSO (200 μL) to each well with gentle mixing (Orbit plate shaker, Labnet international, USA) and the absorbance was read at 570 nm (Synergy 4 Biotek multiplate reader, USA).

For assessing the protective effect of LYC against ACR and GLY induced toxicity, the cells were pre-treated with different concentrations of LYC for 2 h followed by the incubation with ACR and GLY at 37 °C for 24 hrs. Cells without exposure were regarded as the negative control and cells exposed to 500 μM ACR and GLY independently, were assigned as positive control. MTT assay was carried out to estimate the viability. Each experiment was performed in triplicate, and the results are represented as the mean ± SD, using the following calculation

$$\% \text{cell viability} = \frac{\text{The absorbance of test}}{\text{The absorbance of control}} \times 100$$

### 2.4. Intracellular reactive oxygen species (ROS) levels

Intracellular ROS levels was estimated using DCFH-DA staining (Cathcart, Schwiers, & Ames, 1983). The cells were exposed to various subtoxic concentrations of LYC and followed by 500 μM ACR and GLY was added. After the treatment, cells were incubated with DCFH-DA for 20 min and were washed with PBS. The fluorescence intensity of DCF was read fluorescence spectrophotometer (Shimadzu RF5000U) with wavelength of excitation 480 nm and emission s 520 nm (Synergy 4 Biotek multiplate reader, USA).

### 2.5. Antioxidant enzyme analysis

#### 2.5.1. Superoxide dismutase (SOD) and catalase (CAT) activity

HepG2 cells were pre-treated with different concentrations of LYC with 2 hrs followed by exposure to ACR and GLY for 24 h, washed with PBS. Specific enzyme buffer solution was used for lysing the cells which were used for estimating the antioxidant activity. A negative control with cells without treatment and positive control with ACR/GLY alone were also employed. The activity of SOD was estimated using Superoxide Dismutase (SOD) Activity Assay Kit as per the directions provided by the manufacturer (K335-100) and CAT activity was found out according to the Catalase Activity Colorimetric/Fluorometric Assay Kit (K773-100).

#### 2.5.2. Measurement of glutathione (GSH) concentration

The lysate of the cells was prepared as mentioned under the above experiment and the clear supernatant was analysed for GSH level. The

reduced GSH level of the treated lysates was found out based on the reaction of dithionitro benzoic acid (DTNB) with compounds containing sulfhydryl groups that leads to the formation of yellow color. Glutathione assay kit was used for the estimation of glutathione level following the manufacturer instructions provided along with the kit (K261-100).

## 2.6. Oxidative marker analysis

### 2.6.1. Measurement of lipid peroxidation

Quantification of lipid peroxidation was done by commercial lipid peroxidation (LPO) assay kit. HepG2 cells plated in six-well plates ( $1 \times 10^6$  cells/well) were pre-treated with LYC (2h) followed by exposure to ACR and GLY (24 hrs). Negative control and positive control were also employed as mentioned in the previous experiments. Malondialdehyde (MDA) level was tested using Lipid Peroxidation (LPO) Colorimetric/Fluorometric Assay Kit as per the directions given by the manufacturer (K739-100). Absorbance measured at 532 nm (Synergy 4 Biotek multi-plate reader, USA) was used to quantify the amount of MDA formed in the samples.

### 2.6.2. Estimation of 8-oxo-2'-deoxyguanosine (8-oxo-dG) level

DNA damage protection by lycopene against ACR and GLY induced stress was measured using 8-oxo-dG ELISA method. The different sub-toxic concentrations of LYC were pre incubated and followed by ACR and GLY exposure was added to the cells. Then, cells were trypsinized and the genomic DNA was extracted by using genomic DNA isolation kit. 8-oxo-dG, the most abundant DNA oxidative marker, was quantified using Oxidative damage ELISA kit. The quantification of 8-oxo-dG level produced in the cells was analysed spectrophotometrically at 410 nm.

## 2.7. Mitochondrial membrane potential ( $\Delta\Psi_m$ )

Oxidative stress lead to inactivity of mitochondrial membrane potential and the loss of function. Rhodamine123, a fluorescent indicator deposit selectively within the mitochondria based on the membrane potential was used for assessing the mitochondrial membrane potential (Zhang & Wang, 2008). Respiration, by ATP hydrolysis via ATP synthase, generates the proton motive force, that is crucial for keeping the mitochondrial membrane potential. The cells were pre-incubated with LYC before it was exposed to ACR and GLY for stress induction. After incubation, cells were treated with with 2  $\mu$ M Rhodamine 123 directly and rinsed with PBS many times and the fluorescence were read (FACS Aria II, BD Bioscience, USA). Suppression of  $\Delta\Psi_m$  is denoted by decreased level of green rhodamine 123 fluorescence.

## 2.8. Statistical analysis

The results are stated as means  $\pm$  standard deviations of minimum of three experiments. One-way ANOVA was used for analysing the results and the Duncan's multiple range test was employed for assessing the significance using SPSS 16.0. The significance was accepted at  $P \leq 0.05$ .

## 3. Results and discussion

### 3.1. Cytotoxicity assessment of ACR, GLY and LYC

To evaluate the toxicity level of all samples, ACR, GLY and LYC in HepG2 cells were evaluated using MTT assay. The results depicted that LYC did not alter cellular viability up to 30  $\mu$ M concentration (Fig. 1A). Further, LYC at a concentration of below 30  $\mu$ M was chosen for studying the hepatoprotective effect against ACR and GLY induced toxicity.

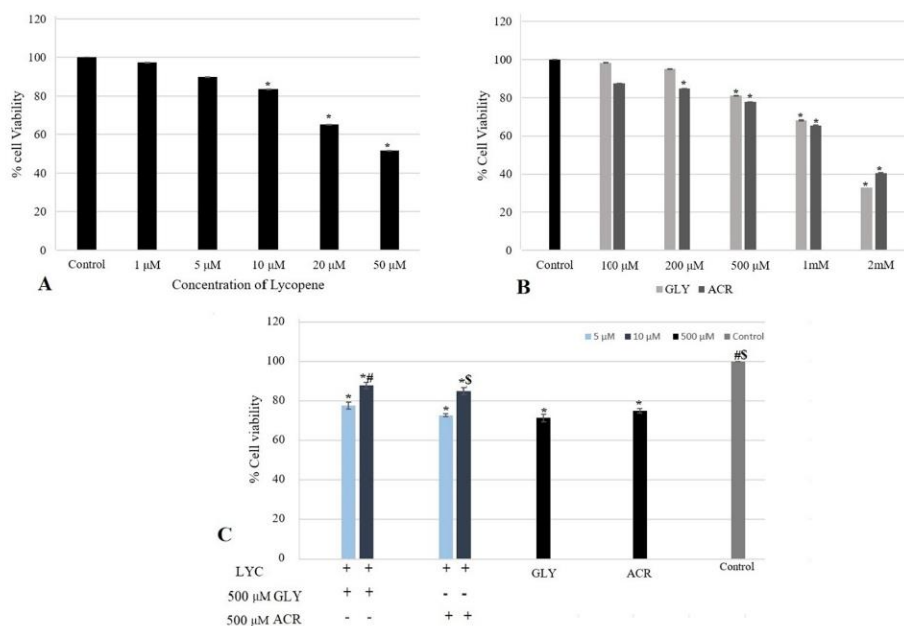


Fig. 1. Determination of cytotoxic effect on HepG2 cells by MTT Assay. (A) Cell viability of various concentrations of LYC (B) Cell viability of ACR and GLY treated cells. (C) The LYC on viability of L6 cell against 500  $\mu$ M ACR and GLY induced toxicity. The data are presented as the means  $\pm$  SD of three experiments. The annotation \* denotes a  $P$  value  $< 0.05$  against control. # denotes  $P < 0.05$  against GLY and \$  $P < 0.05$  against ACR.



To determine the suitable working concentrations of ACR and GLY for inducing toxicity, a dose–response assay was performed with different concentrations of ACR and GLY, ranging from 100  $\mu\text{M}$  to 2 mM. Cells without treatment were taken as negative control group. From the data shown in Fig. 1B, ACR and GLY induced cell death in a concentration-dependent manner. At a concentration of 500  $\mu\text{M}$ , ACR and GLY caused about 30% decrease in cell viability (Fig. 1B). Therefore, this concentration was chosen for inducing the cellular toxicity in further experiments. The concentration was consistent with the previous reports, as acrylamide at concentration above 250  $\mu\text{M}$  showed cytotoxicity in HepG2 cells (Sahinturk, Kacar, Vejselova, & Kutlu, 2018). Similar results were reported for Caco-2 cells (0.2–50 mM), NIH/3T3 fibroblasts, alveolar-basal epithelial cells (A549) and epithelial cells BEAS-2B (normal human lung) (Adriana et al., 2020; Sahinturk, Kacar, Vejselova, & Kutlu, 2018; Kacar, Vejselova, Kutlu, & Sahinturk, 2018; Kacar, Sahinturk, & Kutlu, 2019). The ACR antiproliferative activity was also confirmed in several cancer and normal cell lines (Sahinturk, Kacar, Vejselova, & Kutlu, 2018; Atto et al., 2016; Mallepogu et al., 2017). A study by Kacar et al. (2019) suggested ACR interferes with kinesin proteins, which are responsible for cell division and thereby inhibiting cell proliferation. The cell death induced by intracellular ROS production activate the mitogen activated protein kinase (MAPK)-JNKs, which act an important role in cellular processes including apoptosis (Valiko et al., 2007). Interestingly, several studies showed that the GSH level lead to redox imbalance which promote apoptotic signalling and cell death. Therefore, reduced GSH levels result in oxidative stress, and also lead to cell death as a potential mechanism for ACR toxicity by activating MAPK pathway. ACR induced caspase-3 activation, the final mediator of apoptosis signalling. ACR mechanism in hepatotoxicity was originated from oxidative stress with mitochondrial damage and cell death signalling (Seydi et al., 2015).

### 3.2. Cytoprotective potential of LYC against ACR and GLY-induced toxicity

In order to determine the protective effects of LYC on HepG2 cells against ACR and GLY induced toxicity, the cells were pre-treated with two different concentrations (5  $\mu\text{M}$  and 10  $\mu\text{M}$ ) of LYC followed by the addition of ACR and GLY at their cytotoxic concentration (500  $\mu\text{M}$ ). It was found that the pre-exposure of cells to LYC (Fig. 1C) improved the cell viability in a concentration-dependent manner compared to the cells that are treated only with ACR and GLY. Treatment of cells with 10  $\mu\text{M}$  concentration of LYC prior to ACR treatment increased the cell viability by 10.0% (LYC), compared to ACR treated cells. Likewise, the pre-exposure of LYC (10  $\mu\text{M}$ ) prior to GLY exposure (500  $\mu\text{M}$ ) also proved a similar trend where, an increased cell viability by 16.3% (LYC), was observed (Fig. 1C). The results suggested that LYC could exert hepatoprotective effects against food toxicants such as ACR and GLY in HepG2 cells. A study by Chen et al. (2013) demonstrated that the flavonoid, myricitrin inhibit ACR cytotoxicity on Caco-2 cells.

### 3.3. Protective potential of LYC against ACR and GLY-induced generation of ROS

The ACR toxicity is correlated with antioxidant imbalance that results in an induced oxidative stress. Recent studies confirmed that the ACR toxicity was connected with excessive intracellular ROS build-up in a dose-dependent manner. Adriana et al (2020) showed that ACR (0.2 to 12.5 mM) induced a dose dependent increase in mitochondrial depolarization in Caco2 cells after 24 exposure. According tom Zamani et al, ACR induces oxidative stress on mice splenocytes increase in ROS production, and the peroxidation of lipids and glutathione oxidation, which were accompanied by the collapse of MMP (Zamani et al., 2017). The overproduction of ROS causes the imbalance in the redox status of cells, and it is experimentally demonstrated that augmentation of antioxidants can modulate the cellular homeostasis by scavenging the ROS

(Rodriguez-Ramiro, Ramos, Bravo, Goya, & Angeles Martin, 2011). Therefore, inhibition of ACR and GLY induced ROS formation by natural antioxidants from fruits and vegetables is a hopeful strategy. To establish this concept, we used DCFH-DA, a fluorescence probe specifically for ROS analysis, to evaluate whether LYC could suppress ACR and GLY induced intracellular ROS generation in HepG2 cells. The cells were pre-exposed to 5 and 10  $\mu\text{M}$  of LYC (2 h) followed by treatment with 500  $\mu\text{M}$  ACR and GLY for 24 h incubation. The intensity of DCF fluorescence in HepG2 cells treated with ACR and GLY was significantly increased to 55.6 and 61.2%, respectively compared to the control group (15.0%) (Fig. 2). Interestingly, pre-treatment of 5 and 10  $\mu\text{M}$  LYC scavenged ACR and GLY induced ROS production significantly by reducing the ROS level by 34.0% and 23% compared to GLY treated group and by 41.6% and 34.0% relative to ACR treated group. Results showed that LYC significantly scavenged the ROS generated by ACR and GLY in HepG2 cells in a dose dependent manner. Reduction in the generation of intracellular ROS in LYC pre-exposed HepG2 cells demonstrate the protective capacity of LYC against the ACR and GLY induced ROS generation in the cells. Carotenoids in the foods also possess excellent antioxidant activity, which have been studied for their ability to prevent chronic disease conditions. Beta-carotene, lycopene and others carotenoids exhibit higher antioxidant properties in *in vitro* and *in vivo* models (Mueller, & Boehm, 2011; Bohm, Puspitasari, Ferruzzi, & Schwartz, 2002). It is reported that the ROS generation exerts a vital role in inducing hepatocellular damage. ACR and GLY induced ROS generation have been reported earlier and is known to be linked with oxidative stress (Prasad & Muralidhara, 2012; Mehri, Karami, Hassani, & Hosenzadeh, 2014). Therefore, the importance of LYC in cellular protection against ACR and GLY induced ROS generation is established in the present study.

### 3.4. Estimation of cellular antioxidant enzyme activity

#### 3.4.1. LYC improved Superoxide dismutase and catalase activity

Major antioxidant enzymes such as Superoxide dismutase (SOD) and Catalase (CAT) play a vital role in cellular redox homeostasis (Heikkila, Cabbat, & Cohen, 1976; Winterbourn & Stern, 1987). SOD and CAT are the important cellular antioxidant enzymes that safeguard cellular components against damage caused by free radicals. Hence, the activities of these antioxidant enzymes have been used to evaluate the cellular oxidative stress level (Liu, Ma, & Sun, 2010; Duranti, Ceci, Sgro, Sabatini, & Di Luigi, 2017). Thus, we proceeded to evaluate the effect of LYC on the enzyme activities of SOD and CAT. As demonstrated in Fig. 3A and 3B, incubation of HepG2 cells with ACR and GLY resulted in a significant decrease in both SOD ( $0.31 \pm 0.09$  &  $0.28 \pm 0.12$  U/mg, respectively) and CAT activity ( $3.4 \pm 0.03$  and  $3.10$  U/mg respectively), as compared to the untreated cells ( $0.5 \pm 0.06$  and  $5.4 \pm 0.09$  U/mg respectively for SOD & CAT). When cells were pre-incubated with LYC (10  $\mu\text{M}$  concentration), prior to ACR and GLY exposure, a striking and significant ( $p \leq 0.05$ ) rise in the enzyme activities were noticed. The SOD activity was increased to 0.42 U/mg on pre-exposing the cells to LYC, (Fig. 3A) before ACR treatment. Similarly, SOD activity was increased to 0.41 U/mg when HepG2 cells were treated with LYC before GLY exposure.

Catalase (CAT) is very important in sustaining the cellular redox homeostasis (Autréaux, & Toledano, 2007). CAT activity is one of the commonly employed assays that can provide information about the cell antioxidant defense system. Fig. 3B illustrates the CAT activity in the untreated cells to be  $5.4 \pm 0.09$  U/mg, which on treatment with ACR and GLY decreased to  $3.4 \pm 0.03$  and  $3.1$  U/mg respectively. When cells were pre-incubated with LYC prior to ACR and GLY treatment, a significant ( $p \leq 0.05$ ) elevation in the enzyme activity ( $4.2$  U/mg) was observed (Fig. 2B). Similarly, for GLY exposure, the CAT activity was observed in the order of LYC 4.1 U/mg. From the assay, it was observed that the LYC exposure protected the cells from ACR and GLY induced oxidative damage by maintaining physiological antioxidant enzyme level. Recent



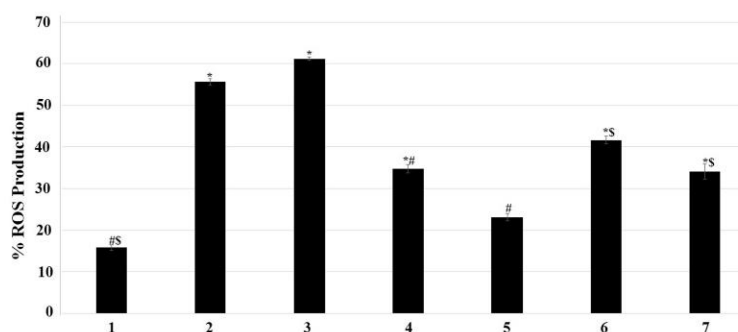


Fig. 2. Estimation of ROS formation by HDCEFA Staining by Fluorescence spectrophotometer. The pretreatment of LYC on the ACR and GLY exposure in HepG2 cells. The numbers depict 1-Control, 2-500  $\mu$ M ACR, 3-500  $\mu$ M LYC, 4-500  $\mu$ M LYC + 500  $\mu$ M ACR, 5-500  $\mu$ M LYC + 500  $\mu$ M ACR, 6-500  $\mu$ M LYC + 500  $\mu$ M ACR + 500  $\mu$ M LYC, 7-500  $\mu$ M LYC + 500  $\mu$ M ACR + 500  $\mu$ M LYC. Data represent the mean  $\pm$  SD of three separate experiments. The annotation \* denotes a  $P < 0.05$  against group Control, # represent  $P < 0.05$  versus the ACR group and # represent  $P < 0.05$  against GLY group.

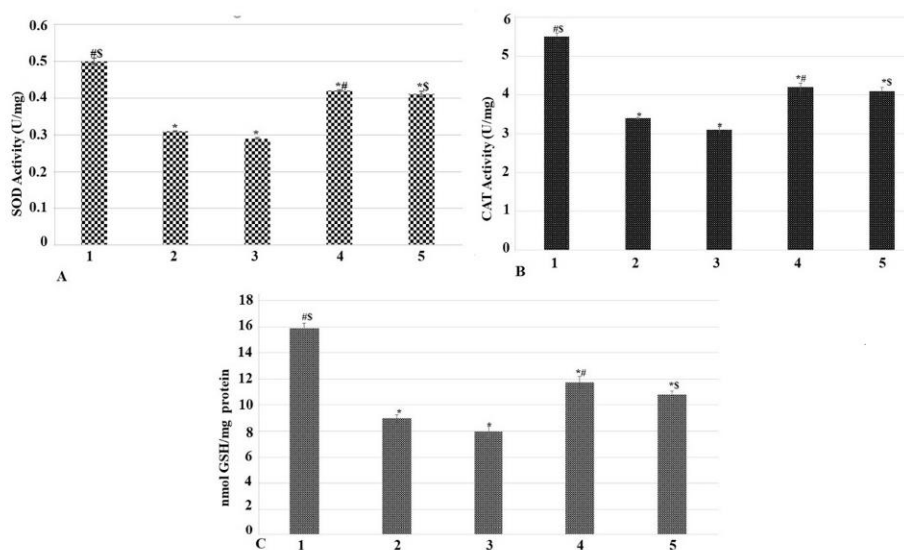


Fig. 3. Effects of LYC on SOD, CAT and GSH in HepG2 cells (A) Protective effect of LYC on SOD activity in presence of ACR and GLY (500  $\mu$ M) (B) Protective effect of LYC on CAT activity in presence of ACR and GLY (500  $\mu$ M) (C) Protective potential of LYC on reduction in the level of glutathione when exposed to ACR and GLY (500  $\mu$ M). The numbers depict 1-Control, 2-500  $\mu$ M ACR, 3-500  $\mu$ M LYC, 4- LYC + 500  $\mu$ M ACR, 5- LYC + 500  $\mu$ M GLY. Data are expressed as the mean  $\pm$  S.D. of three experiments carried out independently. The annotation \* represents  $P < 0.05$  against Control, # represents  $P < 0.05$  against ACR and \$ represents  $P < 0.05$  against GLY group.

studies were focussed on the biological antioxidant and oxidant balancing. Crocin, a carotenoid pigment mainly found in saffron, is reported to attenuate ACR induced damage in male Wistar rats intestines by inhibiting oxidative stress, specifically by upregulating antioxidant enzyme defence system (Gedik et al., 2018). Another study by Gedik et al suggested that the crocin treatment removed ACR induced liver damage in male Wistar rats due to its high antioxidant properties (Gedik et al., 2017).

#### 3.4.2. LYC improved ACR and GLY induced GSH depletion

Glutathione (GSH) performs an important role in the neutralization of free radicals and reactive oxygen species (Shan, Aw, & Jones, 1990). Previous studies reported that ACR exposure can lead to GSH depletion (Autréaux, & Toledano, 2007). Reports suggest that ACR can block the activity of glutathione S-transferase and thereby deplete the GSH level

(Cuzzocrea, & Reiter, 2001; Hsu, Tsai, & Chen, 2009). Subsequently, LYC exhibited a promising effect in scavenging ACR and GLY induced intracellular ROS and thereby ameliorate oxidative damage by maintaining antioxidant enzyme activity. Hence, we postulate that LYC could also attenuate ACR and GLY induced GSH depletion in cells. The results showed that GSH level in HepG2 cells treated with ACR and GLY was significantly depleted ( $8.3 \pm 0.12$  nmol/mg and  $7.9 \pm 0.18$  nmol/mg respectively), compared to the control ( $15.8 \pm 0.09$  nmol/mg) (Fig. 3C). Exposing the cells to LYC before treating with ACR and GLY, restored the GSH activity effectively by increasing it to 11.7 nmol/mg. A similar increase was also found in LYC pre-treatment before GLY exposure, which was 10.7 nmol/mg. It was observed in the study that exogenous exposure of ACR and GLY leads to rise in the generation of intracellular ROS and induce oxidative damage in hepatic cells, which can be counteracted by hepatocyte antioxidant defense mechanisms. Therefore, it may be

inferred that on exposure of the HepG2 cells to the LYC leads to the quenching of intracellular free radical production and elevate the level of glutathione. This enhances the antioxidant status of the cells, guarding against ACR and GLY-induced cellular impairment via controlling GSH antioxidant systems to subsist oxidative stress. These findings implied that LYC might offer protection against ACR and GLY induced oxidative damage in HepG2 cells via maintaining antioxidant defense systems to manage with oxidative stress.

Chronic dietary exposure of ACR induce oxidative stress by increasing ROS formation and GSH oxidation. After intestinal absorption, ACR inhibit glutathione (GSH) that result in depletion of cellular GSH. The reduction in GSH levels enhances the levels of reactive oxygen species (ROS). Experiment conducted by Seydi et al. (2015) on acrylamide toxicity in male rats indicated rapid glutathione depletion, which is another stress marker of the cellular damage. Polyphenols in high concentrations can protect the intestinal epithelium from the oxidative stress induced by ACR. N-acetylcysteine administration in a pharmacological dose also exhibited an antioxidant effect against acrylamide induced oxidative damage in liver and small and large intestine tissues (Altinoz, Turkoz, & Vardi, 2015).

### 3.5. Estimation of oxidative markers formation

#### 3.5.1. Effect of LYC on lipid peroxidation induced by ACR and GLY

MDA level is broadly used as an oxidative stress marker of free radical linked lipid peroxidation. Higher liver Malondialdehyde (MDA) levels indicate the enhanced lipid peroxidation that give rises to tissue impairment and leads to the failure of antioxidant defense mechanisms. In this study, lipid peroxidation, analysed in terms of MDA level, in HepG2 cells were analysed by exposing the cells to 500  $\mu$ M ACR and GLY, which indicated a significant increase in MDA concentration (3.9 nmol/mg and 4.7 nmol/mg respectively), compared to the control group (0.49 nmol/mg). Interestingly, pre-treatment with LYC significantly prevented the formation of MDA induced the cellular damage caused by ACR and GLY in HepG2 cells (Fig. 4A). Pre-treatment with LYC caused a significant reduction in the MDA levels to 2.7 nmol/mg, compared to ACR treated group (3.9 nmol/mg) (Fig. 4A). GLY treated cells with LYC preincubation also exhibited a reduction in MDA level to 3.7 nmol/mg, compared to the GLY alone treated group (4.7 nmol/mg). The results suggest that natural antioxidant LYC can protect against ACR and GLY induced lipid peroxidation in HepG2 cells.

#### 3.5.2. LYC protects DNA from oxidative damage

8-Oxo-dG is the major product of DNA oxidation due to increased oxidative stress (Nakabeppu, Tsuchimoto, Yamaguchi, & Sakumi, 2007). The protective effect of LYC against ACR and GLY induced oxidative DNA damage was quantified by analysing the oxidative marker, 8-oxo-dG in DNA, which is a highly studied DNA oxidation product. In the presence of higher free radical accumulation, dsDNA molecules undergo oxidation to form oxidized product (Bogdanov, Andreassen, Dedeoglu, & Ferrante, 2001). Therefore, here 8-Oxo-dG level in the cells was assessed for investigating the DNA protective effect of LYC against ACR and GLY exposure. As shown in Fig. 4B, on exposure to 500  $\mu$ M ACR and GLY in cells, 8-OH-dG level is significantly increased as compared to the control. However, on LYC pre-treatment prior to ACR and GLY exposure, the 8-OH-dG level was significantly decreased. The dsDNA oxidation was found to increase in ACR and GLY exposure and in LYC pre-treatment decrease the oxidative product level in a dose dependent manner.

#### 3.6. Protective effect of LYC against ACR and GLY induced mitochondrial transmembrane potential ( $\Delta\psi$ m) loss

It is reported that ROS accumulation was related with disruption of mitochondrial membrane potential (MMP) and ACR exposure to cells leads to mitochondrial dysfunction (Chen et al., 2013). Based on these evidences, we studied the impact of promising antioxidant LYC against ACR and GLY induced mitochondrial transmembrane potential loss. To estimate the level of MMP, Rhodamine-123, a cationic fluorescence probe was used in the present study. In Fig. 5B and C depicts ACR and GLY (500  $\mu$ M) treatment, which shows a remarkable decline of MMP level, 62% and 70.6% respectively, as compared to the untreated cells 6.9% shows in Fig. 5A Pre-treatment of cells with LYC was found to exert protective effect in cells against the loss of mitochondrial transmembrane potential induced by ACR and GLY. The MMP was increased when cells were subjected to pre-treatment with the LYC before exposure to ACR and GLY when compared to cells exposed to ACR and GLY without pre-treatment. The MMP on pre-treatment with LYC prior to ACR and GLY were 35.2 and 55.4%, respectively (Fig. 5). Our results suggest that all the LYC-treated cells could significantly attenuate the ACR and GLY induced ROS associated mitochondrial dysfunction. According to Zamani et al. (2017) ACR toxicity depend on mitochondrial dysfunction induced by oxidative damage, which activate cellular death (Zamani et al., 2017). ACR exposure to hepatocytes resulted in mitochondrial injury by the decline of MMP (Seydi et al., 2015).

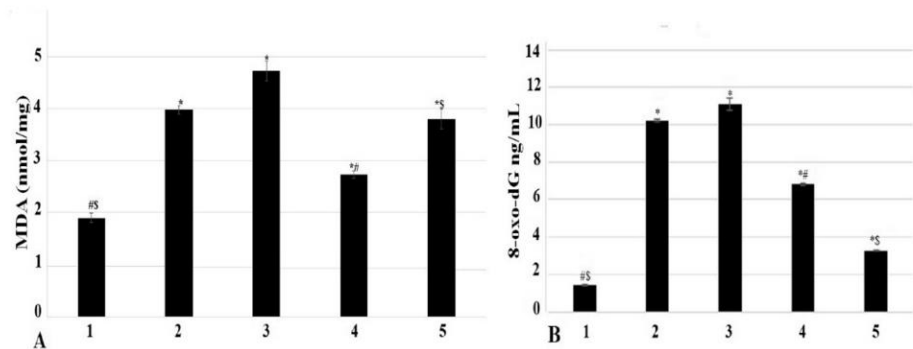


Fig. 4. Quantification of oxidative stress markers. (A) Figure represent Lipid peroxidation determined by MDA level (B) Figure represent the 8-oxo-dG level in cells. The numbers depict 1-Control, 2-500  $\mu$ M ACR, 3-500  $\mu$ M GLY, 4- LYC + 500  $\mu$ M ACR, 5- LYC + 500  $\mu$ M GLY. Each value denotes the mean  $\pm$  SD of triplicate measurements. Significance levels between different groups were determined by using one-way ANOVA, \* $P \leq 0.05$  versus Control; # $P \leq 0.05$  versus ACR and \$ $P < 0.05$  versus GLY.

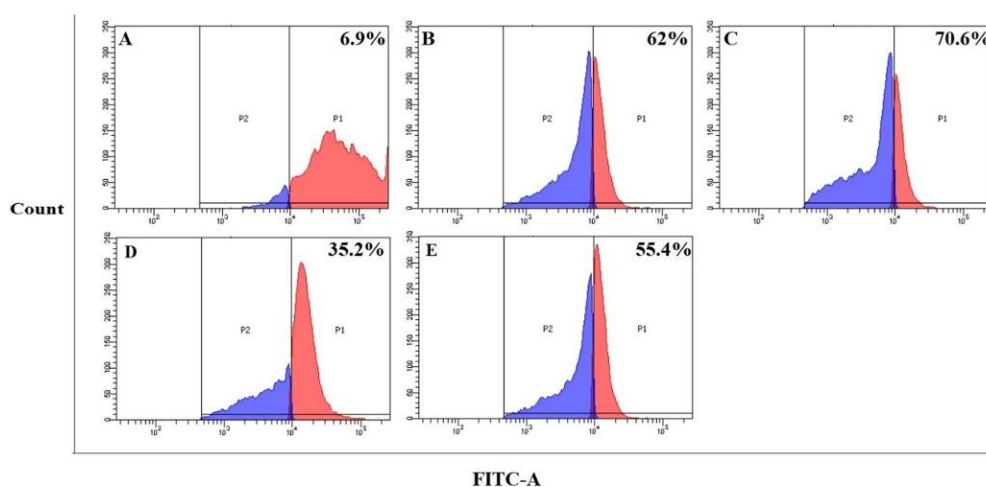


Fig. 5. Estimation of Mitochondrial membrane potential by Rhodamine 123 staining which depicts restoration of MMP on LYC pre-treatment. After incubation, the cells were stained with Rhodamine 123 and read by flow cytometer. In data indicate A- Control, B-500  $\mu$ M ACR, C-500  $\mu$ M GLY, D- 10  $\mu$ M LYC + 500  $\mu$ M ACR, E- 10  $\mu$ M LYC + 500  $\mu$ M GLY.

#### 4. Conclusions

The present study demonstrated the cytoprotective potential of major carotenoid LYC as a bioactive agent to attenuate ACR and GLY-prompted cytotoxicity in HepG2 cells. As biological oxidant to antioxidant ratio imbalance leads to induce oxidative stress, under normal physiological state, free radicals are neutralised by innate antioxidant defence system of our body. LYC is an important carotenoid present in our diet with superior antioxidant property. From the data, LYC protective effect is proposed to be facilitated by the inhibition of intracellular ROS production, enhanced antioxidant enzymes (SOD and CAT), restoration of the GSH level and decreased oxidative product level (MDA and 8-oxo-dG). Collectively, results of this study demonstrate that LYC can protect HepG2 cells against ACR and GLY induced oxidative damage through its antioxidant activity. Therefore, reasonable supplements of the LYC or LYC enriched products, can alleviate the harmful effects caused by the dietary exposure of acrylamide. Further *in vivo* studies are warranted to confirm the findings deduced in the present work.

##### Ethical Statement

The Authors confirm that no animal/human studies have been carried out in the present

##### Credit author statement

P. Nisha designed the work and experimental design. Ms. Reshmitha T.R. executed the experiments and wrote the manuscript. P. Nisha corrected the manuscript and done the proofreading.

##### Declaration of Competing Interest

The authors declared that there is no conflict of interest.

##### Acknowledgments

The authors acknowledge CSIR for the research funding

##### References

- Adriana, N., Szyda, M., Dorota, Z., Agnieszka, K., & Ilona, M. (2020). Acrylamide Decreases Cell Viability, and Provides Oxidative Stress, DNA Damage, and Apoptosis

in Human Colon Adenocarcinoma Cell Line Caco-2. *Molecules*, 25, 368. <https://doi.org/10.3390/molecules25020368>.

Agency for Toxic Substances and Disease Registry (ATSDR). (2012) Toxicological profile for Acrylamide. U.S. Department of Health and Human Services, Public Health Service. <https://www.atsdr.cdc.gov/toxprofiles/TP.asp?tid=1112&tid=236>.

Altinoz, E., Turkoz, Y., & Vardi, N. (2015). The protective effect of N-acetylcysteine against acrylamide toxicity in liver and small and large intestine tissues. *Bratislavske Lekarske Listy*, 116(4). [https://doi.org/10.4149/BLL\\_2015\\_049](https://doi.org/10.4149/BLL_2015_049).

Atto, K., Kertika, D., Lundqvist, J., Oredsson, S., & Forsby, A. (2016). Acrylamide affect proliferation and differentiation of the neural progenitor cell line C17.2 and the neuroblastoma cell line SH-SY5Y. *Toxicology In Vitro*, 35, 100–111. <https://doi.org/10.1016/j.tiv.2016.05.014>.

Autréaux, B. D., & Toledano, M. B. (2007). ROS as signalling molecules: Mechanisms that generate specificity in ROS homeostasis. *Nature Reviews Molecular Cell Biology*, 8, 813–824. <https://doi.org/10.1038/nrm2256>.

Bogdanov, M. B., Andreassen, O. A., Dedeoglu, A., & Ferrante, R. J. (2001). Increased oxidative damage to DNA in a transgenic mouse model of Huntington's disease. *Journal Neurochemistry*, 79, 1246–1249. <https://doi.org/10.1046/j.1471-4159.2001.00689.x>.

Bohm, V., Puspitasari, N. L., Ferruzzi, M. G., & Schwartz, S. J. (2002). Trolox equivalent antioxidant capacity of different geometrical isomers of  $\alpha$ -carotene,  $\beta$ -carotene, lycopene, and zeaxanthin. *Journal of Agricultural and Food Chemistry*, 50, 221–226. <https://doi.org/10.1021/jf010888q>. PMID: 11754571.

Campos, K. K. D., Araújo, G. R., Martins, T. L., Bandeira, A. C. B., Costa, G., de, P., Talvani, A., & Bezerra, F. S. (2017) The antioxidant and anti-inflammatory properties of lycopene in mice lungs exposed to cigarette smoke. *Journal of Nutritional Biochemistry*, 48, 9–20. doi: 10.1016/j.jnutbio.2017.06.004. Epub 2017 Jun 20. PMID: 28651168.

Cancer, IARC monographs on the evaluation of carcinogenic risks to humans: Some industrial chemicals. (International Agency for Research on Cancer), 1994 <http://www.thelancet.com/journals/lanonc/article/PIIS1470-2045%2816%2900137-6>.

Cathcart, R., Schwiers, E., & Ames, B. N. (1983). Detection of picomole levels of hydroperoxides using a fluorescent dichlorofluorescein assay. *Analytical Biochemistry*, 134, 111–116. [https://doi.org/10.1016/0003-2697\(83\)90270-1](https://doi.org/10.1016/0003-2697(83)90270-1).

Chen, J. H., Yang, C. H., Wang, Y. S., Lee, J. G., Cheng, C. H., & Chou, C. (2013a). (2013 a) Acrylamide-induced mitochondria collapse and apoptosis in human astrocytoma cells. *Food and Chemical Toxicology*, 51, 446–452. <https://doi.org/10.1016/j.fct.2012.10.025>.

Chen, W., Feng, L., Shen, Y., Su, H., Li, Y., Zhuang, J., ... Zheng, X. (2013b). Myricitrin inhibits acrylamide-mediated cytotoxicity in human Caco-2 cells by preventing oxidative stress. *BioMed Research International*, 72, 4183. <https://doi.org/10.1155/2013/724183>.

Chiu, Q., Zhao, Y., Shi, X., Han, W., Zhang, Y., Zheng, X., & Zhu, J. (2017). *In vivo*-like 3-D model for sodium nitrite- and acrylamide-induced hepatotoxicity tests utilizing HepG2 cells entrapped in micro-hollow fibers. *Scientific Reports*, 7(1), 14837. <https://doi.org/10.1038/s41598-017-13147-z>.

Cuzzocrea, S., & Reiter, R. J. (2001). Pharmacological action of melatonin in shock, inflammation and ischemia reperfusion injury. *European Journal of Pharmacology*, 426, 1–2. [https://doi.org/10.1016/s0014-2999\(01\)01175-x](https://doi.org/10.1016/s0014-2999(01)01175-x).



- Duranti, G., Ceci, R., Sgro, P., Sabatini, S., & Di Luigi, L. (2017). Influence of the PDE5inhibitor tadalafil on redox status and antioxidant defense system in C<sub>2</sub>Cl<sub>2</sub> skeletal muscle cells. *Cell Stress Chaperon*, 22, 389–396. <https://doi.org/10.1007/s12192-017-0778-9>.
- Erdemli, Z., Erdemli, M. E., Turkoz, Y., Yigitcan, B., Aladag, M. A., Cigremis, Y., ... Bag, H. G. (2021). Vitamin E effects on developmental disorders in fetuses and cognitive dysfunction in adults following acrylamide treatment during pregnancy. *Biotechnic & Histochemistry*, 96(1), 11–19. <https://doi.org/10.1080/10520295.2020.1751880>.
- Gedik, S., Erdemli, M. E., Gul, M., Yigitcan, B., Bag, H. G., Aksungur, Z., & Altinoz, E. (2017). Hepatoprotective effects of crocin on biochemical and histopathological alterations following acrylamide-induced liver injury in Wistar rats. *Biomedicine and Pharmacotherapy*, 95, 764–770. <https://doi.org/10.1016/j.biopha.2017.08.139>.
- Gedik, S., Erdemli, M. E., Gul, M., Yigitcan, B., Bag, H. G., Aksungur, Z., & Altinoz, E. (2018). Investigation of the protective effects of crocin on acrylamide induced small and large intestine damage in rats. *Biotechnic & Histochemistry*, 93(4), 267–276. <https://doi.org/10.1080/10520295.2018.1492888>.
- Ghanayem, B. I., Witt, K. L., Kissling, G. E., Tice, R. R., & Recio, L. (2005). Absence of acrylamide-induced genotoxicity in CYP2E1-null mice: Evidence consistent with a glycidamide mediated effect. *Mutation Research*, 576, 284–297. <https://doi.org/10.1016/j.mrfmmm.2005.05.004>.
- Heikkinen, R. E., Cabbot, F., & Cohen, G. (1976). *in vivo* inhibition of superoxide dismutase in mice by diethylthiocarbamate. *Journal of Biological Chemistry*, 251, 182–2185. PMID: 5443.
- Hsu, Y. W., Tsai, C. F., & Chen, W. K. (2009). Protective effects of sea buckthorn (*Hippophae rhamnoides* L.) seed oil against carbon tetrachloride-induced hepatotoxicity in mice. *Food and Chemical Toxicology*, 47, 2281–2288. <https://doi.org/10.1016/j.fct.2009.06.015>.
- Kacar, S., Sahinturk, V., & Kutlu, H. M. (2019). Effect of acrylamide on BEAS-2B normal human lung cells: Cytotoxic, oxidative, apoptotic and morphometric analysis. *Acta Histochemica*, 121, 595–603. <https://doi.org/10.1016/j.acthis.2019.05.005>.
- Kacar, S., Vejselova, D., Kutlu, H. M., & Sahinturk, V. (2018a). Acrylamide-derived cytotoxic, anti-proliferative, and apoptotic effects on A549 cells. *Human & Experimental Toxicology*, 37, 468–474. <https://doi.org/10.1177/0960327117712386>.
- Kacar, S., Vejselova, D., Kutlu, H. M., & Sahinturk, V. (2018b). Acrylamide-derived cytotoxic, anti-proliferative, and apoptotic effect on A549 cells. *Human & Experimental Toxicology*, 37, 468–474. <https://doi.org/10.1177/0960327117712386>.
- Kelkel, M., Schumacher, M., Dicato, M., & Diederich, M. (2011). Antioxidant and antiproliferative properties of lycopene. *Free Radical Research*, 45(8), 925–940. <https://doi.org/10.3109/10715762.2011.564168>.
- Kunzel, S. G., Subramanya, S., Satapathy, P., Sahoo, I., & Zameer, F. (2019). Acrylamide Induced Toxicity and the Propensity of Phytochemicals in Amelioration: Review. *Central Nervous System Agents in Medicinal Chemistry*, 19(2), 100–113. <https://doi.org/10.2174/1871524919666190207160236>.
- Li, L., Sun, H., Liu, W., Zhao, H., & Shao, M. (2017). Silymarin protects against acrylamide-induced neurotoxicity via Nrf2 signalling in PC12 cells. *Food and Chemical Toxicology*, 102, 93–101. <https://doi.org/10.1016/j.fct.2017.01.021>.
- Liu, C. M., Ma, J. Q., & Sun, Y. Z. (2010). Quercetin protects the rat kidney against oxidative stress-mediated DNA damage and apoptosis induced by lead. *Environmental Toxicology and Pharmacology*, 30, 264–271. <https://doi.org/10.1016/j.etp.2010.07.002>.
- Liu, Z., Song, G., Zou, C., Liu, G., Wu, W., Yuan, T., & Liu, X. (2015). Acrylamide Induces mitochondrial dysfunction and apoptosis in BV-2 microglial cells. *Free radical biology and medicine*, 84, 42–53. <https://doi.org/10.1016/j.freeradbiomed.2015.03.013>.
- Mallepogu, V., Jayasankar Babu, P., Doble, M., Suman, B., Nagalakshamma, V., Chalapathi, P. V., & Thyagaraju, K. (2017). Effects of acrylamide on cervical cancer (HeLa) cells proliferation and few marker enzymes. *Austin Journal of Biotechnology and Bioengineering*, 4, 1087.
- Manjanatha, M. G., Aidoo, A., Shelton, S. D., Bishop, M. E., McDaniel, L. P., & Lyn-Cook, L. E. (2006). Genotoxicity of acrylamide and its metabolite glycidamide administered in drinking water to male and female Big Blue mice. *Environmental and Molecular Mutagenesis*, 47(6–17), 5. <https://doi.org/10.1002/em.20157>.
- Mehri, S., Karami, H. V., Hassani, F. V., & Hosseinzadeh, H. (2014). Chrysin reduced acrylamide-induced neurotoxicity in both *in vitro* and *in vivo* assessments, Iranian Biomedical Journal. 2014, 18 (2),101–106. doi: 10.6091/ibj.1291.2013.
- Mehri, S., Meshki, M. A., & Hosseinzadeh, H. (2015). Linalool as a neuroprotective agent against acrylamide-induced neurotoxicity in Wistar rats. *Drug and Chemical Toxicology*, 38, 162–166.
- Mosmann, T. (1983). Rapid colorimetric assay for cellular growth and survival. Application to proliferation and cytotoxicity assays. *Journal of Immunological Methods*, 65, 55–63. [https://doi.org/10.1016/0022-1759\(83\)90303-4](https://doi.org/10.1016/0022-1759(83)90303-4).
- Motamedharyati, V. S., Farzad, S. A., Nassiri-Asl, M., & Hosseinzadeh, H. (2014). Effects of rutin on acrylamide-induced neurotoxicity. *Journal of Pharmaceutical Sciences*, 22 (1).
- Mueller, L., & Boehm, V. (2011). Antioxidant Activity of  $\beta$ -Carotene Compounds in Different *In Vitro* Assays. *Molecules*, 16, 1055–1069. <https://doi.org/10.3390/molecules16021055>.
- Nakabeppu, Y., Tsuchimoto, D., Yamaguchi, H., & Sakumi, K. (2007). Oxidative damage in nucleic acids and Parkinson's disease. *Journal of Neuroscience*, 2007(85), 919–934. <https://doi.org/10.1002/jnr.21191>.
- Pedreschi, F., Mariotti, M. S., & Granby, K. (2014). Current issues in dietary acrylamide: Formation, mitigation and risk assessment. *Journal of the Science of Food and Agriculture*, 94, 9–20. <https://doi.org/10.1002/jsfa.6349>.
- Prasad, S. N., Muralidhara. (2012). Evidence of acrylamide induced oxidative stress and neurotoxicity in *Drosophila melanogaster*—Its amelioration with spice active enrichment: relevance to neuropathy. *Neurotoxicology*, 33(5),1254–1264. doi: 10.1016/j.neuro.2012.07.006.
- Rahal, A., Kumar, A., Singh, V., Yadav, B., Tiwari, R., & Chakraborty, S. (2014). Oxidative stress, prooxidants, and antioxidants: The interplay. *BioMed Research International*, 761264. <https://doi.org/10.1155/2014/761264>.
- Ren, X., Zou, L., Zhang, X., Branco, V., Wang, J., & Curvalho, C. (2017). Redox Signaling Mediated by Thioredoxin and Glutathione Systems in the Central Nervous System. *Antioxidant Redox Signal*, 27(13):989–1011 doi: 10.1089/ars.2016.6925.
- Rodriguez-Ramiro, I., Ramos, S., Bravo, L., Goya, L., & Angeles Martin, M. (2011). Procyanidin B2 and a cocoa polyphenolic extract inhibit acrylamide-induced apoptosis in human Caco-2 cells by preventing oxidative stress and activation of JNK pathway. *Journal of Nutritional Biochemistry*, 22(12), 1186–1194. <https://doi.org/10.1016/j.jnutbio.2010.10.005>.
- Sabah, A., Nikhat, J. S., Seema, Z., Majid, A. G., & Manal, A. (2016). Hepatoprotective effect of Quercetin supplementation against Acrylamide-induced DNA damage in wistar rats. *BMC Complementary and Alternative Medicine*, 16(1), 327. <https://doi.org/10.1186/s12906-016-1322-7>.
- Sahinturk, V., Kacar, S., Vejselova, D., & Kutlu, H. M. (2018a). Acrylamide exerts its cytotoxicity in NIH/3T3 fibroblast cells by apoptosis. *Toxicology and Industrial Health*, 34, 481–489. <https://doi.org/10.1177/0748233718769806>.
- Sahinturk, V., Kacar, S., Vejselova, D., & Kutlu, H. M. (2018b). Acrylamide exerts its cytotoxicity in NIH/3T3 fibroblast cells by apoptosis. *Toxicology & industrial health*, 34, 481–489. <https://doi.org/10.1177/0748233718769806>.
- Sema, G., Mehmet, E. E., Guk, M., Yigitcan, B., Harika, G. B., Zeynep, A., & Eyup, A. (2017). Hepatoprotective effects of crocin on biochemical and histopathological alterations following acrylamide-induced liver injury in Wistar rats. *Biomedicine & Pharmacotherapy*, 95, 764–777. <https://doi.org/10.1016/j.biopha.2017.08.139>.
- Seydi, E., Rajabi, M., Salimi, A., & Pourahmad, J. (2015). Involvement of mitochondrial-mediated caspase 3 activation and lysosomal labilization in acrylamide-induced liver toxicity. *Environmental Toxicology & Chemistry*, 97, 563–575. <https://doi.org/10.1080/02727248.2015.1047671>.
- Shan, X. Q., Aw, T. Y., & Jones, D. P. (1990). Glutathione-dependent protection against oxidative injury. *Pharmacology & Therapeutics*, 47, 61–71. [https://doi.org/10.1016/0163-7258\(90\)90045-4](https://doi.org/10.1016/0163-7258(90)90045-4).
- Sies, H., & Stahl, W. (1995). Vitamins E and C,  $\beta$ -carotene, and other carotenoids as antioxidants. *American Journal of Clinical Nutrition*, 62(6), 1315S–1321S. <https://doi.org/10.1093/ajcn/62.6.1315S>.
- Soha, M. H., Zakaria, E. K., Abdel, R. F., Ola, N. S., Mervat, M. S., & Diaa, M. (2020). Hepatoprotective effect of Raspberry ketone and white tea against acrylamide-induced toxicity in rats. *Drug and Chemical Toxicology*. <https://doi.org/10.1080/01480545.2020.1772279>.
- Valko, M., Leibfritz, D., Moncol, J., Cronin, M. T., Mazur, M., & Telser, J. (2007). Free radicals and antioxidants in normal physiological functions and human disease. *International Journal of Biochemistry and Cell Biology*, 39, 44–84.
- Winterbourn, C. C., & Stern, A. (1987). Human red cells scavenge extracellular hydrogen peroxide and inhibit formation of hypochlorous acid and hydroxyl radical. *Journal of Clinical Investigation*, 80, 1486. <https://doi.org/10.1172/JCI113230>.
- Zamani, E., Shaki, F., Abedian Kenari, S., & Shokrzadeh, M. (2017). Acrylamide induces immunotoxicity through reactive oxygen species production and caspase-dependent apoptosis in mice splenocytes via the mitochondria-dependent signaling pathways. *Biomedicine & Pharmacotherapy*, 94, 523–530. <https://doi.org/10.1016/j.biopha.2017.07.033>.
- Zhang, L., Wang, E., Chen, F., Yan, H., & Yuan, Y. (2013). Potential protective effects of oral administration of allicin on acrylamide-induced toxicity in male mice. *Food and Function*, 1229–1236. <https://doi.org/10.1039/c3fo60057b>.
- Zhang, W. H., & Wang, H. (2008). Nortriptyline protects mitochondria and reduces cerebral ischemia/hypoxia injury. *Stroke*, 39, 455–462. <https://doi.org/10.1161/STROKEAHA.107.496810>.
- Zhao, M., Wang, P., Zhu, Y., Liu, X., Hu, X., & Chen, F. (2015). Blueberry anthocyanins extract inhibits acrylamide-induced diverse toxicity in mice by preventing oxidative stress and cytochrome P450 2E1 activation. *Journal of Functional Foods*, 14(95–101). <https://doi.org/10.1016/j.jff.2015.01.035>.